UNIVERSITY OF SOUTHAMPTON

FACULTY OF ENGINEERING AND PHYSICAL SCIENCES

School of Engineering

Department of Civil, Maritime and Environmental Engineering

DEVELOPMENT OF TRAVEL TIME ESTIMATION MODELS: CONSIDERATION OF LINK GEOMETRY FOR KOREAN MOTORWAYS

by

SUNGBAE YOON

Thesis for the degree of Doctor of Philosophy

JANUARY 2021

UNIVERSITY OF SOUTHAMPTON

Abstract

FACULTY OF ENGINEERING AND PHYSICAL SCIENCES

Department of Civil, Maritime and Environmental Engineering

Thesis for the degree of Doctor of Philosophy

DEVELOPMENT OF TRAVEL TIME ESTIMATION MODELS: CONSIDERATION OF LINK GEOMETRY FOR KOREAN MOTORWAYS

Sungbae Yoon

Traffic assignment in transport appraisal is an important procedure that allocates future origin-destination trip demand to every route. A link cost function, which is also called a volume-delay function (VDF), has been used to predict travel time consumed by traffic demand passing through each link in traffic assignment. In order to cover various road characteristics such as the number of lanes, road types, different parameters in VDF have been proposed commonly with road capacity and free-flow travel time. VDF has the advantage in that it is simple enough to analyse the entire network, explaining the relationship mainly with traffic flow. However, VDF has two drawbacks: uncertainty in road capacity and difficulty in spatial transferability. The former includes the conceptual uncertainty that there is little consensus of the definition and the measurement uncertainty of which traffic flow is chosen for road capacity (e.g. the highest or 95 percentile one, etc.). The other drawback is that current VDFs cannot account for change in link geometry and as such are not spatially transferable. Because of the two drawbacks, current VDFs could result in inaccurate traffic assignment; and hence cause inappropriate provision of road space.

In order to overcome the limitations, this study implements the empirical analysis of 72 Korean motorway links by quantifying the dependent variable of link travel time and the independent variables of traffic flow and link geometric features. The dataset was collected from intelligent transport systems and road design drawings. Fixed effects modelling by least squares dummy variables identified influential factors on travel time. In order to develop feasible travel time estimation models, three statistical methods were introduced as follows: firstly, this study introduces linear statistical estimations, which are ordinary least squares (OLS) and generalised least squares (GLS) estimated by likelihood maximisation. In the modelling process, strict statistical assumptions of the OLS estimation are tested and different variance-covariance structures in the GLS estimation are scrutinised to deal with statistical violations such as heteroscedasticity and serial correlation. Secondly, nonlinear least squares (NLS) estimation, which is widely used for VDF customisation, is applied by combining link geometric variables with an existing model. In order to clarify the uncertainty of road capacity, sensitivity analysis using different road capacity values shows the impact on NLS estimated models. Lastly, the most appropriate model is selected by the comparison with statistical accuracy measures after a 10-fold cross-validation with the application to practical traffic assignment and transport appraisal.

In conclusion, this study develops new types of travel time estimation models that include link geometric variables by testing many statistical approaches. The results suggest that not only traffic flow in existing models but also many influential factors such as weather, brightness and link attributes can affect travel time. In particular, some link geometric variables of upgrade, downgrade and tunnel ratios are statistically significant as explanatory variables in the models. In addition, it is worth noting that it is possible to develop a new type of VDF with link geometry instead of road capacity. The statistical significance of the developed models and their application to transport planning demonstrate that the selected model can replace existing VDFs in traffic assignment.

Table of Contents

Chapter 1. Introduction **1**

1.1. Background 1

1.2. Motivation 3

1.3. Aim and objectives 6

1.4. Research Scope 8

1.5. Structure of the thesis 11

Chapter 2. Travel Time Estimation Models in Traffic Assignment **13**

2.1. Introduction 13

2.2. Traffic assignment 14

2.2.1. Traffic assignment from the economic perspective 14

2.2.2. Traffic assignment in transport appraisal 16

2.2.3. Two classifications of traffic assignment 18

2.2.4. Implication to thesis 23

2.3. Travel time estimaiton models 25

2.3.1. Theoretical background for traffic modelling 25

2.3.2. Volume Delay Function (VDF) 30

2.3.3. VDF in South Korea 34

2.3.4. Implication to thesis 38

2.4. Free-Flow Speed and Road Capacity 39

2.4.1. FFS and road capacity in highway capacity manuals 39
2.4.2. Uncertainty of FFS and road capacity 41
2.4.3. Implication to thesis 46

2.5. Road geometry in travel time estimation models 47
2.5.1. Observation of traffic data by different road geometry 47
2.5.2. Link geometry in travel time estimation models 48
2.5.3. Road geometry in South Korea 52
2.5.4. Implication to thesis 54

2.6. Research gaps in the current literature and potential improvements 55

Chapter 3. Research Methodology 57

3.1. Introduction 57

3.2. Initial case study 59
3.2.1. Overview of intial case study 59
3.2.2. Measurement of traffic data on each location 61
3.2.3. Estimation of models between travel time and traffic flow 63
3.2.4. Findings 67

3.3. Development of model estimation methdology 69
3.3.1. Overview of model estimation 69
3.3.2. Multivariate linear estimation 70
3.3.3. Nonlinear least squares (NLS) estimation 80

3.4. Identification of variables 84
3.4.1. Variables for model estimations 84
3.4.2. Data collection 87
3.4.3. Data processing 93

3.5. Case study 95

3.5.1. How to select cases 95

3.5.2. Descriptive statistics for the selected cases 97

3.6. Model selection 100

3.6.1. Comparison of results across methodologies 100

3.6.2. 10-fold cross-validation 102

3.7. Summary 104

Chapter 4. Identification of Influential Factors for Models 105

4.1. Introduction 105

4.2. Data selection 106

4.2.1. Plot observation 106

4.2.2. Framing panel data (entity identification) 111

4.3. Analysis of factors by BPR function 114

4.3.1. Model specification 114

4.3.2. Customisation of BPR function (existing approach) 114

4.3.3. Customisation of BPR function including geometric features 116

4.3.4. Sensitivity analysis of differences in road capacity 118

4.3.5. Summary 118

4.4. Analysis of factors by OLS linear estimation 120

4.4.1. Model specification 120

4.4.2. POLS and FE models with DV and TF 121

4.4.3. POLS and FE models including geometric variables 127

4.4.4. Comparison between fixed effects models 133

4.4.5. Model finding with panel data: POLS, FE and RE modelling 135

4.4.6. Summary 139

4.5. Findings 141

Chapter 5. Development of Feasible Models 143

5.1. Introduction 143

5.2. Data selection 144

5.2.1. Data filtering 144

5.2.2. Discussion on one-day data selection 145

5.2.3. Plot observation 148

5.3. Customisation of BPR function by NLS estimation 150

5.3.1. Model specification 151

5.3.2. Sensitivity analysis by road capacity 154

5.3.3. Summary 154

5.4. OLS estimation models 156

5.4.1. Model specification 156

5.4.2. Model findings 156

5.4.3. OLS assumption tests 160

5.4.4. Summary 165

5.5. GLS estimation models 166

5.5.1. Model specification 166

5.5.2. Dealing with heteroscedasticity 167

5.5.3. Dealing with serial correlation 173

5.5.4. Dealing with both heteroscedasticity and serial correlation 176

5.5.5. Summary 179

5.6. Findings 181

Chapter 6. Application 183

6.1. Introduction 183

6.2. Selection of the most appropriate link-cost function 184

6.2.1. Validation of models 184

6.2.2. Investigation of statistical significance between models 186

6.2.3. Practical applicability 188

6.2.4. Summary 192

6.3. Application to transport planning 193

6.3.1. Impacts on travel time estimation 193

6.3.2. Application to traffic assignment 197

6.4. Findings 201

Chapter 7. Conclusion 203

7.1. Main conclusions 203

7.1.1. Uncertainty of FFTT and road capacity in existing VDF approaches 204

7.1.2. Identification of factors affecting travel time 205

7.1.3. Significance of link geometry for travel time estimation 206

7.1.4. Suggestion of new travel time estimation models 207

7.2. Contributions of the thesis 210

7.3. Limitation and future work 212

A. Appendices 215

A.1. Korean motorways 216

A.1.1. Status of motorways in South Korea 216

A.1.2. Design criteria for motorways in South Korea 218

A.2. Cost-Benefit Analysis (CBA) in Transportation 220

A.2.1. CBA in Many Countries 220

A.2.2. CBA Benefit Estimation in the UK 222

A.2.3. CBA limitation or difficulties 227

A.3. CBA in Korea 230

A.3.1. History and significance of CBA in Korean transportation projects 230

A.3.2. The procedure of Korean CBA 231

A.3.3. The benefit factors in Korean CBA 233

A.4. Initial case study 236

A.4.1. Case selection and Data collection 236

A.4.2. Measurement of Traffic data in the intial case study 240

A.5. Statistical results 248

A.5.1. FE modelling 248

A.5.2. OLS estimation on one-day dataset 252

A.5.3. Box-Cox test for selecting log-linear versus linear-linear form 253

A.5.4. Coding for 10-fold cross validation 254

A.5.5. Estimated travel time on three links by three models (part of result) 256

A.5.6. Application to traffic assignment by three models 257

References 259

List of Tables

Table 2-1 Values of travel time savings (VTTS) and vehicle operating cost (VOC) 16

Table 2-2 Environmental impact appraisal on noise, air quality and greenhouse gases............ 17

Table 2-3 Classification of traffic assignment by equilibrium principles.................................. 17

Table 2-4 Comparison between STA and DTA... 23

Table 2-5 Factors of the Korean VDF by different road types 37

Table 2-6 Limitations of road capacity 40

Table 2-7 Formulae for the macroscopic traffic flow on gradient motorways 49

Table 2-8 Design speed in Korea by the type of terrain 53

Table 2-9 The number and ratio of Korean bridges and tunnels.. 54

Table 3-1 Geometrical features with ILDs' locations in the initial case study........................... 60

Table 3-2 Data source and purpose in the initial case study 60

Table 3-3 Observations of FFS and road capacity in the initial case study 61

Table 3-4 Nonlinear estimation based on BPR function in the initial case study....................... 64

Table 3-5 Different curve estimation results in the initial case study.. 66

Table 3-6. Strengths and weaknesses of linear and nonlinear estimation.................................. 69

Table 3-7 Table form for sensitivity analysis focusing on the change in parameters................ 83

Table 3-8 Table form for sensitivity analysis focusing on spatial transferability....................... 83

Table 3-9 Candidates and selection of geometric variables... 85

Table 3-10. Example of DSRC raw data.. 87

Table 3-11 Example of raw data from ILD... 89

Table 3-12 Calculation of average traffic flow 89

Table 3-13 Example of raw data from FTMS... 90

Table 3-14 Procedure for the case selection 95

Table 3-15 List of the selected cases 97

Table 3-16 Descriptive statistics of the 72 selected cases... 99

Table 3-17 Statistical accuracy measures for the model evaluation 102

Table 4-1 Research about reduction rate of traffic values by hourly rainfall 112

Table 4-2 Daily rainfall by regional observatories in September of 2018 113

Table 4-3 Customised models based on BPR function 114

Table 4-4 Existing approach based on BPR function between DV and TF 115

Table 4-5 NLS estimation with TF and geometric variables 116

Table 4-6 Sensitivity analysis of NLS estimation by different values of road capacity 118

Table 4-7 POLS and FE models based on a quadratic function with DV and TF 120

Table 4-8 POLS and FE models after the inclusion of geometric variables on MODEL1 121

Table 4-9 Pooled OLS estimation between DV and IV1 by a quadratic function 122

Table 4-10 Result of FE modelling (LSDV) with the ‘Link’ entity 123

Table 4-11 Result of FE modelling (LSDV) with ‘Date’ entity (without geometric variables) 125

Table 4-12 Result of two-way FE modelling (LSDV) with both ‘Date’ and ‘Link’ entities 126

Table 4-13 Pooled OLS estimation with TF and geometric independent variables 127

Table 4-14 Result of FE modelling (LSDV) with the ‘Route’ entity 128

Table 4-15 Result of FE modelling (LSDV) with the ‘Brightness’ entity 129

Table 4-16 Result of FE modelling (LSDV) with the ‘Day (weekday and weekend)’ entity ... 130

Table 4-17 Result of FE modelling (LSDV) with the ‘Weather’ entity 131

Table 4-18 Result of FE modelling (LSDV) with the ‘Date’ entity (with geometric variables)131

Table 4-19 Summary of FE modelling by LSDV (without geometric variables) 134

Table 4-20 Summary of FE modelling by LSDV (with geometric variables) 134

Table 4-21 Panel data definition with the entity of links and 15-minute intervals 135

Table 4-22 Pooled OLS estimation with the panel data 135

Table 4-23 FE modelling by the method of ‘within’ estimation 136

Table 4-24 RE modelling with panel data 137

Table 4-25 F-test for investigating individual effects 138

Table 4-26 Hausman test for model selection between FE and RE modelling 138

Table 4-27 Breusch and Pagan Lagrangian Multiplier (LM) test 139

Table 4-28 RMSE comparison between OLS and NLS estimation (one-month data analysis) 142

Table 5-1 OLS estimation by different daily data selection 147

Table 5-2 Impact of BEND variable on estimated models from the dataset on 25th of Sep 148

Table 5-3 NLS estimation models by inclusion of geometric variables 150

Table 5-4 Example of NLS estimation (with all geometric variables) 151

Table 5-5 Feasible NLS estimation models by different combinations of IVs 153

Table 5-6 Coefficients of feasible NLS estimation models by different road capacity 154

Table 5-7 OLS estimation models by inclusion of geometric variables 156

Table 5-8 Model estimations by variable selection 157

Table 5-9 Model estimations by interaction variables 158

Table 5-10 Model estimation by log-transformation 159

Table 5-11 Change of R-square by log-transformation of IVs 160

Table 5-12 Result of the variance inflation factor (VIF) 161

Table 5-13 Breusch-Pagan test by using fitted values for FMODEL3-1 162

Table 5-14 Breusch-Pagan test of independent variables for MODEL3-1 163

Table 5-15 Breusch-Pagan test of independent variables for FMODEL3 163

Table 5-16 Durbin-Watson test for MODEL3-1 and FMODEL3 164

Table 5-17 GLS estimation models by different variance-covariance matrices 166

Table 5-18 Various variance structures for dealing with heteroscedasticity 167

Table 5-19 Example of GLS estimation dealing with heteroscedasticity (stratified variance). 168

Table 5-20 GLS estimation considering different variance structures 170

Table 5-21 ANOVA after dealing with heteroscedasticity 172

Table 5-22 Example of GLS estimation dealing with serial correlation (ARMA (2, 2)) 174

Table 5-23 GLS estimation considering different serial correlation structures 175

Table 5-24 ANOVA after dealing with serial correlation 176

Table 5-25 GLS estimation dealing with heteroscedasticity and serial correlation 177

Table 5-26 Selection between OLS and GLS estimated models 180

Table 5-27 Summary of feasible models within each estimation method 181

Table 6-1 RMSE derivation by 10-fold cross-validation 185

Table 6-2 MAPE derivation by 10-fold cross-validation 185

Table 6-3 ANOVA of RMSEs and MAPEs between five models 185
Table 6-4 Comparison of accuracy measures between the feasible models 187
Table 6-5 O-D trip demand depending on transportation in Korea (as of 2013) 190
Table 6-6 Propagation of errors by road capacity uncertainty 192
Table 6-7 Three models for application 193
Table 6-8 Three hypothetical links with different geometric features 196
Table 6-9 Sum of estimated travel times on three links for 30 days by both models 196
Table 6-10 Equilibrium points between motorway and city road 199
Table 6-11 Result of traffic assignment by three models 200
Table A-1 Korean arterial road network 216
Table A-2 Comparison with traffic volume between Korean motorways and highways 216
Table A-3 Minimum width of lane by road types and design speed in Korea 218
Table A-4 Minimum central barrier width by road types in Korea 218
Table A-5 Right clearance by road types and design speed in Korea 218
Table A-6 Left clearance by road types and design speeds in Korea 218
Table A-7 Maximum degree of vertical slope by road types and design speed in Korea 219
Table A-8 Radius of the horizontal curve by design speed and super-elevation in Korea 219
Table A-9 Main contents of UK CBA in WebTAG (DfT, 2018) 224
Table A-10 AMCB table (UK) 224
Table A-11 Valuation of VTTS and VOC in UK 226
Table A-12 Impacts appraisal on noise, air quality and greenhouse gases in UK 227
Table A-13 Preliminary feasibility assessment by project types in Korea 230
Table A-14 Average value of time per vehicle (entire area) in Korea 234
Table A-15. Cost of reducing atmospheric pollutants in Korea 235
Table A-16 Influenced distance by each detector in the initial case 240
Table A-17. Observation of free-flow speed on ILDs in the initial case 242
Table A-18 Measurement of road capacity on ILD locations in the initial case study 243
Table A-19 Various criteria for finding breakdown points 246
Table A-20 Finding traffic flow at breakdown points with Condition 1 247

Table A-21 Finding traffic flow at breakdown points with Condition 2 247

Table A-22 Finding traffic flow at breakdown points with Condition 3 247

Table A-23 Finding traffic flow at breakdown points with Condition 4 247

List of Figures

Figure 2-1 Traffic assignment in traffic demand forecasting 14

Figure 2-2 Change in consumer surplus 15

Figure 2-3 Typical speed–flow (left) and cost–flow (right) relationship in STA........................19

Figure 2-4 General DTA algorithmic procedure 22

Figure 2-5 Flow-density, speed-flow, and speed-density curves...25

Figure 2-6 Practical change of the speed-flow relationship 26

Figure 2-7 Comparison of three flow-density diagrams...27

Figure 2-8 Relationship between flow and density in free-flow (F) and jam (J) conditions 27

Figure 2-9 Two-regime relationship between flow and density..27

Figure 2-10 Three traffic phase based on the spatiotemporal measurement 29

Figure 2-11 Example of flow variation on link AB dependent on the trip demand 30

Figure 2-12 Difference between theoretical and practical relationship......................................31

Figure 2-13 Convex and nonconvex function 32

Figure 2-14 Impact area by the variable and parameters in BPR function.................................36

Figure 2-15 Adjustment of parameters in BPR function..37

Figure 2-16 LOS for basic freeway segments 39

Figure 2-17 Road capacity measurement from boundary conditions..42

Figure 2-18 Road capacity measurement by the average of top 5% traffic flows.......................43

Figure 2-19 Road capacity measurement by regression analysis 43

Figure 2-20 Road capacity measurement by cumulative curve..44

Figure 2-21 Empirical measurement of traffic flow and speed at a bottleneck...........................45

Figure 2-22 Road capacity measurement by finding breakdown effect 45

Figure 3-1 Flow chart for the overall methodological approach 57

Figure 3-2 Diagram for FFS and road capacity in the initial study 61

Figure 3-3 Comparison of traffic flows causing breakdown by two different criteria 62

Figure 3-4 Curve fittings of the initial case study based on the nonlinear estimation 65

Figure 3-5 Curve estimation by different linear equations 66

Figure 3-6 Homoscedastic residual plots (left); heteroscedastic disturbances (right) 73

Figure 3-7 Patterns of serial correlation disturbances.. 74

Figure 3-8 Elements of horizontal curve (L_c: simple curve, L_s: spiral curve)............................ 91

Figure 3-9 Elements of spiral curve 91

Figure 3-10 Example of design drawing: “Kochang-Damyang Motorway (6.08-6.40km) E” ... 92

Figure 3-11 Congestion speed identification from the initial case study.................................... 94

Figure 3-12 Location of the selected cases 96

Figure 3-13 Process of k-fold cross-validation (training and tested set).................................. 103

Figure 4-1 Scatter plot including congestion states 106

Figure 4-2 Scatter plot between DV and IV1 (TF) after data processing 107

Figure 4-3 Box plot of DV by IV2 (TR).. 107

Figure 4-4 Box plot of DV by IV3 (RISE) 108

Figure 4-5 Box plot of DV by IV4 (FALL).. 108

Figure 4-6 Box plot of DV by IV5 (BEND) 109

Figure 4-7 15th percentile values of DV by geometric variables for one month...................... 110

Figure 4-8 85th percentile values of DV by geometric variables for one month...................... 110

Figure 4-9 Fitted line of NLS estimation (BPR function) between DV and TF 116

Figure 4-10 Fitted line between DV and TF in BPR2 117

Figure 4-11 Residual plot of pooled OLS estimation between DV and TF............................. 122

Figure 4-12 Residual plot of fixed effects model within links... 124

Figure 4-13 Residual plot of two-way FE model... 126

Figure 4-14 Residual plot of pooled OLS estimation between DV and TF............................. 128

Figure 5-1 Box plot of daily traffic flows in September of 2018... 144

Figure 5-2 Scatter plot between DV and IV1 (TF) from the one-day dataset........................... 148

Figure 5-3 15th percentile values of DV by geometric variables from the one-day dataset..... 149

Figure 5-4 85th percentile values of DV by geometric variables from the one-day dataset...... 149

Figure 5-5 Scatter residual plots for FMODEL3-1.. 162

Figure 5-6 Residual plot of FMODEL3-1 against the entity of links..172

Figure 6-1 Fitted and observed values according to traffic flow on each model.......................187

Figure 6-2 Standardised residuals vs fitted values plot on feasible models 188

Figure 6-3 Ratio of the error variance depending on links...190

Figure 6-4 Curves of FModel and Korean VDFs 194

Figure 6-5 Curve shift by different link geometry and road capacity 195

Figure 6-6 Comparison of total travel time on three links..196

Figure 6-7 Change in an economic equilibrium from the supply-demand relationship 197

Figure 6-8 Example of a local network for application to transport appraisal 198

Figure 6-9 Change in consumer surplus depending on three models.......................................199

Figure A-1 Korean motorway frame 217

Figure A-2 Appraisal tools and guidance for five types of business cases (UK) 223

Figure A-3 Further appraisal process for the technical project manager (UK) 223

Figure A-4 Overall vehicle operating costs (KRW/km) in Korea 233

Figure A-5 Initial case location 236

Figure A-6. Design Map of the initial case..237

Figure A-7 Example of speed calculation from ILD 238

Figure A-8 Calculation of travel time in a section...239

Figure A-9 Volume-speed relationship for 45 days in the initial case 241

Figure A-10 Breakdown Dynamics during breakdown and recovery (German motorway)......243

Figure A-11 Breakdown effect for 45 days in the initial case 244

Figure A-12 Congestion process from ILD No.30 to No.33 in the initial case study 245

Declaration of Authorship

I, Sungbae Yoon declare that this thesis entitled as “Development of Travel Time Estimation Models: Consideration of Link Geometry for Korean Motorways” and the work presented in it are my own and has been generated by me as the result of my own original research.

I confirm that:

1. This work was done wholly or mainly while in candidature for a research degree at this University;
2. Where any part of this thesis has previously been submitted for a degree or any other qualification at this University or any other institution, this has been clearly stated;
3. Where I have consulted the published work of others, this is always clearly attributed;
4. Where I have quoted from the work of others, the source is always given. With the exception of such quotations, this thesis is entirely my own work;
5. I have acknowledged all main sources of help;
6. Where the thesis is based on work done by myself jointly with others, I have made clear exactly what was done by others and what I have contributed myself;
7. None of this work has been published before submission.

Signed:

Date: January 2021

Acknowledgements

This PhD thesis is dedicated to the memory of my father, Hyunsoo Yoon who always supported and believed me in my life. I wish you had overcome your cancer and stayed with me for a long time. I regretted about why I started my PhD study when you were gone in 2019 but was able to finish my study imagining that if you were alive, you would be very proud of me not to give it up. My mother, Jungja Kim, always gives me her love with devotion, your love has guided me the right way.

My wife, Jihyun Park, always believes and encourages me. Your love and support made me complete my thesis. I cannot imagine my life without you. My children, Soyul, Seojun, Yejun, you are my enjoy and hope. Your existence has empowered and motivated me.

I would like to extend my deepest gratitude to my supervisors who helped me in my PhD course. Professor John Preston, you are my first supervisor who showed me the right direction whenever I lost my way. I am very grateful for the attentive and invisible care that fills my shortcomings. Dr Ioannis Kaparias, I appreciate your delicate supervision and advices.

I cannot finish my study without many persons' help. Professor Taeyoung Heo, you are a very kind and great person who gave me statistical knowledge and solutions. It was great time to discuss many statistical issues during my study. Professor Dongmin Lee and Dr Sang Yeon Hong, you inspired me a lot. I would like to appreciate Korean Expressway Corporation that supported me with the data for modelling. Moreover, I will never forget the time with Wonman Oh, Jongjoon Song and many people during UK life even though I cannot address their names individually.

Lastly, I express my thanks to the Korean Government that sponsored my PhD study.

List of Abbreviations

AIC	Akaike's Information Criterion
ANOVA	Analysis Of Variance
ARMA	Auto-Regressive and Moving Average
AVI	Automatic Vehicle Identification
BEND	Sum of bendiness per link distance
BIC	Bayesian Information Criterion
BPR	Bureau of Public Road (United States of America)
BLUE	Best Linear Unbiased Estimator
DfT	Department for Transport (United Kingdom)
DSRC	Dedicated Short Range Communication
DTA	Dynamic Traffic Assignment
DV	Dependent Variable
ETC	Electric Toll Collection
FALL	Sum of falls per link distance
FFS	Free-Flow Speed
FFTT	Free-Flow Travel Time
FHWA	United States Federal Highway Administration
FIFO	First In First Out
FTMS	Freeway Tunnel Management Systems
GLS	Generalised Least Squares
HCM	Highway Capacity Manual
ILD	Inductive Loop Detector
ITS	Intelligent Transport Systems
IV	Independent variable
KDI	Korean Development Institute
KEC	Korean Expressway Corporation

KHCM	Korean Highway Capacity Manual
KICT	Korean Institute of Civil engineering and building Technology
KOTI	Korean Transport Institute
kph	kilometre per hour
KST	Korean Society of Transportation
LOS	Level Of Service
LSDV	Least-Squares Dummy Variable
MAE	Mean Absolute Error
MAPE	Mean Absolute Percentage Error
MLE	Maximum Likelihood Estimation
MLTM	Ministry of Land, Transport and Maritime affairs (South Korea)
MOLIT	Ministry of Land, Infrastructure and Transport (South Korea)
mph	miles per hour
NATA	New Approach To Appraisal
NLS	Nonlinear Least squares
OBU	On-Board Unit for ETC
OLS	Ordinary Least Squares
O-D	Origin-Destination
pcph	passenger cars per hour
pcpkpl	passenger cars per kilometre per lane
pcphpl	passenger cars per hour per lane
pcpmpl	passenger cars per mile per lane
RISE	Sum of rises per link distance
RSE	Road Side Equipment
RMSE	Root Mean Squared Error
SMS	Space-Mean Speed
SPV	Subjects Per Variables
SSE	Sum of Squared Errors

STA	Static Traffic Assignment
TF(q)	Traffic flow
TF2(q^2)	Square of Traffic flow
TMS	Time-Mean Speed
TR	Tunnel Ratio (sum of tunnel length per link distance)
VDF	Volume-Delay Function
VIF	Variance Inflation Factor
vpk	vehicles per kilometre
vph	vehicles per hour
vphpl	vehicles per hour per lane
WebTAG	Web-based Transport Analysis Guidance (United Kingdom)
WLS	Weighted Least Squares

Chapter 1. Introduction

1.1. Background

Travel time is one of the fundamental arbiters or indicators for assessing efficiency in transportation policy. From the travellers' perspective, travel time is an important factor in selecting transportation modes and their routes. Transportation users predict travel time based on the historical records or real-time measurement, which are provided by many kinds of technologies such as mobile communications. In comparison, from the transportation suppliers' perspective, travel time can be the basic criterion for determining the priority of transportation service. In order to improve the feasibility of the determination, transportation suppliers (governments or planners) need to predict travel time considering various impacts as well as historical records.

In terms of transportation economics, travel time prediction plays an essential role in transport appraisal that would determine the supply of transportation. The supply of transportation is determined by seeking the balance with trip demand (Jones, 1977; Sugden, 1999; Ortúzar and Willumsen, 2012). Suppliers provide additional transportation capacity to meet future trip demand or to meet current latent demand. From the economic perspective, they implement transport appraisal in order to justify their intervention in a market (Boardman *et al.*, 2013). The change in travel time before and after the intervention is one of the comparative measures in transport appraisal. In particular, travel time savings by the intervention are treated as an important benefit factor calculated in quantitative approaches (e.g. cost-benefit analysis), which are introduced in many countries' decision making processes (Hayashi and Morisugi, 2000; KDI, 2008a; DfT, 2018). For example, travel time saving benefits by Korean national highway projects implemented just before making a 2005-2010 plan was about 77.4% of total benefits (KDI, 2008b). Moreover, travel time (or, more correctly, travel speed) affects other benefit factors such as vehicle operating cost savings, traffic safety, noise and air quality (KDI, 2008b; DfT, 2018).

Looking at a transport appraisal process more closely, travel time affects traffic assignment, which is implemented to find the change in future traffic flows on every route before the benefit estimation in transport appraisal. In other words, traffic assignment, which is one of four steps in traffic demand forecasting[1], allocates future trip demand to the entire or local transport network (Ortúzar and Willumsen, 2012; Patriksson, 2015). In the process, the cost (impedance or performance) of each link must be determined, and the predicted travel time accounts for most of the cost. The benefit estimation in transport appraisal includes travel time savings and the relevant

[1] Traffic demand forecasting consists of trip generation, trip distribution, modal split, and traffic assignment (KDI, 2008b; de Dios Ortúzar and Willumsen, 2012).

cost savings that are affected by the travelled distance of vehicles, which is assigned by travelled time. Travel time on each link does not need to be constant, but could differ according to link attributes and traffic flow. Travel time estimation models used for traffic assignment can be divided into two groups: at a microscopic level and a macroscopic level, respectively. At a microscopic level, travel time estimation models focus on the detailed change of a vehicle's individual movement, which is related to instantaneous speed and acceleration focusing on the interactions between vehicles (Hoogendoorn and Bovy, 2001; Rakha and Tawfik, 2009). On the contrary, at a macroscopic level, the models can explain overall travel time on each link, which have been developed from traditional traffic theory (Greenshields *et al.*, 1935; Greenberg, 1959; Underwood, 1961; Rakha and Crowther, 2002; Kerner, 2009). A volume-delay function (VDF), which is a travel time estimation model at a macroscopic level, explains the relationship between travel time and traffic flow as a link cost function in traffic assignment. Traffic assignment tries to find the equilibrium iteratively by principles such as system optimum or user equilibrium (Beckmann *et al.*, 1956; Sheffi, 1985).

Once a transportation project is determined through transport appraisal, the project should be designed in detail before the construction of the project. The design process communicates with transport appraisal. In the design process, engineers decide geometric features suitable for every link considering construction cost, environmental impacts and other limitations based on the predetermined design speed, which could be related to travel time estimation. Design manuals suggest different geometric features such as lane width, slope and curve radius depending on design speed. The geometric features presented in manuals are regarded as the best requirements to maintain the design speed. Moreover, design alternatives are sought in order to minimise the drastic change in average speed because it is directly related to safety and efficiency issues. While seeking the most appropriate road geometry throughout preliminary and detailed design processes, the past transport appraisal result of the project needs to be reviewed in order to reflect changes in total costs and benefits such as construction costs and network travel times as a result of design changes. In other words, the design of transportation projects would affect and be affected by transport appraisal results.

This study focuses on the relationship between travel time and road geometric features. To specify this, this thesis tries to clarify the limitations of current travel time estimation models (VDFs) and to improve the accuracy of them. The variables connecting between travel time and geometric features in existing VDFs are free-flow travel time (FFTT) and road capacity, and as such most types of VDFs include the constant variables of FFTT and road capacity in spite of various forms of functions. (Branston, 1976; Petrik *et al.*, 2014). Therefore, the in-depth investigation of the relationship between the two values in VDFs and link geometric features motivates this thesis.

1.2. Motivation

This thesis is motivated by identifying errors of travel time estimation in using the existing VDFs from two aspects: the inclusion of inappropriate variables in the existing VDFs and relevant modelling process issues. The first aspect is related to the uncertainty of FFTT and road capacity in VDFs and the second aspect starts from the recognition that the modelling process of current VDFs is not suitable for representing link diversity in traffic assignment. Both aspects are connected by the two predetermined constant values in VDFs. Notably, although road capacity has been recognised as a constant value traditionally, several researchers pointed to the stochastic nature of road capacity, which means that it is hard to measure it as a unique value (Minderhoud *et al.*, 1997; Persaud *et al.*, 1998; Lorenz and Elefteriadou, 2001; Brilon *et al.*, 2007; Dong and Mahmassani, 2009; Kalaee, 2010; Kerner, 2016). In particular, Kerner (2016) showed that road capacity, which is closely related to traffic breakdown, is measured differently at moving bottlenecks based on various factors. This uncertainty of road capacity would cause errors in the current VDFs. With regard to these motivations, the initial case study (Section 3.2.3) identifies errors in BPR function (Bureau of Public Roads, 1964) of the current VDFs.

The current approach is that travel time estimation models are dependent only on traffic flow without considering other influential factors that could affect travel time once FFTT and road capacity are predetermined. Current VDFs consist of travel time as a dependent variable, FFTT and road capacity as constant variables, and traffic flow as an independent variable. They focus only on the relationship between travel time and traffic flow after consolidating link attributes into FFTT and road capacity (Campbell *et al.*, 1959; Smock, 1962; Bureau of Public Roads, 1964; Spiess, 1990; Akçelik, 1991; USHCM, 2000; Dowling and Skabardonis, 2008).

However, this study raises the issue about the uncertainty of FFTT and road capacity with regards to their definitions and measurements. Whilst free-flow speed (FFS: distance divided by FFTT) and road capacity are defined theoretically as the maximum hourly rate under prevailing conditions and the mean speed under low to moderate traffic flows respectively in highway capacity manuals (HCM), current VDFs adopt their practical measurements, which are different from theoretical definitions. Based on these findings, this study notes that the uncertainty of both values would cause significant errors in using travel time estimation models because their definitions and measurements for VDFs cannot be unified.

In addition, despite the uncertainty of the two values, many countries have used travel time estimation models that are customised from existing VDF forms after predetermining the values in traffic assignment (Irawan *et al.*, 2010; Leong, 2017; Nobel and Yagi, 2017). Even the comparatively recent studies calibrated the parameters of existing VDFs for the analysed cases without a critical review of the two values (Kalaee, 2010; Huntsinger and Rouphail, 2011; Kim *et al.*, 2014; Leong and Tan, 2015; Kucharski and Drabicki, 2017; Leong, 2017). As a result, they do not account for various geometric features of links that make up a road in the same category, even though their parameters can be classified by the groups such as road types and the number of lanes. They support the current assumptions that link attributes are included by FFTT and road capacity in VDFs and that the analysed links are homogeneous. The assumptions have the advantage of simplifying functions but the drawback of not taking into account the diversity of link attributes. In, particular, Leong and Tan (2015) pointed to the limitation of BPR function in that the model is developed for only accounting for a certain link type and vehicle. In the same vein, Manzo *et al.* (2014) identified the uncertainty of both the parameters and link capacity in the Danish national transport model, which is based on the BPR function, by using a bootstrap resampling method. Although He and Zhao (2014) tried to improve the BPR function by suggesting the model that combines the BPR function with the simple linear function including the variables of bus stop density and intersection density, they still did not focus on how road capacity is determined in the model.

With regard to link geometry, whilst many studies tried to show the impact on traffic characteristics of link geometry based on the change in speed or traffic flow (Iwasaki, 1991; Koshi *et al.*, 1992; Bando *et al.*, 1995; Brilon, 2000; Hong-Di *et al.*, 2009; Komada *et al.*, 2009; Yun and Shengrui, 2012; Zhang *et al.*, 2012; Wu *et al.*, 2014; Zhou *et al.*, 2014), there have been only a few trials that connect it with travel time estimation models in traffic assignment (Brilon and Bressler, 2004; Cartenì and Punzo, 2007; DfT, 2018). In particular, Brilon and Bressler (2004) proposed the speed estimation model with uphill gradient and its length discretely due to the range of the heavy vehicle percentage and the gradient. DfT (2018) applied the variables of bendiness and hilliness to linear speed-flow relationship in an uncongested condition. Despite such studies, there was insufficient effort to develop statistical significant models by identifying various geometric features. Therefore, this study is also motivated by finding link geometric variables that need to be identified in travel time estimation models and by developing statistically and practically appropriate models including the related variables. In this process, not only existing VDF forms but also generalised functional forms need to be scrutinised and compared.

In summary, current VDFs have limitations in that they do not reflect the diversity of links because of the uncertainty sorrounding FFTT and road capacity. Mackie and Preston (1998) suggested 21 reasons about inaccurate transport appraisal, and they illustrated that one of the reasons is that important variables would not be considered at all or exactly. Fagnant and Kockelman (2012) found that link capacity and the parameters of the BPR function had greater impact on the feasibility analysis of transportation projects than other influential factors on the analysis. Although current VDFs are a simple way to estimate future travel time depending on trip demand, they need to be improved by introducing new forms of models with new variables and constants. Link geometry is one of the considerations that can improve the accuracy of travel time estimation models. In order to replace the current VDFs, new travel time estimation models need to be developed by identifying link geometry effects that have an impact on travel time. Therefore, research questions in this study can be organised as follows;

(1) Are FFTT and road capacity appropriate variables for VDFs?
(2) To what extent do uncertainties around FFTT and road capacity result in errors in the current VDFs?
(3) If FFTT and road capacity cause serious errors, is it possible to develop travel time estimation models that could replace current VDFs?
(4) What functional forms can be introduced for travel time estimation models?
(5) What variables need to be included in the new travel time estimation models and how can they be quantified and identified?
(6) Is it possible to apply the developed models to traffic assignment in practice?

1.3. Aim and objectives

This study aims to find feasible travel time estimation models as an alternative to current VDFs based on the better understanding of the relationship between travel time and its influencing factors. Finding models based on the empirical analysis can be implemented statistically and systematically. Therefore, the objectives, which are connected to the previous research questions, can be stated as follows;

(1) To examine factors that can influence travel time over long time periods.
(2) To clarify the impact on travel time of FFTT and road capacity utilisation in VDFs in order to confirm the hypothesis that such values are not appropriate for explaining the diversity of link travel time.
(3) To identify the statistical significance of link geometric features that can be used for travel time estimation models as well as in the appraisal process.
(4) To investigate feasible travel time estimation models that can be used for traffic assignment in practice.

The first objective is to examine what factors have an impact on travel time estimation and by how much. Firstly, with regard to finding influential factors, there may be a number of factors that could affect travel time as well as link geometry. This study tries to isolate the factors such as links, routes, weather, brightness, day and date from the one-month dataset that consists of traffic data and geometric features. A review of existing studies helps select the factors that affect travel time. Moreover, the empirical analysis of the one-month dataset statistically identifies how much the selected factors influence the accuracy of the estimated models. In particular, it is important to investigate the impact by the diversity of links because it is closely related to different geometry on every link.

The second objective can quantitatively show the limitations of existing VDFs including FFTT and road capacity. First, it can investigate how link geometry affects traffic patterns by examining how FFTT and road capacity can change at every location over short time and space intervals. The result can indicate whether it is appropriate to apply the values measured at specific locations to produce generalised functions for link travel time estimation. Furthermore, this study examines the impact of the accuracy of current VDF approaches by sensitivity analysis with respect to FFTT and road capacity. By verifying the hypothesis of this study, link attribute variables need to be set in estimated models in order to replace FFTT and road capacity in current VDFs.

The third objective is to find the statistical significance of the geometric variables and their coefficients when the variables as link attributes are reflected in the estimated models. Firstly, identification is made in respect of which geometric features can be extracted during the design process. Since all variables should represent link characteristics as mentioned above, this study sets the geometric variables that can explain the space of links. In addition, this objective examines how geometric variables play a role on the various models developed by different statistical estimation methodologies in this study. The result can be meaningful through the comparison of the models with and without geometric variables.

The last objective is related to the final goal of this study. Travel time estimation models that can replace current VDFs in traffic assignment need to be developed through many kinds of statistical verification. It can be confirmed that other statistical models with different variables are applicable to travel time estimation by introducing different methodologies from the existing VDFs. Moreover, the developed models should be spatially transferable between links and can be used practically in the traffic assignment of transport appraisal. Therefore, investigation will be carried out to establish that the estimated models satisfy statistical assumptions and can be validated statistically. It is expected that the developed models can overcome the limitations of using road capacity and FFTT in VDFs.

In conclusion, this thesis will make a contribution to knowledge through the development of new statistical travel time estimation models that can replace the current VDFs, through considering geometric features of links after identifying various factors that could affect travel time as well as through clarifying the limitation of current VDFs.

1.4. Research Scope

The final goal of this study is to develop travel time estimation models that depend on link geometric features in order to improve the reliability of transport appraisal. It is necessary to clarify the scope of research because travel time estimation could be different according to the range of cases studied, the selection of link geometric features (variables), and the comparison with existing VDF approaches. Therefore, prior to Chapter 3 for the detailed methodology development, this section narrows the scope of research from a broad range.

Case study: Korean motorways

The cases to be analysed in this study are confined to Korean motorways even though there are many different types of transportation cases that travel time estimation models can be applied to in transport appraisals.

Firstly, motorways are important national infrastructure and as such motorways can be compared to arteries in the body because they account for most of the passenger and freight transport on highways (Appendix A.1). When looking at the aspect of government investment, the investment for motorways requires long-term discussion and detailed transport appraisal such as CBA because the projects involve large budgets. In addition, Korea introduced a hierarchical road construction and maintenance system; especially all motorways other than public-private partnership in Korea are managed by the Korean Expressway Corporation (KEC). As a result, construction and management manuals by KEC exist to improve the consistency of the analysed cases (KEC, 2016).

Secondly, in terms of data collection, intelligent transport systems (ITS) are well established in Korean motorways because of their importance in traffic management. As the traffic data are measured accurately and densely, models can be estimated precisely. As mentioned in Section 3.4 and 3.5, inductive loop detectors (ILDs) and Dedicated Short Range Communication (DSRC) are well established in motorways. In particular, Korea has well-established ITS; specifically DSRC is an efficient way to measure space-mean speed (SMS) that can be essential for link travel time estimation as the dependent variable.

Lastly, link geometry can affect travel time on motorways more than on other types of roads because the homogeneity and continuity on motorways are more important than on other roads. For instance, motorways have smaller curvature, wider lane width and multi-level intersections. These characteristics would be in line with the fact that most motorways are operated without traffic signals. After developing travel time estimation models for motorways first, it is necessary to demonstrate whether the methodologies introduced in this study can be applied to models for other roads.

Range of link geometric features

Roads have their own varying geometric features that are influenced by the terrain where they are located. Although various geometric features for different links could affect travel time estimation, it is necessary to confine the influential features from the viewpoint of traffic demand forecasting to clarify the scope of the study. The measurable factors that could have effects on travel time estimations will be investigated. The condition of "measurable" is very important because this study also aims to develop quantitative feasible models in transport appraisal.

This study focused on the change in three aspects of link geometry, which are tunnel segments, vertical slopes and horizontal curves by referring to the previous studies and manuals that estimate models between the speed and geometric features (Brilon and Bressler, 2004; Cartenì and Punzo, 2007; Kim *et al.*, 2014; DfT, 2018). The scope of geometric features can be described in detail as follows.

Firstly, gradient or curve sections must be clearly one of the considerations for travel time estimation models based on many previous guidelines and studies (Brilon and Bressler, 2004; Cartenì and Punzo, 2007; DfT, 2018). In particular, the geometric features for gradient sections need to be investigated for replacing road capacity because road capacity is affected by the degree of the gradient and its length (USHCM, 2010; MLTM, 2013). On the other hand, lane width and pavement types in this study cannot be identified because most motorway links in South Korea have the same lane width and pavement type.

Moreover, although tunnels could be another influential factor on travel time (Iwasaki, 1991; Koshi *et al.*, 1992; Brilon, 2000; Yun and Shengrui, 2012), the impact of tunnels would not be taken into account as a quantitative variable in travel time estimation models. Many European countries including Norway, Italy and Switzerland, as well as East Asian countries including China and Japan, have many road tunnels. Likewise, Korea has many tunnels because of wide mountainous areas. Overall, 70% of the total area of Korea is covered with mountainous terrain and this terrain has resulted in a large number of tunnels and bridges. According to MOLIT (2016a), tunnels occupy 8.7% of the total Korean motorway length as of 2015. Tunnels would be one of the most unusual environments for drivers because of their enclosed concrete linings or rocks and their different designs and brightness compared with open sections.

Lastly, this study is focusing more on geometric features that can replace FFTT and road capacity in traffic assignment. Although various statistical measures are used to verify the significance of variables (e.g. weather, brightness and day) that are not related to link attributes, they are not quantified in the modelling process. In addition, the current FFTT and road capacity in VDFs do not assume specific situations that could affect travel time estimation. If it is validated to estimate models by quantifying the variables of link geometric features, other variables that could affect travel time are expected to be quantified and added to the models based on the established methodologies.

Consideration of existing VDFs

As mentioned in Section 1.1, this study focuses on travel time prediction in transport appraisal at a macroscopic level. Of the many VDFs already introduced in traffic assignment (Campbell *et al.*, 1959; Smock, 1962; Bureau of Public Roads, 1964; Spiess, 1990; Akçelik, 1991; USHCM, 2000; Dowling and Skabardonis, 2008), only the BPR function is used for modelling and model comparison in this thesis.

Firstly, the BPR function is known to be suitable for travel time prediction on motorways (Kalaee, 2010; Huntsinger and Rouphail, 2011). Secondly, it is also significant to compare the performances of the current VDF and the newly developed estimated models in the selected Korean motorway cases. Currently, the Korean government adopts the BPR function as a VDF for motorways in traffic assignment. Lastly, this study is focusing more on the impact of geometric features and on the development of alternative feasible models rather than the selection of better existing VDFs through the comparison between existing VDF approaches. One of the objectives in this study can be achieved by examining the accuracy of the BPR function to clarify the limitation of FFTT and road capacity. Most VDFs have been developed to more accurately estimate only the relationship between travel time and traffic flow, and little attention has been paid to the impact of FFTT and road capacity (Petrik *et al.*, 2014).

In conclusion, this section suggests three main reasons for a Korean motorway case study, the range of geometric features to be examined, and the need for a consideration of existing VDFs. The detailed methodology can be seen in Chapter 3. Although the research scope needs to be confined in order to clarify the objectives because of practical issues such as data collection, this study has presented methodologies for developing generalised travel time estimation models.

1.5. Structure of the thesis

This thesis consists of eight chapters. The literature review is divided into two chapters. Chapter 2 discusses a theoretical review of traffic assignment in transport appraisal and traffic modelling in traffic assignment comprehensively. In addition, it is investigated that the decisive factors that may affect travel time estimation models in the previous studies. In particular, road capacity and free-flow speed are examined in depth because they are the important factors that motivate this thesis.

Chapter 3 introduces the research methodology to achieve the objectives of this study. The initial case study describe the basis for establishing the methods for travel time model development as well as illustrating the motivation for this research. A large part of the chapter is devoted to explaining the statistical estimation methods for the model development based on the initial data analysis. The uncertainty of road capacity requires alternative variables and statistical estimation methods to overcome the limitations of existing VDFs. Firstly, in order to replace the existing approach that is nonlinear least squares (NLS) estimation, this thesis adopts linear estimation methods including ordinary least squares (OLS) and generalised least squares (GLS) estimation. Moreover, the independent variables of geometric features are suggested to explain travel time for 72 selected motorway links. Lastly, various statistical measures are used to compare the estimated models based on different statistical assumptions and to validate the developed models.

Prior to the feasible model development in traffic assignment, Chapter 4 identifies the influential factors on travel time estimation models. FE modelling by least squares dummy variables is an efficient way to find the explanatory power of each entity as well as to generalise the developed models. In particular, the impact on estimated models by link geometric features is investigated in detail by comparing the estimated models with and without the features.

Chapter 5 shows the modelling results to develop the feasible travel time estimation models for traffic assignment. The OLS linear estimation is used to find appropriate base models by considering the interaction effects and model transformations. The GLS linear estimation is said to be a more advanced approach, reflecting heterogeneity and serial correlation in modelling. In addition to both linear estimations, the NLS estimation with link geometric variables through sensitivity analysis is suggested to minimise the drawbacks of existing approaches.

Chapter 6 selects the most appropriate models to replace the current VDFs from the statistical and practical perspectives. 10-fold cross validation is conducted for verifying the spatial transferability of developed models and various statistical accuracy measures are compared for the selection of the alternative model. This thesis emphasises how the selected model changes the traffic assignment and furthermore transport appraisal. Lastly, Chapter 7 concludes this thesis, suggesting some limitations and required future works.

Chapter 2. Travel Time Estimation Models in Traffic Assignment

2.1. Introduction

This chapter provides the theoretical background to explore the role of traffic assignment in transport appraisal, as well as explaining the theoretical background and potential application of the travel time estimation models to be developed in this thesis. In addition, this chapter reviews existing studies with reference to the road geometry that would affect travel time estimation models in order to find the contributions of this thesis to the knowledge. The contents of this chapter can be summarised in following four ways: an examination of traffic assignment procedures and theories; the theoretical background and utilisation of travel time estimation models; the review of free-flow speed and road capacity; the investigation of the studies about road geometry in transportation.

Section 2.2 examines how traffic assignment play a role in transport economics. In particular, it was scrutinised how traffic assignment have an impact on the benefit estimation in transport appraisal. In addition, this section reviews two main streams in traffic assignment: static traffic assignment (STA), which is the focus of this study, and dynamic traffic assignment (DTA).

After outlining different approaches of travel time estimation models in STA and DTA, Section 2.3 focuses more on a volume-delay function (VDF), which is used as a link cost function in STA, connecting it with the theoretical background of the traffic relationships. In detail, this section investigates the role, principle, overall characteristics and types of VDF including the Korean VDF.

Section 2.4 reviews existing manuals and studies on free-flow speed (FFS) and road capacity because both values are important factors commonly included in VDFs. The unclear definitions of both values are presented in different highway capacity manuals and further different methods for measurements are illustrated from many studies. This study seeks to demonstrate that the uncertainty of both values would affect travel time estimation models.

Section 2.5 introduces the studies that have analysed the effects of road geometry on travel time estimations. Some studies investigate the change in fundamental traffic characteristics on different road geometry such as slopes, interchanges, S-curves, and tunnels. A few studies attempt to develop travel time estimation models using link geometric features.

In summary, based on the literature review, Section 2.6 summarises the research gaps in travel time estimation models from four perspectives: the uncertainty of free-flow travel time and road capacity in existing VDFs; the necessity for the identification of influential factors on travel time; the consideration of link geometric features in travel time estimation models; and the implications for future feasible models.

2.2. Traffic assignment

2.2.1. Traffic assignment from the economic perspective

From general economic perspectives, traffic assignment can be defined as the process that finds the equilibrium points between the marginal cost and benefit across the entire transportation network (Ortúzar and Willumsen, 2012). In practice, traffic assignment can be defined as the process that distributes trip demand between origins and destinations to every link in the entire network (Ortúzar and Willumsen, 2012; Patriksson, 2015). Traffic assignment is one of four steps in traffic demand forecasting or transportation modelling: trip generation, trip distribution, modal split and traffic assignment (KDI, 2008b; Ortúzar and Willumsen, 2012). The output of traffic assignment commonly contains traffic volume and travel times or costs on each link even though its purpose and the detail of cost estimation can vary (Patriksson, 2015).

The traffic assignment model interacts with trip demand, which means it affects trip demand but is also affected by the trip demand (Figure 2-1). Origin-Destination (O-D) trip demand pairs for generating future trip demand, which are initially examined by stated preference surveys and revealed preference information at the base year, are finally verified and calibrated by four steps in traffic demand forecasting (Ortúzar and Willumsen, 2012; MOLIT, 2014; DfT, 2018).

Figure 2-1 Traffic assignment in traffic demand forecasting

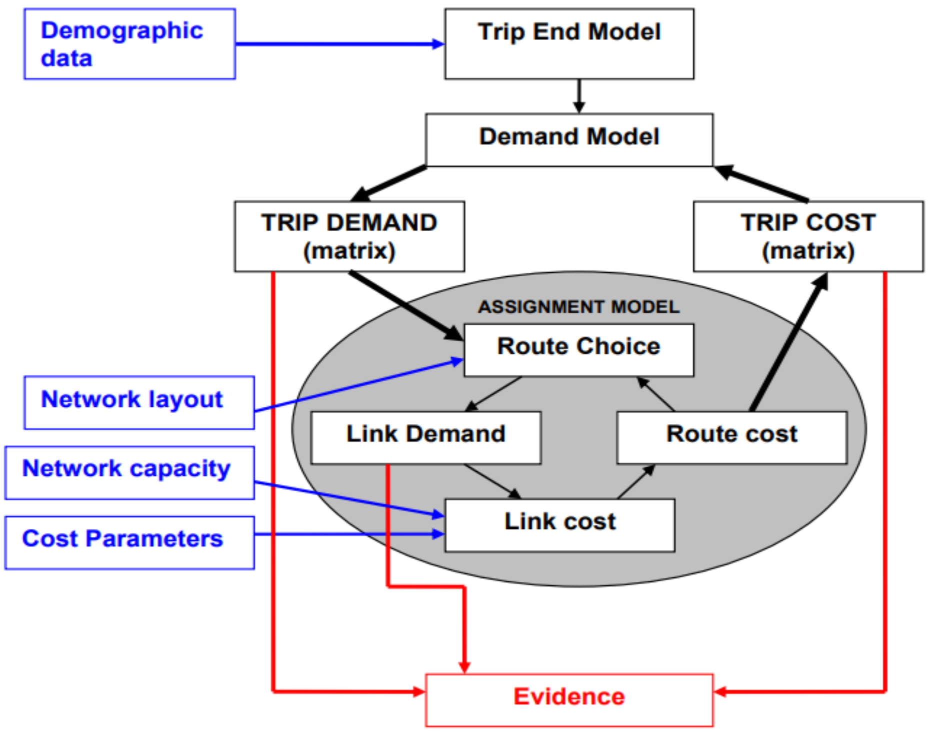

Source: “TAG unit M1-1 principles of modelling and forecasting” in WebTAG (DfT, 2018)

This interaction between traffic assignment and trip demand is connected to the economic theory on user benefits derived from a transport project such as the concept of consumer surplus (Jones, 1977). When demand (e.g. trips) increases from T_0 to T_1 and cost (e.g. travel time) decreases from P_0 to P_1 through an additional supply (e.g. road construction) (Figure 2-2), the change in consumer surplus could be calculated simply using the Rule of a Half (ROH) formula (Equation 2-1). The change by a transport project intervention would be generalised by transport modes such as Equation 2-2 suggested by Sugden (1999). This relationship can be explained in the following two aspects: from the suppliers' perspective, providing additional transport modes or improvement of existing transport modes generates consumer surplus by making existing customers shift from old modes or routes to new ones as well as accommodating newly created demand. From the users' perspective, newly created demand requires additional supply and existing customers can benefit from the additional supply. Traffic assignment is closely related to this demand-supply relationship in that it determines the equilibrium of the relationship based on the cost and benefit estimation.

$$ROH = \frac{1}{2} \times (T^0 + T^1) \times (P^0 - P^1) \qquad \text{Equation 2-1}$$

$$\begin{aligned} ChangeInConsumerSurplus &\approx ROH_m \\ &= \frac{1}{2}\sum_i \sum_j \left(T_{ijm}^0 + T_{ijm}^1\right) \times \left(P_{ijm}^0 - P_{ijm}^1\right) \end{aligned} \qquad \text{Equation 2-2}$$

where T: the number of trips; P: unit cost per trip; and the subscripts of i, j and m: origin, destination and mode (or route) respectively.

Figure 2-2 Change in consumer surplus

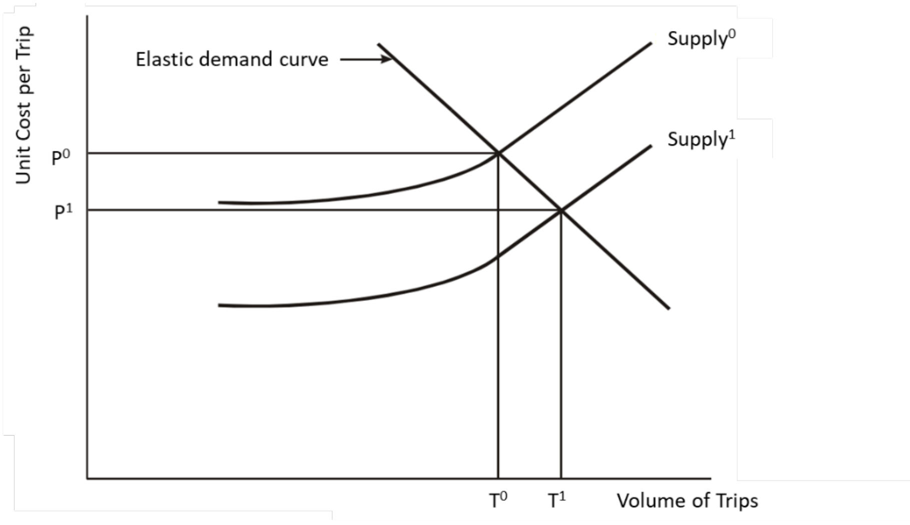

Source: "TAG unit A1.3 user and provider impacts" in WebTAG (DfT, 2018)

2.2.2. Traffic assignment in transport appraisal

Transport appraisal is defined as the feasibility analysis implemented before determining whether to invest in projects (Preston, 2017). Although appraisal includes a qualitative process such as NATA in the UK (Nellthorp and Mackie, 2000), most countries focus more on quantitative results such as cost-benefit analysis (CBA) by which a project can be implemented if benefit exceeds the total cost (Appendix A.2.1). In governmental affairs, CBA is used to justify governmental intervention in a market (Boardman *et al.*, 2013). CBA can be divided into several phases: establishing alternatives, cost and benefit identification, monetisation of value, comparison through sensitivity analysis, and conclusion (Hanley and Spash, 1993; Boardman *et al.*, 2013). More specifically, traffic assignment contributes to cost and benefit identification by simulating the changes in allocated traffic and total travel time across the entire transport network.

The impact of traffic assignment on the benefit estimation

Traffic assignment crucially affects the estimation and valuation of benefit in CBA. As an example of CBA in the UK, WebTAG (DfT, 2018) include travel time savings and vehicle operating costs as impacts on economic efficiency (Table 2-1) and defines environmental impacts including noise, air pollution and greenhouse gasses (Table 2-2). Most of these impacts are predicted based on the traffic flows or travel time (average speed) on each link derived from traffic assignment (see detail in Appendix A.2.2).

Table 2-1 Values of travel time savings (VTTS) and vehicle operating cost (VOC)

<table>
<tr><th colspan="2">Impact</th><th>Methodology of Valuation</th><th>Marginal monetary values</th></tr>
<tr><td rowspan="2">VTTS</td><td>Working time</td><td>- Willingness-To-Pay (WTP)
- Cost Saving Approach (CSA)</td><td>- Car and rail employer's business only:
$VTTS = \frac{U}{\left(1 + e^{\frac{x_{mid}-D}{k}}\right)}$
(U, X_{mid}, k: parameters; D: travel distance)
- Other working time: suggested in TAG Data Book</td></tr>
<tr><td>Non-working time</td><td>WTP</td><td>- Commuting: 9.95 £/hour
- Other: 4.54 £/hour</td></tr>
<tr><td rowspan="2">VOC</td><td>Fuel operating costs</td><td>National Atmospheric Emissions Inventory (NAEI)</td><td>The fuel cost function:
$L = (a + b \cdot v + c \cdot v^2 + d \cdot v^3) / v$
(L: fuel costs; v: speed; a, b, c, d: parameters)</td></tr>
<tr><td>Non-fuel operating costs</td><td>TAG Data Book</td><td>Non-fuel operating costs function
$C = a1 + b1/V$
(C: non-fuel cost; V: speed; a1, b1: parameters)</td></tr>
</table>

Source: Adapted from “TAG unit A1.3 user and provider impacts” in WebTAG (DfT, 2018)

Table 2-2 Environmental impact appraisal on noise, air quality and greenhouse gases

Impact		Quantification or Estimation
Noise		Dependent on a distance, layout, traffic flow and average speed (DMRB 11.3.7)
Air Quality	Local Air Quality: PM10, NO2	Dependent on daily traffic flow, heavy duty vehicles and speed change (DMRB 11.3.1)
	Regional Air Pollution: NOx, CO2	
Greenhouse Gases		Related to fuel consumption prediction by vehicle types

where DMRB is the UK design manual for roads and bridges

Source: Adapted from “TAG Unit A3 Environmental Impact Appraisal” in WebTAG (DfT, 2018)

Equilibrium principles

Traffic assignment aims to allocate link flows from constant O-D pairs during the analysis period and to estimate link and network travel costs mainly with reference to three issues: multiple user classes, stochastic effects and congested equilibrium (Table 2-3). The first issue is caused from the different individual perceptions of benefits and costs. The second one is related to the unreasonable route choices that result from the level of cost information. These two issues are ignored in some cases of traffic assignment (Ortúzar and Willumsen, 2012), even though it is possible to approximate effects by multiple user classes (Leurent, 1998). In comparison, the last issue has been recognised as a basic assumption in most cases of traffic assignment for a long time (Ortúzar and Willumsen, 2012).

Table 2-3 Classification of traffic assignment by equilibrium principles

		Stochastic effects included?	
		No	Yes
Single user class	No capacity restraint	All-or-nothing	Pure stochastic: Dial’s, Burrell’s
	With capacity restraint	Wardrop’s equilibrium	Stochastic user equilibrium SUE
Multiple user classes	No capacity restraint	All-or-nothing with multiple user classes	Multiple user classes stochastic: Dial’s, Burrell’s
	With capacity restraint	Wardrop’s equilibrium with multiple user classes	Stochastic user equilibrium with multiple user classes

Source: Ortúzar and Willumsen (2012)

The widely used principle for explaining congested equilibrium in traffic assignment is Wardrop (1952)'s first principle (Correa and Stier-Moses, 2010) as:

> *"The journey times on all the routes actually used are equal, and less than those which would be experienced by a single vehicle on any unused route."*

Later, this principle has become known more formally as:

> *"Under equilibrium conditions traffic arranges itself in congested networks in such a way that no individual trip maker can reduce his path costs by switching routes."*

The first principle has been used by transportation planners for a long time and is still used today for finding the equilibrium across the entire network. The principle assumes that each user selects routes in order to minimise the cost of travel and unselected routes have more cost than those selected. Most transport modelling packages including TRANSCAD, EMME and VISUM adopt this principle for their assignment function even though their algorithms for convergence to equilibrium vary based on Frank and Wolfe (1956)'s method (Correa and Stier-Moses, 2010).

Limitations of traffic assignment

Ortúzar and Willumsen (2012) defined two basic components in traffic assignment: a trip matrix and a network including links and their properties. In comparison with economic theory, a trip matrix can represent demand and a network can represent supply. In detail, a trip matrix can be derived from O-D pairs, which is usually divided into peak and off-peak hour matrices. With regard to a network, commonly accepted generalised individual costs on every link are travel time and distance even though there could be other costs such as congestion, scenery, signposting, type of road, road works.

Ortúzar and Willumsen (2012) also summarised the limitations of traffic assignment in the following aspects; the inaccurate node-link model of a network; the individual difference and definition error of perceived costs; imperfect information about costs; trip demand dynamics; and the imperfect estimation of travel time and input errors. In particular, they pointed out the problem that link-cost function generally includes only the relationship between travel time and traffic flow and asserted that conventional functions need to be improved.

2.2.3. Two classifications of traffic assignment

According to the level of detail, traffic assignment methods can generally be divided into two groups: static and dynamic traffic assignment (Saw *et al.*, 2015). The difference between the two methods starts from the detail or dynamics of demand and cost as can be inferred from their names. The two methods have different purposes and ranges. Static traffic assignment (STA) is used for appraising overall future traffic changes in traffic flows and travel time in the entire network, whilst dynamic traffic assignment (DTA) is more interested in the details of vehicle's individual movements by inputting the diverse traffic patterns. Accordingly, STA tries to focus more on traffic loading and to find the impact on the entire network with the result that many countries are using it for feasibility analysis in respect of long-term transport projects from a wider perspective than DTA. By contrast, DTA puts more weight on present traffic patterns and thus it is used for comparatively short-term improvement of systems such as the improvement of junction structure, ramp-metering and road pricing.

Static traffic assignment (STA)

STA is a traffic flow allocation method that does not consider the instantaneous change in trip demand but analyses for a relatively long period. O-D pairs are suggested as average daily traffic without the detailed variation of traffic flow over different time period or slices (MOLIT, 2014; DfT, 2018). In particular, the daily traffic can be divided into traffic flow over a number of time periods (e.g. peak and off-peak) according to the detail or the purpose in the assignment model (DfT, 2018). For example, daily traffic flow based on the actual peak-hour traffic can be decided differently depending on countries and local regions (Weijermars and van Berkum, 2004).

Another characteristic of STA is to admit that traffic flow can exceed road capacity while not considering congestion effects such as spillback and queuing even though it is impossible in reality. The dashed line in the left diagram of Figure 2-3 shows the real congestion, but the dashed line in the right diagram assumes the relationship between congested travel time and trip demand, not traffic flow. It can be also rationalised because of the practical reason for the computational iterative process, i.e., one value of traffic flow corresponds to one value of travel time.

Figure 2-3 Typical speed–flow (left) and cost–flow (right) relationship in STA

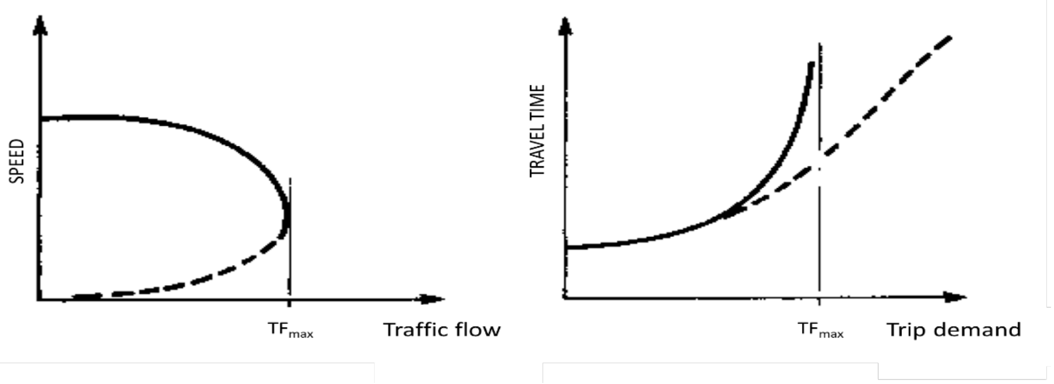

Source: Ortúzar and Willumsen (2012)

Saw *et al.* (2015) categorised STA into six groups by its method of assignment: “All or Nothing Assignment”, “Stochastic traffic assignment”, “Capacity Restrained Assignment”, “Incremental Assignment”, “User Equilibrium (UE) Assignment”, and “System Optimum (SO) Assignment”. Of these methods, UE and SO assignments are the most widely used methods in transport planning because they can reflect Wardrop (1952)’s principles which was referred to earlier.

Sheffi (1985) illustrated the mathematical formulation for programming. Based on the UE principle that all travellers try to minimise the travel time to their destination, he suggested the objective formulation by using Beckmann *et al.* (1956)’s transformation as follows:

$$\min . z(x) = \sum_a \int_0^{x_a} t_a(w)\, dw$$

subject to $\sum_k f_k^{rs} = q_{rs} \quad \forall\, r, s$ (Flow conservation constraints)

$f_k^{rs} \geq 0 \quad \forall\, k, r, s$ (Non-negativity constraints)

$x_a = \sum_r \sum_s \sum_k (f_k^{rs} \cdot \delta_{a,k}^{rs}) \quad \forall\, a.$

where x_a is flow on arc (a), t_a is travel time on arc (a), f_k^{rs} is traffic flow on path (k) connecting O-D pair (r - s), c_k^{rs} is travel time on path (k) connecting O-D pair (r - s), q_{rs} is trip rate between origin (r) and destination (s), and $\delta_{a,k}^{rs}$ is an indicator variable (1 if arc(a) is on path (k), 0 otherwise). The objective formulation is derived by the integrals of the relationship between travel time and traffic flow on each arc. In the formulation, $t_a(x_a)$ is a link performance function, which is also called a volume-delay function or a link cost function. The objective formulation can be solved by using the Lagrangian method for satisfying the first order condition (equivalency conditions) of Beckmann *et al.* (1956)’s transformation as follows:

$$\begin{aligned} f_k^{rs}(c_k^{rs} - u_{rs}) &= 0 && \forall\, k, r, s \\ c_k^{rs} - u_{rs} &\geq 0 && \forall\, k, r, s \\ \textstyle\sum_k f_k^{rs} &= q_{rs} && \forall\, r, s \\ f_k^{rs} &\geq 0 && \forall\, k, r, s \end{aligned}$$

where u_{rs} is the O-D specific Lagrange multiplier and c_k^{rs} is $\sum_a t_a \cdot \delta_{a,k}^{rs}$, which is the sum of travel times of all arcs on path (k) connecting O-D pair (r – s). In addition, in order to satisfy the uniqueness condition of Beckmann *et al.* (1956)’s transformation, the objective formulation should be strictly convex in analysed traffic flows (Sheffi, 1985). The convex condition can be proved by the Hessian derivatives of $z(x)$. In addition, the objective function has a unique solution because $z(x)$ is the integrals of a link performance function and link performance functions have continuously non-decreasing curves (Ortúzar and Willumsen, 2012).

On the other hand, the SO assignment has a different objective formulation because it aims to minimise the total travel time experienced by all vehicles in the entire network. Other constraints and conditions such as flow conservation, non-negativity, equivalency and uniqueness are the same as for the UE assignment. The objective formulation can be set up as follows:

min. $z(x) = \sum_a x_a \cdot t_a(x_a)$

The objective formulation can be solved as follows:

$$f_k^{rs}(\tilde{c}_k^{rs} - \tilde{u}_{rs}) = 0 \qquad \forall\, k, r, s$$
$$\tilde{c}_k^{rs} - \tilde{u}_{rs} \geq 0 \qquad \forall\, k, r, s$$
$$\sum_k f_k^{rs} = q_{rs} \qquad \forall\, r, s$$
$$f_k^{rs} \geq 0 \qquad \forall\, k, r, s$$

where $\tilde{u}_{rs}$ is the Lagrange multiplier and $\tilde{c}_k^{rs}$ is $\sum_a \left[t_a(x_a) + x_a \frac{dt_a(x_a)}{dx_a}\right] \cdot \delta_{a,k}^{rs}$. As mentioned in Section 2.3.1, these principles can be used in some DTA models.

Dynamic traffic assignment (DTA)

DTA has been devised for supporting various considerations about the instantaneous or periodic change in demand and supply reflecting the diversity of human behaviours and traffic systems (Peeta and Ziliaskopoulos, 2001). Although much literature has referred to DTA models since the work of (Merchant and Nemhauser, 1978), the common characteristic of the models is that DTA deals with the interaction between route choice and predicted travel times as recognised by travellers (Chiu *et al.*, 2011). In terms of the interaction, DTA models focus more on congestion because the interaction is assumed to hardly happen in steady-state conditions. To reflect as close a correlation between congestion and reality, DTA follows the capacity constraints that actual traffic flows cannot exceed capacity strictly (Heydecker and Addison, 2005).

Chiu *et al.* (2011) divided general iterative DTA algorithmic procedure into three parts: network loading, path set update and path assignment adjustment (Figure 2-4). The first is the process that evaluates time varying cost (travel times) depending on vehicles loaded on each route (or link) at the previous interval of time. The second is the process that selects the cheapest (fastest) routes depending on every O-D pair and departure time. The last is the process that finds equilibrium in the analysed network. After the last process, the three steps are repeated until a given criterion is satisfied. In particular, many researchers have tried to study the network loading step, which is the main concern of DTA. Chiu et al. (2011) divided the network loading step into two main approaches, which are analytical and simulation-based, and Peeta and Ziliaskopoulos (2001) again subdivided analytical approaches into three groups: mathematical programming, optimal control and variational inequality formulations. They mentioned that the three groups have different characteristics. Mathematical programming models set the analysed time discretely. By contrast, optimal control models assume continuous O-D or link flows. Lastly, variational inequality models can explain the equilibrium about various DTA problems such as asymmetric link interaction (Nagurney, 1998), departure time (Friesz et al., 1993), exit flow function (Wie et al., 1995), link inflow-only function (Chen and Hsueh, 1998). Ortúzar and Willumsen (2012) emphasised that variational inequality models are the most practical of the models. Mitsakis et al. (2011) found that there are several DTA models reflecting the assumptions of STA models while categorising DTA models in detail.

Figure 2-4 General DTA algorithmic procedure

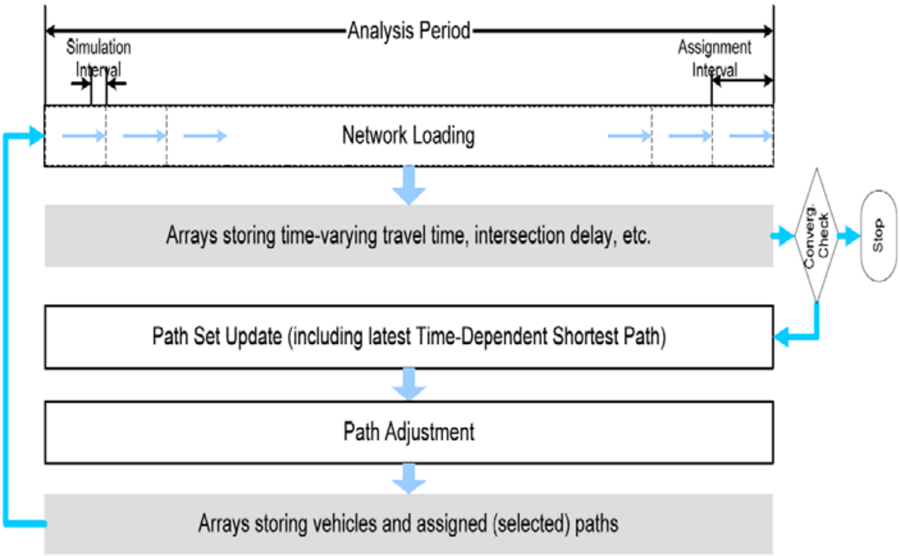

Source: Chiu *et al.* (2011)

In summary, DTA models can offer time-dependent results with more focus on levels of congestions. According to Chiu *et al.* (2011)'s investigation, DTA models were mainly applied to management or operation areas such as corridor management, network disruption, incident or emergency management, urban traffic management, ITS evaluation, HOV-HOT lane operation, congestion charging, air quality analysis and network reliability estimation. In these applications, DTA models estimate different detailed levels of outputs related to time and analysed network level. The models provide time-dependent travel times, travel distances, stop times at network level as well as time-dependent travel times, speeds, densities, queues and stop times at link level.

Comparison between STA and DTA

The difference between STA and DTA can be summarised using one word: "time-dependence". Although intermediate models do exist between them in that some DTA models borrow some STA assumptions, the basic rational behind DTA is to estimate traffic results changing every time interval or continuously during the analysed period. By contrast, STA does not consider change of time-dependent demand and supply (or cost) much even though O-D pairs can be divided into peak and off-peak hours.

Based on literature (Peeta and Ziliaskopoulos, 2001; Chiu *et al.*, 2011; Ortúzar and Willumsen, 2012), other characteristics of STA and DTA can be compared as in Table 2-4. Most of the differences start from the consideration of time-dependence from demand and supply perspectives. A notable difference between STA and DTA is the assumption about queuing conditions. Queuing or congestion on a link is closely related to traffic inflow and outflow. Since STA always assumes that inflow is the same as outflow on a link, queuing conditions are not allowed in STA and congestion is defined as volume exceeds capacity. Instead, DTA can explain congestion and queuing such as spillback by formulating the relationship between inflow, the number of vehicles on a link and outflow. However, the different approaches do not have big variations in steady-state conditions because inflow would be almost the same as outflow. For example, in DynaMIT, which is one of DTA models, Ben-Akiva et al. (1998) assumed that the average speed is constant in the moving part while one of the queuing models is applied to the queuing part after dividing an analysed section into moving and queuing parts.

Table 2-4 Comparison between STA and DTA

Category	STA	DTA
Applied areas	New road construction	Operation and management
Equilibrium	Precisely convergent	Sometimes disequilibrium happens
Usage	Used practically	Used for special purposes
Network size	Larger	Smaller
Computational time	Faster	Slower
Demand	Constant	Variable
Period	Long	Short or mid-term
Inflow and Outflow	Always same	Different in congestion
Congestion	Less focus on congestion	More focus on congestion
Capacity constraint	Defined virually (Volume can exceed capacity)	Defined close to reality (Volume cannot exceed capacity)
Queuing condition	Cannot explain	Try to explain (e.g. spillback effect)
Assumption of FIFO	Always follow	Consider overtaking in some models
Lane-based effects	Not consider	Consider in some models

2.2.4. Implication to thesis

Section 2.2 reviewed that traffic assignment is a process for finding the equilibrium of a network based on supply-demand relationships from the broad perspective of transport economics. Traffic assignment is not only the output for the equilibrium, but also the input for the estimation of costs and benefits in transport appraisal. Moreover, according to the time-dependency, it can be classified into static traffic assignment (STA) and dynamic traffic assignment (DTA), the different features of which are shown in Table 2-4. Whilst STA approximates some traffic effects in the process of finding the equilibrium, DTA takes into consideration the more detailed interaction between vehicles or groups of vehicles.

In summary, it can be said that STA is more suitable for transport appraisal[2] that analyses the feasibility of a long-term (e.g. 30 years or more) investment than DTA, most of which targets the equilibrium at a microscopic level. Although DTA is used for the feasibility analysis that focuses on the short-term improvement of a local transport network such as the intersection structure, traffic signals and lane controls, it would be not easy to take into account the time-dependency for a long-term appraisal. Since this study aims to improve the reliability of the current long-term transport appraisal, this study focuses more on STA in terms of how geometric features affect travel time estimation on relatively long links from a macroscopic perspective.

[2] Cost-benefit analysis (CBA) as one of transport appraisals is examined in Appendix A.2 and A.3.

2.3. Travel time estimaiton models

2.3.1. Theoretical background for traffic modelling

Travel time estimation in STA

A link cost function, which is called VDF in STA, is closely related to classic traffic flow theory. In the traffic flow theory, Equation 2-3 is based on the relationship between three key factors, which are traffic flow (q), density (k), and traffic speed (u) with the assumption that all vehicles move at the same speed (Bell *et al.*, 1997).

$$q = ku \qquad \text{Equation 2-3}$$

Based on this equation, Figure 2-5 shows the empirical relationships between three factors. The curves would start the linear relationship (Figure 2-5c, Equation 2-4) between speed and density, which was suggested by Greenshields *et al.* (1935):

$$u = u_f \left(\frac{k_j - k}{k_j} \right) \qquad \text{Equation 2-4}$$

in which u_f is the free-flow speed and k_j is the jam density.

Figure 2-5 Flow-density, speed-flow, and speed-density curves

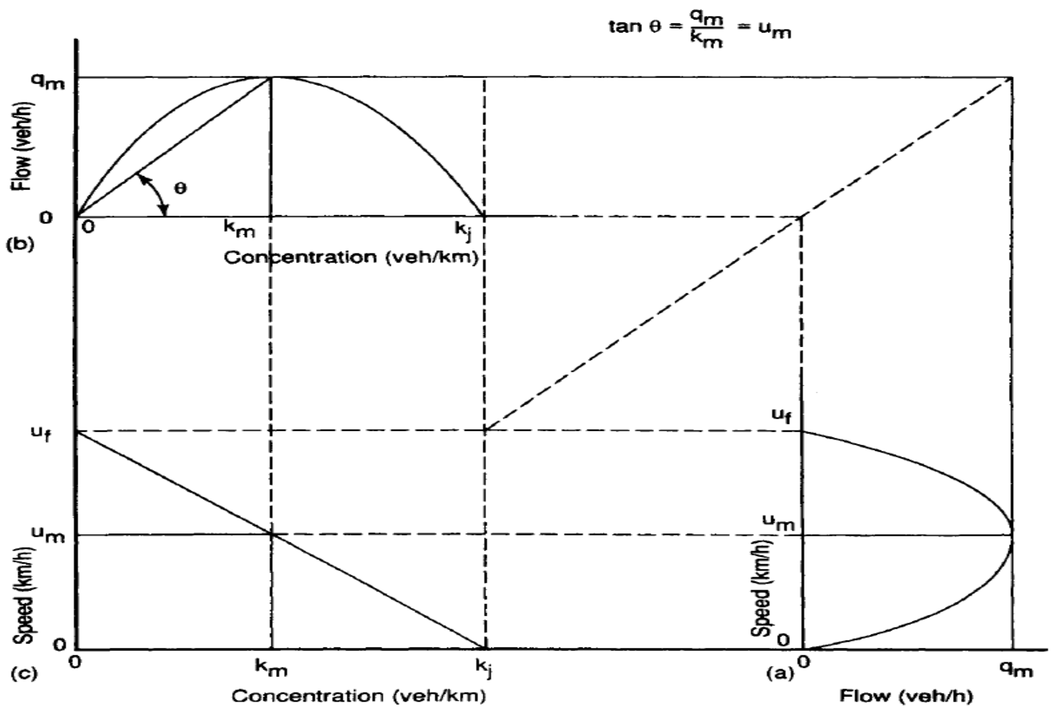

Source: Bell *et al.* (1997)

Combining Equation 2-3 and Equation 2-4, the relationship between flow and density, and between speed and flow are derived as in Figure 2-5b and Equation 2-5, and in Figure 2-5a and Equation 2-6 respectively. In addition, the maximum value of traffic flow, which is defined as the road capacity, is derived when the derivative of Equation 2-6 is equal to zero (q_m in Figure 2-5a). The average speed used for the relationships is space mean speed, but practically time mean speed could be used in many countries because of its simple calculation.

$$q = ku_f\left(\frac{k_j - k}{k_j}\right) \quad \text{Equation 2-5}$$

$$q = k_j\left(1 - \frac{u}{u_f}\right)u \quad \text{Equation 2-6}$$

The Greenshields *et al.* (1935)'s relationships can be applied to VDF after transforming the relationship corresponding to traffic flow over capacity for approximating congestion states like the right dash-dotted line in Figure 2-6. The approximation of traffic flow over road capacity, which is actually equivalent to trip demand, can be allowed in STA because there would be little theoretical backgrounds of the trip demand over road capacity (Nielsen and Jørgensen, 2008; Manzo *et al.*, 2013). Greenberg (1959) and Underwood (1961) suggested that the relationship between speed and density would be defined as logarithmic and exponential function respectively. Rakha and Crowther (2002) compared three types of fundamental diagram, which are the Pipes (1953)'s triangular, the Greenshields *et al.* (1935)'s parabolic, and the Van Aerde (1995)'s diagram, by using microscopic simulation models of CORSIM and VISSIM (Figure 2-7). In addition, Kerner (2009) derived the different relationships between traffic flow and density in free-flow and congested conditions respectively from three-phase theory (Figure 2-8). Likewise, Yousif (2009) proposed two-regime relationship between flow and density based on HCM (Figure 2-9).

Figure 2-6 Practical change of the speed-flow relationship

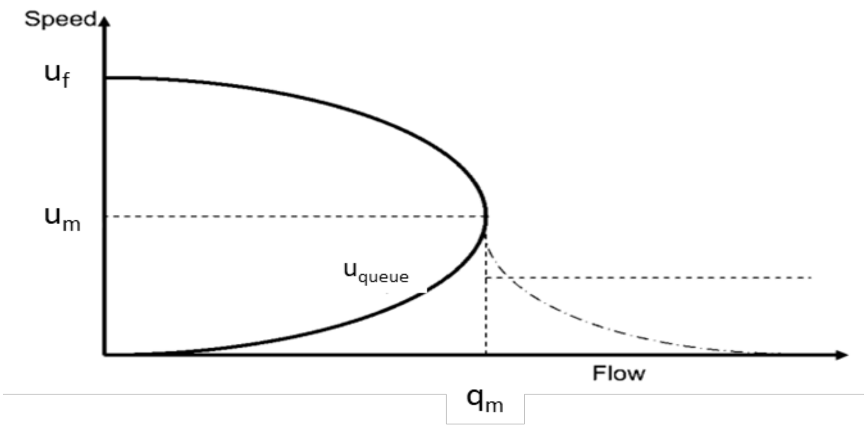

Source: Nielsen and Jørgensen (2008)

Figure 2-7 Comparison of three flow-density diagrams

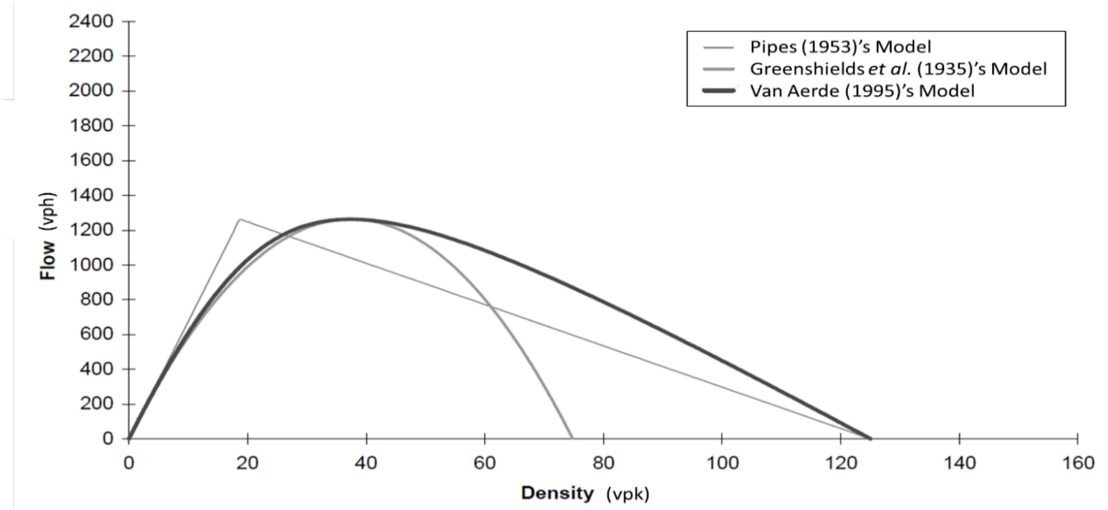

Source: Rakha and Crowther (2002)

Figure 2-8 Relationship between flow and density in free-flow (F) and jam (J) conditions

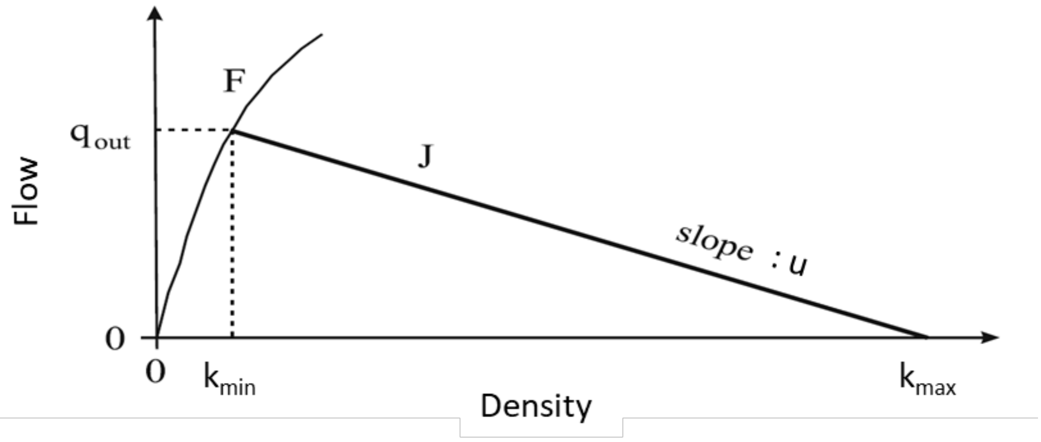

Source: Kerner (2009)

Figure 2-9 Two-regime relationship between flow and density

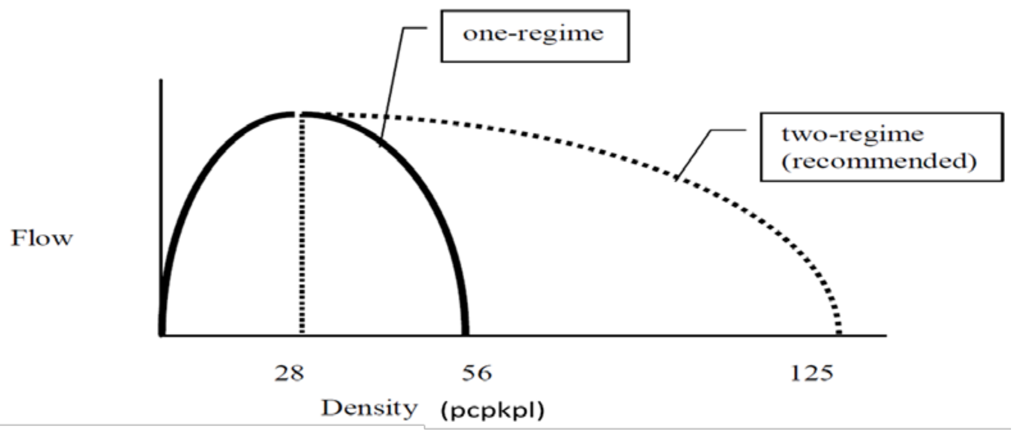

Source: Yousif (2009)

Travel time estimation in DTA

The travel time estimation of an individual vehicle in DTA would not be given much emphasis because DTA takes it into consideration in the process of traffic modelling. Rakha and Tawfik (2009) divided the traffic modelling of DTA into two approaches: analytical modelling and simulation-based modelling. The first approach can be explained as transitional modelling from STA to DTA and it follows theoretical methods of STA mostly. By contrast, the second approach focuses on describing the interaction between vehicles. Peeta and Ziliaskopoulos (2001) explained that simulation-based models can be appropriate for simulation itself or reproduction rather than problem solving by analytical formulation. In other words, travel time estimation is clearer in analytical modelling rather than in simulation-based modelling.

Analytical modelling in DTA assumes that each time interval, which is sliced from the analysed period, has static traffic conditions (Rakha and Tawfik, 2009). In other words, static UE and SO principles as explained in Section 2.2.3 can also be used within the time interval by using standard mathematical static formulation even in analytical modelling in DTA. In addition, the time intervals in analytic modelling are comparatively long similar to STA but different from microscopic simulation-based modelling in DTA. Therefore, it is possible that link cost functions in STA can also be used in analytical modelling in DTA.

As mentioned earlier, simulation-based modelling emphasizes the interaction between vehicles more than analytical modelling does. The interaction can be affected by various traffic environments such as opposing traffic flows, leading vehicles, and signal operation. Rakha and Tawfik (2009) refer to the history of simulation-based modelling. Early models such as SATURN introduced the concept of platoons using 15-30 minutes time intervals, but did not consider congestion patterns such as upstream spillback. Intermediate simulation-based models such as CONTRAM introduced the concept of packets, which are the groups with the same traffic characteristics; and assigned traffic by considering the travel time of previous packets. However, this model is also unable to reflect the possibility of vehicles queuing on links. The recent DTA simulation-based models are more microscopic than the past ones. The models consider car-following, vehicle instantaneous acceleration and lane-changing with an additional function of fuel consumption or emissions at second time intervals. Whilst it is debatable whether microsimulation-based models can explain empirical spatio-temporal data (Rakha and Crowther, 2002; Kerner, 2009), macroscopic and mesoscopic models follow the fundamental relationship between flow and density or are in line with a user specified relationship (Rakha and Tawfik, 2009). Hoogendoorn and Bovy (2001) defined the category of a microscopic, mesoscopic and macroscopic model more clearly depending on three levels of detail relating to analysed units: individuals, traffic entities and aggregated groups respectively.

In addition, Kerner (2009) suggested "Three-Phase Traffic Theory", which means that the traffic state would be divided into free flow, synchronised flow, and wide moving jams (synchronised flow does not always appear). He defined the wide moving jam as having the characteristic that the outflow speed has a small range at the downstream front of the jam. By contrast, the synchronised flow would have an outflow speed that fluctuates greatly (Figure 2-10). He also explained that the synchronised flow could happen to the upstream of a bottleneck. The synchronised flow or the breakdown flow in this study would provide a clue as to whether link geometric features would act as bottlenecks and where a detailed bottleneck point is located.

Figure 2-10 Three traffic phase based on the spatiotemporal measurement

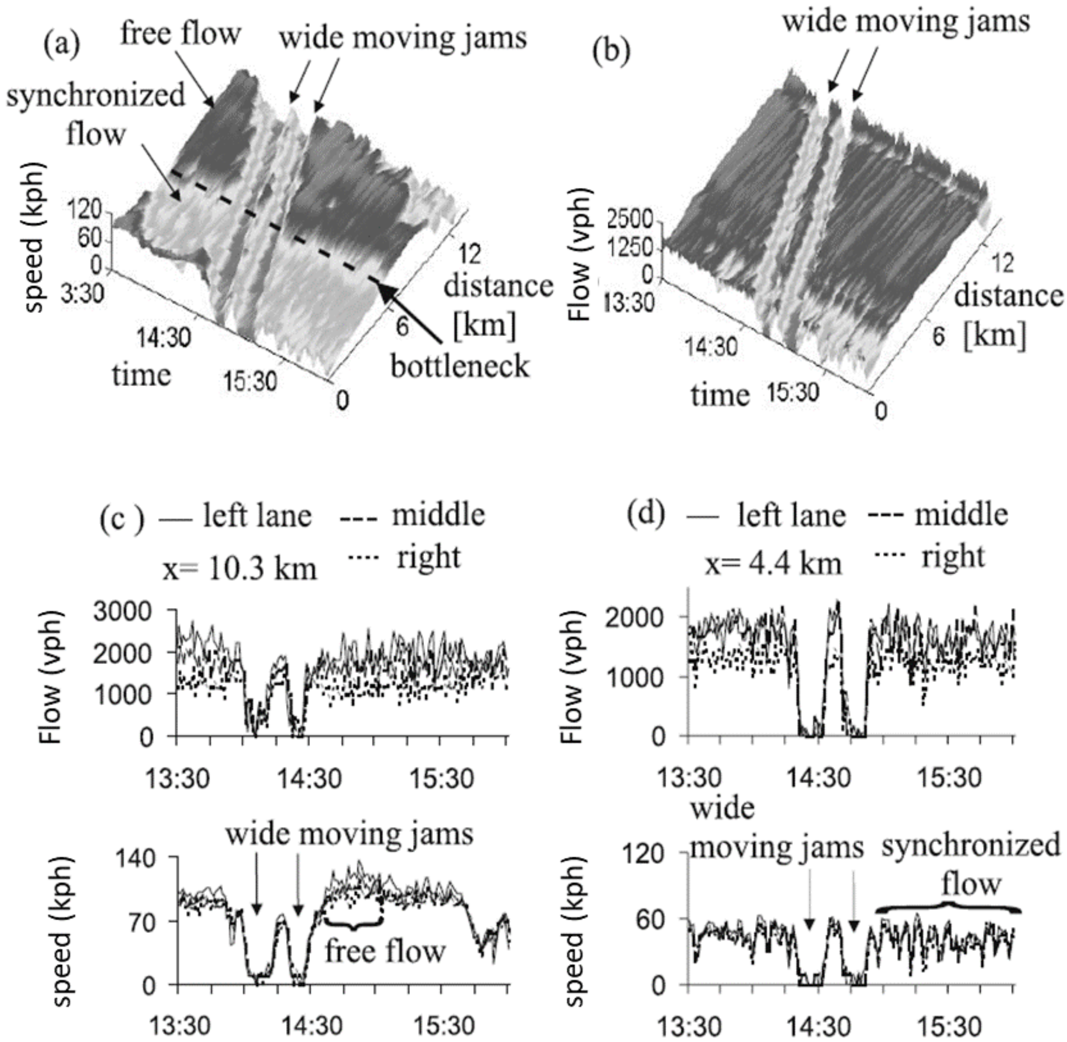

Source: Kerner (2009)

2.3.2. Volume Delay Function (VDF)

Role of VDF

VDF is a function to calculate travel time (or costs) dependent on trip demand and it is generally used in STA at a macroscopic level as mentioned above. VDF affects the route selection with relation to the amount of travel time taken on links consisting of routes connecting journey origins to destinations. VDF is the base formulation to follow the assignment principle such as the Wardrop (1952)'s first principle that road users select the route to minimise their travel time independent of other users in traffic assignment. When searching for the routes to minimise travel time, each analysed unit link would be recognised as an impedance with cost. Therefore, VDF plays an essential role in traffic assignment, because road user's selection could not be modelled without VDF. Moreover, it is very important because almost all benefits in CBA are calculated by travel time, total vehicle kilometres and their speed based on assigned traffic flows on each link (see Appendix A.2.2 and A.3.3)

Principle of VDF

Branston (1976) explained the principle of VDF including the detailed changes in travel time and traffic volume of a link dependent on the time of day, the concept of the "steady state" condition, and the measurement of road capacity.

The overall road capacity that plays a crucial role in travel time estimation would depend on the minimum capacity over a link. It could be naturally measured in a bottleneck section by taking account for the fact that the capacities of all sections that consist of a link cannot be equal. The simplified traffic characteristic could be explained as an example of a link AB assuming that the direction of traffic flow is A to B and that the capacity at node A is higher than that at node B (Branston, 1976). When trip demand increases over the capacity of the link, queues would be formed from the upstream of node B and the maximum traffic flow cannot exceed the capacity at node B, which is the minimum road capacity of the link (Figure 2-11).

Figure 2-11 Example of flow variation on link AB dependent on the trip demand

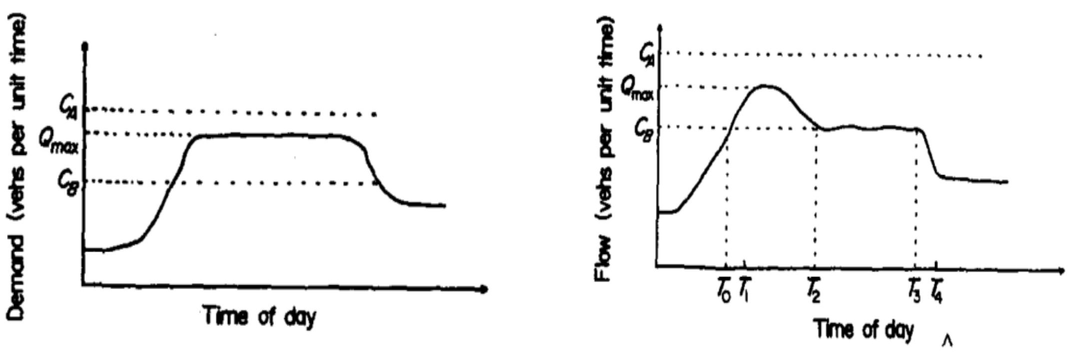

In addition, Branston (1976) mentioned how to use the road capacity in VDFs, which is classified into the steady-state capacity and the practical capacity. The former is the capacity in the steady-state condition that could be supported by the above-mentioned traffic pattern, and it could be the road capacity at the node that could become a bottleneck point. On the other hand, the latter uses traffic flow at the level of service (LOS) D or E, which could be measured at a random point. Therefore, it is closer to the principle of VDF to use the steady-state capacity rather than the practical one. However, it would be difficult to measure the steady-state capacity as demonstrated in the initial case study (Section 3.2). The initial case study attempted to identify the steady-state capacity by introducing different criteria of road capacity at inductive loop detectors having relatively short intervals.

Characteristics of VDF

Ortúzar and Willumsen (2012) suggested the following five characteristics of VDF: realism; non-decreasing and monotone; continuous and differentiable; the existence of traffic flow over road capacity; and easy transferability (Figure 2-12). Of these characteristics, the non-decreasing and monotone condition would be clear based on fundamental traffic theory which was referred to earlier. In addition, to satisfy the fundamental principle of traffic assignment, VDF needs to be not only continuous and differentiable but also convex mathematically. Taking the example for Wardrop (1952)'s principles, the convex condition is necessary to minimise the objective functions (Section 2.2.3) as their first and second derivatives are non-negative (Sheffi, 1985; Ortúzar and Willumsen, 2012). In particular, the condition of a convex function is regarded as very important for the base and feasible model selection in the research methodology (Chapter 3) and the model estimation (Chapter 5). Ortúzar and Willumsen (2012) mentioned that the convex condition is satisfied when the line connecting two points on an examined curve lies above or in the curve (Figure 2-13(a) and (b)).

Figure 2-12 Difference between theoretical and practical relationship

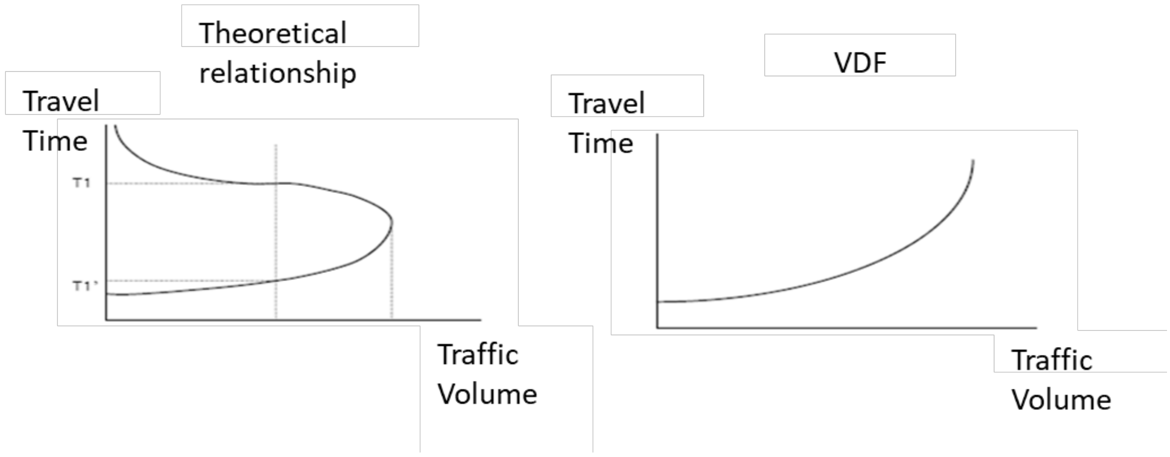

Source: KDI (2015)

Figure 2-13 Convex and nonconvex function

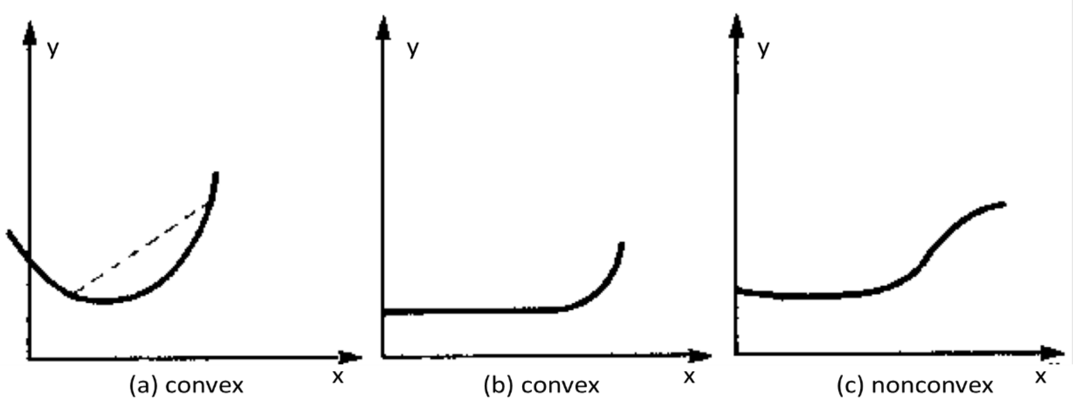

Source: Ortúzar and Willumsen (2012)

Types of VDF

Branston (1976) and Petrik *et al.* (2014) suggested that various functions have been developed in a number of different countries, but there has been little consensus about which function is the most appropriate in the traffic assignment. They asserted that countries with different road environments, demographics and economic characteristics have selected one or more of the VDFs. Branston (1976) classified types of VDF into mathematical and theoretical approaches. Whilst the former is simply defined based on the relationship between observed journey speed and flow without the suggestion of link characteristics, the latter is estimated by introducing the variables of the various network characteristics such as signal (spatial and time) intervals and lane widths and as such it requires more information about the network. Therefore, mathematical functions could not be easily modified without verifying the parameters used in the function. This means that the mathematical forms could not be used for explaining different network characteristics.

In addition, VDFs can be classified into a single equation and multiple equations depending on the level of traffic flows (KDI, 2015). VDFs made up of multiple equations, which are generally composed of two functions, express the relationship by using different functions before and after congested situations. Tipping points would be formed when TF/C reaches a certain level of traffic flow and travel time would increase dramatically after this point. For example, Campbell *et al.* (1959) suggested the two equations for the traffic assignment (Equation 2-7) which has a tipping point when TF/C becomes 0.6. Most VDFs which utilise multiple equations need to be continuous at tipping points between equations.

$$TT = TT_0 \qquad \text{for} \quad TF/C \leq 0.6$$

$$TT = TT_0 + \alpha\left(\frac{TF}{C} - 0.6\right) \qquad \text{for} \quad TF/C > 0.6$$

Equation 2-7

where TT: travel time (TT_0: free-flow TT); TF: traffic flow; C: road capacity; α: parameter.

For developing travel time estimation models in this study, it is necessary to verify the availability of existing functions. Petrik *et al.* (2014) reported that the exponential function (Smock, 1962), the BPR function (Bureau of Public Roads, 1964) and its modifications, and the conical function (Spiess, 1990) have been widely used recently. Smock (1962) suggested the curvilinear function (Equation 2-8) for Detroit, USA by using an average of the intersection capacities without parameters. Spiess (1990) tried to overcome the limitation that other VDFs could show in predicting the travel time of congested links (Equation 2-9).

$$TT = TT_0 \, exp[TF/C] \qquad \text{Equation 2-8}$$

$$TT = TT_0 \left(2 - \beta + \alpha \left(1 - \frac{TF}{C}\right) + \sqrt{\alpha^2 \left(1 - \frac{TF}{C}\right)^2 + \beta^2} \right) \qquad \text{Equation 2-9}$$

where α is larger than 1, and $\beta = {(2\alpha - 1)}\big/{(2\alpha - 2)}$.

Davidson (1978) tried to overcome the limitation of VDF that cannot express the trip demand over road capacity by adding queuing theory to the function (Equation 2-10).

$$TT = TT_0 \left(1 + \frac{J_d \cdot \frac{TF}{C}}{(1 - \frac{TF}{C})} \right) \qquad \text{Equation 2-10}$$

where J_d is delay parameter (time per unit distance).

Akçelik (1991) proposed another type of time-dependent travel time function based on Davidson's function as follows:

$$TT = TT_0 + 0.25D \left[\left(\frac{TF}{C} - 1\right) + \sqrt{\left(\frac{TF}{C} - 1\right)^2 + \frac{8J_A \cdot \frac{TF}{C}}{C \cdot D}} \right] \qquad \text{Equation 2-11}$$

where D is duration of analysis period (hour) and J_A is delay parameter (without a unit).

USHCM (2000) provided the travel time estimation function developed from Akçelik's function and modified it in 2002 as follows:

$$TT = TT_0 + d_0 + d_m + 0.25ND\left[\left(\frac{TF}{C} - 1\right) + \sqrt{\left(\frac{TF}{C} - 1\right)^2 + \frac{16J \cdot \frac{TF}{C} \cdot L^2}{N^2 \cdot D^2}}\right] \qquad \text{Equation 2-12}$$

where d_0 is delay (hour) at signalized intersection without traffic flow, d_m is segment delay (hour) between signals (equals zero if no signals), L is link length (mile), N is the number of signals and J is delay parameter ($\mathrm{hour}^2/\mathrm{mile}^2$).

Afterward, Dowling and Skabardonis (2008) simplified Akçelik's function as follows:

$$TT = TT_0 + 0.25D\left[\left(\frac{TF}{C} - 1\right) + \sqrt{\left(\frac{TF}{C} - 1\right)^2 + J \cdot \frac{TF}{C}}\right] \qquad \text{Equation 2-13}$$

The function developed by US Bureau of Public Roads (1964), which is the main concern analysed in the modelling process (Chapter 4 and Chapter 5), is investigated in detail in the next section.

2.3.3. VDF in South Korea

Transport appraisal in South Korea

As mentioned above, forecasting traffic demand is one of the most important procedures in transport appraisal that predicts costs and benefits. Like other countries, traffic demand forecasting plays a very important part in Korean transport appraisal because if an incorrect trip demand forecast is made this will affect the estimation of benefits on every link and thereby cause a distortion of the total benefit (KDI, 2008b). Two kinds of software, namely EMME and TransCAD, are widely used for traffic demand analysis in Korea. A volume-delay function (VDF) is installed for trip assignment to the software. The Korean Transportation DataBase (KTDB), which has O-D trip demand dependent on the type of transportation in the future, is the input in forecasting traffic demand. The benefits of a road project intervention in transport appraisal are classified into four categories: vehicle operating costs reduction, travel time savings, road safety increases and environmental improvement (especially in respect of emission and noise) in Korea. When investigating the CBA results of national highway projects implemented just before making a 2005-2010 plan, 77.4% of the total estimated benefits for those projects is represented by travel time savings (KDI, 2008b). With the current system of benefit estimation and valuation in transport appraisal, the benefit of travel time savings occupies a very large proportion of the total benefit in

CBA. In addition to the direct impact of the travel time savings, other benefits are closely related to the change in travel time on every route (Appendix A.3.3). For example, the traffic accidents reduction benefit is estimated considering allocated traffic flow on different types of roads; and the environmental costs reduction benefit such as emission is estimated depending on vehicles' speed and travelled distance. Namely, traffic flow, average speed and travelled distance derived by traffic assignment based on travel time estimation become the essential factors on which to determine other benefits. Therefore, it can be said that travel time estimation is the starting point for most benefit estimation in transport appraisal.

Korean VDF: BPR function

The VDF that is widely used in Korea is the BPR function (Equation 2-14). The essential factors of BPR function are free-flow speed, road capacity and the parameters of α, β as with other VDFs. However, current VDFs cannot reflect the characteristics of networks in detail even though the amendment of the VDF is sometimes required to reflect the actual traffic situation more accurately in the feasibility analysis (KDI, 2015).

$$TT = TT_0 \left(1 + \alpha \left(\frac{TF}{C}\right)^{\beta}\right) \qquad \text{Equation 2-14}$$

where TT: travel time (TT_0: free flow TT); TF: traffic flow; C: road capacity; α, β: parameter.

Many countries including Korea use the BPR function for traffic demand forecasting. The original type of function (Equation 2-14) would have used the practical road capacity and the parameters would be generally suggested as 0.15 and 4 for α and β respectively (Branston, 1976; KDI, 2015). The replacement to steady-state road capacity could make the parameters change into 2.62 and 5 for α and β respectively, which is higher than those in the original type (Steenbrink, 1974). Many researchers calibrated the parameters of BPR function with the measurement of road capacity and free-flow travel time (Singh, 1995; Kurth *et al.*, 1996; Dowling *et al.*, 1997; Skabardonis and Dowling, 1997; Singh and Dowling, 2002; Hansen *et al.*, 2005). In particular, Hansen *et al.* (2005) modified BPR function by using 75% of road capacity and the parameters of α = 0.15 and β = 7. In addition, Manzo *et al.* (2013) modified the function from the general point of view, which is relevant in the cases where there are no separated lanes (Equation 2-15).

$$TT = TT_0 (1 + \alpha \left(\frac{TF + \gamma\, TF'}{C}\right)^{\beta}\Bigg) \qquad \text{Equation 2-15}$$

where TF' is the traffic volume on the opposite direction and γ is the parameter due to no separated lane types.

Inputs of BPR function

BPR function consists of the inputs including free flow speed, link capacity, and the parameters of α, β. If BPR function is assumed to be optimal in all road sections and the road capacity in VDF is measured accurately, the parameters of α, β would have a huge impact on the curve of the function. The parameter of α would be the main factor in determining the travel time in VDF in the section where the ratio of traffic volume to the road capacity (TF/C) is between 0.5 and 1.0. If TF/C were over 1.0, the parameter of β would start to affect the result (Figure 2-14). In addition, the parameters of α, β could be adjusted and derived from the actual measurement of various capacities in many links and the statistical analysis of calculated travel time dependent on varying levels of traffic volume (Figure 2-15).

Consideration of link geometry in Korean VDF

Korean VDF is classified into 32 types depending on road types, the region (urban, rural), the number of lanes and the density of intersection (Table 2-5). Korean VDF is developed by the empirical analysis based on the traffic data observations in the links that would be in line with a basic segment in HCM (KOTI, 2009; KDI, 2015). In other words, the impact of link geometry was not considered in the modelling process. When link geometric features are reflected in the process of trip assignment, the only factors that can change in Korean VDFs are free-flow speed and road capacity. Korean VDFs do not suggest various parameters depending on different free-flow speed and road capacity, ignoring the fact that all the factors could have an influence on each other.

Figure 2-14 Impact area by the variable and parameters in BPR function

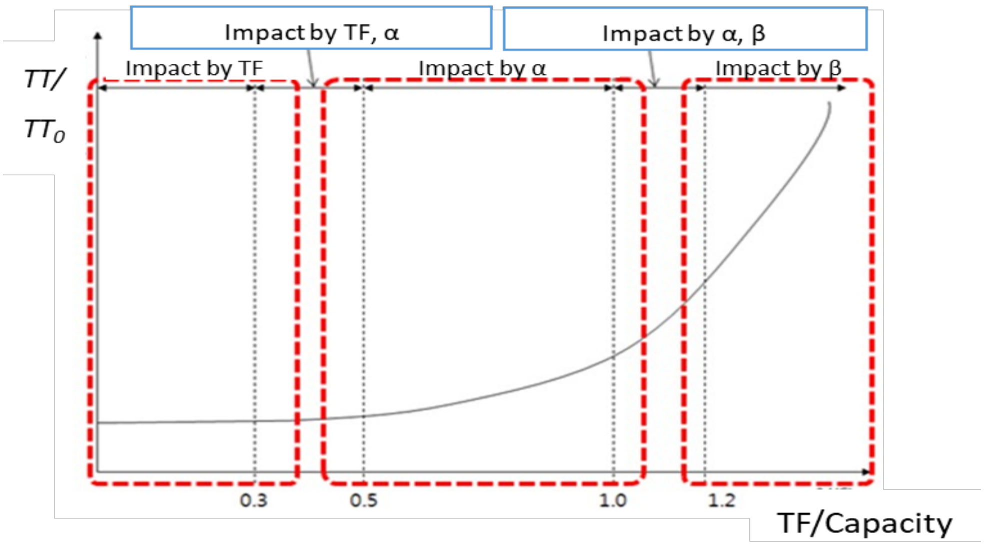

Source: KDI (2015)

Figure 2-15 Adjustment of parameters in BPR function

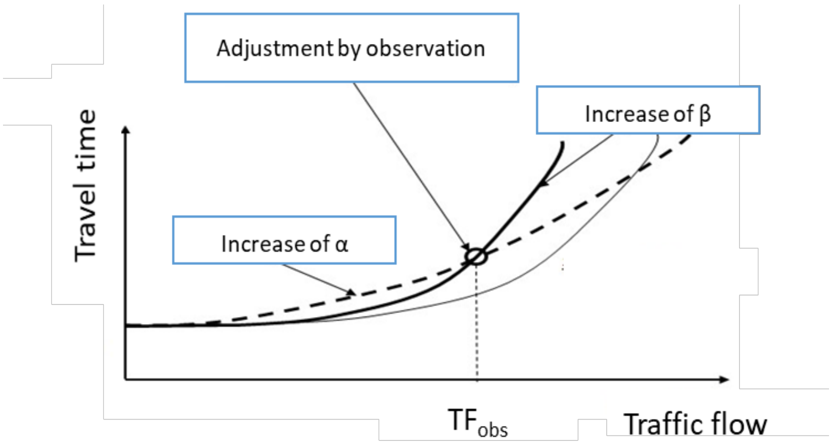

Source: KDI (2015)

Table 2-5 Factors of the Korean VDF by different road types

Road Type	Region	BPR Type	No. of Lanes	Intersection Density (No./km)	Recommended Value			
					Free-flow speed (km/h)	α	β	Capacity (pcphpl)
Freeway	Urban	1	≤ 2	0	100.7	**0.56**	**1.80**	1,846
	Rural	2		0	95.2	**0.55**	**2.09**	1,786
	Urban	3	> 3	0	115.1	**0.57**	**1.68**	2,028
	Rural	4		0	108.2	**0.57**	**2.07**	1,987
Urban Highway	Urban	5	≤ 2	0	95.5	**0.47**	**2.43**	1,773
	Urban	7	> 3	0	97.5	**0.48**	**2.40**	2,182
General Road	Urban	9	1	≤0.3	66.5	**0.51**	**2.69**	1,100
	Rural	10			67.5	**0.51**	**2.82**	1,090
	Urban	11	≥2		80.7	**0.67**	**2.16**	1,420
	Rural	12			82.3	**0.65**	**2.24**	1,400
	Urban	13	1	≤0.7	63.9	**0.54**	**2.47**	957
	Rural	14			65.0	**0.54**	**2.16**	925
	Urban	15	≥2		79.2	**0.68**	**2.08**	1,341
	Rural	16			80.7	**0.72**	**2.14**	1,188
	Urban	17	1	≤1.0	55.7	**0.60**	**2.15**	873
	Rural	18			62.8	**0.59**	**1.87**	767
	Urban	19	≥2		71.0	**0.69**	**1.93**	1,242
	Rural	20			72.2	**0.73**	**1.82**	971
	Urban	21	1	≤2.0	51.0	**0.60**	**1.92**	862
	Rural	22			58.1	**0.63**	**1.87**	583
	Urban	23	≥2		69.6	**0.71**	**1.80**	985
	Rural	24			70.0	**0.80**	**1.81**	831
	Urban	25	1	≤4.0	44.1	**0.67**	**1.86**	636
	Rural	26			54.4	**0.68**	**1.79**	580
	Urban	27	≥2		62.4	**0.72**	**1.79**	936
	Rural	28			69.3	**0.82**	**1.72**	756
	Urban	29	1	> 4.0	38.3	**0.80**	**1.82**	595
	Rural	30			44.2	**0.72**	**1.72**	465
	Urban	31	≥2		57.0	**0.82**	**1.66**	801
	Rural	32			60.0	**0.83**	**1.70**	736

Source: KDI (2015)

2.3.4. Implication to thesis

Section 2.3 investigates travel time estimation models in traffic assignment reviewing theoretical backgrounds on travel time estimation models. Before examining VDFs in detail, which are used as link cost functions in STA, the section tried to scrutinise travel time estimation models in both STA and DTA. Although there are some approaches using travel time estimation models in DTA, most of DTA approaches give a more emphasis on the interaction between vehicles. The finding suggests that the statistically estimated travel time models based on the empirical data analysis as with this thesis would be more appropriate for STA. The implications from reviewing VDFs in STA can be summarised as follows.

Firstly, it was confirmed that the examined VDFs commonly include road capacity and FFS, which are the only two values could express link attributes in VDFs. In the literature, it was not clarified why both values are used and how they are measured in VDFs. Although Branston (1976) tried to classify the link capacity as into the steady-state capacity and the practical capacity, most studies used the values without critical reviews and proposed different forms of models with both values. Therefore, the review of VDF studies motivated the necessity for a more detailed investigation of free-flow travel time (FFTT) and road capacity.

Furthermore, the finding that all VDFs in STA have monotonically increasing convex curves depending on traffic flow contributed significantly to the selection of the base function of the models estimated in research methodology (Chapter 3). Although this study does not overcome a limitation that VDF approximates oversaturated or congested states based on the statistical estimation of travel time in uncongested states (see details in Section 7.3), it would also be significant to clarify the relationship between travel time, traffic flow and geometric features in uncongested and synchronised states.

Lastly, it was reviewed that the Korean VDF (BPR function) also follows the common feature of VDFs, which include FFTT and road capacity. In common with many countries, the Korean VDF (BPR function) is useful for traffic assignment in transport appraisal, but it has a limitation in that it was developed based on the traffic data of links that are not affected by geometry. This study attempts to overcome this limitation in existing VDFs. This is also a reason why Korean motorways are selected for the case study and the Korean VDF is used as a reference model for the comparison with the developed models in this study.

2.4. Free-Flow Speed and Road Capacity

2.4.1. FFS and road capacity in highway capacity manuals

Road capacity can be defined and theoretically calculated based on HCMs in many countries. USHCM (2010) suggests road capacity based on the intersection between the curve related to FFS reflecting link geometry and the dashed line of road density at each LOS (maximum traffic flow: LOS E) in Figure 2-16. Thus, it could represent the performance of each link and as a result it could connect with link performance function. USHCM (2010) suggests the equation of free-flow speed in a basic segment as follows:

$$FFS = 75.4 - f_{LW} - f_{LC} - 3.22TRD^{0.84} \qquad \text{Equation 2-16}$$

where f_{LW} is adjustment for lane width, f_{LC} is adjustment for right-side lateral clearance, and TRD is total ramp density.

Figure 2-16 LOS for basic freeway segments

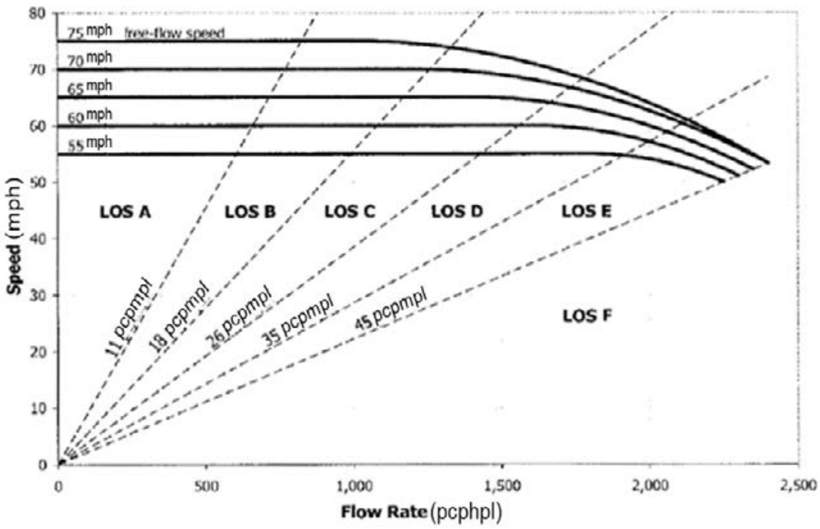

Source: USHCM (2010)

The concept of road capacity is related to traffic flow theory because it is the output combined with traffic speed, road density and traffic flow. Figure 2-16 shows the relationship between speed and traffic flow with the areas of LOS, which is related to road density. Road capacity is generally defined as the traffic flow at LOS E. USHCM (2010) considered gradient effects including upgrades, downgrades, and composite grades as well as ramp density. For example, the uniform gradient effects as three categories of level, rolling and mountainous terrain where grades below 2% are below 0.25 miles long, or where grades between 2% and 3% are below 0.5 miles long. Other gradient links between 2% and 3% and longer than 0.5 miles; or 3% or greater and longer than 0.25 miles need to be regarded as separate segments. However, USHCM (2010) does not include assessment of the impact of other link geometric features such as tunnels. It admits the limitations in the methods of current road capacity estimation and suggests the development of performance measurement related to this study (Table 2-6). Both the German Highway Capacity Manual (HBS, 2015) and Korean Highway Capacity Manual (KHCM, 2013) respectively, take into account the following road geometric features- grades, ramp or weaving section in their definitions of capacity. Compared to USHCM (2010), both HBS (2015) and KHCM (2013) analyse a segment over 3% grade and longer than 500m separately. Notably, even though the difference is small compared with a basic segment, HBS (2015) takes into consideration tunnel impact on the capacity (Wu, 2017).

Table 2-6 Limitations of road capacity

Limitation	Potential for Improved Treatment by Alternative Tools
Special lanes reserved for a single vehicle type, such as HOV, truck, and climbing lanes	Modeled explicitly by simulation
Extended bridge and tunnel segments	Can be approximated by using assumptions related to desired speed and number of lanes along each segment
Segments near a toll plaza	Can be approximated by using assumptions related to discharge at toll plaza
Facilities with FFS less than 55 mi/h or more than 75 mi/h	Modeled explicitly by simulation
Oversaturated conditions (refer to Chapters 10 and 26 for further discussion)	Modeled explicitly by simulation
Influence of downstream blockages or queuing on a segment	Modeled explicitly by simulation
Posted speed limit and extent of police enforcement	Can be approximated by using assumptions related to desired speed along a given segment
Presence of ITS features related to vehicle or driver guidance	Several features modeled explicitly by simulation; others may be approximated by using assumptions (for example, by modifying origin–destination demands by time interval)

Source: USHCM (2010)

The Korean Highway Capacity Manual (KHCM, 1992) was also developed based on USHCM (1985). The methodology for calculating capacity is similar, but some factors for other special conditions such as the impact of differing weather conditions, road maintenance works and the effect of night time are customised for the Korean road environment. There were many changes in the methodology of USHCM (1997) such as the introduction of free flow speed adjusted by correction factors based on base free-flow speed, but KHCM (2001, 2013) didn't follow these major changes and uses the road capacity adjusted by correction factors based on maximum service traffic flow. KHCM (2013) consists of 15 chapters and they are about a motorway, a highway (multilane and two lane roads), an urban street (signalised, non-signalised, etc.), a roundabout, a transit road, a pedestrian road and a bicycle path. The basic geometric conditions for analysis in Korean motorway capacity are that width is over 3.5m, that lateral clearance is over 1.5m on a level terrain. The factors that are used in the process of calculating basic motorway segment capacity are related to road width, clearance, the percentage of heavy vehicles, and the degree and distance of a slope.

HCMs in many countries do suggest some impact on motorway capacity as a result of geometric factors. The factors identified as causing a reduction in capacity are motorway weaving, merging and diverting segments, whose capacity are lower than basic segments in HCMs. With reference to weaving segments these are divided into the configuration, the length, and the width of a weaving segment. The capacity of merging or diverting segments in ramp junctions is determined by the design speed of a ramp, the distance between adjacent ramps, the traffic volume between adjacent ramps, the accelerating or decelerating distance in a ramp, and the percentage of heavy vehicles in a ramp and adjacent ramps.

2.4.2. Uncertainty of FFS and road capacity

As mentioned in Section 2.3.2, what most VDFs have in common is is the inclusion of FFTT, which is derived from FFS, and road capacity. The parameters of the VDFs can be calibrated based on empirical traffic data analysis, but the effect that these differing parameters have on FFTT and road capacity is not shown. In addition, the methodology for measurement of FFS and road capacity differs in many studies or manuals. Therefore, both values in link performance functions can be said to lack clarity and to be ambiguous.

First of all, USHCM (2010) defines road capacity as follows:

> *"The capacity of a system element is the maximum sustainable hourly flow rate at which persons or vehicles reasonably can be expected to traverse a point or a uniform section of a lane or roadway during a given time period under prevailing roadway, environmental, traffic, and control conditions."*

Instead of the quantitative value, the definition of road capacity in USHCM (2010) is expressed using vague and imprecise words such as "sustainable", "uniform", "expected", "reasonably" and "prevailing". Although it can be said that the definition and the measurement of road capacity are different issues, USHCM (2010) does not outline the definite methodology to measure road capacity. Notably, in USHCM (1950), road capacity was divided into three categories: basic, possible and practical road capacity, even though these categories were merged in later versions (Roess and Prassas, 2014).

In addition, USHCM (2010) defines FFS as *"the theoretical speed when the density and flow rate on the study segment are both zero"*, describing that FFS can be examined as a constant speed in traffic flows between 0 and 1,000pcphpl. The definition of FFS is clearer than that of road capacity, but even so its measurement methodology contains uncertainty because it is questionable whether there will be constant values in the low traffic flows.

Because of the unclear measurement methodology for both fundamental values in the traffic theory, many studies interpreted FFS and road capacity differently. Kim (2013) divided the methodology for measuring road capacity into three categories: the average of high traffic flows, the derivation by regression analysis and the measurement by a descending cumulative traffic flow line. Another methodology which is based on breakdown traffic flow estimation can be added to the three categories.

Capacity measurement from average of high traffic flows

This approach is a widely used methodology for capacity measurement. The maximum or the average of high traffic flows is estimated as the road capacity of traffic flows observed at one or more locations during a given period (e.g. hour, day, month, or year). KICT *et al.* (1999) suggested the average (q_m) of the two highest values (q_1 andq_2) in two curves that show the relationship between speed and traffic flow (Figure 2-17). Agarwal *et al.* (2005) used the average of the top 5% of traffic flows as road capacity (Figure 2-18). In addition, Huntsinger and Rouphail (2011) adopted the average of the top 1% of traffic flows and Kucharski and Drabicki (2017) used 95 percentile traffic flow. This methodology tries to follow the description of HCM as closely as possible. However, the method for establishing the criterion for distinguishing between low and high traffic flows (e.g. 1% or 5%) is unclear.

Figure 2-17 Road capacity measurement from boundary conditions

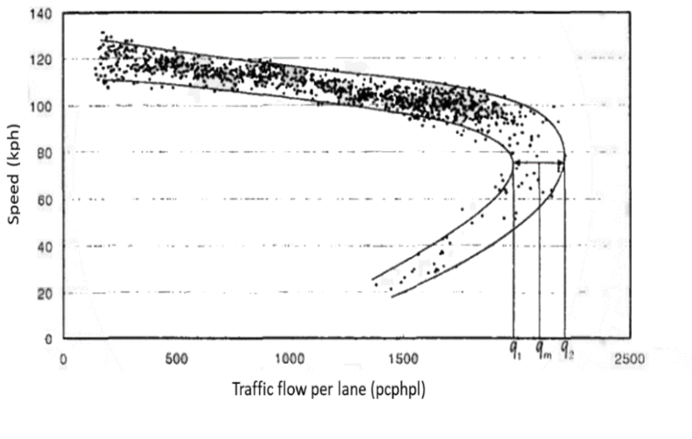

Source: KICT *et al.* (1999)

Figure 2-18 Road capacity measurement by the average of top 5% traffic flows

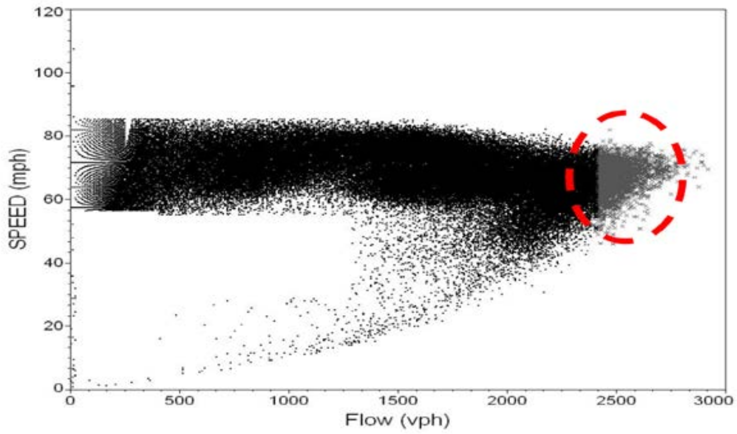

Source: Agarwal *et al.* (2005)

Capacity Derivation by regression analysis

This approach measures road capacity based on existing traffic models (e.g. Pipes triangular, Greenshield parabolic, and Van Aerde diagram) or newly developed regression equations. KICT *et al.* (1999) derived the maximum traffic flow after implementing regression analysis from observed speed and traffic flow data (Figure 2-19). The regression equation for Jungbu Motorway in South Korea is as follows:

$\mathrm{s} = -14.2984 \times e^{0.0006128\times \mathrm{TF}} + 140$ for uncongested conditions

$\mathrm{s} = 5.388 \times e^{0.0012\times \mathrm{TF}}$ for congested conditions

where q is traffic flow (pcphpl) and s is speed. The derived road capacity by these regression equations was 2,304pcphpl. Kim (2013) mentioned that this approach can best statistically reflect the features of the observed dataset although the result would depend on the distribution and quality of the dataset. However, if the dataset was separated into uncongested and congested traffic, the criteria used for this separation would also be unclear.

Figure 2-19 Road capacity measurement by regression analysis

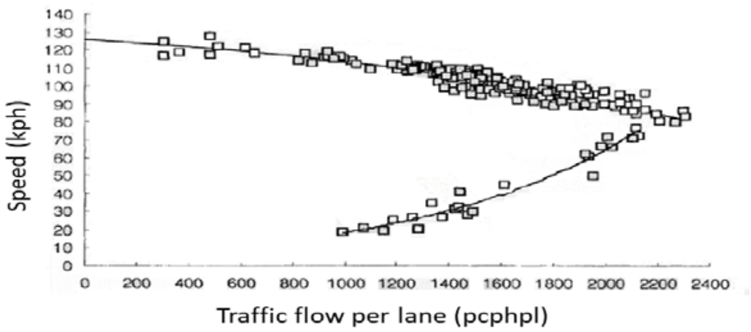

Source: KICT *et al.* (1999)

Capacity measurement by descending cumulative traffic flow line

This approach aims to find the inflection point from the descending cumulative curve of daily maximum traffic flows. For example, Kim and Seo (1999) extracted the first inflection point that began to record the several highest similar traffic flows from 100-day maximum traffic flows from 1-min interval observation (Figure 2-20). It can be said that this methodology follows the concept of "reasonable expectation" from the road capacity definition in USHCM (2010) in that the repeatedly measured high traffic flow can be selected as road capacity. However, this method could also have the limitation in that the average of similar traffic flows would become an inflection point even when the values accidently happen a few times.

Figure 2-20 Road capacity measurement by cumulative curve

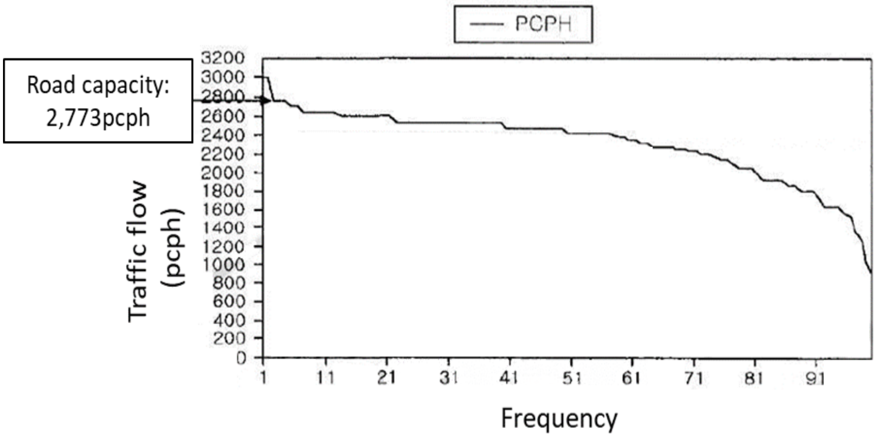

Source: Kim and Seo (1999)

Capacity measurement by breakdown traffic flow estimation

In addition to the classic relationships between speed and traffic flow, many studies have been carried out demonstrating and developing this relationship based on empirical data. The sudden speed decrease between a fluid and congested state at a bottleneck, which is called the traffic breakdown, began to be defined (May, 1990). Afterwards, from the probabilistic perspective, it was suggested that traffic breakdown would not always happen at the same traffic flow level (Elefteriadou *et al.*, 1995; Persaud *et al.*, 1998). Kerner (2009) found that the maximum traffic flow would precede the breakdown traffic flow, and that it would be greater than the breakdown flow (Figure 2-21).

In line with the introduction of the breakdown effect, studies have been developed that try to use breakdown traffic flow for measuring road capacity. Lorenz and Elefteriadou (2001) suggested road capacity based on probability of breakdown under prevailing conditions. Kalaee (2010) used breakdown traffic flow by adopting the threshold speed of 55mph (88kph) and the speed drop of 10mph between five and fifteen-minute intervals in a US highway, whose FFS is assumed to be

65mph. In addition, he used 75% of breakdown traffic flow as a constant of road capacity in VDF. Kim (2013) found road capacity by calculating the change (from minus to plus) in the derivative of the function between traffic flow and speed (Figure 2-22). This approach can find road capacity by reflecting real traffic characteristics, but it has the limitation of the subjective selection of criteria such as threshold speed and the level of speed reduction.

Figure 2-21 Empirical measurement of traffic flow and speed at a bottleneck

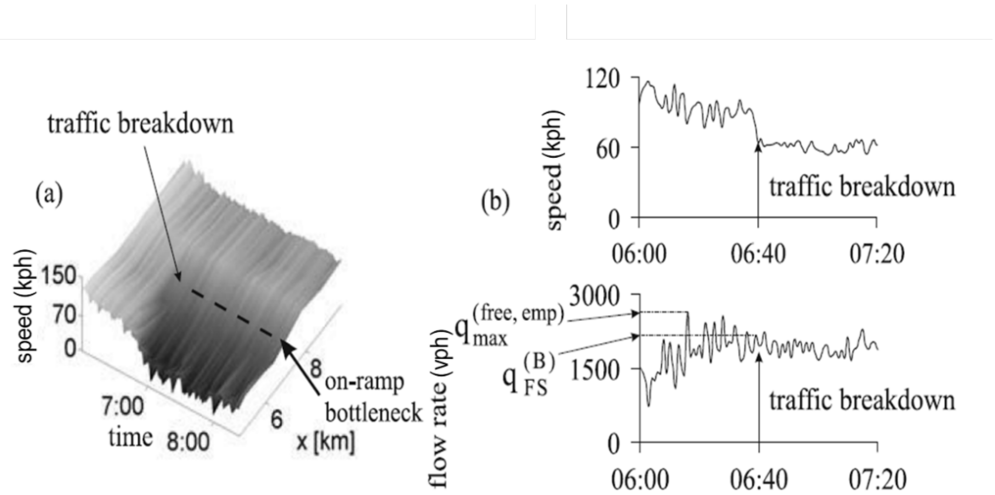

Source: Kerner (2009)

Figure 2-22 Road capacity measurement by finding breakdown effect

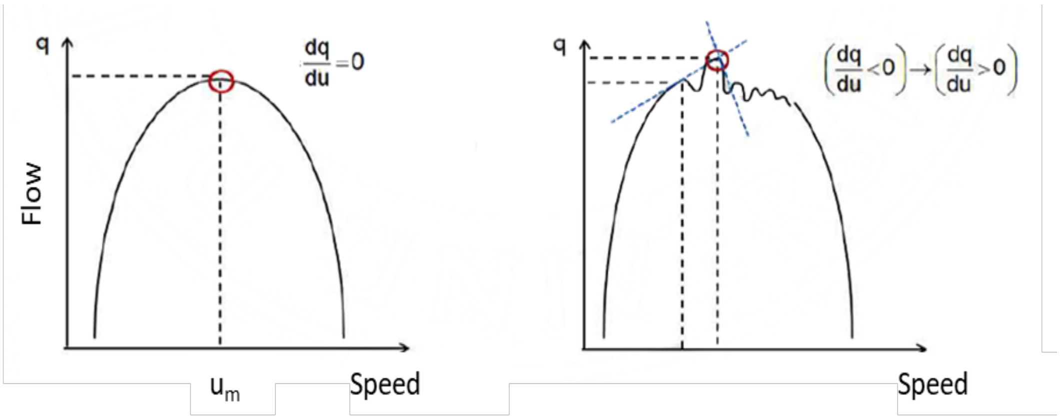

Source: Kim (2013)

Various FFS measurement

As with road capacity measurement, FFS can be estimated using different criteria. Some studies used design speed or enforcement speed without detailed measurement of FFS in VDF calibration. KDI (2015) proposed FFS for South Korean 2-lane motorways as 100.7kph in urban areas and 95.2kph in rural areas (Table 2-5). DfT (2018) provided FFS of light vehicles as 111kph for dual 2-lane motorways in TAG Unit M3.1. “Highway assignment modelling” (2014). USHCM (2010) proposed the highest FFS in the equation for basic freeway segments as 75.4mph (121.3kph) (Equation 2-16). Kalaee (2010) calculated FFS as the mean value of speeds corresponding to traffic flows under 360vph. Kucharski and Drabicki (2017) extracted FFS as 85 percentile speed from its distribution. Brilon and Bressler (2004) derived FFS as 141.3kph (without consideration of heavy vehicle percentage) and 154.8kph (with consideration of heavy vehicle percentage) in a 2-lane German autobahn VDF. Therefore, as with road capacity, there was no consistent methodology for FFS measurement.

2.4.3. Implication to thesis

Section 2.4 reviewed FFS and road capacity in HCMs and other studies. The investigation of both values is a starting point of this study because most VDFs include the values and as such most studies adopted the methods that calibrate the parameters after predetermining the values. The implications from reviewing the values can be summarised from two aspects: the theoretical definition and the measurement.

Firstly, whilst the definition of road capacity has the advantage of incorporating many situations, it has the drawback of having difficulty in being defined as a unique value. This ambivalence would give a flexibility but at the same time cause an error in VDFs when applying both values to VDFs. This study investigates the impact of both values on VDFs based on the review here. Moreover, it is worth noting that HCMs cannot cover all geometric features. The link geometry including the presence of a tunnel, which is investigated in this research, could be one of the geometric features reducing capacity, but this is not taken into consideration in HCMs. In the same context, HCMs admit varying road capacity depending on many situations that cannot be suggested in HCMs. Therefore, the definition of FFS and road capacity would be unclear to apply to VDFs.

In addition, it was reviewed that existing research selected different methods of FFS and road capacity measurement. The different measurements on empirical data analysis could affect the development of VDFs. However, most existing VDFs do not propose how the values were measured. Even though the measurement methods would be described clearly in VDF manuals, it would be impossible to measure or predict those values for existing and planned roads. Therefore, this finding motivates to reconsider the applicability of both FFS and road capacity in VDFs.

2.5. Road geometry in travel time estimation models

2.5.1. Observation of traffic data by different road geometry

Iwasaki (1991) collected traffic data from 106 detectors in a Japanese motorway and found three causes of severe bottlenecks, these were an interchange decreasing from three lanes to two lanes, an S-curve and sag section, and the entrance to a tunnel. He asserted that the geometric features at each detector would affect traffic characteristics including FFS and traffic flow; and in particular that the maximum traffic flow in the analysed tunnel was estimated with 1,550vphpl although he did not suggest the equation that could explain traffic characteristics in those sections.

Koshi et al. (1992) identified bottlenecks at sags and tunnels by measuring traffic flow and the average speed. They demonstrated the result of capacity measurement in ten sags and seven tunnels and the results ranged from 2,200vph to 2,700vph per two lanes, whilst the theoretical capacity would be 4,000vph per two lanes. They also observed the location of congestion, as being normally at the entrance of tunnels and sags, and the transition and congestion traffic patterns in the sections. However, as with Iwasaki (1991), they did not suggest any model for estimating traffic movements in tunnels.

Brilon (2000) introduced two tunnel projects that predicted costs depending on the random and time-dependent characteristics of road capacity; and on time-variant average daily traffic including high peak trip demand. The firstly analysed project is a tunnel plan between Denmark and Germany (Brilon and Lemke, 1997; Brilon and Lemke, 2000; Lemke, 2000). Many scenarios were applied to the project considering ferry transportation, accident (or breakdown) and various average daily traffic. In particular, it was examined that without ferry transportation, there would be no significant delay for average annual daily traffic up to 15,000 vehicles per day, but the sum of delays dramatically increases above the level. He emphasised that flow patterns can affect design decision. The other project estimated the costs of travel time and vehicle operation in several German tunnels investigated by the German federal department of transportation (Brilon and Lemke, 1999). After applying the different speed-flow curves from several studies of tunnels to the project, the analysis result concluded that the average annual daily traffic of 70,000 vehicles per day without a hard shoulder could become a starting point that increases the costs; and that there was no significant impact of a hard shoulder below the traffic of 50,000 vehicles per day. Two projects attempted to identify the change in costs that happen in tunnel sections depending on different situations, but travel time estimation models by tunnel characteristics were not specified.

Yun and Shengrui (2012) investigated the speed-density relationship from six inductive loop detectors in a 4,740m motorway tunnel: 400m before the entrance, at the entrance, 350m before the middle, at the middle, at the exit, and 100m after the exit. They derived the road capacity at each detector assuming that the speed-density relationship is linear based on the Greenshields *et al.* (1935)'s traditional diagrams (Figure 2-5); and thus the road capacity was calculated from multiplying the half of free-flow speed and the half of jam density. After comparing the maximum traffic flows at each point, they selected the maximum traffic flow at the middle of the tunnel section as road capacity, which is the lowest among the maximum traffic flows. In addition, they recommended that a bottleneck would happen at the middle of the tunnel section where the lowest road capacity was derived. From this study, it was identified that a tunnel section would be a bottleneck that decrease the road capacity, but it was not proved how tunnel characteristics affect traffic characteristics quantitatively.

Komada *et al.* (2009) and Hong-Di *et al.* (2009) revised the optimal velocity model developed by Bando *et al.* (1995). From the physical perspective, they connected a vehicle's movement with the basic physical theory (Equation 2-17) considering gravitational and braking force.

$$m\frac{d^2x_i(t)}{dt^2} = F(\Delta x_i(t)) - \gamma\frac{dx_i(t)}{dt} - mgsin\theta B(\Delta x_i(t)) \qquad \text{Equation 2-17}$$

where *m* is a vehicle mass, the $x_i(t)$ is the position of vehicle *i* at time *t*, $\Delta x_i(t)(= x_{i+1}(t) - x_i(t))$ is the spacing of vehicle *i* at time *t*, $F(\Delta x_i(t))$ is the accelerating force, γ is the friction coefficient, *g* is the gravity, and *θ* is a gradient degree, and $B(\Delta x_i(t))$ is braking-related function. In particular, they suggested that the third term $mgsin\theta B(\Delta x_i(t))$ consists of the maximal reduced speed (for uphill gradient), the spacing of vehicles and the braking distance. Komada *et al.* (2009) attempted to find where and when traffic jams happen by simulating the change in speed and spacing depending on the density in hypothetical different uphill and downhill gradients. In addition, Hong-Di et al. (2009) simulated traffic flow in hypothetical gradient sections under the periodic boundary condition, i.e. vehicles move within a circuit. They found that the slope affects the beginning of traffic flow and the phenomenon such as stop-and-go traffic. From the physical perspective, the studies by Komada *et al.* (2009) and Hong-Di et al. (2009) theoretically clarified the impact of gravity and further interaction with braking force.

2.5.2. Link geometry in travel time estimation models

Whilst the literature review in the previous section emphasises whether or which road geometry affects the traffic characteristics, this section focuses more on link geometry in travel time estimation models. It was examined that there are only a few studies that estimate travel time models with link geometry based on the empirical data.

Brilon and Bressler (2004) analysed traffic characteristics on uphill motorways in Germany. They measured travel time by placing video cameras between two uphill locations. The variation of gradients and slope lengths is 2%-6% and 2.5km-5.6km respectively. Based on this measurement and microscopic simulation (VISSIM) results, they found a mathematical model for predicting average speed and based on the division of traffic into two stages (steady and congested) (Table 2-7). The variables for the model are the number of lanes, traffic composition, uphill grade, uphill section length, and traffic density. In a steady state (stage I), the variables of lane number and heavy vehicle percentage were considered not to have much significance. They also found that whilst road capacity on gradient motorways was affected by the grade, not the uphill length, the average speed was affected by both variables.

Table 2-7 Formulae for the macroscopic traffic flow on gradient motorways

		stage I		stage II	
		2 lanes	**3** lanes	**2** lanes	**3** lanes
Model		$v_{P,I}(k) = v_0 + b_{grade} \bullet c_{length} + d \bullet k$		$v_{P,II}(k) = v_0 + a_{truck} + b_{grade} \bullet c_{length} + d \bullet k$	
		$v(k) = \min((v_{P,I}(k); v_{P,II}(k))$ $q = k \cdot v(k)$			
Parameter					
v_0		141.30		154.88	156.13
a_{truck}	Proportion of heavy vehicles 5% 10% 15% 20% 30%			0 –0.38 –0.76 –1.15 –1.91	0 –3.18 –4.18 –5.18 –7.19
b_{grade}	gradient s [%] ≤ 2 3 4 5	0 –1.90 –5.74 –11.00		0 –5.39 –13.24 –20.09	
c_{length}		$c_{length} = -1.181 \bullet 10^{-11} L^3 + 2.192 \bullet 10^{-8} L^2 + 3.498 \bullet 10^{-4} L$ $L \leq 3800$ m $c_{length} = 1$ elsewhere L = length of the upgrade section [m]			
d		-0.6187		-1.4516	-0.9711

v_P	average passenger car travel velocity	[km/h]
v_0	free flow speed	[km/h]
a_{truck}	factor for influence of trucks	[km/h]
b_{grade}	factor for influence of gradient	[km/h]
c_{length}	influence of length (= proportion of speed reduction for a section of length L relative to the maximum speed reduction for the same degree of gradient)	[-]
k	traffic density	[veh/km]
d	coefficient for the influence of traffic density	$[km^2/(veh \cdot h)]$
q	traffic volume	[veh/h]

Source: Brilon and Bressler (2004)

They adopted the generalised model for predicting the simple linear relationship between average speed and traffic density in steady and congested states by using the independent variables of a gradient and a slope length that could reduce average speed and by estimating their corresponding parameters. The study estimated models based on both empirical and simulated data while it would not focus much on the statistical significance of the estimated model and of its coefficients. In addition, they did not analyse the impact of other geometric features except for upgrades on motorways.

Cartenì and Punzo (2007) tried to find a travel time function for urban road sections taking into account many geometric features and in particular the effects of road side parking. They collected data from video recordings between two points for 17 roads in Italy. Then, they calibrated their results by using a micro-simulation (AIMSUN) and found an equation with parameters (Equation 2-18). They also tried to validate their function with results from six other roads that are not included in the calibration process.

$$TT = \frac{L}{\beta_0 + \beta_1 LW + \beta_2 SL + \beta_3 B + \beta_4 D + \beta_5 SP + \beta_6 PV + \dfrac{\beta_7 \cdot \left(\frac{TF}{LW}\right)^2}{1 + B + SP + D}} \qquad \text{Equation 2-18}$$

where TT is the travel time in an urban road section L (km); TF is traffic flow (vph); LW is the road width (m); SL is the average road slope (%); B is the average road bendiness discrete variable; D is the distress index (0.00, 0.33, 0.66, 1.00) referring to external factors such as bus stops and pedestrian crossing roads; SP is the percentage of the road side parking (%); PV is a type of pavement dummy variable (asphalt =1, other=0); and β_i $(i = 0,1 \ldots 7)$ are parameters. Although this model is only for urban roads, it would be significant to identify which factors would affect travel time estimation models. Of the analysed factors, the factors with respect to road width, slope, bendiness and pavement types can be applied to models for motorways. In addition, it can be noted that the relationship between travel time and traffic flow is estimated based on the quadratic form.

Kim *et al.* (2014) customised the BPR function to find the travel time prediction model for an urban underground tunnel. They calibrated the parameters by using traffic data at ILDs set in two consecutive tunnels with six lanes and a speed limit of 70kph as on an urban highway in Seoul, South Korea. They adopted “Golden Section Search” methodology originally developed by Kiefer (1953). The parameters for an urban tunnel were developed for the fixed capacity, which is 2,200vphpl assuming different free-flow speeds. They selected the parameters by finding the lowest Root Mean Square Error (RMSE) with the free-flow speed of 110kph and the derived parameters of α, β in the BPR function were 0.894 and 2.003 respectively. Moreover, the parameters were validated for two motorway tunnels having four and six lanes with a speed limit of

100kph. Although this study would be meaningful in that it attempted to find the BPR function that can be used for tunnel sections, it follows the existing approach, which is the calibration of parameters in the current VDF with the predetermination of road capacity. In addition, other quantitative factors for grade sections were not taken into account in their research.

DfT (2018) includes hilliness and bendiness in the speed-flow function of TAG Unit M3.1. "Highway assignment modelling" (2014). At traffic flow less than the breakpoint ($\mathrm{TF_B}$), estimated speed has the linear relationship with link geometric features and traffic flow as follows:

$$s_L = \mathrm{FFS_L} - 0.1 \text{ x BEND} - 0.14 \text{ x HILL (two} - \text{way links only)} - 0.28 \text{ x RISE (one} - \text{way links only)} - \frac{6}{1000} \text{ x TF} \quad \text{Equation 2-19}$$

where s_L is speed of light vehicles (kph), $\mathrm{FFS_L}$ is FFS (111kph for dual 2-lane motorways) for light vehicles, BEND is bendiness per link length (deg/km), HILL is sum of rises and falls per link length (m/km), and RISE is sum of rises per link length (m/km). $\mathrm{TF_B}$ is the traffic breakdown point, which is the traffic flow where the speed-flow coefficient changes, is set at 1,200 and 1,080vphpl for motorway and dual carriageways respectively. At traffic flow greater than the breakpoint ($\mathrm{TF_B}$), the speed has the linear relationship only with traffic flow as follows:

$$s_\mathrm{L} = s_\mathrm{B} - 33(\mathrm{TF} - \mathrm{TF_B})/1000 \quad \text{Equation 2-20}$$

where s_B is speed at the breakpoint traffic flow of $\mathrm{TF_B}$. The speed prediction formula for heavy vehicles is suggested as follows:

$$\mathrm{s_H} = \mathrm{FFS_H} - 0.1 \text{ x BEND} - 0.25 \text{ x HILL (two} - \text{way links only)} - 0.5 \text{ x RISE (one} - \text{way links only)} \quad \text{Equation 2-21}$$

where s_H is speed of heavy vehicles, and FFS_H is FFS for heavy vehicles, which is 93kph for motorways. DfT (2018) proposed two relationships at traffic flow over capacity (C), which are referred to as 'Advice Note 1A' (AN1A) relationship (Equation 2-22) and the Akçelik relationship (Equation 2-11)

$$\mathrm{s} = \frac{s_C}{1 + \frac{s_C}{8L}(\frac{TF}{C} - 1)} \quad \text{Equation 2-22}$$

where TF is trip demand for traffic assignment, s_C is speed at the road capacity of C, L is link length (km). The UK government proposed three piecewise simple linear models for motorway speed-flow models taking into account vertical and horizontal link geometric features. Four points that need to be focused here were found as follows: firstly, although the research for developing the models is not reviewed in this study, the reason why the piecewise functions are suggested in the TAG would be because the split functions can approximate the nonlinear relationship between average speed and traffic flow. Secondly, since UK roads do not have many tunnel sections, the effects of tunnels would not be taken into account. Thirdly, except for in congested states, the models cannot include the constant of road capacity in the models. This result is in line with the trial that would minimise the uncertainty of road capacity raised in this study. However, the breakdown point traffic flow (TF_B) and road capacity (C) are used for splitting the level of traffic flow in the models. In other words, UK models would include the uncertainty of both values near connecting points between the models. Lastly, the analysis of statistical significance of the models is not suggested in TAG.

2.5.3. Road geometry in South Korea

According to Korean Land Classification Research (1982), as much as 71.5% of South Korea is made up of mountainous terrain. When designing roads in South Korea as with many countries, engineers should consider link geometry by referring to the manual called “Road Standard Regulation about Structures and Facilities”. The manual had classified terrain only into a mountainous area or a flat area, but the category of a hilly area was added for detailed design in 2011. In addition, Kim *et al.* (2011) stated that KHCM defined the flat, hilly and mountainous areas in order to calculate heavy vehicle adjustment parameters and it classified the gradient of a road into below 2% (flat), 2%-5% (hilly), over 5% (mountainous) and introduced the special slope section, which is for areas of over 500m of continuous slope with a gradient over 3%.

According to MLTM (2015), the design speed in a motorway (Table 2-8) is described as 120kph on a level terrain and 100kph in a mountainous terrain or in an urban area (The operating speed limit is divided into 100kph or 110kph). Other motorway design criteria can be shown as follows (see details in Appendix A.1.2): with regard to the cross-section characteristics, every motorway generally has a minimum lane width of 3.5m and a minimum central (left) barrier width of 3.0m in a rural area and 2.0m in an urban area. In addition, the minimum right lane clearance is 3.0m in a rural area and 2.0m in an urban area, and the minimum left lane clearance is 1.0m in both rural and urban areas. In spite of the clearance regulation, the minimum clearance in a segment where a structure such as a tunnel or a bridge exists can be reduced into 1m. When looking at a longitudinal section, the maximum degree of slope in a motorway ranges from 3% on a level terrain to 4% in a mountainous terrain in the case of the 120kph design speed and from 3% on a level terrain to 5% in a mountainous terrain in the case of the 100-110kph design speed. However, in practice the slope of a motorway does not seem to exceed 3% even if a road is located in a mountainous area. The minimum radius of the horizontal curve in a motorway ranges from 420m to 710m depending upon the design speed and superelevation. Lastly, the regulation restricting all vhicles from changing lanes applies in most Korean tunnels. These geometric features interact the average speed as can be seen from the fact that most design manuals suggest different geometry with reference to design speed. In other words, these features can also be regarded as important factors on travel time estimaiton models.

Table 2-8 Design speed in Korea by the type of terrain

		Design Speed (km/h)			
		Rural Area			Urban Area
		Flat	Hilly	Mountainous	
Motorway		120	110	100	100
Highway	Major Arterial	80	70	60	80
	Minor Arterial	70	60	50	60
	Collector	60	50	40	50
	Local	50	40	40	40

Source: MOLIT (2015)

Note: The shadowed area is the classification of a hilly area that was added to the design manual in 2011

Given Korea’s mountainous terrain, it is no surprise that Korean roads have a high percentage of bridges and tunnels. According to Table 2-9, the total bridge and tunnel length make up 2.1% of the total road length. However, the more notable fact is that around 23% of Korean motorways consist of bridges and tunnels. This observation would be in line with that a motorway should seek to accommodate high-speed traffic by reducing the overall change in the road geometry such as that created by a change in gradient. The geometric features of tunnels were given an emphasis in this thesis, but the impact of relatively long bridges was not identified in this study because of the difficulty in the data collection.

Table 2-9 The number and ratio of Korean bridges and tunnels

(As of 2015)

	Total	Motorway	National Highway	Provincial Road	Metropolitan Road	City, County Road
Road lenth (Km)	107,527	4,193	13,948	18,087	20,313	50,985
Bridges (Number)	30,983	9,018	8,338	4,979	1,911	7,451
Bridges (Km) (%)	3,077 1.4%	1,190 14.2%	880 3.2%	333 0.9%	346 0.9%	421 0.4%
Tunnels (Number)	1,944	925	565	178	183	126
Tunnels (Km) (%)	1,419 0.7%	729 8.7%	402 1.4%	128 0.4%	129 0.3%	52 0.1%

Source: MOLIT (2016a)

Note: When calculating the percentage of bridge and tunnel length over road length, the road length doubled because the number and length of bridges and tunnels were measured separately in each direction of roads.

2.5.4. Implication to thesis

Section 2.5 reviewed road geometry that would affect traffic characteristics and further travel time estimation models in the literature. Some studies tried to determine the change in traffic characteristics according to different road geometry, observing the empirical traffic data. There are the studies that attempted to find theoretical models to clarify the geometric features such as gradients without the empirical data analysis. Many of these studies used the maximum traffic flow as a comparative measure regarding it as road capacity. Moreover, it is worth noting that the reviewed studies recognise that tunnels and gradients would affect traffic characteristics.

Whilst more studies focused on the comparison of the discrete traffic data according to the sections that have different road geometry, only a few studies tried to quantify the impact of geometric features in the travel time (or speed) – flow relationship. Most of the studies are in line with this thesis in that they introduced link travel time or speed estimation models without road capacity, but they quantified only the variables of vertical or horizontal alignments in the models. In addition, they only assumed the simple linear relationship between travel time and traffic flow (or traffic density) without specifying different functional forms.

2.6. Research gaps in the current literature and potential improvements

The comprehensive literature review of traffic assignment confirms that the travel time estimation models are the essential elements in traffic assignment to determine cost (impediment) on each link. Inappropriate travel time estimation models in traffic assignment can be one of the reasons for inaccurate traffic demand forecasting and as such can reduce the reliability of transport appraisal. Flyvbjerg et al. (2005) investigated that over half of the road projects showed the error over 20% between the actual and forecasted demand. In addition, Korean National Assembly (2017) examined that the error for 23 motorway projects constructed after 2000 was 40%.

Of travel time estimation models, this study focuses on VDFs based on the statistical analysis of empirical data from the viewpoint of STA at a macroscopic level. Because of the uncertainty of FFTT and road capacity, VDFs are not well adapted to explaining travel time on different links. More generalised models need to be developed to satisfy the spatial transferability of travel time estimation models by replacing FFTT and road capacity. Therefore, the research gaps to be filled by this study can be summarised as follows: the proof of the uncertainty of FFTT and road capacity; the identification of those factors which have an influence on travel time; the investigation of the statistical significance of link geometry in travel time estimation models; and the development of feasible models.

Uncertainty of FFTT and road capacity in VDFs

Although FFS and road capacity imply uncertainty in their definitions and measurement as mentioned in Section 2.4.2, most studies have ignored the effects of the uncertainty thus suggesting inconsistent measurement methods. The previous studies have rarely tried to analyse how the variation of FFS and road capacity affects the performance of VDF. This study seeks to examine the impact of the variation, which is related to the change in parameters by predetermining FFS and road capacity using different measurements. In addition, the travel time estimation models developed in this study can be compared with the traditional calibration of existing VDFs with predetermining FFS and road capacity.

Identification of influential factors on travel time (spatiotemporal data analysis)

Most studies used the data measured from only a few locations, which are supposed to be ideal links, to calibrate the parameters of existing VDFs for weeks or months (Singh, 1995; Kurth *et al.*, 1996; Dowling *et al.*, 1997; Skabardonis and Dowling, 1997; Singh and Dowling, 2002; Hansen *et al.*, 2005; Kalaee, 2010; Huntsinger and Rouphail, 2011; Manzo *et al.*, 2013; Kucharski and Drabicki, 2017). In other words, they aimed to calibrate existing parameters for some analysed links. These trials can verify only the temporal extension of existing VDFs but cannot justify the spatial extension of them even though it is meaningful that the trials could customise the existing

VDFs for the analysed countries. Because many links have different factors that could affect travel time, analysing only a few links would not identify the influential factors on travel time. This study can statistically justify the developed travel time estimation models by identifying the influential factors from the spatiotemporal data.

Consideration of link geometric variables

Since road capacity is affected by the link geometry as provided in HCMs, geometric features would be the variables that could replace road capacity in travel time estimation models. However, there are only a few studies which reflect link geometric variables in VDFs. Brilon and Bressler (2004) developed the speed estimation model which does incorporate the variables of uphill gradient with its length, heavy vehicle percentage and density. The model was developed using the real data measured from five German motorway links and was extrapolated by the simulated data produced from VISSIM. Cartenì and Punzo (2007) proposed a travel time estimation model for urban roads by turning road width, slope, bendiness, side parking and pavement type as well as traffic flow into variables. DfT (2018) is providing piecewise linear functions in an uncongested situation by applying the variables of bendiness and hilliness as well as traffic flow to speed-flow relationship for UK motorways without detailed references. This study tries to generalise travel time estimation models more by taking into consideration the geometric features, including tunnel sections and using a different functional form from the previous studies. In addition, whilst the previous studies did not give much emphasis on the statistical significance of developed models including link geometric variables, this study verifies the models with link geometric variables statistically by using the empirical dataset.

Implication of linear estimation models

As reviewed in Section 2.3.2, many studies or guidelines have proposed many types of VDFs. These VDFs can differ based on the various relationships between speed, density and traffic flow as in Section 2.3.1. Although there have been a few trials to find new forms of travel estimation models (Brilon and Bressler, 2004; Cartenì and Punzo, 2007; DfT, 2018), most studies have tried to calibrate the existing VDFs (Kalaee, 2010; Huntsinger and Rouphail, 2011; Kim *et al.*, 2014; Kucharski and Drabicki, 2017). However, the studies that calibrate the parameters of existing VDFs share the limitation of being estimated based on statistically nonlinear estimation with predetermined FFS and road capacity. When using a nonlinear estimation, it is difficult to guarantee the statistical significance of derived parameters (Montgomery *et al.*, 2012). This study tries to develop feasible travel time models with the empirical dataset based on both linear and nonlinear statistical estimations. Consequently, it is expected that the investigation of the statistical significance of the developed model can be extended in its application to other sections of Korean motorways.

Chapter 3. Research Methodology

3.1. Introduction

The main objective of this study is to develop travel time estimation models that can replace the current VDFs by identifying and incorporating influence factors such as geometric features. This chapter consists of five parts: initial case study (Section 3.2); the development of model estimation methodology (Section 3.3); the identification of variables (Section 3.4); case study (Section 3.5); and the model selection (Section 3.6). Figure 3-1 illustrates how the sections in this chapter establish the methodology in this thesis.

Figure 3-1 Flow chart for the overall methodological approach

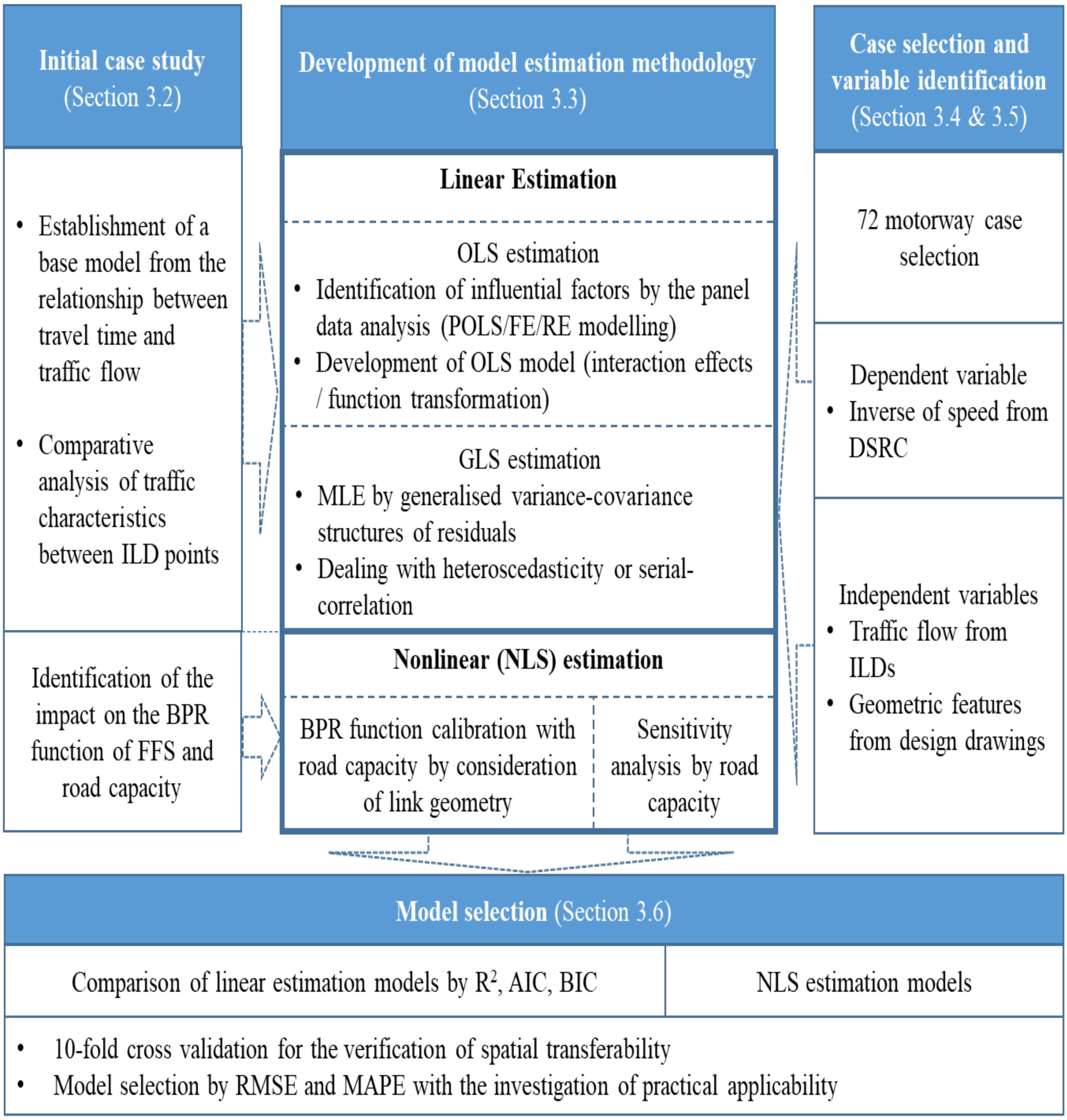

Firstly, Section 3.2 provides the motivation and some fundamental findings for the model development. The initial case study analyses a tunnel motorway link in Korean in order to reduce trial and error before analysing the main case study. The methodology of this thesis is based on the fundamental results derived from the initial case study in the following aspects: the observation of FFTT and road capacity; the comparative analysis of traffic characteristics; the direction for data processing; and the establishment of base functions.

Secondly, Section 3.3 introduces statistical estimation methods used in this study: multivariate linear estimation and nonlinear estimation. The multivariate linear estimation is subdivided into ordinary least squares (OLS) estimation and generalised least squares (GLS) estimation. The OLS estimation not only finds the fundamental models, but also proposes fixed effects modelling to identify influence factors by recognizing the dataset as panel data. In addition, the GLS estimation generalised models by assuming the differing variance and covariance structures of residuals. Lastly, the nonlinear least square (NLS) estimation suggests a model form in which geometric variable are added to the existing BPR function.

Thirdly, Section 3.4 presents the detailed method used for collecting variables and for selecting cases to be used for model estimations. The section explains by what criteria the dependent and independent variables are selected and how they are quantified. In particular, not only traffic flow, which is included in existing VDFs, but geometric variables, which can represent the attributes of links, are collected as independent variables. In addition, Section 3.5 shows how the cases for model development are selected with descriptive statistics for the cases.

Lastly, Section 3.6 explains the methodology for selecting the appropriate travel time estimation models. 10-fold cross-validation is used to verify the spatial transferability of each model. Moreover, this study introduces adjusted R-squared, Akaike's Information Criterion (AIC), and Bayesian Information Criterion (BIC) as comparative measures for linear estimations as well as Root Mean Squared Error (RMSE) and Mean Absolute Percentage Error (MAPE) as accuracy criteria across all models.

3.2. Initial case study

3.2.1. Overview of intial case study

The initial case analysis motivates this study, and at the same time provides the direction of research methodology. The ways in which the initial case study is used can be summarised as follows.

Firstly, the uncertainty of FFS and road capacity needs to be clarified because most of previous studies used both values for travel time estimation models without the critical review. As mentioned in Section 1.2 and 2.4, this study started from the hypothesis that FFTT and road capacity in VDFs are uncertain and ambiguous for explaining road geometry. Thus, the initial analysis is necessary in order to confirm the hypothesis.

Secondly, the initial case study investigates whether geometric features can be used for independent variables of travel time estimation models. The initial case study identifies a section having geometric features like the hilly tunnel section and establishes the fact that this would cause a change in traffic characteristics including FFS and road capacity. Although FFS and road capacity were expected to be uncertain in VDFs, they can be used as fundamental comparative criteria. The change in traffic characteristics is identified by comparing both values measured at different ILD points.

Thirdly, data collection in the initial case study helps develop more appropriate methodology for the data quantification in this study. The initial study is based on the data from each location, but the data is inappropriate for the travel time estimation of links. Therefore, initial data processing provides an important opportunity for improving the data processing in the main study.

Lastly, the data analysis in the initial case study provides the basis for establishing the methodologies for travel time estimation models in this study. Various models are applied in order to estimate the relationship between travel time and traffic flow. The statistical methods for model estimation and the base functions are determined by exploratory data analysis.

Initial case selection (geometric features)

The initial case is a hilly tunnel section between 36.02km and 37.86km from the starting point in “Seoul-Chuncheon Motorway” (Appendix A.4.1). The section includes ‘Songsan Tunnel’ the length of which is 1,135m; the degree of slope in the tunnel is 2.74%; the minimum radius of the horizontal curve is 1,900m; and the lane width is 3.5m. The clearance of 2.0m in the tunnel section is shorter than that (3.0m) of the open section. The reasons why this section was selected for the initial case study are as follows: firstly, since the section is located on a route which is frequently congested, the section is suitable for the investigation of significant traffic data from steady to congested states. In addition, the geometric features of the initial case have a hilly gradient and long tunnel. Lastly, six inductive loop detectors (two outside and four inside the tunnel), which are installed every 280-530m within 1.8km, enable the observation of the change in traffic characteristics. The detailed information is summarised in Table 3-1.

Table 3-1 Geometrical features with ILDs' locations in the initial case study

ID No.	Location	Distance from tunnel entrance	Slope	Reference
29	36.02km	840m* (before)	-0.78%	Outside the tunnel
30	36.55km	310m (before)	2.74%	Outside the tunnel
31	36.89km	30m (after)	2.74%	Inside the tunnel
32	37.19km	330m (after)	2.74%	Inside the tunnel
33	37.49km	630m (after)	2.74%	Inside the tunnel
34	37.86km	1,000m (after)	2.74%	Inside the tunnel

Data collection in the initial case study

The dataset for the initial case study was collected in Korean ITS from August of 2016 to August of 2017. Table 3-2 summarises the data source and its purpose. Traffic flow and average speed, which are collected from inductive loop detectors, are essential data in the initial study. All data were measured on each location as well as the time-mean speed, which is calculated by arithmetically averaging the values of instantaneous speed. Travel time was calculated from the distance between ILDs divided by time-mean speed weighted by traffic flow. More detailed processes for data collection can be seen in Appendix A.4.1.

Table 3-2 Data source and purpose in the initial case study

Data	Source	Purpose
Traffic flow (TF)	ITS (ILD)	- Measurement of road capacity - Identifying free-flow state - Measurement of traffic flow at traffic breakdowns - Independent variable of travel time model
Average speed (SPD)	ITS (ILD)	- Measurement of free-flow speed - Identifying breakdown effects
Travel time (TT)	Output from SPD and ILD location	- Travel time model estimation
ILD Location	ITS	- Comparison of traffic data on locations - Matching with tunnel locations

3.2.2. Measurement of traffic data on each location

Measurement of FFS and road capacity

Continuous changes in road capacity and FFS in one tunnel section were examined for one year (Table 3-3). FFS, which is calculated for the average of speeds corresponding to traffic flows below 360vph (Kalaee, 2010), dropped considerably from 103.1kph to 95.4kph after the tunnel entrance and increased slightly inside the tunnel. Road capacity measurements at six detectors were lower inside the tunnel, while recording maximum value near the entrance. The maximum traffic flows are much lower ranging from 2,748 to 2,948vph than the theoretical road capacity of 3,310vph, which was calculated by reflecting the average heavy vehicle percentage of 18.1% in traffic survey in 2016 (MOLIT, 2017) based on KHCM (2013). The observed 10th largest traffic flows show the similar trend with the maximum traffic flows. From these observations, it was found that the tunnel section forms a virtual bottleneck, which negatively affects traffic characteristics. However, the calculation of road capacity is still uncertain and it is also unclear at which location the road capacity should be used in travel time estimation.

Table 3-3 Observations of FFS and road capacity in the initial case study

ID No.	Distance from tunnel entrance	FFS (kph)	Max. TF (vph)	10th largest TF (vph)	Theoretical road capacity (vph)
29	840m (before)	106.0	2,872	2,772	3,310
30	310m (before)	103.1	2,948	2,872	
31	30m (after)	95.4	2,836	2,768	
32	330m (after)	98.5	2,872	2,748	
33	630m (after)	99.2	2,748	2,704	
34	1,000m (after)	98.6	2,820	2,748	

Note. The criteria for FFS and capacity are suggested differently here because of their uncertainty.

Figure 3-2 Diagram for FFS and road capacity in the initial study

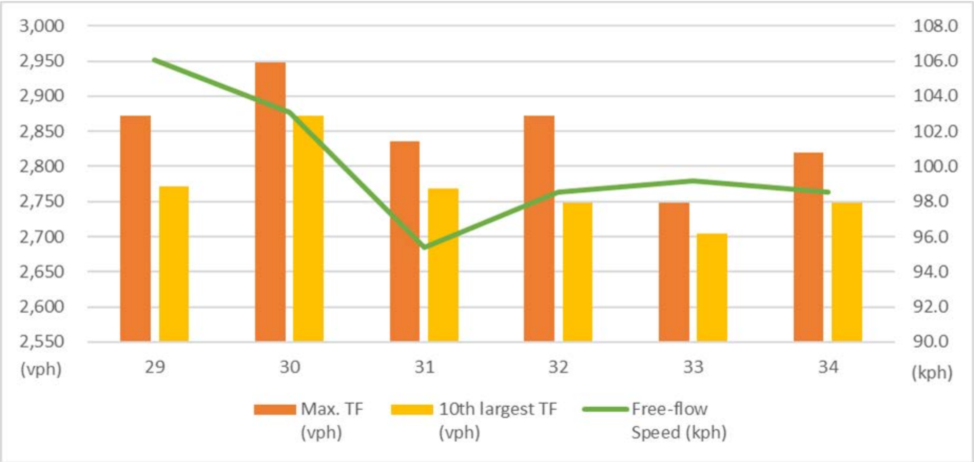

Measurement of traffic flow causing breakdown

Secondly, breakdown effects, which can be defined as a forerunner of congestion, were identified in the tunnel section. Traffic flows at traffic breakdown points can be regarded as an important indicator for identifying traffic characteristics. Some studies treated the traffic flow at a breakdown point as road capacity or used it as a substitute of road capacity in VDFs (Lorenz and Elefteriadou, 2001; Kalaee, 2010; Kim, 2013). Through observing scatter plots and time-series processes (Appendix A.4.2), the breakdown effects in the initial case study were identified. In addition, traffic flows at breakdown points were measured depending on the different criteria of threshold speed, speed drop between time intervals and the duration time of low speed (Brilon *et al.*, 2005; Dong and Mahmassani, 2009; Kalaee, 2010). Figure 3-3 compares traffic flows at breakdown points and the number of breakdown points using two different criteria. From the two graphs, it can be seen that traffic flows at breakdown points are in line with the trend of the maximum traffic flows. However, as with road capacity, it is not clear which value, at which location and which condition can be adopted in travel time estimation. Other measurements of traffic data in the section can be found in Appendix A.4.2.

Figure 3-3 Comparison of traffic flows causing breakdown by two different criteria

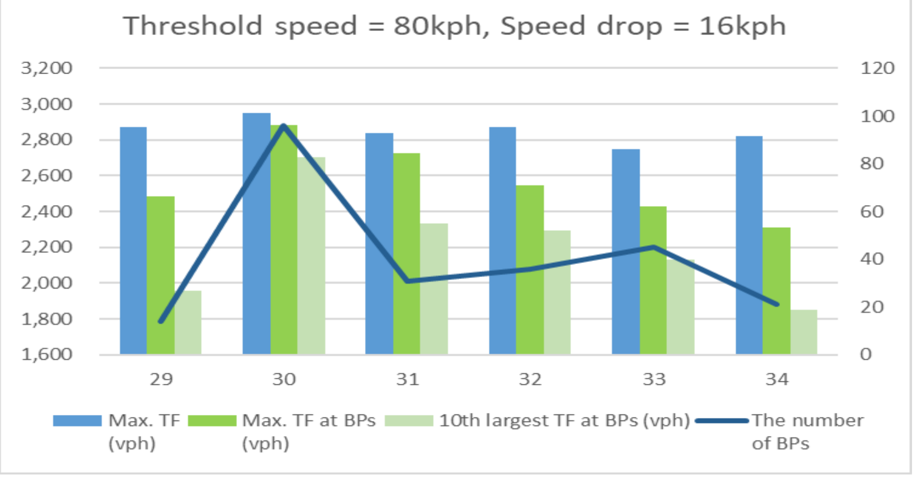

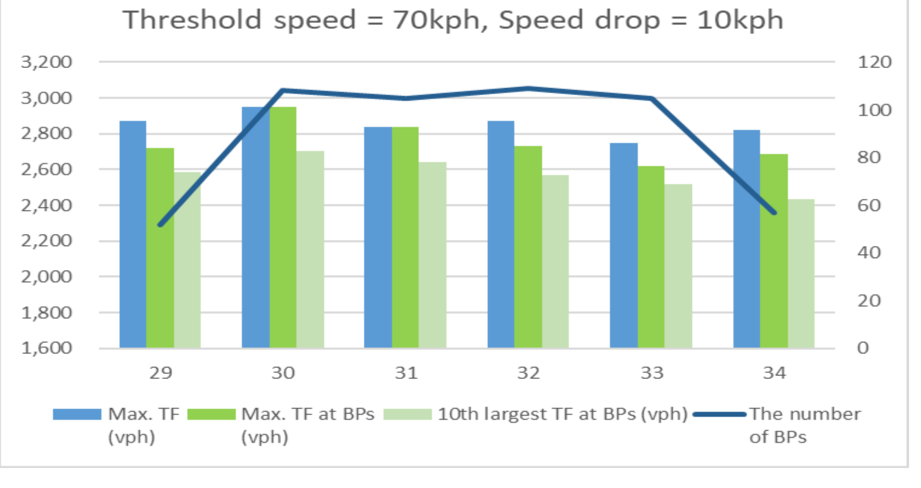

3.2.3. Estimation of models between travel time and traffic flow

Modelling the relationship between travel time and traffic flow in the initial case study helped in finding the methodologies for this study. The estimation did not take into account the impact of geometric features because the estimate cannot include the variation of road geometry based on only one section. As mentioned in Section 3.2.1, travel time was calculated from the distance between ILDs divided by the speed measured at each ILD (Appendix A.4.2). Data was filtered according to three conditions: rainy days, brightness and congestion. The data for non-rainy days and during daylight hours between 07:00 and 19:00 were included as for the feasible model estimation in Section 5.2.1; and traffic data in congested states were not used in this analysis (Section 3.4.3). The initial modelling can be divided into two parts: by the existing BPR function approach and by the generalised function forms designed to scrutinise base functions in this study.

Calibration of BPR function by predetermining FFS and road capacity

Most studies for calibrating the parameters of existing VDFs adopt the nonlinear estimation methodology after predetermining FFS (FFTT) and road capacity (Hansen *et al.*, 2005; Kalaee, 2010; Huntsinger and Rouphail, 2011; Manzo *et al.*, 2013). To clarify the motivation, which is the uncertainty of FFS and road capacity, the initial case study also follows the previous studies. The selected algorithm for the analysis is the "Gauss-Newton" algorithm (Montgomery et al., 2012), which is also adopted as a nonlinear estimation method in this study (Section 3.3.3). As mentioned in Section 1.4, this study uses the BPR function form for the existing VDF approach as follows;

$$\mathrm{TT} = \mathrm{TT}_0\left(1 + \alpha\left(\frac{TF}{C}\right)^{\beta}\right) \qquad \text{Equation 3-1}$$

where TT: travel time (TT_0 is FFTT); TF: traffic flow; C: road capacity; and α, β: parameters.

The results of the nonlinear estimation to minimise Root Mean Squared Error (RMSE)[3] vary depending on predetermined FFTT and road capacity (Table 3-4). As with the previous studies, the predetermined road capacity was inevitable for the nonlinear estimation, but it was possible to estimate parameters without predetermining FFS (FFTT). When the maximum traffic flow (2,948vph) is applied to the road capacity in the estimation, the minimum RMSE was 6.319. The uniquely estimated values are FFS (FFTT) and the parameter 'β': 101.4kph (102.2seconds)[4] and 3.59 respectively. However, although different combinations of road capacity and the parameter 'α'

[3] Since nonlinear estimation finds the best coefficient for minimising the sum of squared errors, RMSE is one of the best comparative measures for nonlinear estimation (see Chapter 3.6.1).
[4] Since the total influenced distance by ILDs is 2.88km (Appendix A.4.2), the free-flow travel time (FFTT) can be calculated from the influence distance divided by FFS.

can minimise RMSE of the estimated models, they could not be estimated uniquely. The parameter ‘α’ is proportional to road capacity in the nonlinear estimation.

When compared with both the standard BPR function (α=0.15, β=4) and the Korean BPR function (α=0.55, β=2.09, C=3,572vph, FFS=95.2kph) for motorways (KDI, 2015), estimated curves (orange lines in Figure 3-4) better reflect the relationship between observed travel time and traffic flow. The standard BPR function underestimates whilst the Korean BPR function overestimates observed travel time. However, if FFS and road capacity are predetermined inappropriately, this will cause an error in model estimations. In particular, whilst any predetermined road capacity from 2,748vph to 3,884vph can minimise RMSE (Graph ‘A’ and ‘B’ in Figure 3-4), fixing both FFS and road capacity will cause a significant error in the existing VDF approach (Graph ‘C’ and ‘D’ in Figure 3-4). Therefore, this initial nonlinear estimation demonstrates how FFTT (FFS) and road capacity affect travel time estimation models negatively based on the nonlinear estimation.

Table 3-4 Nonlinear estimation based on BPR function in the initial case study

Fixed variables	Road capacity (vph)	Free-flow travel time (sec)	Free-flow speed (kph)	RMSE	Parameters		Graph
Road capacity	2,748	102.2	101.4	6.319	α	0.42	
					β	3.59	
Road capacity	2,948	102.2	101.4	6.319	α	0.54	A
					β	3.59	
Road capacity	3,260	102.2	101.4	6.319	α	0.78	
					β	3.59	
Road capacity	3,572	102.2	101.4	6.319	α	1.08	B
					β	3.59	
Road capacity	3,884	102.2	101.4	6.319	α	1.46	
					β	3.59	
Road capacity, Free-flow travel time	2,948	90.0	115.2	7.090	α	0.48	C
					β	1.15	
Road capacity, Free-flow travel time	2,948	108.9	95.2	7.655	α	0.64	
					β	6.39	
Road capacity, Free-flow travel time	3,572	108.9	95.2	7.655	α	2.18	D
					β	6.39	

Note 1. Shadowed areas represent the predetermined values during the estimation
2. 2,948vph is the maximum traffic flow in the measurement of the initial case study
3. 3,572vph and 95.2kph are road capacity and FFS defined in the Korean VDF manual (KDI, 2015)
4. ‘Graph’ represents each graph in Figure 3-4

Figure 3-4 Curve fittings of the initial case study based on the nonlinear estimation

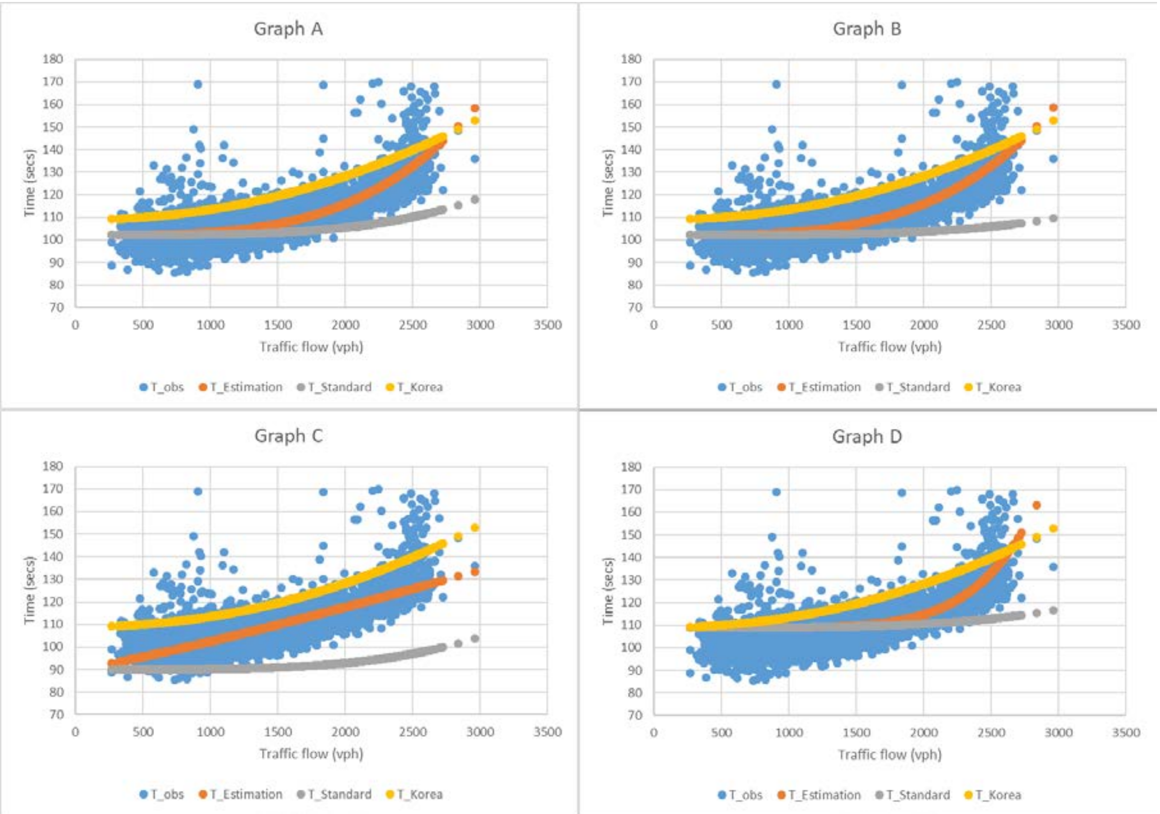

Note. Graph 'A', 'B', 'C', and 'D' show curves by FFS, road capacity and parameters in Table 3-4

Curve estimation without FFS and road capacity

Various function forms were applied for curve estimation: linear, quadratic, cubic, power, growth, and exponential functions from Equation 3-2 to Equation 3-7. Quadratic and cubic functions achieved the best fit for this estimation with adjusted R-squared of 0.619 and 0.626 respectively (Table 3-5), but the quadratic functional form is more appropriate for the statistical linear estimation in this study because the objective function of traffic assignment should be strictly convex as mentioned in Section 2.2.3. The advantage of this approach is that this model can be derived without defining road capacity in advance, for which there is no consensus. The intercept and coefficients of the estimated TF and TF^2 variables in Equation 3-3 are 108.7, -0.016 and 1.004e-05 respectively (Table 3-5). The linear regression analysis will be consolidated with results from the other independent variables such as geometric features (Section 3.3.2).

$$Linear: TT = \beta_0 + \beta_1 \cdot \mathrm{TF} \qquad \text{Equation 3-2}$$

$$Quadratic: \mathrm{TT} = \beta_0 + \beta_1 \cdot \mathrm{TF} + \beta_2 \cdot TF^2 \qquad \text{Equation 3-3}$$

$$Cubic: \mathrm{TT} = \beta_0 + \beta_1 \cdot \mathrm{TF} + \beta_2 \cdot TF^2 + \beta_3 \cdot TF^3 \qquad \text{Equation 3-4}$$

$$Power: \text{TT} = \beta_0 \cdot TF^{\beta_1} \quad \text{Equation 3-5}$$

$$Growth: \text{TT} = e^{\beta_0 + \beta_1 \cdot \text{TF}} \quad \text{Equation 3-6}$$

$$Exponential: t = \beta_0 e^{\beta_1 \cdot \text{TF}} \quad \text{Equation 3-7}$$

where β_0: an intercept (constant); β_i $(i = 1, 2, 3)$: parameters; and others: same as above.

Table 3-5 Different curve estimation results in the initial case study

Model Summary and Parameter Estimates

Dependent Variable: Travel time

	Model Summary				Parameter Estimates			
Equation	Adj. R Square	F	df	Sig.	Constant	b1	b2	b3
Linear	0.522	4955.988	4546	0.000	89.9	0.014		
Quadratic	0.619	3690.087	4545	0.000	108.7	-0.016	1.004E-05	
Cubic	0.626	2539.780	4544	0.000	97.6	0.012	-1.104E-05	4.711E-09
Power	0.428	3408.306	4546	0.000	40.7	0.137		
Growth	0.539	5307.973	4546	0.000	4.5	0.000		
Exponential	0.539	5307.973	4546	0.000	91.7	0.000		

The independent variable is Traffic flow.

Figure 3-5 Curve estimation by different linear equations

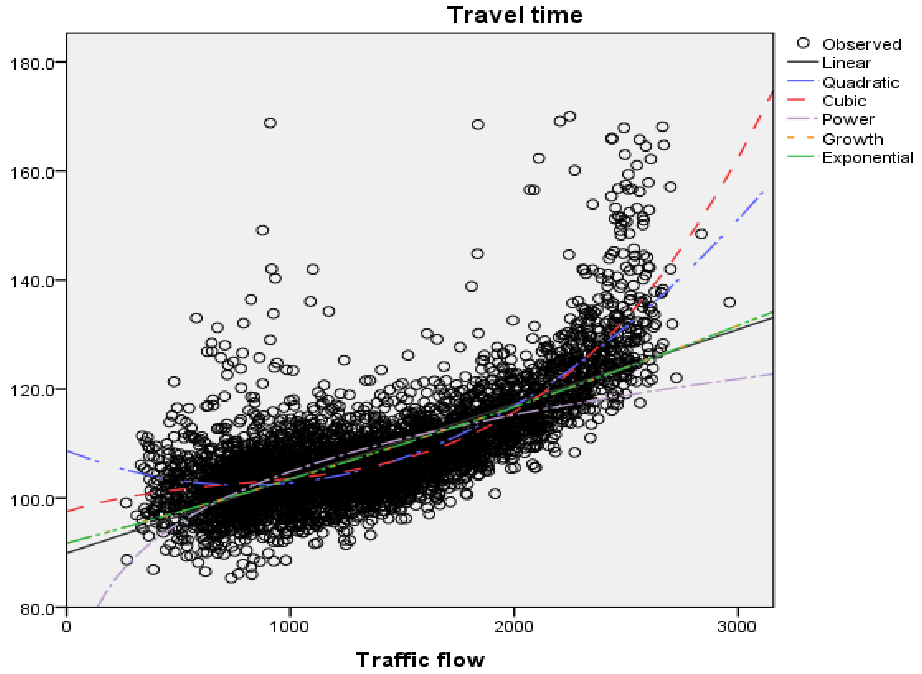

3.2.4. Findings

Limitations of FFTT and road capacity in travel time estimation models

The initial case study confirms the hypothesis of this study that FFTT and road capacity are a cause of the error in travel time estimation or transport appraisal because of the uncertainty of both values.

Firstly, from the perspective of the measurement of both values, it is not clear which criterion is the best for road capacity. Although the initial study measured the maximum, the 10^{th} largest and traffic flow causing breakdown effects, nonetheless, it is difficult to determine which value is the best for travel time estimation models. In addition, since the values are fluctuated at the measurement (ILD) points, it would also not be easy to select the measurement point for road capacity. This is in the same line with Branston (1976)'s suggestion of using the practical road capacity instead of the steady-state road capacity for VDFs (Section 2.3.2). Even if the most suitable road capacity measurement location is identified, it is not realistic to measure traffic flow empirically at all locations.

Secondly, from the perspective of model estimations, the predetermination of both values would cause an error in the model. The initial case study showed that the error increases if inappropriate values are fixed in the modelling process. In addition, the existing methodology of nonlinear estimation shows that it is difficult to create estimation models without the predetermination of road capacity. Therefore, it is concluded that the uncertainty of road capacity would be fed into the whole model when using the existing VDF modelling approach.

The change in traffic characteristics: virtual bottleneck

Although the definitions of FFS and road capacity were unclear in travel time estimation, both values are useful in many areas of transport research. As comparative measures of traffic characteristics, both values are investigated in the initial case study. The measurement of various traffic data indicates that traffic characteristics in the initial case are affected by geometric features, including the tunnel environment. In particular, the identification of breakdown effects on each location in the initial case study suggests the presence of a virtual bottleneck near the entrance to the tunnel. Traffic breakdowns are known generally to occur at the beginning of bottlenecks which result in the formation of a change in vehicles' movements (Persaud *et al.*, 1998). In order words, the tunnel section forms a virtual bottleneck without a decrease in the number or width of lanes, and as such the bottleneck affects travel time estimation and traffic assignment in these sections. Therefore, the initial case study confirmed that new feasible travel time estimation models which take into account link attributes instead of road capacity should be developed for traffic assignment.

Suggestion of direction for data processing

The initial data analysis became the intermediate milestone for the main data processing in this study. The dataset used for feasible model estimations in this study should incorporate the attributes of links and likewise, traffic flow and travel time should also be measured on a link basis. In this regard, the initial study showed some limitations. Firstly, point-based ILD data does not measure the overall vehicle speed on a link but the instantaneous speed on a point, so the methodology in Section 3.4.2 suggests the concept of space-mean speed by using DSRC equipment from Korean ITS. Furthermore, geometric features were measured over the entirety of each link unlike the location-based measurement in the initial analysis. Lastly, the initial data analysis assisted in creating the methodology for filtering the dataset.

Discovery of base functions

Above all, the most important contribution from the initial case study was the discovery of the base functions for the main model development in this study. The functions are used for establishing the methodologies for statistical model estimation and geometric features consideration in Section 3.3.

Firstly, the initial study demonstrates that the quadratic function form would become the base function for the multivariate linear estimation as one stream of the methodology. Although the cubic function has a little better curve fitting result than the quadratic function, it was not analysed in this study because it is not convex. Again the linear estimation was divided into two main parts (Section 3.3.2): ordinary least squares (OLS) and generalised least squares (GLS) linear estimation. The former is to focus on the sum of square errors based on five statistical assumptions and the latter to consider the violations of the OLS estimation assumptions. In particular, the GLS linear estimation considers the variance structure and the time-series correlation between errors by recognising the dataset as the panel data.

Secondly, the BPR function form became the base function as another stream of the methodology in this study, which is the nonlinear estimation (Section 3.3.3). As well as trying to introduce new model forms for travel time estimation, this study also tries to improve the existing VDF approach by adding geometric features to the models. Moreover, the customised models can be used for comparison with the newly estimated models. However, this methodology would continue to bear the limitation of road capacity uncertainty as discussed through the sensitivity analysis (Section 4.3.4 and 5.3.2)

3.3. Development of model estimation methdology

3.3.1. Overview of model estimation

Summary of existing approaches

As previously reviewed in the literature, travel time estimation models are used in many countries as link cost (or performance) functions in traffic assignment. In particular, current VDFs predict travel time on different road links mainly at a macroscopic level. The feature which is in common to many types of VDFs is the inclusion of FFS and road capacity with parameters. In order to cover the diversity of link performance, VDFs incorporate different FFS, road capacity and parameters depending on link characteristics such as road classification, region and the number of lanes.

When examining the process of customisation in detail, many studies predetermine FFS and road capacity based on real data before customising the parameters of analysed VDFs (Kalaee, 2010; Huntsinger and Rouphail, 2011; Kim *et al.*, 2014). Firstly the studies selected a few links for a day or several days. Second, as mentioned in Section 2.4.2, FFS and road capacity were measured in different ways. Third, the studies adopted nonlinear estimation methodology most commonly by minimising least squares of errors. Finally, some of the studies tried to validate the derived models by applying them to hold-out samples.

Two main streams for new methodology

Two approaches for developing new travel time estimation models by the regression analysis were selected in this study. The strategy used for modelling can be categorised as the multivariate linear estimation and the nonlinear estimation. Even though most VDFs have been derived by nonlinear estimation methods with the nonlinear functional forms that cannot be linearised, the linear estimation with linearised functional forms was also selected because it has many advantages including clarity and transferability. The strengths and weaknesses of either approach are presented in Table 3-6.

Table 3-6. Strengths and weaknesses of linear and nonlinear estimation

	Multivariate linear estimation (Using linearised functional forms)	Nonlinear estimation (Using BPR function)
Strengths	• Widely used for regression analysis • Unique solution can be derived. • Easy to find the best solution (simpler than nonlinear estimation) • Possible to extend the model to population	• Possible to have the best curve fit • Possible to use existing models or theories

	• Possible to confirm the significance of derived parameters • Straightforward as it uses the absolute coefficient of determination such as R-squared	
Weaknesses	• Difficult to find the best curve fit. • Some existing theories might be ignored. • Strictly satisfies/adheres to statistical assumptions.	• Iterative method is necessary (computationally intensive). • Sometimes multiple solutions exist. • Sometimes local optimisation issues arise (constraints may be necessary) • Initial (starting) values are necessary. • Solutions could be confined to analysed samples (difficult to validate inferred results) • Difficult to guarantee the significance of derived parameters

Source: summarised from Montgomery et al. (2012)

3.3.2. Multivariate linear estimation

Base model selection for linear estimation

Montgomery *et al.* (2012) defined multivariate linear estimation models broadly as in Equation 3-8,

$$y = \beta_0 + \sum \beta_i z_i + u \qquad \text{Equation 3-8}$$

where z_i can be any types of functions with one or more independent variables of x_i without parameters in the functions; and u is the error term. For example, y =$\beta_0 + \beta_1 x_1 + \beta_2 \sin(x_2) + \beta_3 x_1 x_3 + \beta_4 \exp(x_4) + \beta_5 x_5^2 + u$ can be a functional form for the multivariate linear estimation.

As mentioned in Section 3.2.3, the quadratic function was chosen as a base function type for the multivariate linear estimation. In particular, the linear estimation has the advantage that FFS and road capacity do not need to be predetermined as which contrasts with the existing nonlinear approach. After collecting data for the geometric features, the linear estimation is consolidated with results from the other IVs. The analysed base model for the linear estimation reflecting link geometric variables can be seen in Equation 3-9. As derived in Section 3.2.3, the relationship between travel time and traffic flow can be represented as a quadratic function and the relationship between travel time and geometric features as a linear function. Even though the functional forms for geometric variables can be various as in Equation 3-8, this study assumes the functional form is linear because the relationship between travel time and geometric features has not been identified well unlike the relationship between travel time and traffic flow. In addition, Montgomery *et al.* (2012) explains that empirical models can be approximated with the simple linear functional form if the true function is unknown.

$$TT = \beta_0 + \beta_1 TF + \beta_2 TF^2 + \sum \gamma_k Geometry_k + u \qquad \text{Equation 3-9}$$

where the dependent variable is TT (travel time), IVs are TF (traffic flow); $Geometry_k$ (k refers to different link geometric features); parameters are β_0, β_1, β_2 and γ_k; and u is the error term.

OLS linear estimation analysis

OLS linear estimation is widely used in many studies including econometrics and engineering because of its simplicity and the utilisation of comparative statistical measures. However, a model using the OLS estimation should satisfy many assumptions (these are described later in this section).

OLS derives the estimators by minimising the sum of squares, which is calculated from the differences between the observed dependent variables and the predicted ones by the estimated function. Firstly, the linear matrix formulation can be described as follows;

$$\boldsymbol{Y} = \boldsymbol{X\beta} + \boldsymbol{\varepsilon} \qquad \text{Equation 3-10}$$

where Y is a dependent variable matrix (n×1, n = the number of samples), X is an independent variable matrix (n×p, p = the number of independent variables), $\boldsymbol{\beta}$ is a coefficient matrix (p×1) and $\boldsymbol{\varepsilon}$ is a residual error matrix (n×1). In order to attain the basic OLS objective, the objective function can be defined as follows;

$$S(\beta) = \sum_{i=1}^{n}\left(y_i - \sum_{j=1}^{p} X_{ij}\beta_j\right)^2 = (\boldsymbol{Y} - \boldsymbol{X\beta})^T(\boldsymbol{Y} - \boldsymbol{X\beta}) \qquad \text{Equation 3-11}$$

The OLS estimator $\widehat{\boldsymbol{\beta_{OLS}}}$ can be derived by solving normal equations for minimising the function of $S(\beta)$ as follows;

$$\widehat{\boldsymbol{\beta_{OLS}}} = \underset{\beta}{\operatorname{argmin}}\, S(\beta) \qquad \text{Equation 3-12}$$

$$(\boldsymbol{X^T X})\widehat{\boldsymbol{\beta_{OLS}}} = \boldsymbol{X^T Y}, \quad therefore \quad \widehat{\boldsymbol{\beta_{OLS}}} = (\boldsymbol{X^T X})^{-1}\boldsymbol{X^T Y}$$ Equation 3-13

OLS assumptions

Although some studies adopted OLS linear regression analysis in the development of travel time estimation models, they were not much interested in statistical assumptions (Brilon and Bressler, 2004; Cartenì and Punzo, 2007; DfT, 2018). It is imperative to check that statistical assumptions are satisfied because real traffic data can be influenced by many factors. There are numerous statistical fundamental assumptions that OLS linear regression modelling should satisfy (Washington *et al.*, 2010). If any models cannot meet the assumptions, the linear regression model cannot have the best linear unbiased estimators (BLUE).

Washington *et al.* (2010) emphasises the six main assumptions as follows: the zero mean of disturbances; the normality of disturbances; the uncorrelatedness of independent variables and disturbances; the homoscedasticity of disturbances; no serial correlation in the disturbances; and model specification errors. The last assumption is related to the fundamental issue of model estimation, so the violation of the last assumption would require a different model selection. It is related to the reasons such as omitting important variables, including irrelevant variables, using incorrect functional form and multicollinearity. Therefore, the statistical tests for OLS estimation models are closely related to the first five assumptions.

The first and second assumptions can be denoted in the expression of the simple linear regression model (Equation 3-14) as follows;

$$Y_i = \beta_0 + \beta X_i + u_i$$ Equation 3-14

$$E[u_i] = 0$$ Equation 3-15

$$u_i \approx N(0, \sigma^2)$$ Equation 3-16

where Y_i is the dependent variable; X_i is the independent variable; β_0 is the intercept; β is the coefficient of X_i; and u_i is the error term. Equation 3-15 shows that the expected value of errors or the sum of errors is zero and Equation 3-16 means that errors are approximately normally distributed with the mean of zero and the variance of σ^2. With regards to these two assumptions, the dataset used in this study can be assumed to be normally distributed by central limit theorem[5] because it has a large sample measured every 15 minutes. In addition, the large sample size could help find exact parameters in the analysed models (Washington *et al.*, 2010).

The third assumption implies that independent variables are influenced by factors outside the model; that is, the dependent variable does not directly determine independent variables. This requirement can be described as follows;

$$COV[X_i, u_j] = 0 \quad \text{for all } i \text{ and } j \qquad \text{Equation 3-17}$$

The fourth assumption, the violation of which is called heteroscedasticity, requires constant variance of residuals in the OLS regression model in Equation 3-18. The violation of this assumption could reduce the precision of OLS estimated parameters. Notwithstanding this, heteroscedasticity only affects the efficiency of estimators, but does not affect consistency and unbiasedness (Washington *et al.*, 2010).

$$VAR[u_i] = \sigma^2 \qquad \text{Equation 3-18}$$

Scatter residual error plots can be used for finding heteroscedasticity intuitively (Figure 3-6). If the variance has an increasing or decreasing tendency on residual plots, the regression is said to be heteroscedastic. There are numerous statistical tests for detecting heteroscedasticity, which are supported by statistical software packages including R. (Goldfeld and Quandt, 1965; Park, 1966; Breusch and Pagan, 1979; White, 1980)

Figure 3-6 Homoscedastic residual plots (left); heteroscedastic disturbances (right)

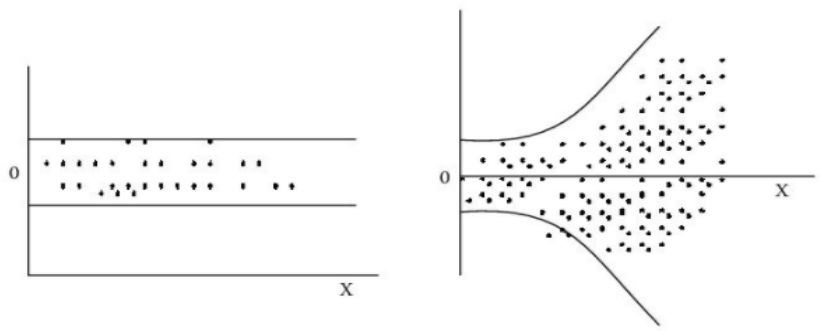

Source: Washington *et al.* (2010)

[5] If a sample has a large number of observations and each observation is calculated from the mean of the observed values, the sample is closely normally distributed regardless of the population distribution.

The fifth assumption, the violation of which is called serial correlation, requires the condition that disturbances are not correlated with adjacent disturbances. Serial correlation is related to the efficiency of parameters, but not to the unbiasedness and consistency of models, similar to heteroscedasticity (Washington *et al.*, 2010). Serial correlation is known to occur in time-series datasets. This assumption can be shown as follows;

$$COV[u_i, u_j] = 0 \quad \text{if } i \neq j \qquad \text{Equation 3-19}$$

Figure 3-7 shows the various serial correlation patterns of scatter residual plots that result in a trend over independent variables. The widely used statistical test for detecting serial correlation is the Durbin-Watson (DW) test (Durbin and Watson, 1951). The DW statistic is derived from the relationship between adjacent residuals. The serial correlation is expected not to exist when the DW statistic is near two. There are other tests for serial correlation such as the Breusch-Godfrey test and the Wooldridge test (Breusch, 1978; Godfrey, 1978; Wooldridge, 2010). It is noteworthy that Washington *et al.* (2010) raised the issue that many transportation studies and projects ignored this assumption.

Figure 3-7 Patterns of serial correlation disturbances

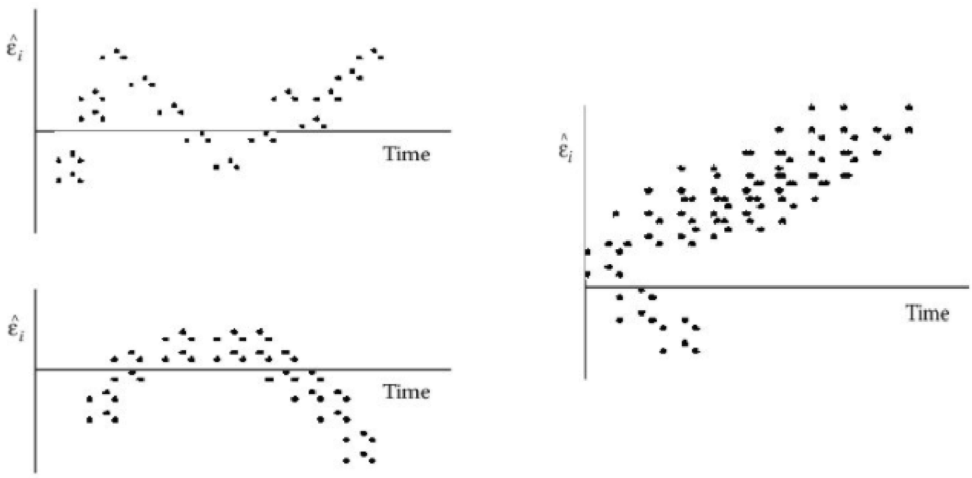

Source: Washington *et al.* (2010)

Panel data

In order to specify models in the linear model estimation, it is necessary to consider the characteristic of dataset used in the study. The explanatory variables in the dataset are traffic flows measured every 15 minutes and five time-invariant geometric features varying according to sections. Therefore, statistical approaches which take account of the characteristics of panel data are worth scrutiny in this study even though the independent variables of geometric features are fixed over time.

In statistics and econometrics, panel data are defined as the combination of time-series data and cross-section data (Diggle *et al.*, 2002; Fitzmaurice *et al.*, 2004; Washington *et al.*, 2010). Hsiao (2014) mentioned three advantages to panel data analysis: one is to improve the efficiency of parameter estimation by increasing degrees of freedom with time-series data; the second is to enable researchers to analyse the intervention of the specific subjects varying according to different periods; and the third is to make it possible to test the cross-sectional homogeneity by including additional parameters in estimated models.

While cross-section data is observed on n subjects (entities), panel data incorporates observations on n entities at $T \geq 2$ time periods. This can be denoted as follows;

$$(X_{it}, Y_{it}), i = 1, \ldots, n \text{ and } t = 1, \ldots, T \qquad \text{Equation 3-20}$$

where the index i refers to each subject (e.g. n = 72 analysed links in this study) while t refers to the analysed time period (e.g. T = 1 (month) * 30 (days) * 24 (hours) * 4 (*15 minutes) = 2,880 time intervals in each link).

Fixed effects modelling for panel data

Fixed effects modelling can reflect entity (or individual) or time heterogeneity in panel data analysis (Baltagi, 2008; Washington *et al.*, 2010). As travel time can be influenced by many factors as well as traffic volume and geometric features, it is imperative to investigate the change in the estimation of each model according to different entities, times or both entities and times. In addition, Washington *et al.* (2010) found that many transportation studies adopted these models (Eskeland and Feyzioğlu, 1997; Dee, 1999; Loizides and Tsionas, 2002; Chu and Durango-Cohen, 2008).

Fixed effects modelling can be divided into one-way (fixing effects by entity) and two-way (fixing effects by both entity and time) error component models. Heterogeneity effects across entities (or times) or across both entities and times can be absorbed by the intercept term under the assumption that heterogeneity effects are constant for each entity (or time period) or for each entity during each time period (Hsiao, 2014). Therefore, the model for this study (Equation 3-9) can be generalised as follows;

$$TT_{it} = \beta_0 + \beta_1 TF_{it} + \beta_2 TF_{it}^2 + \sum \boldsymbol{\gamma_k Geometry_{k,it}} + u_{it} \qquad \text{Equation 3-21}$$

where i refers to the cross-sectional units; t refers to time periods; β_0 is the intercept; β_1 and β_2 are the parameters of traffic flow variables (scalars); $\boldsymbol{\gamma_k}$ is the parameters of geometric feature variables (k×1 vector); TF_{it} is a traffic flow variable according to entities and times; $Geometry_{k,it}$ is geometric feature variables (1×k vector) in this study; and u_{it} is the section-specific error term. In particular, the residual term can be written as $u_{it} = \mu_i\ (or\ \lambda_t) + \varepsilon_{it}$ in one-way error component modelling and $u_{it} = \mu_i + \lambda_t + \varepsilon_{it}$ in two-way error component modelling where μ_i is the unobserved cross-sectional specific effects, λ_t is the unobservable time effects, and ε_{it} are random or idiosyncratic disturbances.

The statistical estimation methods for fixed effects can mainly be divided into two; the least squares dummy variable (LSDV) and the fixed effects estimation within the group (or entity). Equation 3-21 can be transformed for LSDV as follows;

$$TT_{it} = \beta_1^{LSDV} TF_{it} + \beta_2^{LSDV} TF_{it}^2 + \sum \boldsymbol{\gamma_k^{LSDV} Geometry_{k,it}} + \sum \delta_i Dummy_i + u_{it} \quad \text{Equation 3-22}$$

where $Dummy_i$ (i=1, 2, 3…, n) is dummy variables for entities (e.g. 72 sections, days, routes) and δ_i is the coefficient for each dummy variable. On the other hand, fixed effects estimation within the group uses OLS regression with the demeaning variables. In other words, after calculating the mean from the original variables, the demeaned variables are used for OLS regression. The equation after averaging the observation across time can be derived from Equation 3-21 as follows;

$$\overline{\mathrm{TT}_{it}} = \beta_0 + \beta_1 \overline{TF_{it}} + \beta_2 \overline{TF_{it}^2} + \sum \boldsymbol{\gamma_k \overline{Geometry_{k,it}}} + \overline{u_{it}} \quad \text{Equation 3-23}$$

where $\overline{\mathrm{TT}_{it}} = \frac{1}{T}\sum_{t=1}^{T} TT_{it}$; $\overline{TF_{it}} = \frac{1}{T}\sum_{t=1}^{T} TF_{it}$; $\overline{TF_{it}^2} = \frac{1}{T}\sum_{t=1}^{T} TF_{it}^2$; $\boldsymbol{\overline{Geometry_{k,it}}} = \frac{1}{T}\sum_{t=1}^{T} \boldsymbol{Geometry_{k,it}}$; $\overline{u_{it}} = \frac{1}{T}\sum_{t=1}^{T} u_{it}$; and T is the count of observations. After subtracting Equation 3-23 from Equation 3-21, the coefficients of demeaned variables can be derived as β_1^{FE}, β_2^{FE}, $\boldsymbol{\gamma_k^{FE}}$ without an intercept because β_0 is eliminated. In addition, the unobserved cross-sectional specific effects (μ_i) are eliminated and idiosyncratic disturbances (ε_{it}) remain.

As mentioned above, both approaches of LSDV and fixed effects estimation within a group can be commonly used for eliminating unobserved fixed effects not varying according to time. However, LSDV estimation would be more appropriate for this study because the approach can identify the effects of entities on the model as the coefficients of dummy variables. In addition, by applying various entities to the model estimation, the effects of each entity were investigated. The entities that can be separated from the dataset were divided into links, routes (lines), brightness (daytime and nighttime), date, days (weekdays and weekends), and weather. The first two entities can be classified as cross-sectional fixed effects and the last four ones as time fixed effects. The combination of cross-sectional and time fixed effects was considered in this study.

Random effects modelling with panel data

The biggest difference between FE modelling and random effects (RE) modelling is that whilst FE modelling assumes that the cross-sectional specific effects (μ_i in Equation 3-21) are correlated with the explanatory variables, RE modelling does not allow the correlation (Kurt, 2018). In other words, FE modelling can eliminate unobserved time-invariant (potentially omitted) variables and their constant effects, but RE modelling cannot reflect the omitted variables. In addition, unlike FE modelling, RE modelling can include time-invariant explanatory variables across entities (e.g. geometric features across links in this study). When recalling Equation 3-21 (Equation 3-24), RE modelling defines the expected value and variance of cross-sectional specific effects (μ_i in Equation 3-25 and Equation 3-26) unlike FE modelling. Whilst FE modelling has the same statistical assumptions as OLS, RE modelling assumes a homoscedastic variance of residuals together with serially correlated covariance of residuals. $VAR(u_{it}) = \sigma_\mu^2 + \sigma_\varepsilon^2 \ (for\ all\ i\ and\ t)$, and as such RE modelling considers serial correlation only for the residuals of the same cross-sectional unit with a constant covariance, which is $COV(u_{it}, u_{js}) = \sigma_\mu^2 \ (for\ i = j, t \neq s)$ (Washington *et al.*, 2010; Kurt, 2018).

$$TT_{it} = \beta_0 + \beta_1 TF_{it} + \beta_2 TF_{it}^2 + \sum \boldsymbol{\gamma_k Geometry_{k,it}} + \mu_i + \varepsilon_{it}$$ Equation 3-24

$$E\left[\mu_i | TF_i, TF_i^2, \boldsymbol{Geometry_{k,i}}\right] = 0$$ Equation 3-25

$$VAR\left[\mu_i \middle| TF_i, TF_i^2, \boldsymbol{Geometry_{k,i}}\right] = \sigma_\mu^2$$ Equation 3-26

GLS (Generalised least squares) linear estimation analysis

Once one or more of the OLS statistical assumptions are violated, the first thing to do is to question the model specification. On the assumption that the established models can explain the dataset, some remedies can deal with the violations without discarding the predetermined models. Washington *et al.* (2010) suggested several methods for dealing with heteroscedasticity: transformation of the dependent variable; WLS estimation; ridge regression; and GLS estimation. In addition, they presented the GLS linear estimation as the time-series analysis for treating serial correlation. Therefore, the GLS linear estimation considering time-series data can provide an alternative to the OLS linear estimation for the purposes of this study. Since the GLS estimation would cause the decrease of the sum of squared errors, the GLS estimation needs to be chosen only when the OLS statistical assumptions are violated.

The fundamental difference between OLS and GLS is that GLS can generalise the disturbance terms while OLS strictly assumes that the disturbances have constant variance and are not correlated (Fox and Weisberg, 2010; Washington *et al.*, 2010). For demonstrating GLS, the linear equation can be set out by using vectors as follows;

$$\boldsymbol{Y} = \boldsymbol{X\beta} + \boldsymbol{\varepsilon} \qquad \text{Equation 3-27}$$

where the statistical conditions of the matrix of disturbances ($\boldsymbol{\varepsilon}$) under OLS assumptions can be shown as follows;

$$E[\boldsymbol{\varepsilon} \mid \boldsymbol{X}] = 0, \qquad VAR[\boldsymbol{\varepsilon} \mid \boldsymbol{X}] = \sigma^2 \boldsymbol{I} \qquad \text{Equation 3-28}$$

where I is the n×n identity matrix (where n is the total number of observations). Conversely, the conditions of disturbances in GLS can be generalised as follows;

$$E[\boldsymbol{\varepsilon} \mid \boldsymbol{X}] = 0, \qquad VAR[\boldsymbol{\varepsilon} \mid \boldsymbol{X}] = \boldsymbol{E}[\boldsymbol{\varepsilon\varepsilon^T}] = \sigma^2 \boldsymbol{\Omega} \qquad \text{Equation 3-29}$$

where $\boldsymbol{\sigma^2\Omega}$ is a variance-covariance matrix and $\boldsymbol{\Omega}$ is a symmetric non-singular matrix. $\boldsymbol{\Omega^{-1}} = \boldsymbol{C^T C}$ using the lower triangular matrix $\boldsymbol{C}$ for computational iterative calculations (Amemiya, 1985). The general linear function (Equation 3-27) can be transformed into Equation 3-31 by pre-multiplying $\boldsymbol{C}$ as follows;

$$\boldsymbol{Y}^* = \boldsymbol{CY}, \quad \boldsymbol{X}^* = \boldsymbol{CX}, \quad \boldsymbol{\varepsilon}^* = \boldsymbol{C\varepsilon} \qquad \text{Equation 3-30}$$

$$\boldsymbol{Y}^* = \boldsymbol{X}^*\boldsymbol{\beta} + \boldsymbol{\varepsilon}^* \qquad \text{Equation 3-31}$$

Equation 3-31 is satisfied with OLS assumptions as follows;

$$E[\boldsymbol{\varepsilon}^*] = \boldsymbol{C}E[\boldsymbol{\varepsilon}] = \boldsymbol{0} \qquad \text{Equation 3-32}$$

$$VAR[\boldsymbol{\varepsilon}^*] = E\left[\boldsymbol{\varepsilon}^*\boldsymbol{\varepsilon}^{*T}\right] = E[\boldsymbol{C\varepsilon\varepsilon^T C^T}] = \boldsymbol{CE}[\boldsymbol{\varepsilon\varepsilon^T}]\boldsymbol{C^T} = \sigma^2\boldsymbol{C\Omega C^T} = \sigma^2\boldsymbol{I} \qquad \text{Equation 3-33}$$

Therefore, GLS minimises the objective function as with OLS and the GLS estimator of $\boldsymbol{\beta}$ can be derived as follows;

$$S(\beta) = (\boldsymbol{Y}^* - \boldsymbol{X}^*\boldsymbol{\beta})^T(\boldsymbol{Y}^* - \boldsymbol{X}^*\boldsymbol{\beta}) = (\boldsymbol{Y} - \boldsymbol{X\beta})^T\boldsymbol{\Omega^{-1}}(\boldsymbol{Y} - \boldsymbol{X\beta}) \qquad \text{Equation 3-34}$$

$$\widehat{\boldsymbol{\beta_{GLS}}} = \left(\boldsymbol{X^T\Omega^{-1}X}\right)^{-\boldsymbol{1}}\boldsymbol{X^T\Omega^{-1}Y} \qquad \text{Equation 3-35}$$

Compared to Equation 3-13, it can be seen that the GLS estimator is derived by weighting $\boldsymbol{\Omega^{-1}}$ to the equation. The GLS estimator is also derived for maximising log-likelihood (LL) function by using MLE for normally distributed disturbances as follows (Fox and Weisberg, 2010);

$$LL = -\frac{n}{2}\ln(2\pi) - \frac{1}{2}\ln(\det(\boldsymbol{\Omega})) - \frac{1}{2}(\boldsymbol{Y} - \boldsymbol{X\beta})^T\boldsymbol{\Omega^{-1}}(\boldsymbol{Y} - \boldsymbol{X\beta}) \qquad \text{Equation 3-36}$$

Especially when heteroscedasticity exists, $\boldsymbol{E}[\boldsymbol{\varepsilon\varepsilon^T}] = \sigma^2\boldsymbol{\Omega}$, where $\sigma^2\boldsymbol{\Omega}$ is n×n matrix as follows;

$$\sigma^2\boldsymbol{\Omega} = \begin{pmatrix} \sigma_1^2 & 0 & . & 0 \\ 0 & \sigma_2^2 & . & 0 \\ . & . & . & . \\ 0 & 0 & . & \sigma_n^2 \end{pmatrix} \qquad \text{Equation 3-37}$$

As the matrix is a diagonal matrix of unequal error variances, which corresponds to the definition of heteroscedasticity, $\widehat{\boldsymbol{\beta_{GLS}}}$ is the same as the WLS estimators, which can be derived just by "*lm()*" function in software package R after adding weights to each of the variables (Fox and Weisberg, 2010). In this context, WLS can be said to be a special case of GLS.

When serial correlation is present, $\boldsymbol{E}[\boldsymbol{\varepsilon\varepsilon^T}] = \sigma^2\boldsymbol{\Omega}$, where $\sigma^2\boldsymbol{\Omega}$ is n×n matrix as follows;

$$\sigma^2\boldsymbol{\Omega} = \sigma^2\begin{pmatrix} 1 & \rho_1 & \rho_2 & . & \rho_{n-1} \\ \rho_1 & 1 & \rho_1 & . & \rho_{n-2} \\ \rho_2 & \rho_1 & 1 & . & \rho_{n-3} \\ . & . & . & . & . \\ \rho_{n-1} & \rho_{n-2} & \rho_{n-3} & . & 1 \end{pmatrix} \qquad \text{Equation 3-38}$$

In practice, if the matrix has different (n-1) values of ρ_i, it is impossible to estimate models with GLS (Fox and Weisberg, 2010). Therefore, GLS needs to establish additional structure for dealing with serial correlation. Assuming that time-series data are stationary, ARMA models can be used for specifying the structure (Washington *et al.*, 2010). ARMA models are the combination of the autoregressive models (AR) and the moving average models (MA). In ARMA (*p, q*), *p* refers to the autoregressive order and *q* refers to the moving average order. For example, the first-order auto-regressive process, AR(1) is described as follows;

$$\varepsilon_t = \phi\, \varepsilon_{t-1} + \nu_t \qquad \text{Equation 3-39}$$

where ν_t is called "Gaussian" white noise, which means ν_t is independent and normally distributed, $\nu_t \approx$ NID(0, σ_ν^2) (Fox and Weisberg, 2010). After applying the AR(1) model to Equation 3-38, $\rho_1 = \phi$, $\rho_i = \phi^i$, and $\sigma^2 = \sigma_\nu^2/(1-\phi^2)$.

By contrast, the MA model assumes that the current disturbances of ε_t depend on white noises during the current and previous periods. For the example, the first-order moving average process, MA(1) is denoted as follows;

$$\varepsilon_t = \nu_t + \theta\nu_{t-1} \qquad \text{Equation 3-40}$$

Therefore, ARMA(1,1) can be expressed as follows;

$$\varepsilon_t = \phi\, \varepsilon_{t-1} + \nu_t + \theta\nu_{t-1} \qquad \text{Equation 3-41}$$

The '*gls()*' function in the "**nlme"** library of the software package R enables regression analysis by using GLS with a non-constant error-variance structure including dealing with heteroscedasticity and serial correlation (Pinheiro and Bates, 2000). In order to derive GLS estimators, the maximum likelihood estimation (MLE) method can be used, which the '*gls()*' function also supports.

3.3.3. Nonlinear least squares (NLS) estimation

Base model selection for NLS estimation

This approach follows the methodology of existing VDF studies that predetermine road capacity and free-flow speed, but differs in that it separates link geometric variables, rather than condensing these features by set parameters. The analysed base function reflecting link geometric variables for the NLS estimation is seen in Equation 3-42. This model combines the finding that link geometry affects travel time with the way in which existing studies set FFS and road capacity as constant values. As with the linear estimation (Section 3.3.2), it is approximated that the relationship between travel time and geometric variables is linear because the relationship has not been clearly identified in the previous studies. The BPR function, which is a combination of a linear and power equation, was used as a base model because the BPR function has a good performance for motorways compared with other VDFs (Kalaee, 2010; Huntsinger and Rouphail, 2011).

$$TT = FFTT\left(1 + \alpha\left(\frac{TF}{C}\right)^{\beta}\right) + \sum \gamma_k Geometry_k + u \qquad \text{Equation 3-42}$$

Selection of estimation method

An iterative method used in this study is the "Gauss-Newton" algorithm, which is widely used for non-linear regression analysis (Montgomery et al., 2012). Linearisation by Taylor Series theorem is used for this analysis, which uses partial derivatives of parameters with initial values. If $f(x_i, \theta)$ is a non-linear function with *i* IVs and p parameters, the function can be linearised with the initial values $\theta_0^{'} = [\theta_{10}, \theta_{20}, \dots, \theta_{p0}]$ as

$$f(x_i, \theta) = f(x_i, \theta_0) + \sum_{j=1}^{p}\left[\frac{\partial f(x_i, \theta)}{\partial \theta_j}\right]_{\theta=\theta_0}(\theta_j - \theta_{j0}) \qquad \text{Equation 3-43}$$

$$y_i - f_i^0 = \sum_{j=1}^{p} \beta_j^0 Z_{ij}^0 + \varepsilon_i, \qquad i = 1,2,\dots,n \qquad \text{Equation 3-44}$$

where $f_i^0 = f(x_i, \theta_0)$, $\beta_j^0 = \theta_j - \theta_{j0}$ and $Z_{ij}^0 = \left[\frac{\partial f(x_i,\theta)}{\partial \theta_j}\right]_{\theta=\theta_0}$. Equation 3-44 can be simplified as

$$y_0 = Z_0\beta_0 + \varepsilon \qquad \text{Equation 3-45}$$

so the parameter β_0 after linearization can be estimated as

$$\widehat{\beta_0} = (Z_0^T Z_0)^{-1} Z_0^T y_0 = (Z_0^T Z_0)^{-1} Z_0^T (y - f_0) \qquad \text{Equation 3-46}$$

Since $\beta_0 = \theta - \theta_0$, θ_1 for the next calculation can be set as

$$\widehat{\theta_1} = \widehat{\beta_0} + \theta_0 \qquad \text{Equation 3-47}$$

The iteration can be finished after convergence satisfying the set small number of δ

$$[(\widehat{\theta_{J,k+1}} - \widehat{\theta_{Jk}})/\widehat{\theta_{Jk}}] < \delta \qquad j = 1,2,\dots,p$$ Equation 3-48

Unlike R-squared as an absolute coefficient of determination in OLS linear estimation, Root Mean Square Error (RMSE) in nonlinear estimation can be a comparative statistical measure. This analysis would be significant through the comparison with RMSEs of previously analysed models, including the theoretical BPR function with parameters. However, nonlinear estimation needs careful consideration because it involves the issue of local optimisation as well as providing multiple solutions as mentioned in Table 3-6. The starting values or constraints need to be set because they could affect the convergence of estimators in this analysis. The starting values for α and β parameters in Equation 3-42 are set at 0.15 and 4 respectively, with reference to the standard BPR function. The starting value of an intercept for FFTT is set at 36 (seconds/km), which is equivalent to time per km with a speed limit of 100kph. The starting values of other parameters for geometric independent variables are set at zero.

Sensitivity Analysis by road capacity

In the literature review (Section 2.4), there is no consensus about the value of road capacity in VDF models even though many studies adopt various methods for measuring it. Again, as most VDF models commonly include road capacity and FFTT, the stochastic values of road capacity would be insufficient to account for travel time in the road sections. Moreover, although USHCM (2010) suggested a different value for road capacity according to its geometry (e.g. grade, width), it is unclear how much the change in road capacity affects the statistical measures of VDF models. Therefore, sensitivity analysis is imperative for nonlinear regression analysis to find the impact of the road capacity variation.

Sensitivity analysis aims to find the level of uncertainty of the results caused by the uncertainty of the independent variables in many studies (Saltelli *et al.*, 2008). The only factor for sensitivity analysis in this study is the predetermined road capacity in VDF models including Equation 3-42, therefore the sensitivity analysis can be subdivided as follows: the derivation of different parameters depending on the range of road capacity and an investigation of the change in outputs as affected by different values of road capacity when applying the derived nonlinear model to different sections.

Even if there are no clear criteria used in establishing road capacity in VDF, it is necessary to define the value of road capacity as a reference of sensitivity analysis, which is called nominal road capacity ($C=C_n$ in Equation 3-42) in this study. Moreover, although it is debatable how to fix one value of road capacity for covering all analysed sections, the nominal road capacity was defined as the mean of traffic flows corresponding to speeds from 60 to 80kph referring to various measurement in many studies (see Section 2.4.2). In addition, the minimum traffic flow for the nominal capacity measurement was limited to 2,000vph per two lanes because abnormal traffic flows (caused by for example vehicle breakdown, road maintenance or measurement error) should be excluded. The range of threshold speeds is also related to breakdown effects and the historical speed at which congestion begins in motorways (see Section 2.4.2).

The first approach for sensitivity analysis is to examine the change in parameters depending on the range of road capacity (fluctuation from 80% to 120%[6] of the nominal capacity). The increment is determined as 10% of the nominal road capacity, which can be adjusted after analysing the result. This approach aims to find how road capacity affects the current VDF models (Table 3-7). The second approach is to examine the spatial transferability of the models developed from the first approach. Once a model had been derived from each road capacity, the model was applied to other road sections with each road capacity measured using the same method as the nominal capacity. The second approach is conducted to find out how the sum of squared errors (SSE) between observed travel time and the outputs by the model can vary depending on the variation of road capacity (Table 3-8).

Table 3-7 Table form for sensitivity analysis focusing on the change in parameters

	α	β	γ_k	RMSE
80% of C_n				
90% of C_n				
C_n				
110% of C_n				
120% of C_n				

Table 3-8 Table form for sensitivity analysis focusing on spatial transferability

	80% of C_n		C_n		120% of C_n	
	C (Measured)	SSE	C (Measured)	SSE	C (Measured)	SSE
Selected Case 1						
Selected Case 2						
Selected Case 3						
Selected Case 4						
Selected Case 5						

Note. SSE can be replaced by other accuracy measures (e.g. RMSE, MAPE, etc.)

[6] The range was determined by considering twice the standard deviation of extracted traffic flows based on the criteria of the selection of nominal capacity.

3.4. Identification of variables

3.4.1. Variables for model estimations

Dependent variable (DV)

DV is the inverse value of SMS in each selected link, the unit of which is seconds/km. The reason why the inverse value of speed is selected is that every link has a different length. Speed can be measured and calculated according to two types: TMS and SMS (FHWA, 1998). TMS can simply be calculated as the arithmetical average value of vehicles' speeds (Equation 3-49). By contrast, SMS, which is the harmonic average speed, is the link length divided by the average time of vehicles passing between the starting and end points of a link (Equation 3-50). Both speeds can be approximated by using SMS variance (Equation 3-51), but SMS calculated from the travel time measurement is more accurate than the approximation. It is reasonable to use SMS in this study because the accuracy of DV measurement is very important. In addition, FHWA recommended the use of SMS for analysing travel time data.

$$Time - Mean\ Speed, \bar{s}_{TMS} = avg.speed = \frac{\sum s_i}{n} = \frac{\sum \frac{d}{t_i}}{n} \qquad \text{Equation 3-49}$$

$$Space - Mean\ Speed, \bar{s}_{SMS} = \frac{distance\ travelled}{avg.travel\ time} = \frac{d}{\frac{\sum t_i}{n}} = \frac{n \times d}{\sum t_i} \qquad \text{Equation 3-50}$$

$$\bar{s}_{TMS} \approx \bar{s}_{SMS} + \frac{\sigma_{SMS}^2}{\bar{s}_{SMS}} \qquad \text{Equation 3-51}$$

where d = distance travelled; n = number of observations; s_i = speed of the *i*th vehicle; t_i= travel time of the *i*th vehicle; and σ_{SMS}^2 = variance of SMS.

Independent variables (IVs)

IVs in this study can mainly be divided into two groups: traffic flow and link geometry. The selected IVs are five: traffic flow (IV1, vph), tunnel ratio (IV2, the total tunnel length per distance, m/km), the sum of rises per distance (IV3, m/km), the sum of falls per distance (IV4, -m/km), and the sum of bendiness per distance (IV5, deg/km). Table 3-9 summarises the potential candidate independent variables and the reasons why only the five variables are slelected. Some of factors that could affect link travel time are identified by LSDV or fixed effects modelling even though they cannot be included in feasible models because it is difficult to measure them quantitatively.

Table 3-9 Candidates and selection of geometric variables

Name	Considerations
Traffic flow	All VDFs show the relationship between travel time and trip demand in common.
Traffic composition	Mentioned in the limitation of this study (Section 7.3).
The number of lanes	Not considered (Exclusion in the case selection).
Lane width	All motorways have the same lane width.
Lane clearance	All motorways have the same lane clearance.
Intersection existence (type)	Intersections are nodes that separate links (VDFs are defined for each link) and additional traffic flows arise from them.
Tunnel length	Tunnel length can be a representative variable for tunnels because most characteristics of a tunnel are constant.
Tunnel light brightness	Difficult to measure.
Rises of slope (degree of slope)	The criteria to define road capacity theoretically and to be selected by the reviewed studies.
Falls of slope (degree of slope)	The UK manual (DfT, 2018) include this variable.
Bendiness	The UK manual (DfT, 2018) include this variable.
Barrier (or guard rail) type	Most motorways have the same types of barrier.
Signpost	Difficult to measure.
Emergency parking (service)	Not considered (Exclusion in the case selection).
Daily change	Identified by fixed effects modelling.
Weather (rain) impact	Difficult to measure. Identified by fixed effects modelling.
Day (week/weekend) impact	Identified by fixed effects modelling.

Note. Shadowed areas are the selected independent variables in feasible models.

Traffic flow is the independent variable that is commonly included in existing models. The variable is also included in this study because the fundamental relationship in all traffic theories demonstrates travel time that depends on traffic flow in order to explain steady and congested states. Traffic composition (heavy vehicle percentage) is an important variable in relation to traffic flow, but this variable is not included in this study because current Korean ITS does not provide the data for it in sufficient detail. Automatic vehicle identification (AVI) systems, which operate by recognising the vehicle registration number plate, are a very efficient way of classifying vehicle types (Ahmed and Abdel-Aty, 2011). However, these are seldom used on Korean motorways and they are not therefore part of the selected links for this case study. In addition, this study tries to overcome this limitation through fixed effects modelling with the entity of date in the panel data (Section 4.2.2) and through the selection of the one-day dataset during a national holiday that could decrease the impact of heavy vehicle percentage for the feasible model estimation (Section 5.2.1). Although the traffic composition is an important variable, the three reviewed studies (Section 2.5.2) that generalise travel time estimation models without road capacity do not include this variable in their models (Cartenì and Punzo, 2007; DfT, 2018) or include the variable only in congested states (Brilon and Bressler, 2004)

Link geometry is the other group of IVs, which are analysed in this study. The selected IVs in this study should be measurable and quantifiable (or binary). According to the Korean road design manual (MOLIT, 2015), link geometric features which affect design speed in motorways are the number of lanes; lane width; the central barrier type and width; lane clearance; degree of slope; radius of the horizontal curve; types of intersection; tunnels; and road accessories for safety and maintenance. These features are therefore the candidates for the variables of link geometry in this study, but not all these features were selected as IVs as mentioned in the scope of research (Section 1.4). First, the number of lanes is one of the criteria determining FFS, road capacity and the parameters in the current Korean VDF, but the variable is not included in this study. This study analyses only 2-lane motorway sections because the low number of 3-lane (or more) tunnel sections cannot confirm the spatial transferability depending on the diversity of link geometry. Second, lane width, central barrier width and lane clearance can be excluded from the variables in this study because they almost always have the same values in every motorway section. Third, types of intersection were not considered in this study because one of the base conditions for the link division is homogeneous (Rakha and Tawfik, 2009). Intersections are locations that divide routes into links. Lastly, variables such as road accessories cannot be measured from the freeway management system (FMS) for Korean motorways. Therefore, degree of slope, the radius of the horizontal curve and tunnels are analysed as IVs for this study. In addition, the selected geometric features are in line with the existing studies and manuals (Koshi, 1985; Iwasaki, 1991; Koshi *et al.*, 1992; Brilon and Bressler, 2004; Yun and Shengrui, 2012; Kim *et al.*, 2014; DfT, 2018)

In order to quantify variables and offset the effects of the different lengths of analysed links, it is necessary to transform the selected raw road features into adequate variables. Firstly, the degree of slope is divided into rises in upgrades and falls in downgrades for identifying the effects by upgrade and downgrade respectively with reference to UK guidance (DfT, 2018). The sum of rises in upgrade sections and the sum of falls in downgrade sections are divided by the total length of each link. Secondly, the radius of the horizontal curve is transformed into the total bendiness of the horizontal curve. A horizontal curve segment consists of simple curves and spiral (transition) curves even though a spiral curve is not necessary when the radius of simple curves is large. (UK Highways Agency, 2002; MOLIT, 2015). The radius cannot be used as a variable because the radius of a transition curve changes along the distance from the starting point. Therefore, the sum of bendiness of simple curves and transition curves is used as an IV in this study. Lastly, the tunnel ratio, which is the sum of tunnel lengths divided by the total link length, is selected as an IV because most tunnels have the same structure in Korean motorways and data for other tunnel features such as light factors and interior design cannot be collected from FTMS.

3.4.2. Data collection

DV: Inverse of SMS (Inv_SPD)

As mentioned in Section 3.4.1, speed can be divided into TMS and SMS. SMS is used in this study in order to improve the reliability of data analysis even though TMS measured from the ILDs in a motorway tunnel section was used for finding base models as mentioned in Section 3.3.1. There are two systems for measuring travel time between two or more points for calculating SMS: AVI and the DSRC system. The AVI system has the advantage that it collects the information from all vehicles but the drawback is that it is used sparsely on motorways because of the cost of CCTV installation. The DSRC system, which is related to ETC, collects the travel time of vehicles with OBU between locations of RSE. Around 71% (14.6 million) of registered vehicles have OBU and the usage rate of ETC is 74.2% in South Korea (ITS KOREA, 2016). This study collects the data for the dependent variable from the DSRC system because the distance of RSE in the DSRC system is very dense and the usage rate of ETC can confirm the reliability of the data. Table 3-10 illustrates data collected from the DSRC system. The collection period covers the month of September 2018. During this period, one of Korea's biggest national holidays occurred from the 23rd to the 25th of the month, so many vehicles moved across the nation at that time.

Table 3-10. Example of DSRC raw data

DSRC_DATE	DSRC_SECT_ID	AVG_TRAVL_TM	WHOLE_DATA_CNT	MAX_TRAVL_TM	MIN_TRAVL_TM	M_TRAVL_TM	USE_DATA_CNT	SPD_SMS
201809241215	0140LNE030	202	80	222	183	203	52	95.17
201809241220	0140LNE030	193	61	211	183	193	41	99.61
201809241225	0140LNE030	198	66	217	185	198	46	97.09
201809241230	0140LNE030	192	84	206	177	192	54	100.13
201809241235	0140LNE030	191	74	207	177	190	53	100.65
201809241240	0140LNE030	187	64	209	171	186	47	102.8
201809241245	0140LNE030	186	52	202	172	185	35	103.35
201809241250	0140LNE030	195	71	218	176	194	44	98.58
201809241255	0140LNE030	193	63	219	173	193	48	99.61
201809241300	0140LNE030	189	59	207	175	186	48	101.71
201809241305	0140LNE030	190	58	210	172	189	41	101.18
201809241310	0140LNE030	210	105	228	193	209	77	91.54

where DSRC_DATE is measured time (5-min interval); DSRC_SECT_ID is the name of RSE unit pairs; AVG_TRAVL_TM is the average travel time of all vehicles having OBU during the measurement period; WHOLE_DATA_CNT is the number of vehicles having OBU during the period; MAX_TRAVL_TM is the longest travel time of all data; MIN_TRAVL_TM is the shortest travel time of all data; M_TRAVL_TM is the average travel time except for the longest and shortest travel times; USE_DATA_CNT is the number of vehicles not having the highest and lowest travel times; and SPD_SMS is the space-mean speed that is calculated from the distance of RSE unit pairs divided by AVG_TRAVL_TM.

Travel time (TT) is used in this study after aggregating the value over 15-minute intervals; this is for reasons of conformity with most existing models and also because this study does not pursue modelling based on the instantaneous change of travel time. This data collection method is in line with the traffic flow measurement method, which counts vehicles passing at a point for 15 minutes and converts them into hourly rates by multiplying by four. When considering concepts of SMS and TMS in Section 3.4.1, errors can be included in analysed datasets where use is made of the arithmetical mean of three consecutive values of 5-minute travel time in DSRC without considering the number of vehicles every five minutes. Therefore, DV must be calculated from the total sum of travel times recorded in DSRC for 15 minutes divided by the total number of recorded vehicles during the same period. DV is finally created from mean travel time for 15 minutes divided by the distance between RSEs in DSRC, which is equivalent to the inverse of space-mean speed for 15 minutes. The derivation of DV can be shown as follows;

$$Average\ TT\ for\ 15\ minutes = \frac{Total\ TT_{15min}}{Total\ NV_{15min}}$$

$$= \frac{\sum(AVG\_TRAVL\_TM_{5min} * WHOLE\_DATA\_CNT_{5min})}{\sum WHOLE\_DATA\_CNT_{5min}} \qquad \text{Equation 3-52}$$

$$Inverse\ of\ SPD = \frac{Average\ TT\ for\ 15\ minutes}{The\ length\ (km)\ of\ each\ link}$$

where TT is travel time; NV is the number of vehicles; the subscripts mean the observation duration; others are the same as in Table 3-10.

IV1: Traffic flow (TF, vehicles per hour: vph)

The data for traffic flow, which is referred to as “TF” in this study and is the first IV, were collected from the average of the numbers measured at the different ILDs. Traffic flow can be differently measured depending on the measurement points because traffic flow has accordion-like patterns, so bottleneck point would be the best place for the measurement (Iwasaki, 1991).

However, it is impossible to measure traffic flow at every bottleneck point because the detecting location from ILDs is already fixed and the bottleneck is not stationary in real traffic situations. Therefore, this study used the average traffic flow measured at ILDs included in selected cases.

ILDs include traffic information including time, location, traffic flow, TMS and occupancy rate (Table 3-11). The traffic data is produced every minute, but aggregated traffic information data for five minutes is stored in ITS servers regardless of vehicle's types. Average traffic flow is the sum of traffic flows measured at ILDs divided by the number of ILDs and TF is calculated from multiplying the sum of three 5-min average traffic flows by four (Table 3-12). The collection period is the month of September 2018 as with the dependent variable. The unit of this IV is vehicles per hour (vph).

Table 3-11 Example of raw data from ILD

ST_YMDHM	VDS_ID	VOL	SPD_TMS
201809241215	0140VDE00606	135	99.83
201809241220	0140VDE00606	139	98.02
201809241225	0140VDE00606	138	104.52
201809241230	0140VDE00606	121	104.04
201809241235	0140VDE00606	134	105.17
201809241240	0140VDE00606	122	104.87
201809241245	0140VDE00606	130	100.43
201809241250	0140VDE00606	114	101.86
201809241255	0140VDE00606	120	103.32
201809241300	0140VDE00606	121	104.26
201809241305	0140VDE00606	141	97.24
201809241310	0140VDE00606	132	102.12

where ST_YMDHM is measured time (5-min interval); VDS_ID is the name of each ILD; VOL is traffic flow (vehicle count); and SPD_TMS is time-mean speed at each ILD.

Table 3-12 Calculation of average traffic flow

VDS_DATE	VDE00602_VOL	VDE00606_VOL	VDE00610_VOL	AVG_TF	TF_15Min*4
201809241205	152	122	129	134.33	
201809241210	150	134	131	138.33	
201809241215	154	135	129	139.33	1648.00
201809241220	172	139	144	151.67	
201809241225	162	138	133	144.33	
201809241230	180	121	136	145.67	1766.67
201809241235	154	134	127	138.33	
201809241240	138	122	119	126.33	
201809241245	162	130	133	141.67	1625.33
201809241250	150	114	124	129.33	
201809241255	124	120	98	114.00	
201809241300	154	121	116	130.33	1494.67

IV2: Tunnel ratio (TR, sum of tunnel lengths per link distance: m/km)

Tunnel ratio, which is referred to as "TR" in this study and is the second IV, was collected from FTMS. In order to offset the effects of the different length of links, the sum of tunnel lengths was divided by the length of each link. The unit of this IV is m/km. FTMS has much information on tunnel management, it includes not only tunnel length but also the tunnel entrance or exit milepost, tunnel slope degree, and the number of lanes and the horizontal curve radius (Table 3-13). Milepost and tunnel length were also used for matching tunnel locations with DSRC locations.

Table 3-13 Example of raw data from FTMS

Route	Tunnel_Name	Milepost(km)	Tunnel_length(m)	Deg_Slope	No._lanes	Radius_Curve (m)
Kochang-Damyang	Munsoosan_E*	7.20	3805	-0.5026	2	8000
Kochang-Damyang	Munsoosan_S**	7.20	3820	0.5065	2	8000

Note: _E (toward ending point) and _S (toward starting point) mean the direction of tunnels

IV3: Sum of rises per link distance (RISE, m/km)

The sum of rises per distance, which is referred to as "RISE" in this study and is the third IV, was measured directly from design drawings. Design drawings contain much information for construction along every 20-m station such as the current ground level, horizontal alignment, vertical alignment, and cut and fill for earthworks (Figure 3-10). Rises were extracted from the difference in elevation between two stations only in upgrade segments and then the sum of rises was divided by the total length of each case (Equation 3-53). With reference to the UK manual (DfT, 2018), in order to represent the attributes of a link, not a point, the difference in elevation was taken into account rather than the maximum degree of slope. The unit of this IV is m/km.

IV4: Sum of falls per link distance (FALL, m/km)

The method for collecting the sum of falls per distance, which is referred to as "FALL" in this study and is the fourth IV, is the same as IV3 of RISE (Equation 3-53). This IV always has a negative value (-m/km) because it was extracted only in downgrade segments.

$$RISE\ or\ FALL = \frac{\sum(Elevation_{ending} - Elevation_{starting})}{Total\ length\ of\ link} \quad \text{Equation 3-53}$$

IV5: Sum of bendiness per link distance (BEND, deg/km)

The sum of bendiness per distance, which is referred to as "BEND" here and is the fifth IV, is calculated from the sum of central angles in each horizontal curve and the sum was divided by the length of each case. In Figure 3-8 and Figure 3-9, the central angle is equal to the intersecting angle

(I), which is the sum of simple curve angle (Δ_c) and spiral angles (θ_s). According to Findley *et al.* (2015), these angles are derived from Equation 3-54 and Equation 3-56. The values for this calculation were collected from design drawings (Figure 3-10).

$$I = \Delta_c + 2\theta_s \qquad \text{Equation 3-54}$$

$$\Delta_c \approx \frac{L_c}{R} \qquad \text{Equation 3-55}$$

$$\theta_s \approx \frac{L_s}{2R} \qquad \text{Equation 3-56}$$

Figure 3-8 Elements of horizontal curve (L_c: simple curve, L_s: spiral curve)

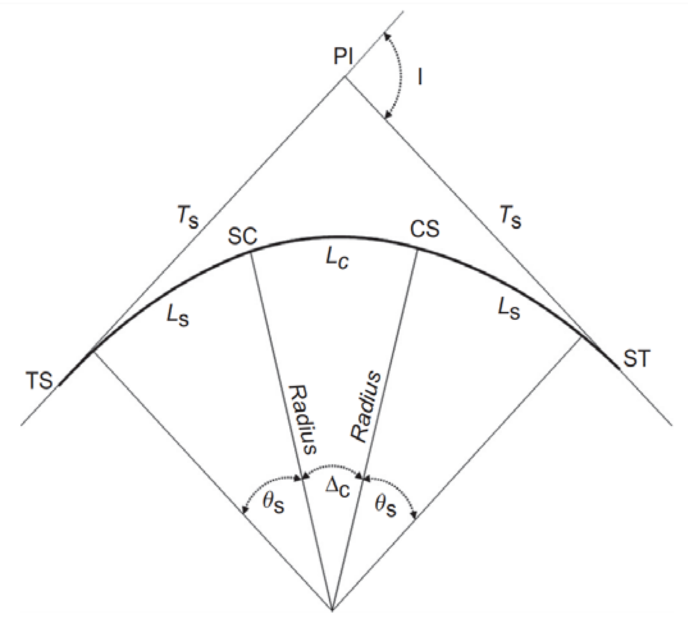

Source: Findley *et al.* (2015)

Figure 3-9 Elements of spiral curve

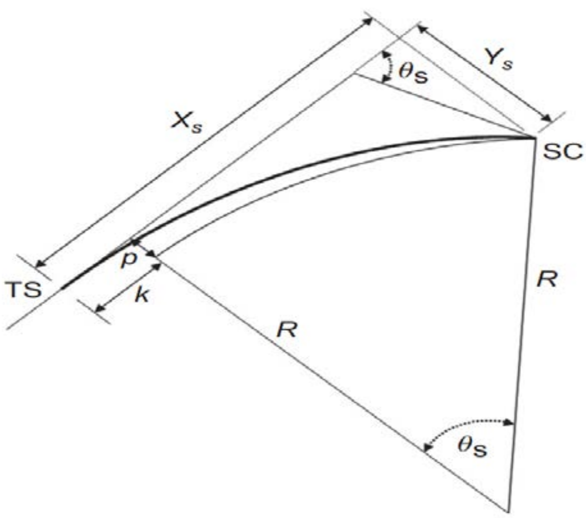

Source: Findley *et al.* (2015)

Figure 3-10 Example of design drawing: "Kochang-Damyang Motorway (6.08-6.40km) E"

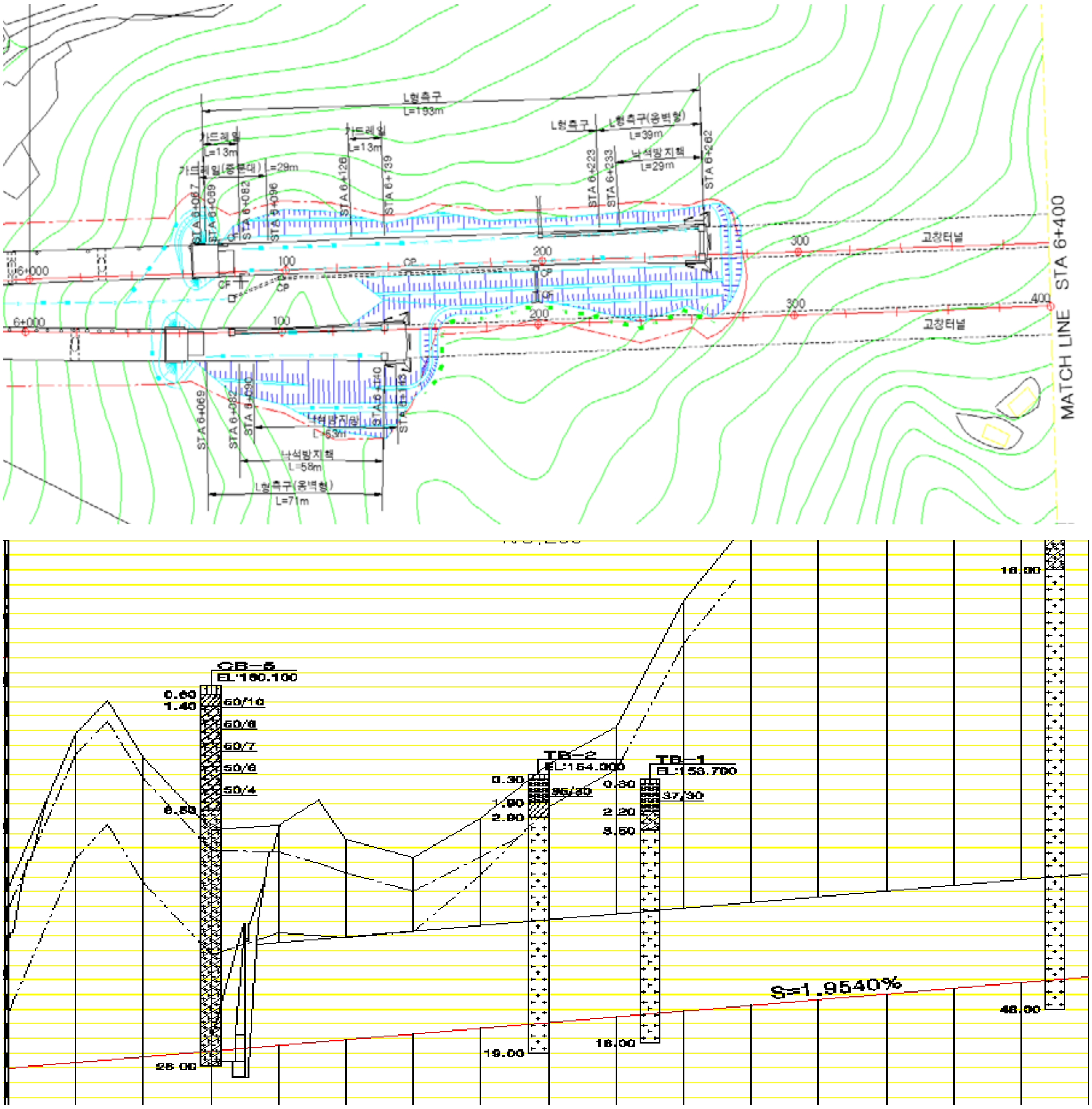

Design Elevation	133.96	134.35	134.74	135.13	135.52	135.91	136.30	136.69	137.08	137.47	137.86	138.25	138.65	139.04	139.43	139.82	140.21
Existing Ground	146.23	156.75	155.17	150.20	150.51	149.56	148.33	151.01	154.70	157.24	165.87	171.55	171.88	177.93	180.74	181.51	185.01
Cut- / Fill+	−12.28	−22.41	−20.43	−15.07	−14.99	−13.65	−12.03	−14.32	−17.62	−19.77	−28.01	−33.28	−33.24	−38.89	−41.31	−41.70	−44.80
Super-elevation Right	+2.0	+2.0	+2.0	+2.0	+1.6	+0.3	−1.0	−2.0	−2.0	−2.0	−2.0	−2.0	−2.0	−2.0	−2.0	−2.0	−2.0
Super-elevation Left	−2.0	−2.0	−2.0	−2.0	−2.0	−2.0	−2.0	−2.0	−2.0	−2.0	−2.0	−2.0	−2.0	−2.0	−2.0	−2.0	−2.0
Vertical allign	S = 1.9540% L = 1095.00																
Horizontal allign	IP = 1 R = 3400.0 CL=518.462																
Milepost	+6.080	+100	+120	+140	+160	+180	+200	+220	+240	+260	+280	+300	+320	+340	+360	+380	+400

Source: provided by Korean Express Corporation (KEC)

3.4.3. Data processing

As road traffic has many situations that cannot be quantified as independent variables in travel time estimation models, raw traffic data must be filtered or cleaned. The data measured in abnormal situations would reduce the accuracy and precision of estimation models and their estimators. In the process of data refinement, a researcher's personal perspective should be minimised. Therefore, raw data were filtered in the following ways.

Exclusion of data including extremely low traffic flow

Inevitably, there are abnormal samples in a one-month dataset for many differing reasons such as traffic accidents, road maintenance and vehicle breakdowns. However, such samples cannot be easily identified without additional information. First of all, measurement errors due to temporary technical failures of ILD or DSRC were excluded in the data analysis. Secondly, the rows where traffic flow is below 120vph (10 vehicles per five minutes) were excluded from the dataset. The initial data analysis found out that the variation of travel time in low traffic flow is much wider than that in mid or high traffic flow (Figure 3-11). Moreover, based on the frequency analysis of travel time recorded in DSRC, 22.8% of the raw data were not recognised in DSRC corresponding to hourly traffic flow from 12vph (one vehicle per five minutes) to 120vph. This means that the values of travel time observed on the low traffic flow would depend on a few vehicles having OBU. Conversely, only 0.6% of the raw data was not recorded in DSRC from 120vph to 240vph.

Exclusion of data in congested situations

From Greenshields *et al.* (1935) to Greenberg (1959) and Underwood (1961), the relationship between speed, density and traffic flow has been investigated. These comparative older studies assumed or conceptually defined the relationship between speed and traffic flow as symmetrical, so the half of free-flow speed is supposed to be the point at which congestion starts (the speed in the point is referred to as "congestion speed" hereafter). Congestion speed is also related to the speed at road capacity. However, this relationship has been reinvestigated by many more recent empirical studies (Section 2.3.1). The studies commonly defined the relationship as two-regime showing different curves before and after the congestion speed; and they do not therefore endorse the symmetrical curve assumed in earlier studies.

VDF assumes that traffic flow can increase continuously in oversaturation states because it reflects the cost of travel time depending on trip demand in traffic assignment (Section 2.3.1). The analysis of traffic characteristics in congested states can be the area of DTA which focuses on the interaction of vehicles rather than VDF modelling. Therefore, this study requires the definition of congestion speed that is the criterion for excluding congested data from the dataset. As the value of congestion speed differs according to road types and countries, it was necessary to examine studies to analyse the traffic data for Korean motorways. Kim (2013) found that congestion speed varies from 78kph to 83kph in finding maximum traffic flow and from 64kph to 70kph by using regression analysis. In addition, as can be seen from the initial case study (Figure 3-11), the congestion speed varies depending on six detecting points even in a comparatively short section (1.8km). Therefore, although the criterion cannot be defined uniquely, this study selected the congestion speed of 60kph to minimise the data exclusion referring to previous studies and the initial analysis.

Figure 3-11 Congestion speed identification from the initial case study

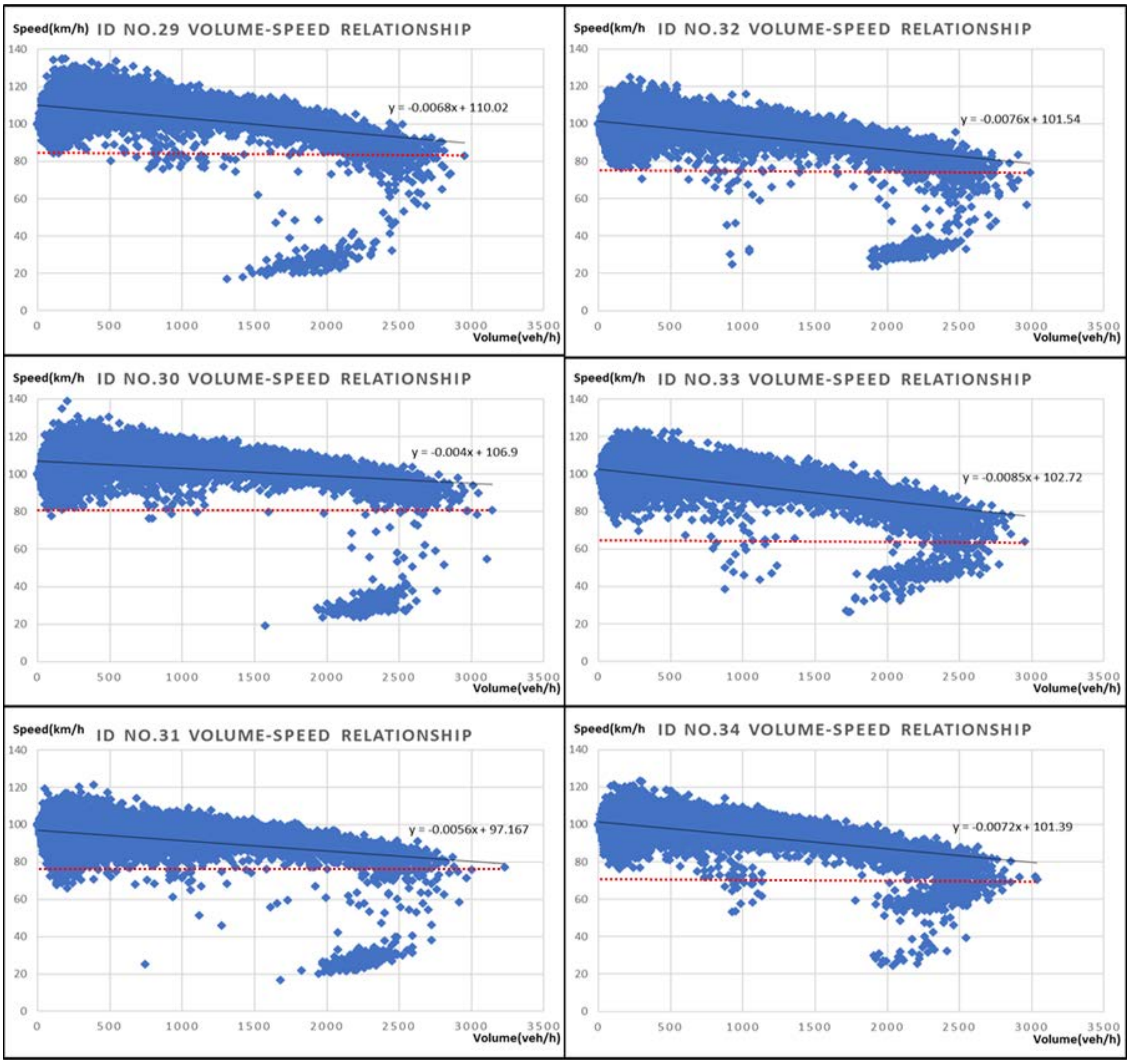

Note. Red dotted lines represent congestion speeds correspoding to the maximum traffic flows (five-minute observation) measured at ILDs

3.5. Case study

3.5.1. How to select cases

The choice of the number of cases for developing travel time estimation models is related to subjects per variable (SPV) (Schmidt, 1971; Green, 1991; Harrell, 2001) where subjects mean the estimated data varying according to the variable. Schmidt (1971) described the minimum number of SPV ranges as being from 15 to 20. Harrell (2001) suggested 10 SPV as the minimum number of required samples for linear regression analysis. The data to estimate the relationship between travel time and traffic flow are enough because the data are observed every 15 minutes. Given the geometric variables, subjects represent selected cases (links) because each link has a set of time-invariant geometric features. Thus, the number of SPV needs to be taken into consideration only by the number of geometric independent variables. If all independent variables are included in the final model, the necessary number of cases would range from 40 (=4×10) to 80 (=4×20) because the number of geometric independent variables is four. Moreover, the number of cases can be finally verified referring to various statistical results in the process of regression analysis.

The number of cases for this study is 72 sections (Table 3-14). The number of 2-lane tunnels is 935 of a total of 1,060 Korean motorway tunnels. As it is mandatory to install ILDs in tunnel sections of over 1km in Korea, 239 two-lane tunnel sections with a length over 1km were examined in the case selection process. Firstly, 132 sections were selected after excluding routes having low traffic flow during the analysis period. Secondly, 40 sections where speed enforcement cameras are installed and data collection errors happened during the month, were excluded from this study. Lastly, while collecting link geometric data from design drawings, 20 sections including interchanges or service areas were excluded. Therefore, 72 cases were used for modelling in this study. As shown in Figure 3-12, the cases in this study are located in nationwide 2-lane motorways.

Table 3-14 Procedure for the case selection

	Total	First cut	Second cut	Third cut
No. of cases (sections)		132	92	72
No. of Included tunnels	935	191	137	112
No. of Included tunnels over 1km	239	162	116	93
Criteria	2-lane tunnels	DSRC matching after Low-traffic cases exclusion	Exclusion of speed enforcement or data error sections (40)	Exclusion of sections including Interchage or service area (20)

Note: ( ); the number of excluded cases after every cut

Figure 3-12 Location of the selected cases

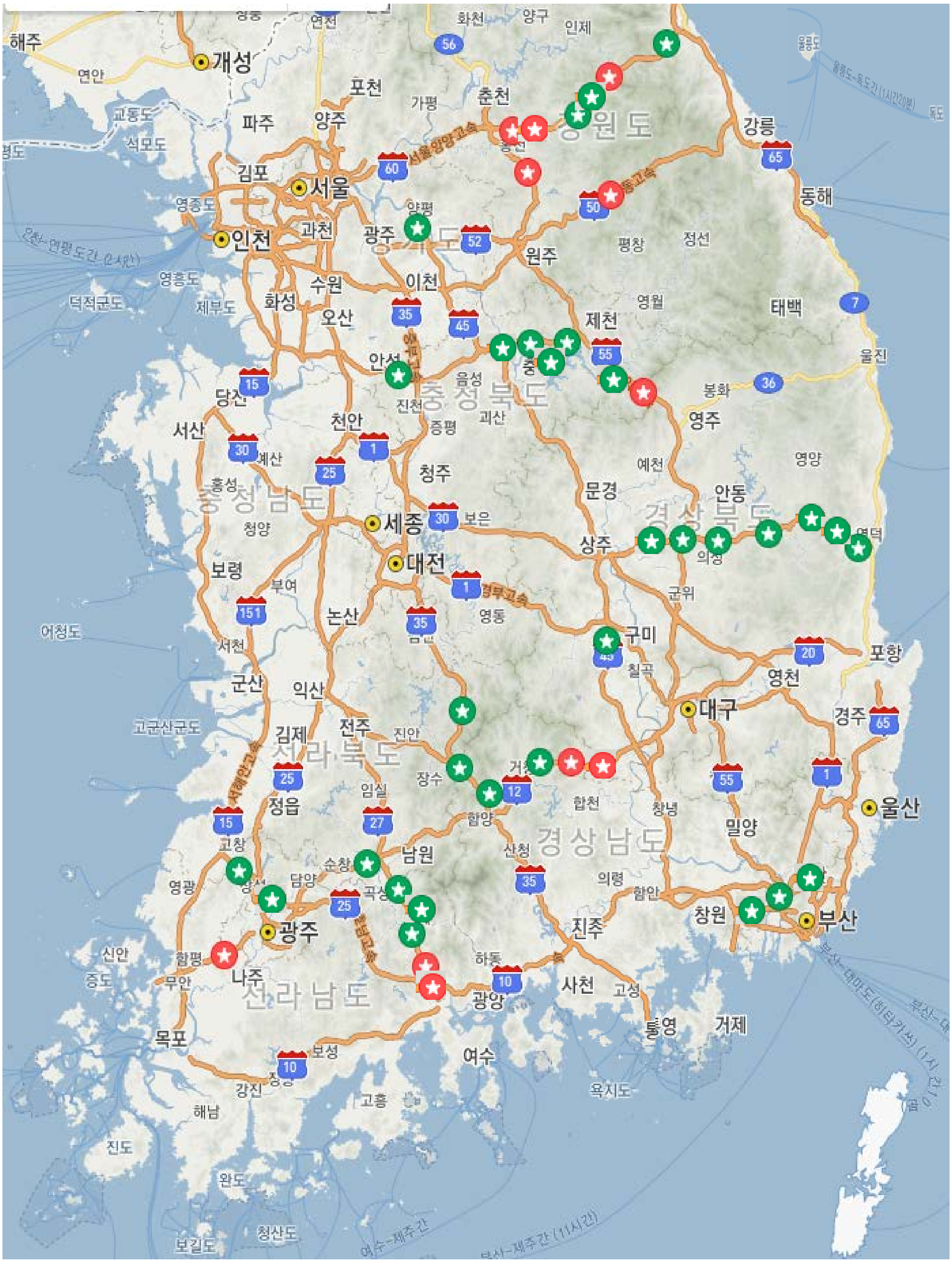

Source: https://map.kakao.com

Note 1. The orange lines represent Korean motorways.

2. Green marks (31*2=62 sections) denote the selection of both direction tunnels.

3. Red marks (10 sections) denote the selection of one of both direction tunnels.

3.5.2. Descriptive statistics for the selected cases

Dataset of cases including link geometry

There are 72 geometric feature sets because each case has one geometric feature set of TR, RISE, FALL and BEND as IVs. Moreover, each case contains one-month data including 15-minute interval travel time and traffic flow. Dataset including geometric features was completed by combining data from DSRC locations, FTMS and design drawings. As shown in Table 3-15, IVs were derived from measured data including total length of cases, tunnel length, the sum of rises in upgrade segments, the sum of falls in downgrade segments and the sum of intersection angles (bendiness).

Table 3-15 List of the selected cases

Case_Route_Milepost_Direction	Total length (km)	Total tunnel length (m)	Tunnel Ratio (IV2)	Upgrade sum of rises (m)	RISE (IV3)	Downgrade sum of falls (m)	FALL (IV4)	Sum of bendiness (deg)	BEND (IV5)
1. KochangDamyang (6.23-11.57k)_E	5.34	3,805	712.55	21.96	4.11	-33.78	-6.32	4.04	0.76
2. KochangDamyang (6.23-11.57k)_S	5.34	3,820	715.36	33.78	6.32	-21.96	-4.11	4.04	0.76
5. KochangDamyang (19.92-24.06k) E	4.14	3,598	869.08	20.16	4.87	-2.89	-0.70	0.00	0.00
6. KochangDamyang (19.92-24.06k) S	4.14	3,581	864.98	2.89	0.70	-20.16	-4.87	0.00	0.00
7. GwangjuDaegu (41.2-43.7K) E	2.5	1,592	636.80	2.04	0.82	-50.39	-20.16	56.68	22.67
8. GwangjuDaegu (41.2-43.7K) S	2.5	1,544	617.60	50.39	20.16	-2.04	-0.82	56.68	22.67
9. GwangjuDaegu (125.9-128.0K) E	2.1	1,170	557.14	32.50	15.48	-6.37	-3.03	46.85	22.31
10. GwangjuDaegu (125.9-128.0K) S	2.1	1,175	559.52	6.37	3.03	-32.50	-15.48	46.85	22.31
12. GwangjuDaegu (135.0-138.6K) S	3.6	2,787	774.17	61.68	17.13	-5.88	-1.63	24.75	6.87
14. GwangjuDaegu (138.6-143.3K) S	4.7	2,434	517.87	134.81	28.68	0.00	0.00	46.36	9.86
22. MuanGwangju (26.57-29.57) S	3	1,180	393.33	44.56	14.85	-16.08	-5.36	31.19	10.40
25. SangjuYoungduk (105.1-110.3) E	5.2	4,117	791.73	14.12	2.72	-50.05	-9.63	38.20	7.35
26. Sangju Youngduk (105.1-110.3) S	5.2	4,121	792.50	50.05	9.63	-14.12	-2.72	38.20	7.35
27. SangjuYoungduk(110.3-115.0) E	4.7	1,840	391.49	84.46	17.97	-15.19	-3.23	76.41	16.26
28. SangjuYoungduk (110.3-115.0) S	4.7	1,872	398.30	15.19	3.23	-84.46	-17.97	64.72	13.77
29. SangjuYoungduk (124.7-128.1) E	3.4	1,789	526.18	16.53	4.86	-7.58	-2.23	40.76	11.99
30. SangjuYoungduk(124.7-128.1) S	3.4	1,815	533.82	7.58	2.23	-16.53	-4.86	40.76	11.99
31. SangjuYoungduk (146.3-152.2) E	5.9	4,408	747.12	35.08	5.95	-21.81	-3.70	46.31	7.85
32. SangjuYoungduk (146.3-152.2) S	5.9	4,435	751.69	21.81	3.70	-35.08	-5.95	46.31	7.85
35. SangjuYoungduk (172.3-176.2) E	3.9	1,319	338.21	50.41	12.93	-13.15	-3.37	105.73	27.11
36. SangjuYoungduk(172.3-176.2) S	3.9	1,157	296.67	13.15	3.37	-50.41	-12.93	105.73	27.11
37. SangjuYoungduk (181.3-185.5) E	4.2	3,023	719.76	0.00	0.00	-26.15	-6.23	58.37	13.90
38. SangjuYoungduk (181.3-185.5) S	4.2	3,031	721.67	26.15	6.23	0.00	0.00	58.37	13.90
39. SangjuYoungduk(185.5-188.7) E	3.2	2,813	879.06	17.83	5.57	-9.45	-2.95	1.81	0.57
40. SangjuYoungduk (185.5-188.7) S	3.2	2,862	894.38	9.45	2.95	-17.83	-5.57	1.81	0.57
41. SeoulYangyang (63.8-70.1) E	6.33	3,431	542.04	44.59	7.04	-54.77	-8.65	33.73	5.33
43. SeoulYangyang (70.1-73.7) E	3.57	1,844	516.53	16.08	4.50	-24.32	-6.81	43.92	12.30
47. Seoul Yangyang(97.7-103.9) E	6.18	4,688	758.58	124.32	20.12	0.00	0.00	93.33	15.10

48. Seoul Yangyang (97.7-103.9) S	6.18	4,609	745.79	0.00	0.00	-124.32	-20.12	93.33	15.10
49. Seoul Yangyang(106.9-110.9) E	4.04	3,153	780.45	0.00	0.00	-43.53	-10.77	33.59	8.31
50. Seoul Yangyang(106.9-110.9) S	4.04	3,166	783.66	43.53	10.77	0.00	0.00	33.59	8.31
54. Seoul Yangyang(115.7-119.0) S	3.39	2,257	665.78	2.50	0.74	-12.73	-3.76	50.43	14.88
55. Seoul Yangyang(143.0-149.6) E	6.53	5,052	773.66	8.10	1.24	-95.92	-14.69	111.26	17.04
56. Seoul Yangyang(143.0-149.6) S	6.53	4,976	762.02	95.92	14.69	-8.10	-1.24	111.26	17.04
57. Suncheon Wyanju (7.8-12.5) E	4.74	2,736	577.22	28.90	6.10	-14.21	-3.00	81.57	17.21
59. Suncheon Wyanju (12.5-20.0) E	7.42	4,637	624.93	64.05	8.63	-25.87	-3.49	107.49	14.49
61. Suncheon Wyanju (25.1-32.6) E	7.53	2,520	334.66	75.66	10.05	-31.04	-4.12	125.91	16.72
62. Suncheon Wyanju (25.1-32.6) S	7.53	2,532	336.25	31.04	4.12	-75.66	-10.05	125.91	16.72
65. Suncheon Wyanju (37.9-41.8) E	3.87	1,310	338.50	53.61	13.85	-7.84	-2.03	63.25	16.34
66. Suncheon Wyanju (37.9-41.8) S	3.87	1,295	334.63	7.84	2.03	-53.61	-13.85	63.25	16.34
67. Suncheon Wyanju (41.8-46.6) E	4.78	3,987	834.10	0.00	0.00	-23.25	-4.86	27.87	5.83
68. Suncheon Wyanju (41.8-46.6) S	4.78	3,944	825.10	23.25	4.86	0.00	0.00	27.87	5.83
83. Jungbunaeryuk (106.4-108.1-109.50) E	3.1	1,055	340.32	12.07	3.89	-23.28	-7.51	76.72	24.75
84. Jungbunaeryuk (106.4-108.1-109.50) S	3.1	1,045	337.10	23.28	7.51	-12.07	-3.89	76.72	24.75
93. Jungbunaeryuk (290.6-295.4) E	4.8	3,084	642.50	35.80	7.46	-27.10	-5.65	101.45	21.14
94. Jungbunaeryuk (290.6-295.4) S	4.8	3,094	644.58	27.10	5.65	-35.80	-7.46	101.45	21.14
97. Jungang (237.4-244.9) E	7.5	4,600	613.33	22.41	2.99	-77.14	-10.29	72.47	9.66
99. Jungang (267.8-270.4) E	2.6	1,190	457.69	0.00	0.00	-36.04	-13.86	33.60	12.92
100. Jungang (267.8-270.4) S	2.6	1,150	442.31	36.04	13.86	0.00	0.00	33.60	12.92
102. Jungang (349.3-351.4) S	2.1	1,429	680.48	27.99	13.33	-5.06	-2.41	13.46	6.41
103. Jungang-Branch (1.1-3.4) E	2.3	1,851	804.78	17.41	7.57	-1.87	-0.81	9.95	4.33
104. Jungang-Branch (1.1-3.4) S	2.3	1,850	804.35	1.87	0.81	-17.41	-7.57	9.95	4.33
105. Jungang-Branch (4.3-5.4) E	1.1	540	490.91	2.46	2.24	-6.44	-5.85	22.68	20.62
106. Jungang-Branch (4.3-5.4) S	1.1	550	500.00	6.44	5.85	-2.46	-2.24	22.68	20.62
107. Jungang-Branch (5.4-8.0) E	2.6	1,295	498.08	19.10	7.35	-16.73	-6.43	35.64	13.71
108. Jungang-Branch (5.4-8.0) S	2.6	1,300	500.00	16.73	6.43	-19.10	-7.35	35.64	13.71
117. TongyoungDaejeon (113.2-115.6) E	2.4	1,455	606.25	11.93	4.97	0.00	0.00	45.84	19.10
118. TongyoungDaejeon (113.2-115.6) S	2.4	1,505	627.08	0.00	0.00	-11.93	-4.97	45.84	19.10
119. TongyoungDaejeon (127.6-131.8) E	4.2	3,170	754.76	4.45	1.06	-30.35	-7.23	46.66	11.11
120. TongyoungDaejeon (127.6-131.8) S	4.2	3,170	754.76	30.35	7.23	-4.45	-1.06	46.66	11.11
121. TongyoungDaejeon (153.1-155.9) E	2.8	1,148	410.00	0.00	0.00	-46.60	-16.64	25.80	9.21
122. TongyoungDaejeon (153.1-155.9) S	2.8	1,126	402.14	46.60	16.64	0.00	0.00	25.80	9.21
123. Pyungtaek Jaecheon (48.9-52.1) E	3.2	2,300	718.75	6.12	1.91	-20.63	-6.45	27.09	8.46
124. Pyungtaek Jaecheon (48.9-52.1) S	3.2	2,355	735.94	20.63	6.45	-6.12	-1.91	27.09	8.46
125. Pyungtaek Jaecheon (105.1-107.3) E	2.2	1,062	482.73	22.93	10.42	0.00	0.00	37.90	17.23
126. Pyungtaek Jaecheon (105.1-107.3) S	2.2	1,079	490.45	0.00	0.00	-22.93	-10.42	37.90	17.23
127. Pyungtaek Jaecheon (112.0-115.7) E	3.7	2,645	714.86	0.00	0.00	-22.03	-5.95	41.24	11.15
128. Pyungtaek Jaecheon (112.0-115.7) S	3.7	2,619	707.84	22.03	5.95	0.00	0.00	41.24	11.15
129. Pyungtaek Jaecheon (115.7-118.9) E	3.2	2,499	780.94	51.28	16.03	-0.61	-0.19	25.65	8.02
130. Pyungtaek Jaecheon (115.7-118.9) S	3.2	2,465	770.31	0.61	0.19	-51.28	-16.03	25.65	8.02
131. Pyungtaek Jaecheon (118.9-123.9) E	5	4,427	885.40	0.53	0.11	-33.75	-6.75	36.18	7.24
132. Pyungtaek Jaecheon (118.9-123.9) S	5	4,465	893.00	33.75	6.75	-0.53	-0.11	36.18	7.24

Descriptive statistics of the selected cases

Before modelling by using the dataset, it is necessary to investigate the frequencies of the selected cases. As shown in Table 3-16, the descriptive statistics of geometric features for the selected 72 cases were scrutinised briefly. The total length of the 72 cases ranges from 1.1km to 7.53km and the tunnel ratio (IV2) ranges from 296.67 to 894.38 (m/km) with the mean statistic of 627.78 (m/km) and the standard deviation of 169.02 (m/km). Moreover, RISE (IV3) and FALL (IV4) are skewed towards zero (a flat terrain) because road engineers aim to design flat roads considering special constraints such as earthwork balance because of safety and energy consumption. The variation of both variables ranges from 0 (a flat link) to 28.68 (m/km) and from -20.16 (m/km) to 0 (a flat link) respectively. The mean values of both variables are 6.51 (m/km) and -5.70 (m/km) respectively. Lastly, BEND (IV5) is examined from 0 (a straight link) to 27.11 (deg/km) with the mean statistic of 12.54 (deg/km).

Table 3-16 Descriptive statistics of the 72 selected cases

	N	Minimum	Maximum	Mean	Std. Deviation
Total length (km)	72	1.10	7.53	4.00	1.53
Sum of tunnel lengths (m)	72	540	5052	2541	1250
Tunnel Ratio (IV2, m/km)	72	296.67	894.38	627.78	169.02
Upgrade sum of rises (m)	72	0.00	134.81	26.28	27.73
RISE (IV3, m/km)	72	0.00	28.68	6.51	6.08
Downgrade sum of falls (m)	72	-124.32	0.00	-23.34	24.76
FALL (IV4, m/km)	72	-20.16	0.00	-5.70	5.22
Sum of bendiness (deg)	72	0.00	125.91	48.43	31.47
BEND (IV5, deg/km)	72	0.00	27.11	12.54	6.75

3.6. Model selection

3.6.1. Comparison of results across methodologies

This section presented the different aspects of statistical estimations for the dataset from 72 cases. The methodology for model development can be divided into two main streams: the regression analysis based on linearity between the dependent variable and independent variables; and nonlinear regression analysis based on BPR function among existing VDF models. Moreover, linear estimations consist of the OLS and GLS estimation according to the respective detailed assumptions for satisfying the linearity. Therefore, the models in this study can be classified into three groups: models by OLS, models by GLS, and models by NLS. The optimal model within each group can be determined according to the statistical measures produced by the estimated method of the group. However, other statistical measures are needed to evaluate models between groups. This study adopted the statistical measures of AIC, BIC, RMSE and MAPE as follows.

AIC and BIC (comparison between linear models)

R-squared is defined as the ratio of the regression sum of squares to the total sum of squares calculated from the independent variable(s) (Equation 3-57). Adjusted R-squared is calculated after reflecting degrees of freedom (Equation 3-58). Both measures have been widely used as coefficients of determination for comparison in the OLS estimation (Washington *et al.*, 2010). However, the measures are not used in the GLS estimation because the GLS estimation is based on maximising the (log)-likelihood function (Equation 3-36)

$$R^2 = \frac{SST - SSE}{SST} = \frac{SSR}{SST} = 1 - \frac{SSE}{SST} \qquad \text{Equation 3-57}$$

where SST= total sum of squares ($= \sum(Y_i - \bar{Y}_i)^2$), SSE = sum of square errors or residuals ($= \sum\left(Y_i - \hat{Y}_i\right)^2$), SSR = the regression sum of squares ($= \sum\left(\hat{Y}_i - \bar{Y}_i\right)^2$).

$$R^2_{adjusted} = 1 - \left(\frac{n-1}{n-p}\right)\frac{SSE}{SST} \qquad \text{Equation 3-58}$$

where n is the number of observations and p is the number of independent variables.

Instead of R-square, the corrected Akaike's Information Criterion (AIC) (Equation 3-59) and the Bayesian Information Criterion (BIC, Equation 3-60) can be used for comparing linear models (Akaike, 1974; Burnham and Anderson, 2004). Since the results both from minimising the least squares function (Equation 3-11) and from maximising likelihood function are identical in the OLS estimation (Washington *et al.*, 2010), the statistics of AIC and BIC can be derived in OLS as well as GLS estimations. Therefore, the criteria can also be used for comparison between OLS and GLS estimated models. Both criteria are calculated from multiplying the log-likelihood by -2, so the models having the smallest AIC and BIC from the same dataset are regarded as better models. The difference between the two criteria is that BIC penalises models as the number of parameters increases more than AIC does.

$$AIC = -2LogLikelihood + 2k + \frac{2k(k+1)}{(n-k-1)} \qquad \text{Equation 3-59}$$

$$BIC = -2LogLikelihood + kln(n) \qquad \text{Equation 3-60}$$

where k is the number of parameters and n is the number of observations in the estimated models.

RMSE and MAPE (comparison between linear and nonlinear models)

In addition to the comparison between linear estimation models, finding optimal models through the comparison between linear and nonlinear estimation models is also important in this study. This is also meaningful in that the newly introduced model in this thesis is compared with the existing modelling approach. As discussed above, nonlinear regression analysis does not produce many statistical measures of determination unlike linear estimation because it estimates models through iterative calculations to minimize the errors between observations and predicted values without prior assumptions including the distribution and variance of residuals.

Therefore, statistical accuracy measures, which are calculated from errors and observations, can be used to compare linear and nonlinear models. Most of the measures commonly include the absolute or squared of the errors in the equation, and evaluate how well the model can explain the observations. Among these measures, it is known that RMSE (MSE), MAD and MAPE are mainly used for transportation studies (Washington *et al.*, 2010). Since RMSE gives comparatively high weights to large errors before they are averaged, RMSE is more useful than MAD when evaluating models where large errors are undesirable. In addition, MAPE can be useful in that it produces the average of the ratio of the predicted values to actual values. Therefore, both measures of RMSE and MAPE are used to compare the accuracy of all models in this study.

Table 3-17 Statistical accuracy measures for the model evaluation

Measure	**Equation**	**Measure**	**Equation**
Mean error	$ME = \frac{\sum \varepsilon_i}{n}$	Mean absolute deviation	$MAD = \frac{\sum \lvert\varepsilon_i\rvert}{n}$
Sum of squared errors	$SSE = \sum \varepsilon_i^2$	Mean squared error	$MSE = \frac{\sum \varepsilon_i^2}{n}$
Root mean squared error	$RMSE = \sqrt{\frac{\sum \varepsilon_i^2}{n}}$	Standard deviation of errors	$SDE = \sqrt{\frac{\sum \varepsilon_i^2}{n-1}}$
Percentage error	$PE_t = \frac{Y_t - \hat{Y}_t}{Y_t} \times 100\%$	Mean percentage error	$MPE = \frac{\sum PE_i}{n}$
Mean absolute percentage error	$MAPE = \frac{\sum \lvert PE_i\rvert}{n}$		

Source: Washington *et al.* (2010)

3.6.2. 10-fold cross-validation

Classification in statistics or machine learning is implemented for identifying the difference between a new observation and analysed dataset and as such classifiers can be defined as the algorithm for classification. Thus, classifiers enable a comparison of models by presenting meaningful conclusions in a systemic manner. Kohavi (1995) suggests that k-fold cross-validation (CV) has good performance when comparing the predictability of analysed models for reducing biases. In k-fold CV, the whole dataset is randomly split into k subsets having almost equal size (Figure 3-13). Firstly, (k-1) subsets are regarded as training samples and the other subset is set as the test samples. By using training samples, the analysed models are derived and the accuracy measure (A_i in Equation 3-61, e.g. MAPE, RMSE) of each model is calculated from true (observed) in test samples and predicted values. This process is repeated k times and therefore k individual accuracy measures are calculated. The overall accuracy of analysed models is compared from calculating the average of k measures as in Equation 3-58.

Figure 3-13 Process of k-fold cross-validation (training and tested set)

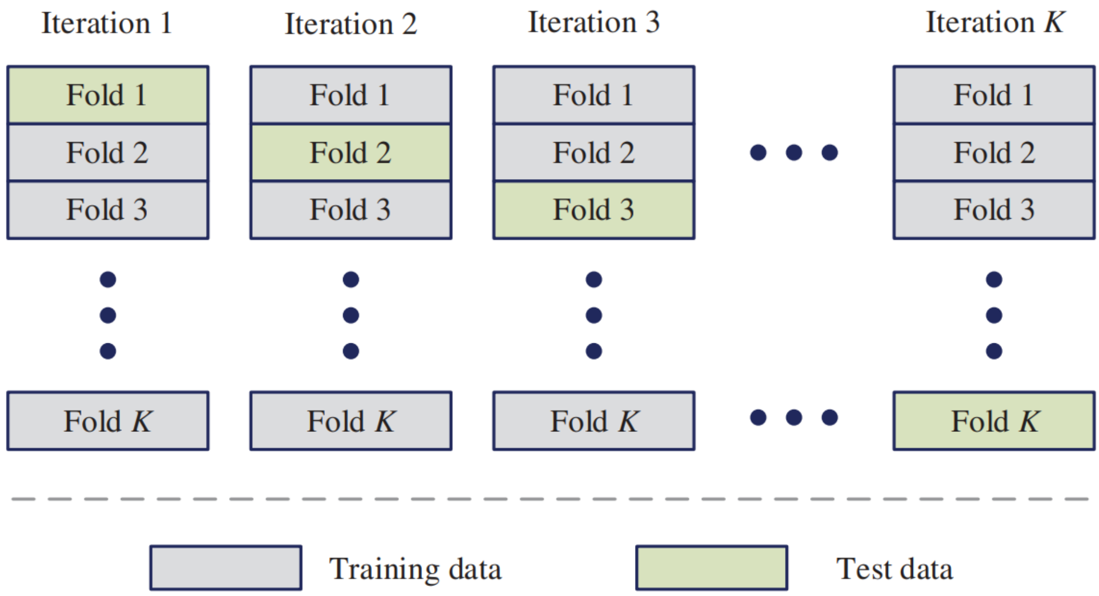

Source: Ren *et al.* (2019)

$$\mathrm{CV_k} = \frac{1}{k}\sum_{i=1}^{k} A_i \qquad \text{Equation 3-61}$$

where $\mathrm{CV_k}$ is the overall accuracy from k-fold CV, A_i is the accuracy measure of the *i*th fold.

It is necessary to select the k value carefully in k-fold CV even though there is no formal rule for k (Kuhn and Johnson, 2013). k=5 or k=10 are common choices in many studies. This study adopted 10-fold CV because 5-fold CV could cause statistical problems caused by there being low number of training samples. In other words, the number of training samples (63=7*9) in 10-fold CV is more appropriate for modelling than that (56=14*4) in 5-fold CV. Although both approaches would be eligible to this study in that the minimum number of samples for model estimations ranges from 40 to 80 (Section 3.5.1), it can be said that it would be less statistically problematic to adopt 10-fold CV that has more number of training samples.

3.7. Summary

From the literature review and the initial case study, this study raised the research issue of whether the current VDFs are appropriate for explaining the diversity of links only with free-flow travel time (FFTT) and road capacity. This chapter suggests the way in which this thesis will seek to overcome the limitations of current VDFs with the following two approaches: the identification of influential factors on travel time and the establishment of new reliable approaches for the empirical data analysis. The first one aims to incorporate additional variables to travel time estimation models and the second to develop other statistical estimation methods.

The part of the research methodology for identifying the influential factors is as follows. The initial case study (Section 3.2) confirmed that the uncertainty of FFTT and road capacity cause the error in travel time estimation for a virtual bottleneck section. FE modelling by LSDV in Section 3.3 suggests how to identify the influential factors on travel time estimation models to replace the current FFTT and road capacity. In addition, Section 3.4 explains how to represent each link attributes effectively, focusing on the spatial values such as space-mean speed and the overall geometric features of the link.

The other part of the research methodology for establishing new statistical estimation methods is as follows: unlike the previous studies that used the NLS estimation with FFTT and road capacity, Section 3.3 devised linear estimation methods. Whilst the previous approach has the drawbacks of confining the estimated models to the dataset used for modelling, the linear estimation has merits of generalising the models by verifying the statistical significance. According to their statistical assumptions, the linear estimation was divided into two methods: OLS and GLS estimations. The base model was determined as a quadratic function from the initial case study (Section 3.2). The OLS estimation is appropriate when to consider the interaction effects between variables as well as the model transformation. However, the OLS estimation cannot guarantee the statistical significance when violating its assumptions, especially with regard to the variance-covariance structure of residuals. The GLS estimation is a more general approach than the OLS estimation in that the GLS estimation assumes the varying structure of residuals based on the maximum likelihood estimation. Therefore, this study focuses more on the GLS estimation as a means of replacing the current approach of the NLS estimation.

To select the most appropriate feasible model, this chapter suggests many statistical accuracy measures for the comparison of the estimated models. After verifying spatial transferability by 10-fold validation, the statistical measures including AIC, BIC, RMSE, MAPE, etc. are used for the comparison. As well as the statistical significance, from the viewpoint of traffic assignment, this study proposed the practical applicability of the estimated models.

Chapter 4. Identification of Influential Factors for Models

4.1. Introduction

The main concern of this study is to develop travel time estimation models which take into account geometric features; more specifically, its purpose is to develop link-performance functions that can replace the existing VDFs, which have road capacity and free speed as constants. Prior to developing feasible models, it is necessary to investigate which factors influence statistically estimated models and how much these factors contribute to the models. Using the dataset collected from the selected cases for a month, this study quantitatively measured the impact of various external conditions as well as geometric features. For ease of identification of these factors, this chapter is divided into three sections: data selection; factors identification by the OLS estimation; and factors identification by the NLS estimation. The GLS estimation method is excluded from this chapter because the estimation requires a large number of iterative calculations with one-month time-series data and because this chapter needs overall goodness of fit from various models, not the efficiency of coefficients.

Firstly, Section 4.2 presents the descriptive analysis of the entire data depending on traffic flow and geometric features. In addition, the one-month dataset is identified as panel data for fixed effects (FE) modelling, which is one of the key points in this chapter. The entities of the panel data noted in this study are links, routes, brightness, date, day (weekday and weekend) and weather. Among these, geometric features are endogenous to the link entity.

Secondly, Section 4.3 suggests that the existing VDF (BPR function) can customise the one-month dataset as a reference model in this chapter. The NLS estimation also shows how geometric variables change the sum of errors by adding geometric IVs to BPR function. In addition, since existing VDFs need to determine road capacity in advance, sensitivity analysis is conducted to investigate how the variation in road capacity affects model accuracy.

Lastly, Section 4.4 attempts to identify predictors that could be included in the model through two OLS estimations. The comparison of pooled OLS (POLS) estimation with and without geometric features suggests how geometric features can affect the models. FE modelling by least squares dummy variables (LSDV) can determine generalized effects, dividing the entire dataset according to the abovementioned entities. In addition, RE modelling is implemented by recognising the dataset as the panel data for the comparison with FE modelling.

4.2. Data selection

4.2.1. Plot observation

Before carrying out various statistical estimations, scatter plots were examined to find the overall relationships between variables. Figure 4-1 shows all scatter plots including data from congested states. The scatter plot used for statistical estimations can be seen in Figure 4-2 after the data processing mentioned in Section 3.4.3. As the scatter plot between DV and TF has large variation because it was observed in all 72 cases every 15 minutes for one month, it is difficult to explain the observations in terms only of the relationship between two variables. Therefore, a more detailed analysis considering geometric variables was required in order to clarify the relationship between variables more precisely.

Figure 4-1 Scatter plot including congestion states

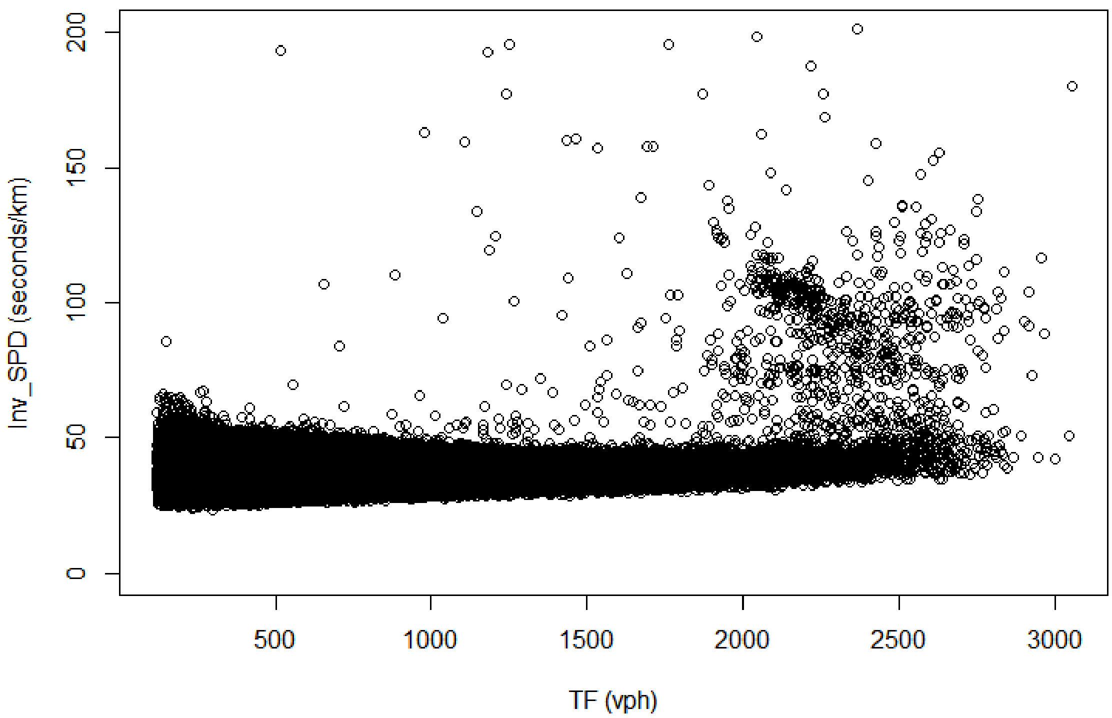

Box plots of DV by geometric features

Box plots were investigated for finding linear trends of the relationships between DV and each geometric variable. Four box plots depending on geometric variables can show the approximate mean and standard errors of DV according to each section (From Figure 4-3 to Figure 4-6). All geometric features act to increase the average travel time without considering traffic flow; in particular, RISE and FALL variables have a comparatively high slope of linear relationship with average travel time. However, it is necessary to note that the distribution (variation of box plots) of DV depends on the average traffic volume in each section. In other words, the mean value of the box plot of a busy motorway is higher than that of a quiet motorway.

Figure 4-2 Scatter plot between DV and IV1 (TF) after data processing

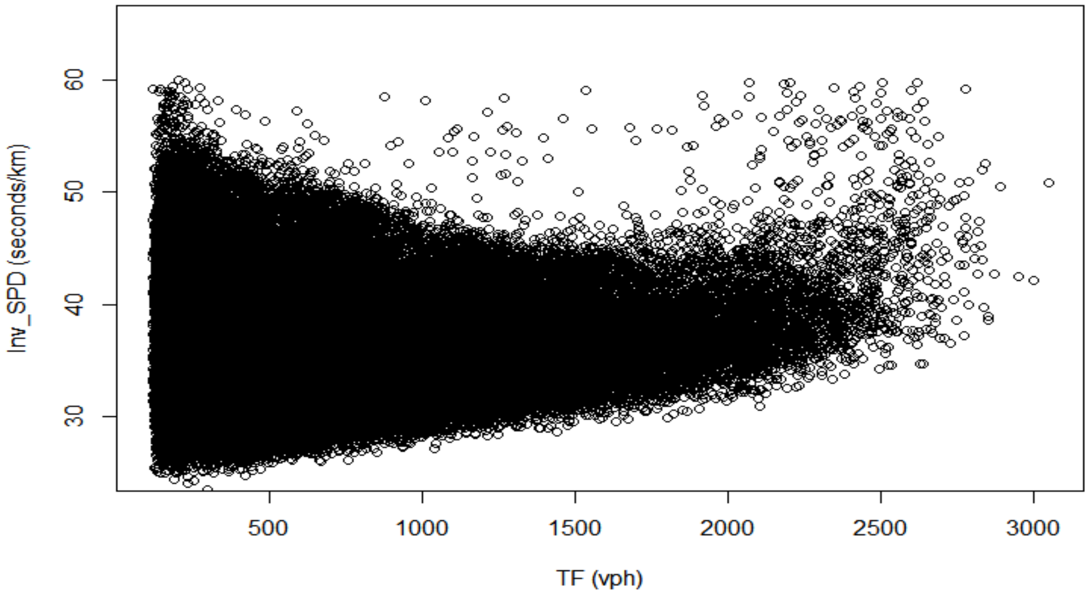

Figure 4-3 Box plot of DV by IV2 (TR)

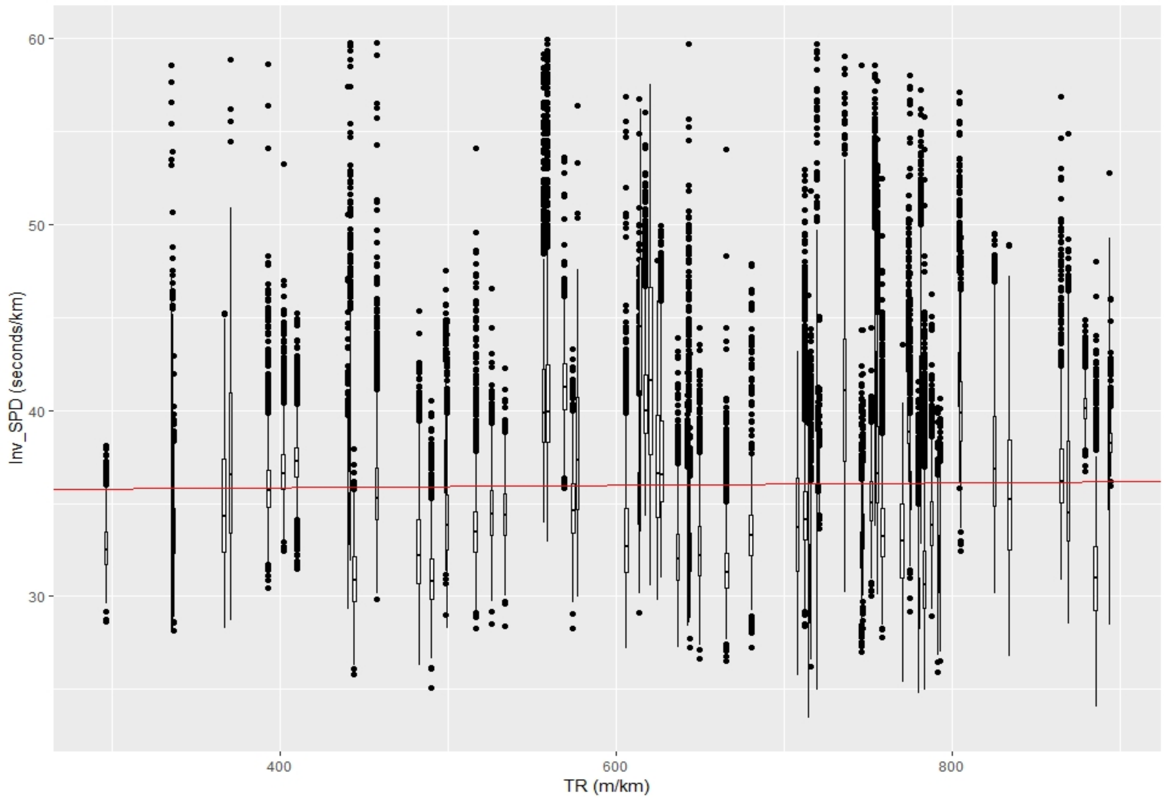

Note: The red line is a reference for finding the trend between Inv_SPD and TR.

Figure 4-4 Box plot of DV by IV3 (RISE)

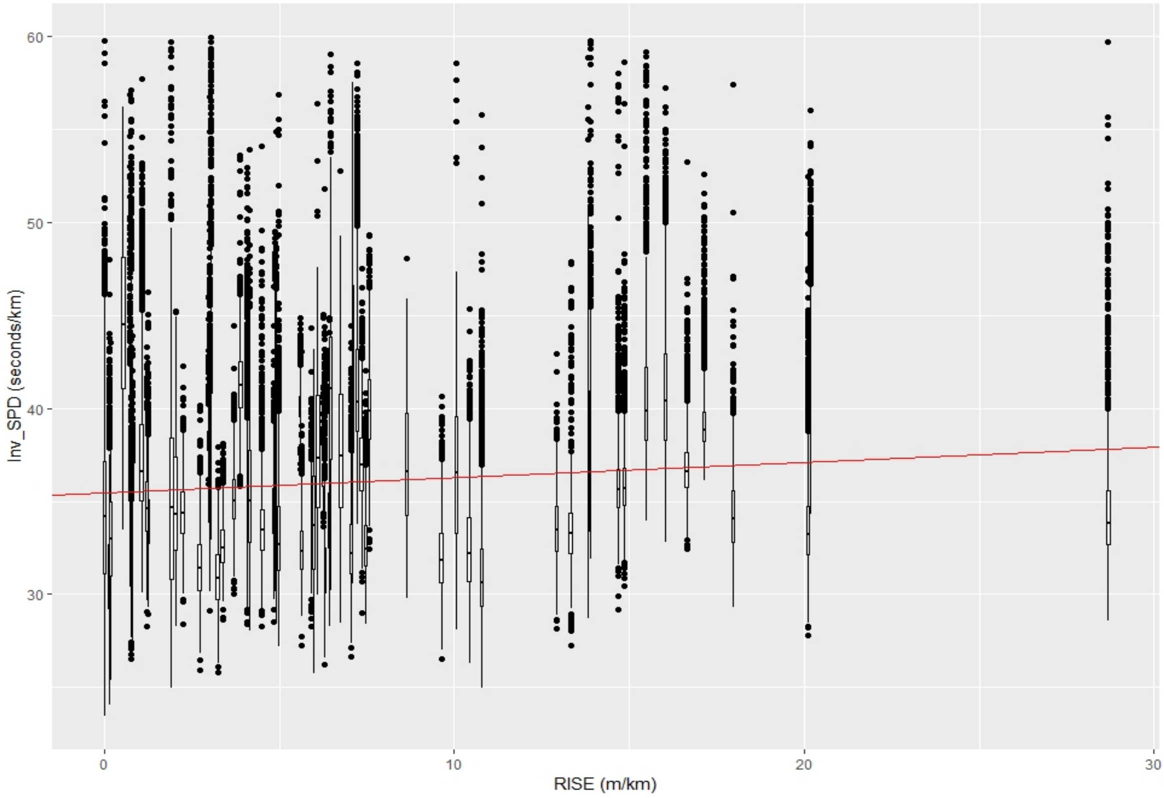

Figure 4-5 Box plot of DV by IV4 (FALL)

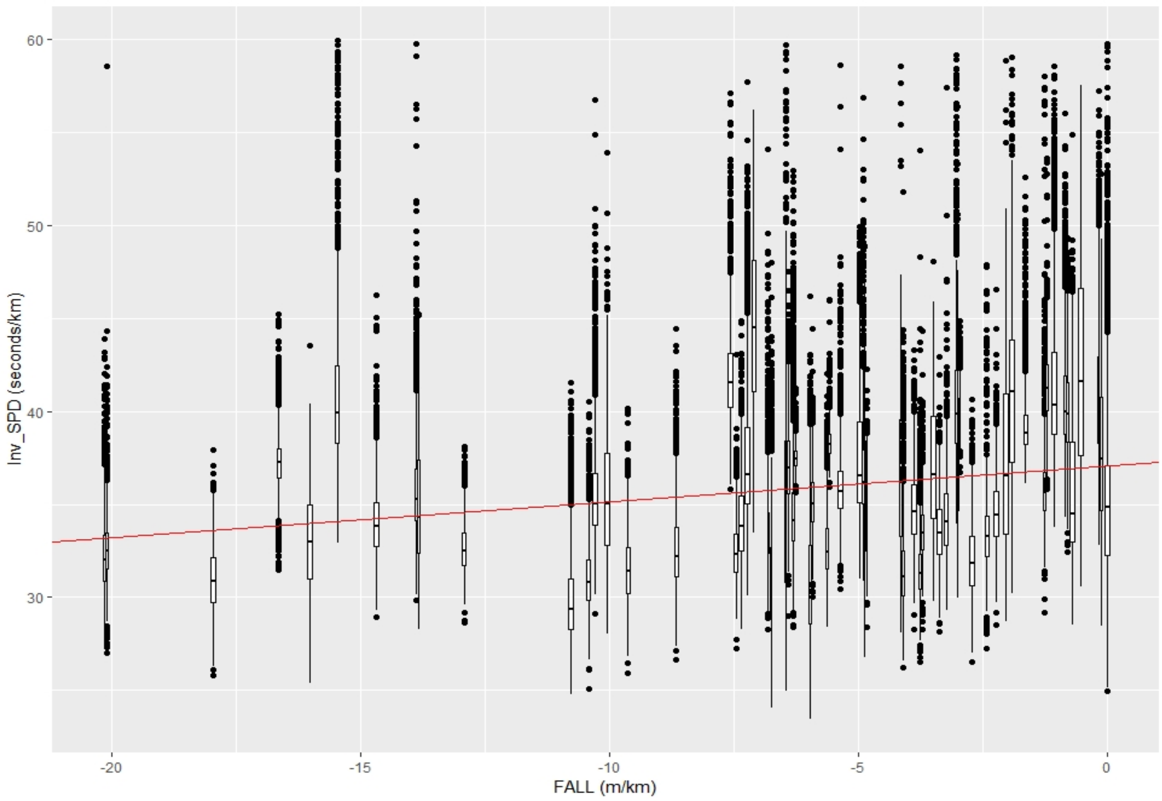

Figure 4-6 Box plot of DV by IV5 (BEND)

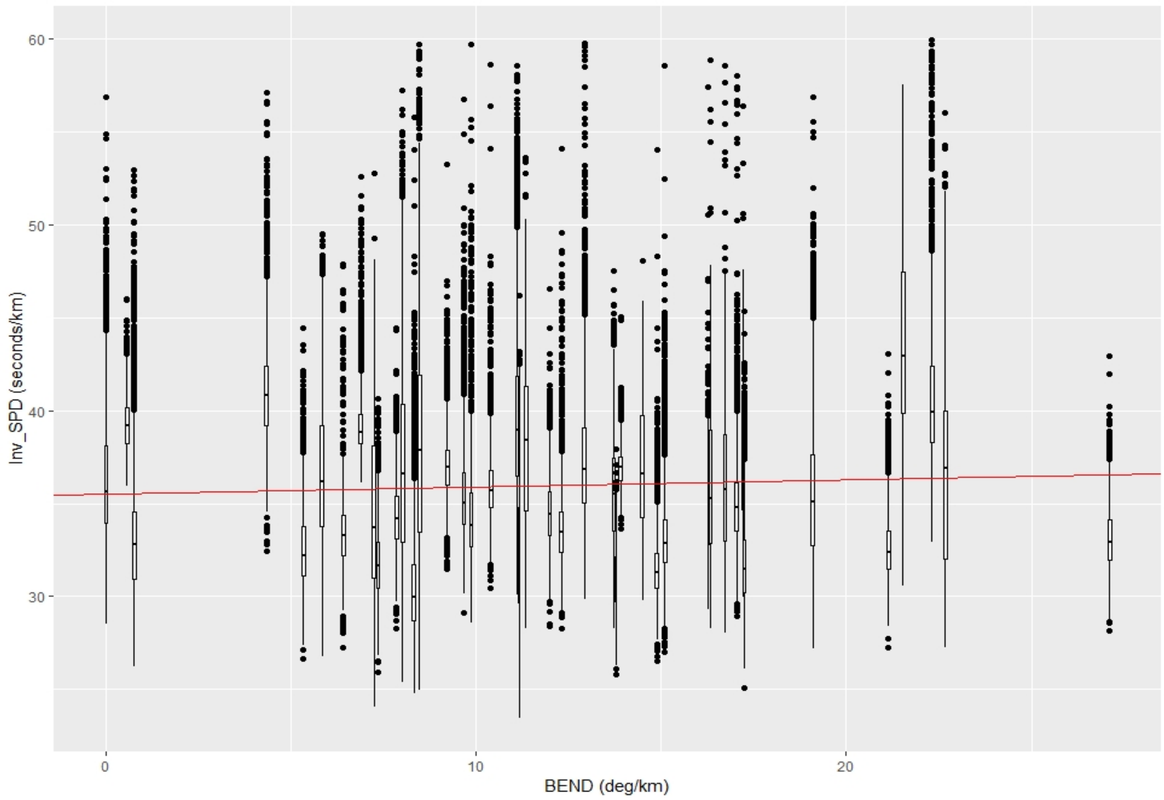

Observation of the 15th percentile values of DV by geometric features

The 85th percentile value of speed in transportation studies is generally used for road design or data comparison (Abbas *et al.*, 2011; Castro *et al.*, 2011). The 85th percentile value of speed is equivalent to the 15th percentile value of inverse speed, which is close to FFS. The 15th percentile value of DV is useful for determining how each geometric variable changes the travel time in free-flow states (Figure 4-7). Notably, BEND has the negative linear relationship with the 15th percentile value of DV, which is the opposite result compared to the box plot analysis.

Observation of the 85th percentile values of DV by geometric features

The 85th percentile value of DV can explain moderate or congested traffic situations. The linear relationship between the 85th percentile values and each geometric value can enable an examination to be made of how much each geometric feature can affect travel time in comparatively high traffic flow. Three geometric features of TR, RISE and FALL exhibit the same trends with the analysis from box plots and the 15th percentile values, but BEND has a different direction from the analysis of the 15th percentile values, which means the same direction with box plots by BEND.

Figure 4-7 15th percentile values of DV by geometric variables for one month

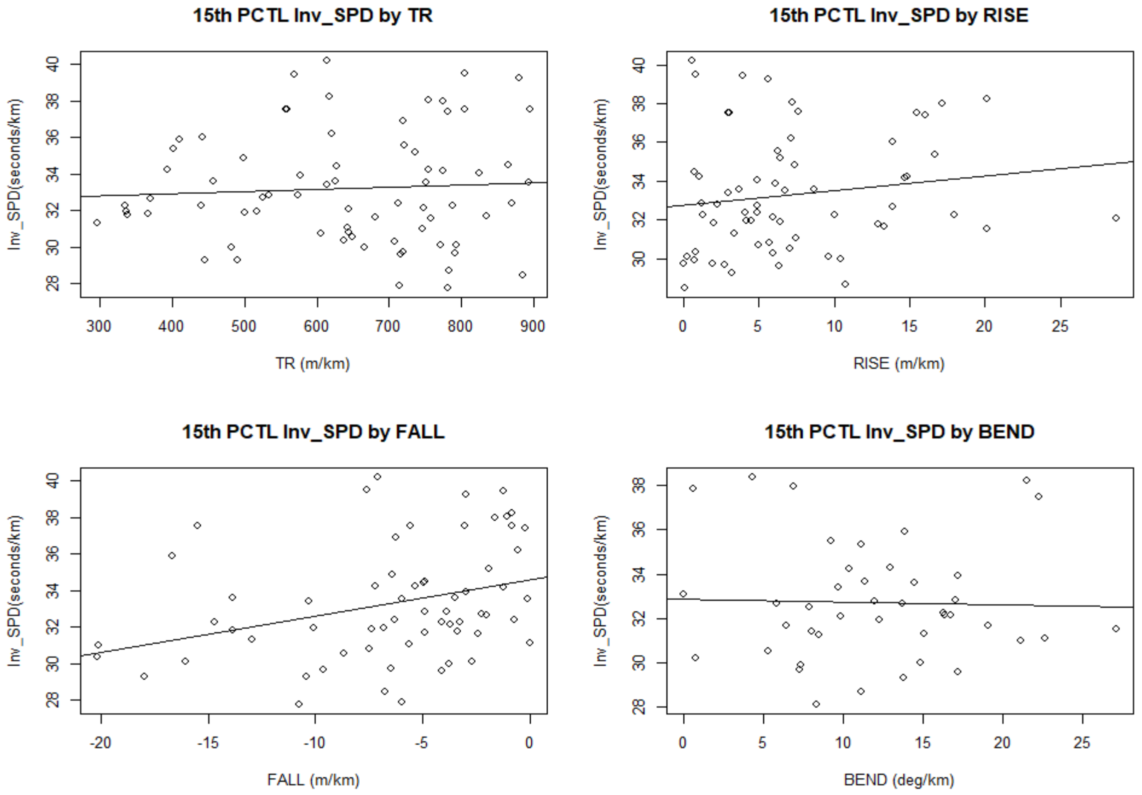

Figure 4-8 85th percentile values of DV by geometric variables for one month

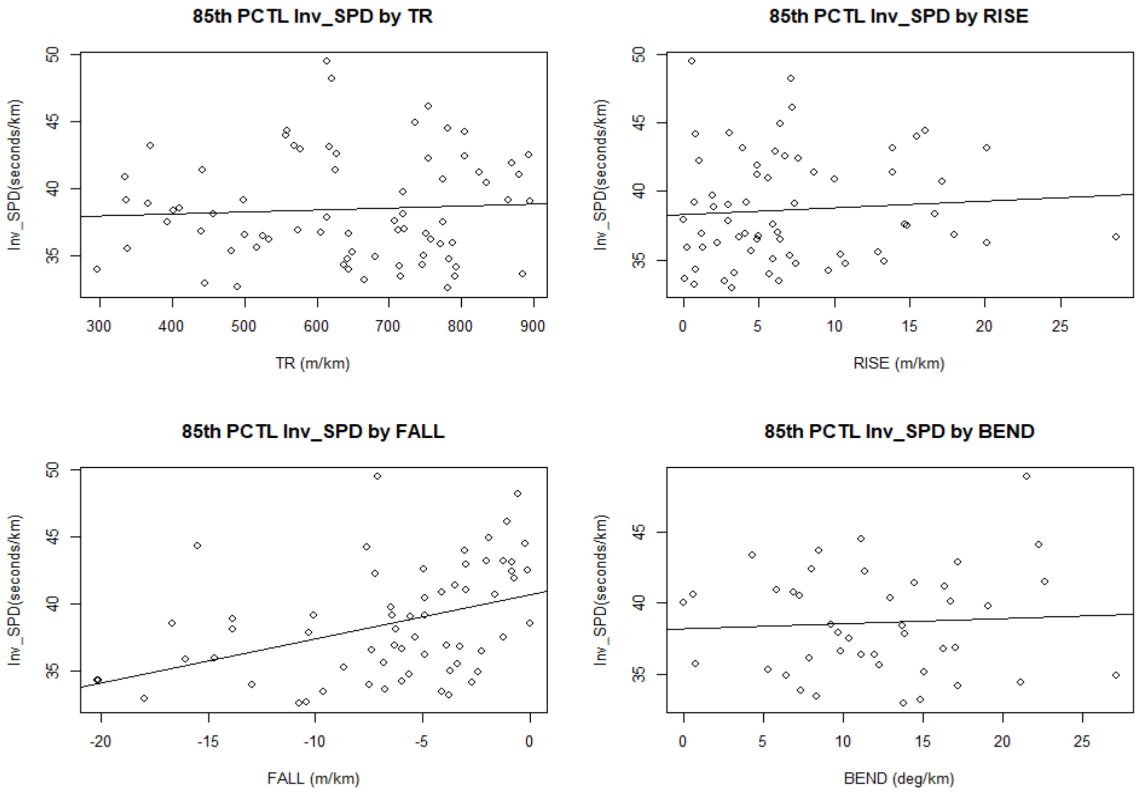

4.2.2. Framing panel data (entity identification)

As mentioned in Section 3.3.2, panel data, which is also known as longitudinal or cross-sectional time-series data, enables the control of variables that cannot be measured across entities or time by fixed effects modelling. In addition, panel data allows multilevel or hierarchical modelling at different levels of entities. Therefore, identifying entities and time from the dataset should precede fixed effects modelling. The identified entities can be divided into the six groups: links, routes, dates, weather, weekday and weekend, and brightness.

Links

The number of links in this study is 72, which is the same as the number of cases. The entity of a link can explain the effects that cannot be measured between links. The effects by the link entity can include link geometric features (including other features not considered in this study): landscape, the distance from an interchange, road accessories (e.g. road signs, guardrail types), pavement quality and other features that vary across links but do not change across time.

Routes (Lines)

The entity of routes is a broader classification than links. As can be seen from Table 3-15, routes consist of several links. The number of routes in this study is 12 and the number of links in one route ranges from one to twelve. The entity of routes can reflect differences according to the region and overall terrain where the routes are located.

Brightness

Brightness can affect drivers' behaviour because of differences in visibility between daytime and nighttime (Bella *et al.*, 2014). The effects of the brightness entity were also considered in this study. The dataset was divided into daytime and nighttime data rows based on two time periods - the average time of sunrise and sunset in September 2018, which worked out as around 07.00 and 19.00 hours respectively. This entity can explain in one model, the extent to which travel time is different between daytime and nighttime.

Date

Whilst models using the above two entities can control time-invariant effects, date can control time-varying unobserved variables, which are time-fixed effects. For example, traffic patterns can vary on any individual day in September 2018 for many different reasons such as logistics (related to traffic composition), road maintenance, and national holidays. The dummy variables of date can explain this daily change in travel time estimation models in detail.

Weekday and Weekend

Days of the week are known to affect traffic patterns (Weijermars and van Berkum, 2004; Cools *et al.*, 2007; Gao and Niemeier, 2007). In particular, Cools *et al.* (2007) found that daily traffic flows during weekends have different patterns from those on weekdays. By dividing the dataset into weekdays and weekends, this study found the effects on travel time estimation models according to days of the week. With this approach, the data on rainy days was excluded because the impact of weather could affect travel time in one model and thus the impact of days cannot be separated.

Weather

Weather is also one of the influential factors in travel time estimation models. Many studies found the reduction of FFS and road capacity due to the weather condition (Agarwal *et al.*, 2005; Rakha *et al.*, 2007; USHCM, 2010; Kim, 2013). The only factor related to weather in the dataset is based on the amount of rainfall because the dataset is measured during the autumn season in South Korea. There is no specific correlation made between traffic values and the amount of rainfall in USHCM (2010), but Agarwal *et al.* (2005), Rakha *et al.* (2007) and Kim (2013) suggested a reduction in their in proportion to the amount of hourly rainfall (Table 4-1). Although it is necessary to collect the information of hourly rainfall to identify weather effects in detail, this study considered only the amount of daily rainfall (Table 4-2) referring to the website[7] of the Korean meteorological administration because this study does not aim to quantify the effects of rainfall. The data rows recorded in locally rainfall days were excluded from fixed effects modelling because it is difficult to identify the impact of rainfall, which is affected by how far weather observatories are from the selected cases.

Table 4-1 Research about reduction rate of traffic values by hourly rainfall

Study	Rainfall	Road capacity	Congestion speed	FFS
Manish Agarwal et al. (2005)	trace (~0.01inch/h)	1~3%	1~2%	
	light(0.01~0.25inch/h)	5~10%	2~4%	
	Heavy(0.25inch/h~)	10~17%	4~7%	
Hesham Rakha et al. (2006)	light(~0.1mm/h)	10~11%	8~10%	2~3.6%
	rain(~16mm/h)	10~11%	8~14%	6~9%
Kim (2013)	0~5mm/h	20.58%	2.88%	
	5~10mm/h	30.42%	6.42%	
	10~20mm/h	31.63%	8.38%	
	20mm/h~	35.25%	13.07%	

[7] http://www.weather.go.kr/weather/climate/past_cal.jsp

Table 4-2 Daily rainfall by regional observatories in September of 2018

Date	Gwangju	Suncheon	Namwon	Busan	Changwon	Sangju	Youngju	Choongju	Jecheon	Wonju	Chuncheon	Gangreung
0901	1	34.2		82.8	46.4							
0902		4.8	1.2	3.3	0.6		0.5					
0903	12.7	11	4.2	57.2	48.2	8.4	22	125.7	96.5	80.3	34.1	14
0904	76.1	100	48.5	0	17	59.9	91	14.2	20	5.1		3.4
0905												
0906	1.7	0	0.1	0	0			0.5		3.2		
0907	8.2	6	10.3	15.6	8.5		0.4	3.3	5.5	0.9	4.2	
0908				0							0.2	
0909												5.7
0910												0
0911												
0912					0							
0913	3.9	19.5	0.9	8.6	11.6	0.9						
0914	3.4	9.8	1.3	47.7	29.4	15.3	6	0.8	1.5	1	0	0.1
0915	2	0	3.6	1.4	7	2.8	5.5	1.7	4	7.5	0	0.4
0916			0.3				0.5	0.7	0.5	0.2	0.5	0.6
0917	0		0.2				0.3	0.3	0	0		
0918												
0919	1	1.9		0	0.5				0.5	0.7	0.7	0.3
0920	1.7	11.3	0.7	11.4	12.2	11	12.5	3.9	23.5	13.5	12.2	17.2
0921	18	20	20	27.2	28	35.5	27.5	33.4	33.5	35.1	17.9	24.4
0922							0.1			0.1		
0923							0.2	0.4		0	0.1	
0924												
0925												
0926				2.4								
0927												
0928	0			0								
0929				37.1	6.4							
0930				13.7	0.6							
Sum	129.7	218.5	91.3	308.4	216.4	133.8	166.5	184.9	185.5	147.6	69.9	66.1

Note. Blue shades: nationwide rainfall days; Grey shades: local rainfall days.

Source: Collected from http://www.weather.go.kr/weather/climate/past_table.jsp

4.3. Analysis of factors by BPR function

4.3.1. Model specification

When recalling the NLS estimation model based on BPR function (Equation 4-1), the model consists of two relationships: the relationship between travel time (DV) and traffic flow (IV1); and the relationship between travel time (DV) and geometric variables (from IV2 to IV5). As previously discussed in Section 3.3.3, the first relationship is the existing approach of BPR function, which is widely used for motorway VDFs. In order to compare both estimation results, the dataset used for the NLS estimation is the one-month dataset as with the OLS estimation in Section 4.3. As investigated in the initial data analysis (Section 3.2.3), the predetermination of road capacity is essential for the NLS estimation. The nominal capacity (C_n), which is calculated as 2,404vph from the one-month dataset, is used for the NLS estimation (Section 3.3.3).

$$TT = FFTT\left(1 + \alpha\left(\frac{TF}{C}\right)^{\beta}\right) + \sum \boldsymbol{\gamma_k Geometry_k} + u \qquad \text{Equation 4-1}$$

The estimated models based on BPR function are denoted as Table 4-3 according to the inclusion of geometric variables. In particular, BPR1 can be a reference model for the comparison between derived models because it is a customised model based on the BPR function by using the dataset collected in this study. The difference between BPR1 and BPR2 is whether geometric variables are included in estimated models.

Table 4-3 Customised models based on BPR function

Model Name	Independent Variables	Explanation
BPR1	TF	Customisation of BPR function by predetermining road capacity (existing approach)
BPR2	TF, TR, RISE, FALL, BEND	Inclusion of geometric variables in addition to the customised BPR function

4.3.2. Customisation of BPR function (existing approach)

Similar with the existing BPR function, this approach does not consider the geometric variables in the model. Namely, the term of $\sum \boldsymbol{\gamma_k Geometry_k}$ in Equation 4-1 is not included. The estimated model assumes that road capacity could capture all link characteristics. The difference with the existing BPR function customising approaches is that this approach does not predetermine FFTT. As FFTT is the intercept in estimated models, it is not necessary to predetermine FFTT in the iteration process of "Gauss-Newton" algorithm (Section 3.3.3). This finding is in line with the initial data analysis. '*nls()*' function, which is based on "Gauss-Newton" algorithm in the software package "R", was used for the NLS estimation.

The iteration results and thereafter derived parameters of the estimated model (BPR1) are shown in Table 4-3. The starting value of FFTT for the iteration is 36 (seconds per km), which is travel time corresponding to most motorway speed limit (100kph) in South Korea. The starting values of parameters are 0.15 and 4 for parameters respectively, which are the same values of the standard BPR function. FFTT in BPR1 is 35.8, and the derived parameters ('a' and 'b' in Table 4-3) of the models are 0.1704 and 4.040. RMSE of this model is calculated as 4.49 and the convergence tolerance, which means the difference of estimated errors between iterations (as it is smaller, the model accuracy increases), is 1.695e-06, which is the ratio change before and after iterations (Equation 3-48). The blue points (fitted line) in Figure 4-9 show the typical form of VDF without geometric variables.

Table 4-4 Existing approach based on BPR function between DV and TF

```
#Predetermination of road capacity
Data.NLS$capacity <-2404

# Nonlinear estimation without geometric IVs
BPR1 <- nls(Data.NLS$Inv_SPD ~ FFTT*(1+a*(Data.NLS$TF/Data.NLS$capacity)^b),
start = list(FFTT=36, a =0.15, b = 4), data=Data.NLS, trace = TRUE)
## 2986698 :  36.00  0.15  4.00
## 2980454 :  35.7898646  0.1703606  4.0484791
## 2980453 :  35.7895966  0.1704273  4.0391423
## 2980453 :  35.789640  0.170437  4.039913
summary(BPR1)
##
## Formula: Data.NLS$Inv_SPD ~ FFTT * (1 + a * (Data.NLS$TF/Data.NLS$capacit
y)^b)
##
## Parameters:
##       Estimate Std. Error t value Pr(>|t|)
## FFTT 35.789640   0.013418 2667.33   <2e-16 ***
## a      0.170437   0.003184   53.52   <2e-16 ***
## b      4.039913   0.095716   42.21   <2e-16 ***
## ---
## Signif. codes:  0 '***' 0.001 '**' 0.01 '*' 0.05 '.' 0.1 ' ' 1
##
## Residual standard error (≈RMSE): 4.490 on 147828 degrees of freedom
##
## Number of iterations to convergence: 3
## Achieved convergence tolerance: 1.695e-06
```

where the coefficients of 'a' and 'b' represent 'α' and 'β' in Equation 4-1.

Figure 4-9 Fitted line of NLS estimation (BPR function) between DV and TF

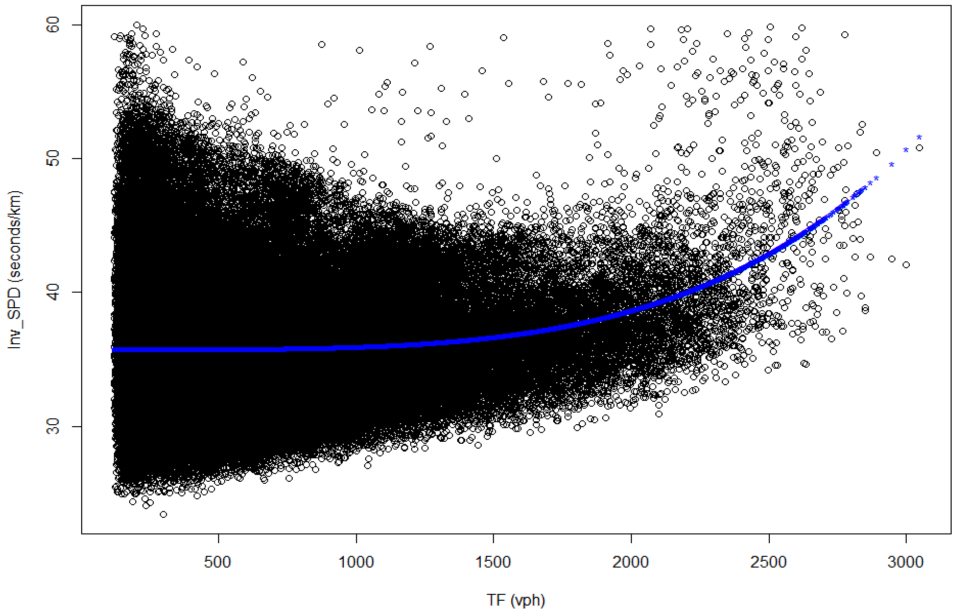

4.3.3. Customisation of BPR function including geometric features

Based on BPR1, this approach does consider the geometric variables in the model. In other words, all the terms in Equation 4-1 are used for model estimation. The estimated model (BPR2) is based on the assumptions that road capacity cannot capture all link characteristics and that geometric features can be separated from road capacity in the model. Other estimation methods are the same as for BPR1.

FFTT and the derived parameters of BPR2 are shown as yellow shades in Table 4-5. The starting values of the geometry-related parameters are set at zero based on the assumptions that there would be no effects of link geometry once road capacity is defined and that the other starting values, except for geometry-related parameters, are same as BPR1. FFTT in BPR2 was estimated as 35.22, and TF-related parameters ('a' and 'b' in Table 4-5) were derived as 0.1779 and 4.051 respectively. The parameters of geometric independent variables (from 'c' and 'f' in Table 4-5) are 1.238e-03 for TR, -2.560e-02 for RISE, 2.222e-01 for FALL and 9.524e-02 for BEND respectively. Moreover, RMSE of BPR2 is estimated as 4.35. Finally, the fitted lines of BPR2 between DV and TF reflecting geometric variables were derived (Figure 4-10).

Table 4-5 NLS estimation with TF and geometric variables

```
#Definition of road capacity
Data.NLS$capacity <-2404

# Nonlinear estimation with geometric IVs
BPR2 <- nls(Data.NLS$Inv_SPD ~ FFTT*(1+a*(Data.NLS$TF/Data.NLS$capacity)^b) +
 c*Data.NLS$TR + d*Data.NLS$RISE + e*Data.NLS$FALL + f*Data.NLS$BEND, start =
```

```
 list(FFTT=36, a =0.15, b =4, c=0, d=0, e=0, f=0), data=Data.NLS, trace = TRU
E)
## 2986698 :  36.00  0.15  4.00  0.00  0.00  0.00  0.00
## 2797301 :  35.2212  0.1774  4.0665  0.0012 -0.0256  0.2222  0.0952
## 2797299 :  35.2200  0.1779  4.0484  0.0012 -0.0255  0.2222  0.0952
## 2797299 :  35.2203  0.1779  4.0510  0.0012 -0.0256  0.2222  0.0952

summary(BPR2)
##
## Formula: Data.NLS$Inv_SPD ~ FFTT * (1 + a * (Data.NLS$TF/Data.NLS$capacit
y)^b) + c * Data.NLS$TR + d * Data.NLS$RISE + e * Data.NLS$FALL +
f * Data.NLS$BEND
##
## Parameters:
##         Estimate Std. Error t value Pr(>|t|)
## FFTT  3.522e+01  8.756e-02  402.22   <2e-16 ***
## a      1.779e-01  3.170e-03   56.13   <2e-16 ***
## b      4.051e+00  9.076e-02   44.63   <2e-16 ***
## c      1.238e-03  9.199e-05   13.46   <2e-16 ***
## d     -2.560e-02  2.404e-03  -10.65   <2e-16 ***
## e      2.222e-01  2.857e-03   77.77   <2e-16 ***
## f      9.524e-02  2.230e-03   42.70   <2e-16 ***
## ---
## Signif. codes:  0 '***' 0.001 '**' 0.01 '*' 0.05 '.' 0.1 ' ' 1
##
## Residual standard error (≈RMSE): 4.350 on 147824 degrees of freedom
##
## Number of iterations to convergence: 3
## Achieved convergence tolerance: 9.915e-06
```

where the coefficients of ‘a’ and ‘b’ represent ‘α’ and ‘β’ in Equation 4-1; and the coefficients of ‘c’, ‘d’, ‘e’ and ‘f’ represent ‘$\boldsymbol{\gamma_k}$’ (a vector) in Equation 4-1.

Figure 4-10 Fitted line between DV and TF in BPR2

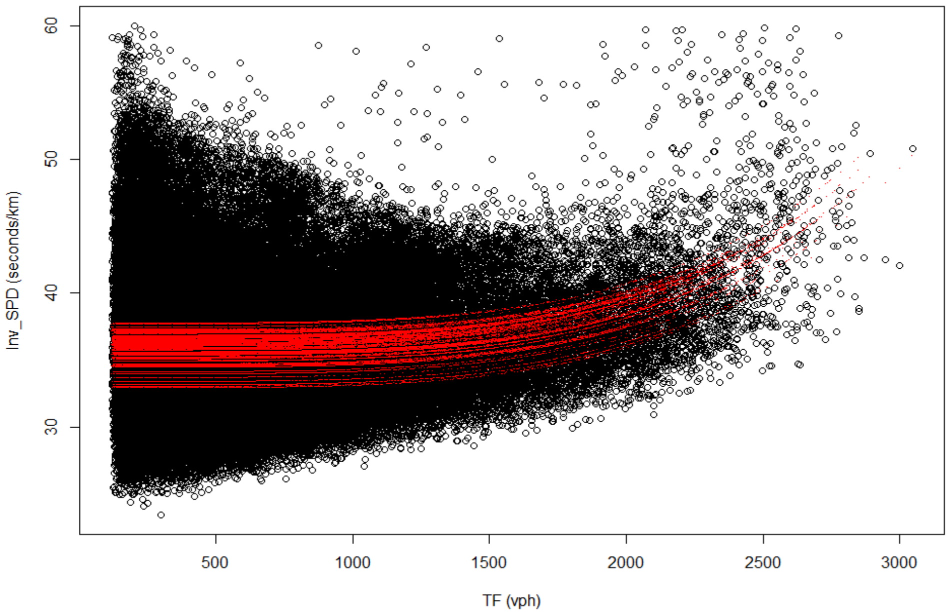

4.3.4. Sensitivity analysis of differences in road capacity

As previously discussed in Section 3.3.3, it is questionable whether the nominal road capacity (C_n) defined in this study would be suitable for the NLS estimation because of the road capacity uncertainty. Therefore, this section examines how estimated models vary according to different values of road capacity. Table 4-6 shows the parameters which have been estimated differently based on 80-120% of the nominal road capacity as well as by the road capacity of 3,572vph used in Korea; the latter is used for 2-lane rural motorways in the Korean VDF (Table 2-5). Only the parameter 'a' of all parameters has a positive correlation with the predetermined value of road capacity and the other parameters do not change despite the different values of road capacity. The parameter 'a' varies from 0.0692 for 80% of C_n to 0.3556 for 120% of C_n in BPR1; and from 0.0720 for 80% of C_n to 0.3720 for 120% of C_n in BPR2. In particular, the value increases significantly in the estimated model from the road capacity proposed in the Korean VDF.

Table 4-6 Sensitivity analysis of NLS estimation by different values of road capacity

Model / Road Capacity	BPR1			BPR2						
	FFTT	a	b	FFTT	a	b	c	d	e	f
80% of C_n (1,923vph)	35.79	0.0692	4.0397	35.22	0.0720	4.0510	0.0012	-0.0256	0.2222	0.0953
90% of C_n (2,164vph)	35.79	0.1114	4.0397	35.22	0.1162	4.0510	0.0012	-0.0256	0.2222	0.0953
C_n (2,404vph)	35.79	0.1704	4.0397	35.22	0.1779	4.0510	0.0012	-0.0256	0.2222	0.0953
110% of C_n (2,644vph)	35.79	0.2503	4.0397	35.22	0.2616	4.0510	0.0012	-0.0256	0.2222	0.0953
120% of C_n (2,884vph)	35.79	0.3556	4.0397	35.22	0.3720	4.0510	0.0012	-0.0256	0.2222	0.0953
C_{Korea} (3,572vph)	35.79	0.8439	4.0397	35.22	0.8850	4.0510	0.0012	-0.0256	0.2222	0.0953
RMSE	4.490			4.350						

Note 1. 'C_{Korea}' is the road capacity defined for 2-lane motorways in Korean VDF.
2. The coefficients of 'a' and 'b' are TF-related parameters ('α' and 'β' in Equation 4-1); and the coefficients from 'c' to 'f' are link geometry-related parameters ('$\boldsymbol{\gamma_k}$' in Equation 4-1).

4.3.5. Summary

Two phased approaches were adopted by NLS estimation based on the BPR function. Firstly, in order to clarify the effects of link geometry, two NLS estimation models were derived; BPR1 without geometric variables as a reference model and BPR2 with them for comparison. These models predetermined the nominal road capacity as defined in this study, but the uncertainty of road capacity measurement and definition still remains. Secondly, sensitivity analysis was implemented in order to identify the uncertainty of road capacity in the process of NLS modelling. The statistical significance test and validation of each of the derived coefficients of variables are dealt in Chapter 5 while the overall change in coefficient values was investigated in this section.

As a result of a two phased approach, the NLS estimation results from the one-month dataset can be subdivided into two: the effects of geometric features and the variation of parameters by different road capacity. Firstly, it is noteworthy that the geometry-related parameters can change FFTT and TF-related parameters between both models of BPR1 and BPR2 (Table 4-4 and Table 4-5). This result was confirmed from the fitted red points (line) (Figure 4-10) between DV and TF in BPR2. Each red line represents shifts that take into account the different geometry in 72 cases of this study. Conversely, the blue fitted line (Figure 4-9) in BPR1 cannot explain the different geometry and aggregated the observations into FFTT and the parameters of ‘a’ and ‘b’. Therefore, this suggests that the geometry-related parameters can cover some of the different link characteristics apart from road capacity.

Secondly, through the sensitivity analysis, it can be concluded that the parameter of ‘a’ is strongly correlated with road capacity (Table 4-6). In addition, it was established that RMSE is dependent only on model specification regardless of road capacity. In other words, the result supports the need for clarification of one of the research gaps (Section 2.6) in that it is difficult to determine which value of road capacity is the most suitable for current VDFs.

4.4. Analysis of factors by OLS linear estimation

4.4.1. Model specification

When recalling the linear estimation model for this study (Equation 4-2), pooled OLS (POLS) estimation can be used by making the assumption that all the selected variables can capture all time-fixed and entity-fixed characteristics. When POLS estimation is applied to this study, if five independent variables can explain travel time perfectly, the developed model can be used for every motorway section. In this situation, μ_i in Equation 4-2, which is the unobserved individual specific effects, can be dropped. In order to examine how geometric features affect the one-month dataset, POLS estimation was divided into two parts: the estimation between only DV and TF, and the estimation by adding geometric features.

$$TT_{it} = \beta_0 + \beta_1 TF_{it} + \beta_2 TF_{it}^2 + \sum \boldsymbol{\gamma_k Geometry_{k,it}} + \mu_i + \lambda_t + \varepsilon_{it} \qquad \text{Equation 4-2}$$

Moreover, as mentioned in Section 3.3.2, fixed effects modelling is an efficient way to find entity or time heterogeneity. As travel time can be affected by various factors that cannot be observed in ITS, this study tried to exclude those fixed effects in modelling. LSDV estimation was selected in this study because the approach can monitor the impact by each entity. In addition, fixed effects modelling is closely related to classifying entities. As mentioned in Section 4.2.2, the entities can be classified into six: links, routes (lines), brightness, date, day (weekday and weekend), and weather (rain).

The models estimated by the OLS linear estimation can be denoted as Table 4-7 and Table 4-8, which classify the OLS linear models based on Equation 4-2. The reference model (MODEL1) in Table 4-7 is POLS linear estimation model by a quadratic function between only DV and IV1 (TF and TF2) without geometric variables because the link entity has the perfect correlation with geometric variables (Section 4.4.2) and the influential factors can be identified by FE models including link, date and both dummy variables. In comparison with MODEL1, MODEL2 in Table 4-8 is POLS linear estimation model based on both a quadratic function between DV and IV1 (TF and TF2) and a simple linear function with geometric features. FE models from MODEL 2-1 to 2-4 in Table 4-8 take into consideration the influential factors by routes, weekend, weather and date.

Table 4-7 POLS and FE models based on a quadratic function with DV and TF

Model Name	Independent Variables	Explanation
MODEL1	TF, TF2	Quadratic model between Inv_SPD and TF. Replacement of existing BPR function.

		Exclusion of road capacity and FFTT.
MODEL1-1	TF, TF2, Dummy_Link	Identification of fixed effects across links in comparison with MODEL1.
MODEL1-2	TF, TF2, Dummy_Date	Identification of fixed effects by date in comparison with MODEL1.
MODEL1-3	TF, TF2, Dummy_Link, Dummy_Date	Identification of two-way fixed effects by links and date in comparison with MODEL1, 1-1 and 1-2.

Table 4-8 POLS and FE models after the inclusion of geometric variables on MODEL1

Model Name	Independent Variables	Explanation
MODEL2	TF, TF2, TR, RISE, FALL, BEND	Quadratic model among Inv_SPD, TF and geometric variables. Inclusion of four geometric variables Exclusion of road capacity and FFTT.
MODEL2-1	TF, TF2, TR, RISE, FALL, BEND, Dummy_Route	Identification of fixed effects across routes in comparison with MODEL2.
MODEL2-2	TF, TF2, TR, RISE, FALL, BEND, Dummy_Brightness	Identification of fixed effects by day and night time in comparison with MODEL2.
MODEL2-3	TF, TF2, TR, RISE, FALL, BEND, Dummy_Weekend	Identification of fixed effects by weekday and weekend in comparison with MODEL2.
MODEL2-4	TF, TF2, TR, RISE, FALL, BEND, Dummy_Weather	Identification of fixed effects by rainy days in comparison with MODEL2.
MODEL2-5	TF, TF2, TR, RISE, FALL, BEND, Dummy_Date	Identification of fixed effects by date in comparison with MODEL2.

4.4.2. POLS and FE models with DV and TF

"MODEL1": POLS estimation between DV and IV1 (TF and TF2)

This approach follows the assumption of most existing studies about VDF models where travel time is dependent only on traffic flow. As this study cannot deny the basic relationship between travel time and traffic flow, so the relationship became the starting point of model estimation. Based on the initial analysis (Section 3.2.3), the base model was set as a quadratic function. The variables of $\boldsymbol{Geometry_{k,it}}$ in Equation 4-2 are not considered in this model. By using *'lm()'* function for OLS linear estimation in "R", the model ("MODEL1") was derived (Table 4-9) with its estimators and the residual plot (Figure 4-11). However, the adjusted R-squared of this model, which is known as the coefficient of determination, is only 2.5% (0.02523).

Table 4-9 Pooled OLS estimation between DV and IV1 by a quadratic function

```
# Pooled OLS: Model estimation between DV and IV1
MODEL1<-lm(mydf$Inv_SPD~mydf$TF+mydf$TF2)
summary(MODEL1)
## Call:
## lm(formula = mydf$Inv_SPD ~ mydf$TF + mydf$TF2)
##
## Residuals:
##      Min       1Q   Median       3Q      Max
## -12.4774  -3.2450  -0.7021   2.6852  23.8481
##
## Coefficients:
##               Estimate Std. Error t value Pr(>|t|)
## (Intercept)  3.663e+01  3.304e-02 1108.79   <2e-16 ***
## mydf$TF     -2.957e-03  8.434e-05  -35.06   <2e-16 ***
## mydf$TF2     2.087e-06  4.210e-08   49.58   <2e-16 ***
## ---
## Signif. codes:  0 '***' 0.001 '**' 0.01 '*' 0.05 '.' 0.1 ' ' 1
##
## Residual standard error: 4.484 on 147828 degrees of freedom
## Multiple R-squared:  0.02524,     Adjusted R-squared:  0.02523
## F-statistic:  1914 on 2 and 147828 DF,  p-value: < 2.2e-16
```

Figure 4-11 Residual plot of pooled OLS estimation between DV and TF

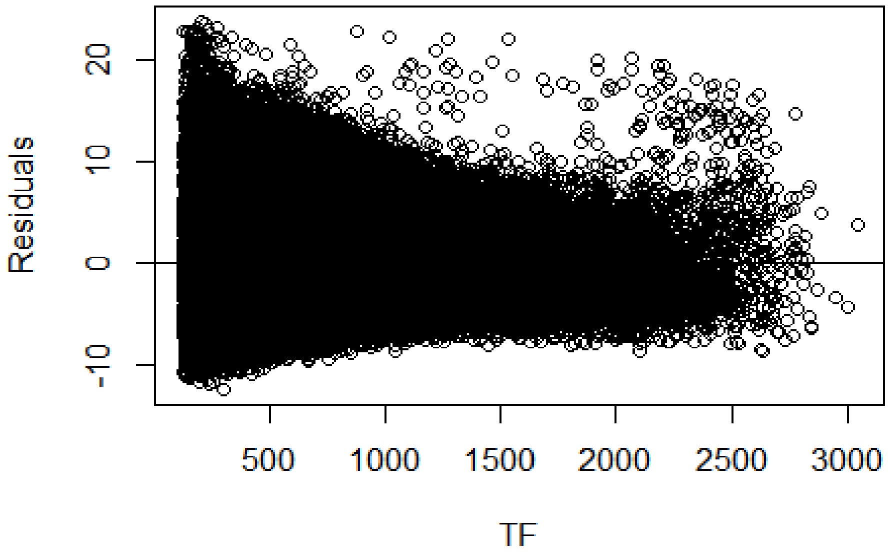

"MODEL1-1": FE model across links

The LSDV model with the dummy variables of links can control time-invariant fixed effects within each link. As can be seen from Table 4-9 and Table 4-10, compared with MODEL1 whose R-squared is 2.5%, the R-squared of MODEL1-1 was 59.4%. Likewise, the range of residuals, which is from -12.5 to 23.8 in MODEL1, was reduced to from -12.3 to 23.5 in MODEL1-1. The estimated intercept of the model represents one of the 1st selected link ("1. KochangDamyang (6.23-11.57k)_E")[8] because the number of dummy variables is always one less than the number of the entity (links). The estimated coefficient of each dummy variable means the difference of FFTT between "1. KochangDamyang (6.23-11.57k)_E" and each section. The result suggests that unobserved effects included in each link can affect travel time considerably. In other words, every link has its own characteristics that can determine travel time. In addition, it is noteworthy that the FE within links contains link geometry because geometric features in each section are fixed across time. Therefore, it is natural not to consider geometric variables from IV2 to IV5 in the FE model with the link entity (Table 4-10). Otherwise, the coefficients of the last four dummy variables (No. 93, 94, 97 and 99 cases) in Table 4-10 cannot be estimated (denoted as 'NA') due to perfect correlation (Appendix A.5.1).

Table 4-10 Result of FE modelling (LSDV) with the 'Link' entity

```
#Model with Link dummies
MODEL1_1<-lm(mydf$Inv_SPD ~ mydf$TF + mydf$TF2 + as.factor(mydf$Link))
summary(MODEL1_1)
Call:
lm(formula = mydf$Inv_SPD ~ mydf$TF + mydf$TF2 + as.factor(mydf$Link))

Residuals:
     Min       1Q   Median       3Q      Max 
-12.3328  -1.7406  -0.2246   1.3763  23.4625 

Coefficients:
                                                           Estimate Std. Error  t value Pr(>|t|)    
(Intercept)                                               3.700e+01  6.745e-02  548.493  < 2e-16 ***
mydf$TF                                                  -6.417e-03  5.827e-05 -110.131  < 2e-16 ***
mydf$TF2                                                  3.492e-06  2.835e-08  123.138  < 2e-16 ***
as.factor(mydf$Link)10. GwangjuDaegu (125.9-128.0K) S     6.151e+00  8.939e-02   68.811  < 2e-16 ***
as.factor(mydf$Link)100. Jungang (267.8-270.4) S          3.891e+00  8.785e-02   44.286  < 2e-16 ***
as.factor(mydf$Link)102. Jungang (349.3-351.4) S         -1.271e+00  9.066e-02  -14.019  < 2e-16 ***
as.factor(mydf$Link)103. Jungang-Branch (1.1-3.4) E       5.375e+00  8.702e-02   61.761  < 2e-16 ***
as.factor(mydf$Link)104. Jungang-Branch (1.1-3.4) S       7.285e+00  8.669e-02   84.037  < 2e-16 ***
as.factor(mydf$Link)105. Jungang-Branch (3.4-5.4) E       1.926e-01  8.732e-02    2.205  0.02743 *  
as.factor(mydf$Link)106. Jungang-Branch (3.4-5.4) S       6.692e+00  8.679e-02   77.107  < 2e-16 ***
as.factor(mydf$Link)107. Jungang-Branch (5.4-8.0) E       2.436e+00  8.734e-02   27.886  < 2e-16 ***
as.factor(mydf$Link)108. Jungang-Branch (5.4-8.0) S      -4.868e-01  8.702e-02   -5.594 2.22e-08 ***
as.factor(mydf$Link)117. TongyoungDaejeon (113.2-115.6) E -1.362e+00  8.749e-02  -15.570  < 2e-16 ***
as.factor(mydf$Link)118. TongyoungDaejeon (113.2-115.6) S  2.877e+00  8.532e-02   33.716  < 2e-16 ***
as.factor(mydf$Link)119. TongyoungDaejeon (127.6-131.8) E  2.961e+00  8.782e-02   33.714  < 2e-16 ***
as.factor(mydf$Link)12. GwangjuDaegu (135.0-138.6K) S     4.629e+00  8.932e-02   51.830  < 2e-16 ***
as.factor(mydf$Link)120. TongyoungDaejeon (127.6-131.8) S  6.771e+00  8.542e-02   79.269  < 2e-16 ***
as.factor(mydf$Link)121. TongyoungDaejeon (153.1-155.9) E  2.266e+00  9.004e-02   25.165  < 2e-16 ***
as.factor(mydf$Link)122. TongyoungDaejeon (153.1-155.9) S  1.987e+00  8.800e-02   22.575  < 2e-16 ***
as.factor(mydf$Link)123. Pyungtaek Jaecheon (48.9-52.1) E -8.293e-01  8.699e-02   -9.533  < 2e-16 ***
as.factor(mydf$Link)124. Pyungtaek Jaecheon (48.9-52.1) S  5.202e+00  8.777e-02   59.263  < 2e-16 ***
as.factor(mydf$Link)125. Pyungtaek Jaecheon (105.1-107.3) E -2.267e+00  8.905e-02  -25.459  < 2e-16 ***
as.factor(mydf$Link)126. Pyungtaek Jaecheon (105.1-107.3) S -4.093e+00  8.987e-02  -45.542  < 2e-16 ***
as.factor(mydf$Link)127. Pyungtaek Jaecheon (112.0-115.7) E -3.982e+00  8.902e-02  -44.733  < 2e-16 ***
as.factor(mydf$Link)128. Pyungtaek Jaecheon (112.0-115.7) S -1.213e+00  8.848e-02  -13.705  < 2e-16 ***
as.factor(mydf$Link)129. Pyungtaek Jaecheon (115.7-118.9) E  6.127e+00  8.899e-02   68.847  < 2e-16 ***
as.factor(mydf$Link)130. Pyungtaek Jaecheon (115.7-118.9) S -2.101e+00  8.854e-02  -23.728  < 2e-16 ***
as.factor(mydf$Link)131. Pyungtaek Jaecheon (118.9-123.9) E -3.576e+00  8.917e-02  -40.107  < 2e-16 ***
as.factor(mydf$Link)132. Pyungtaek Jaecheon (118.9-123.9) S  2.743e+00  8.799e-02   31.181  < 2e-16 ***
```

[8] See the first case of the list of cases in Section 3.5.2

```
as.factor(mydf$Link)14. GwangjuDaegu (138.6-143.3K) S       -2.127e-01  8.905e-02   -2.388  0.01692 *
as.factor(mydf$Link)2. KochangDamyang (6.23-11.57k)_S       -3.077e+00  8.847e-02  -34.773  < 2e-16 ***
as.factor(mydf$Link)22. MuanGwangju (26.57-29.57) S          1.137e+00  8.753e-02   12.994  < 2e-16 ***
as.factor(mydf$Link)25. SangjuYoungduk (105.1-110.3) E      -3.913e+00  9.870e-02  -39.644  < 2e-16 ***
as.factor(mydf$Link)26. SangjuYoungduk (105.1-110.3) S      -3.384e+00  9.936e-02  -34.061  < 2e-16 ***
as.factor(mydf$Link)27. SangjuYoungduk(110.3-115.0) E       -1.069e+00  9.880e-02  -10.822  < 2e-16 ***
as.factor(mydf$Link)28. SangjuYoungduk (110.3-115.0) S      -4.426e+00  9.910e-02  -44.657  < 2e-16 ***
as.factor(mydf$Link)29. SangjuYoungduk (124.7-128.1) E      -7.597e-01  9.637e-02   -7.883 3.23e-15 ***
as.factor(mydf$Link)30. SangjuYoungduk(124.7-128.1) S       -8.267e-01  9.995e-02   -8.272  < 2e-16 ***
as.factor(mydf$Link)31. SangjuYoungduk (146.3-152.2) E      -1.557e+00  9.303e-02  -16.737  < 2e-16 ***
as.factor(mydf$Link)32. SangjuYoungduk (146.3-152.2) S      -4.206e-03  9.538e-02   -0.044  0.96483
as.factor(mydf$Link)35. SangjuYoungduk (172.3-176.2) E      -1.817e+00  1.015e-01  -17.911  < 2e-16 ***
as.factor(mydf$Link)36. SangjuYoungduk(172.3-176.2) S       -2.750e+00  1.025e-01  -26.835  < 2e-16 ***
as.factor(mydf$Link)37. SangjuYoungduk (181.3-185.5) E       2.075e+00  1.019e-01   20.370  < 2e-16 ***
as.factor(mydf$Link)38. SangjuYoungduk (181.3-185.5) S       9.355e-01  1.026e-01    9.119  < 2e-16 ***
as.factor(mydf$Link)39. SangjuYoungduk(185.5-188.7) E        4.699e+00  1.017e-01   46.220  < 2e-16 ***
as.factor(mydf$Link)40. SangjuYoungduk (185.5-188.7) S       2.958e+00  1.027e-01   28.811  < 2e-16 ***
as.factor(mydf$Link)41. SeoulYangyang (63.8-70.1) E         -2.336e+00  8.767e-02  -26.645  < 2e-16 ***
as.factor(mydf$Link)43. SeoulYangyang (70.1-73.7) E         -1.193e+00  8.724e-02  -13.675  < 2e-16 ***
as.factor(mydf$Link)47. Seoul Yangyang(97.7-103.9) E        -1.132e+00  8.831e-02  -12.824  < 2e-16 ***
as.factor(mydf$Link)48. Seoul Yangyang (97.7-103.9) S       -2.409e+00  9.105e-02  -26.458  < 2e-16 ***
as.factor(mydf$Link)49. Seoul Yangyang(106.9-110.9) E       -5.036e+00  8.843e-02  -56.941  < 2e-16 ***
as.factor(mydf$Link)5. KochangDamyang (19.92-24.06k) E       9.966e-01  9.368e-02   10.638  < 2e-16 ***
as.factor(mydf$Link)50. Seoul Yangyang(106.9-110.9) S       -3.509e+00  9.113e-02  -38.502  < 2e-16 ***
as.factor(mydf$Link)54. Seoul Yangyang(115.7-119.0) S       -3.425e+00  9.100e-02  -37.633  < 2e-16 ***
as.factor(mydf$Link)55. Seoul Yangyang(143.0-149.6) E       -9.388e-01  8.910e-02  -10.536  < 2e-16 ***
as.factor(mydf$Link)56. Seoul Yangyang(143.0-149.6) S        9.816e-01  9.109e-02   10.776  < 2e-16 ***
as.factor(mydf$Link)57. Suncheon Wyanju (7.8-12.5) E         3.153e+00  8.780e-02   35.906  < 2e-16 ***
as.factor(mydf$Link)59. Suncheon Wyanju (12.5-20.0) E        2.217e+00  8.790e-02   25.217  < 2e-16 ***
as.factor(mydf$Link)6. KochangDamyang (19.92-24.06k) S       1.833e+00  9.301e-02   19.708  < 2e-16 ***
as.factor(mydf$Link)61. Suncheon Wyanju (25.1-32.6) E        1.729e+00  8.818e-02   19.612  < 2e-16 ***
as.factor(mydf$Link)62. Suncheon Wyanju (25.1-32.6) S        5.969e-01  8.783e-02    6.796 1.08e-11 ***
as.factor(mydf$Link)65. Suncheon Wyanju (37.9-41.8) E        2.445e+00  8.793e-02   27.801  < 2e-16 ***
as.factor(mydf$Link)66. Suncheon Wyanju (37.9-41.8) S        2.548e-01  8.754e-02    2.911  0.00361 **
as.factor(mydf$Link)67. Suncheon Wyanju (41.8-46.6) E        7.111e-01  8.746e-02    8.130 4.32e-16 ***
as.factor(mydf$Link)68. Suncheon Wyanju (41.8-46.6) S        2.663e+00  8.724e-02   30.526  < 2e-16 ***
as.factor(mydf$Link)7. GwangjuDaegu (41.2-43.7K) E          -2.646e+00  9.164e-02  -28.879  < 2e-16 ***
as.factor(mydf$Link)8. GwangjuDaegu (41.2-43.7K) S           5.725e+00  9.175e-02   62.402  < 2e-16 ***
as.factor(mydf$Link)83. Jungbunaeryuk (106.4-108.1) E        7.346e+00  8.431e-02   87.132  < 2e-16 ***
as.factor(mydf$Link)84. Jungbunaeryuk (106.4-108.1) S        1.003e+01  8.434e-02  118.894  < 2e-16 ***
as.factor(mydf$Link)9. GwangjuDaegu (125.9-128.0K) E         5.821e+00  9.006e-02   64.638  < 2e-16 ***
as.factor(mydf$Link)93. Jungbunaeryuk (290.6-295.4) E       -2.425e+00  9.720e-02  -24.954  < 2e-16 ***
as.factor(mydf$Link)94. Jungbunaeryuk (290.6-295.4) S       -2.744e+00  9.643e-02  -28.461  < 2e-16 ***
as.factor(mydf$Link)97. Jungang (237.4-244.9) E              7.425e-01  9.026e-02    8.226  < 2e-16 ***
as.factor(mydf$Link)99. Jungang (267.8-270.4) E              8.746e-01  8.932e-02    9.792  < 2e-16 ***
---
Signif. codes:  0 '***' 0.001 '**' 0.01 '*' 0.05 '.' 0.1 ' ' 1

Residual standard error: 2.894 on 147757 degrees of freedom
Multiple R-squared:  0.5942,    Adjusted R-squared:  0.594
F-statistic:  2964 on 73 and 147757 DF,  p-value: < 2.2e-16
```

Figure 4-12 Residual plot of fixed effects model within links

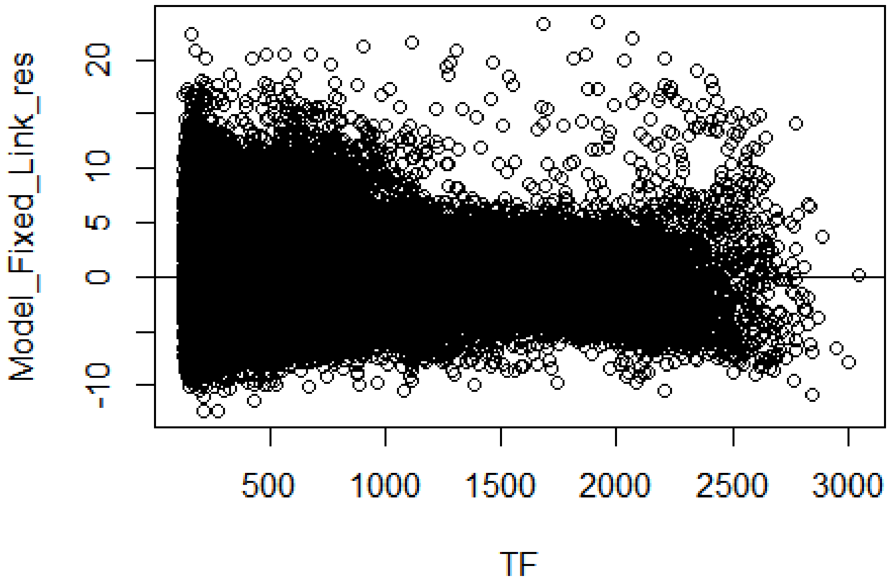

"MODEL1-2": time-fixed effects model by date

The LSDV model (MODEL1-2) that eliminates invariant effects by date can be derived as Table 4-11. R^2 of the model is 13.4%, which means that time-fixed effects have less impact on travel time than the link entity. The intercept of the model represents FFTT on 1st of September, which is 34.98 (seconds/km). As with MODEL 1-1, the estimated coefficients of dummy variables means the difference of FFTT between 1st of September and each date.

Table 4-11 Result of FE modelling (LSDV) with 'Date' entity (without geometric variables)

```
#Model with date dummies (No geometry)
MODEL1_2<-lm(mydf$Inv_SPD~mydf$TF+mydf$TF2+as.factor(mydf$Date))
summary(MODEL1_2)
##
##
## Call:
## lm(formula = mydf$Inv_SPD ~ mydf$TF + mydf$TF2 + as.factor(mydf$Date))
##
## Residuals:
##      Min       1Q   Median       3Q      Max
## -13.6965  -3.0044  -0.6062   2.5675  25.0786
##
## Coefficients:
##                          Estimate Std. Error t value Pr(>|t|)
## (Intercept)             3.498e+01  6.710e-02 521.293  < 2e-16 ***
## mydf$TF                -2.292e-03  8.023e-05 -28.568  < 2e-16 ***
## mydf$TF2                2.262e-06  4.043e-08  55.951  < 2e-16 ***
## as.factor(mydf$Date)2  -6.600e-01  8.520e-02  -7.747 9.47e-15 ***
## as.factor(mydf$Date)3   2.405e+00  8.669e-02  27.741  < 2e-16 ***
                                         ⋮
## as.factor(mydf$Date)29  6.412e-01  8.457e-02   7.582 3.44e-14 ***
## as.factor(mydf$Date)30 -5.053e-01  8.674e-02  -5.826 5.69e-09 ***
---
Signif. codes:  0 '***' 0.001 '**' 0.01 '*' 0.05 '.' 0.1 ' ' 1

Residual standard error: 4.227 on 147799 degrees of freedom
Multiple R-squared:  0.1341,           Adjusted R-squared:  0.1339
F-statistic: 738.1 on 31 and 147799 DF,  p-value: < 2.2e-16
```

"MODEL1-3": two-way FE modelling with link and date entities

Lastly, the two-way fixed effects modelling was implemented. The selected two fixed effects are link and date because the two entities have the minimum number of observations in cross-sectional and time-fixed effects. In addition, each R-squared of FE modelling by both entities of link and date is the highest value of cross-sectional and time specific entities respectively. The result of FE modelling by considering both entities can be shown in Table 4-12 (all coefficients can be seen in Appendix A.5.1). R-squared of the model is 68.2% and the range of residuals varies from -11.5 to 24.1 (Table 4-12).

Table 4-12 Result of two-way FE modelling (LSDV) with both 'Date' and 'Link' entities

```
#Model with date and link dummies
MODEL1_3<-lm(mydf$Inv_SPD ~ mydf$TF + mydf$TF2 + as.factor(mydf$Date) + as.fa
ctor(mydf$Link))
summary(MODEL1_3)
##
## Call:
## lm(formula = mydf$Inv_SPD ~ mydf$TF + mydf$TF2 + as.factor(mydf$Date) + a
s.factor(mydf$Link))
##
## Residuals:
##      Min       1Q   Median       3Q      Max
## -11.4554  -1.6166  -0.2194   1.2662  24.0820
##
## Coefficients:

##                              Estimate Std. Error  t value Pr(>|t|)
## (Intercept)                 3.525e+01  6.993e-02  504.062  < 2e-16 ***
## mydf$TF                    -5.284e-03  5.217e-05 -101.277  < 2e-16 ***
## mydf$TF2                    3.507e-06  2.551e-08  137.469  < 2e-16 ***
## as.factor(mydf$Date)2      -5.959e-01  5.161e-02  -11.546  < 2e-16 ***
                                                   ⋮
## as.factor(mydf$Date)30     -5.353e-01  5.256e-02  -10.185  < 2e-16 ***
## (Link)10.GwangjuDaegu()S    6.190e+00  7.909e-02   78.271  < 2e-16 ***
                                                   ⋮
## (Link)99.Jungang()E         6.960e-01  7.903e-02    8.806  < 2e-16 ***

## ---
## Signif. codes:  0 '***' 0.001 '**' 0.01 '*' 0.05 '.' 0.1 ' ' 1
##
## Residual standard error: 2.56 on 147728 degrees of freedom
## Multiple R-squared:  0.6825, Adjusted R-squared:  0.6823
## F-statistic:  3113 on 102 and 147728 DF,  p-value: < 2.2e-16
```

Figure 4-13 Residual plot of two-way FE model

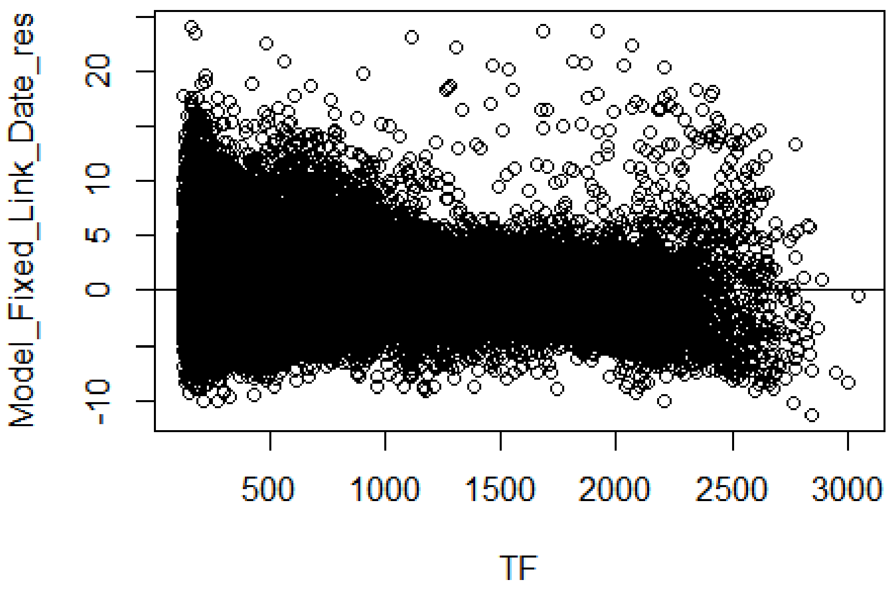

4.4.3. POLS and FE models including geometric variables

"MODEL2": POLS estimation with geometric variables:

In order to investigate the effects of link geometry, four link geometric variables obtained from 72 motorway sections are added to MODEL1 as independent variables. Therefore, the number of independent variables of the model ("MODEL2") becomes six (Table 4-13). The model can explain the relationship between DV and IV1 (TF and TF2) with four geometric variables. Adjusted R-squared of MODEL2 was 8.6% (0.08584), which is improved by around 6.1% compared to MODEL1. In the same vein, the width of residual variation decreased (Figure 4-14).

Table 4-13 Pooled OLS estimation with TF and geometric independent variables

```
# Pooled OLS: Model with geometric features
MODEL2<-lm(mydf$Inv_SPD~mydf$TF+mydf$TF2+mydf$TR+mydf$RISE+mydf$FALL+mydf$BEN
D)
summary(MODEL2)
##
## Call:
## lm(formula = mydf$Inv_SPD ~ mydf$TF + mydf$TF2 + mydf$TR + mydf$RISE +
##     mydf$FALL + mydf$BEND)
##
## Residuals:
##      Min       1Q   Median       3Q      Max
## -12.5457  -3.0571  -0.6077   2.6507  25.0981
##
## Coefficients:
##               Estimate Std. Error t value Pr(>|t|)
## (Intercept)  3.618e+01  9.380e-02  385.74   <2e-16 ***
## mydf$TF     -3.163e-03  8.183e-05  -38.65   <2e-16 ***
## mydf$TF2     2.197e-06  4.081e-08   53.83   <2e-16 ***
## mydf$TR      1.178e-03  9.193e-05   12.81   <2e-16 ***
## mydf$RISE   -2.565e-02  2.401e-03  -10.69   <2e-16 ***
## mydf$FALL    2.237e-01  2.855e-03   78.38   <2e-16 ***
## mydf$BEND    9.488e-02  2.227e-03   42.61   <2e-16 ***
## ---
## Signif. codes:  0 '***' 0.001 '**' 0.01 '*' 0.05 '.' 0.1 ' ' 1
##
## Residual standard error: 4.342 on 147824 degrees of freedom
## Multiple R-squared:  0.08588,    Adjusted R-squared:  0.08584
## F-statistic:  2315 on 6 and 147824 DF,  p-value: < 2.2e-16
```

Figure 4-14 Residual plot of pooled OLS estimation between DV and TF

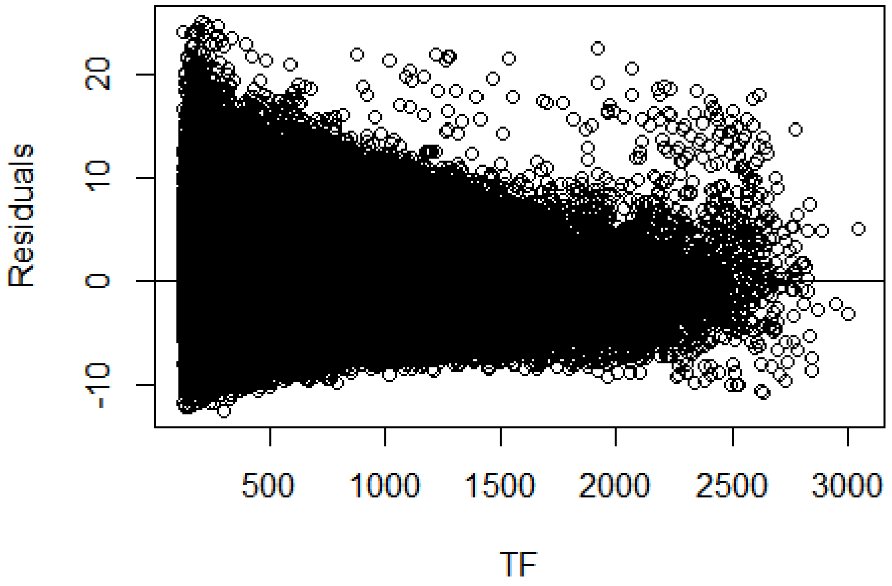

"MODEL2-1": FE model across routes (lines)

Routes consist of links and as such the entity of routes is the collective concept of links. The purpose of FE modelling by this classification is to find how routes affect travel time. For example, some routes can be mainly used for logistics and others can be used for tourism. The result of route-specific FE modelling can be seen from Table 4-14. The estimated intercept of each route dummy variable is the difference with "Gwangju-Daegu" route. R-squared (26.6%) of MODEL2-1 is improved by 18.3% compared to MODEL2 (8.6%), but the coefficient of determination is much lower than MODEL1-1 (59.3%). This result would be natural in that MODEL1-1 estimates the model in more detail than MODEL2-1 because each route consists of links.

Table 4-14 Result of FE modelling (LSDV) with the 'Route' entity

```
#Model with route dummies
MODEL2_1 <-lm(mydf$Inv_SPD ~ mydf$TF + mydf$TF2 + mydf$TR + mydf$RISE + mydf
$FALL + mydf$BEND + as.factor(mydf$Line))
summary(MODEL2_1)
##
## Call:
## lm(formula = mydf$Inv_SPD ~ mydf$TF + mydf$TF2 + mydf$TR + mydf$RISE + myd
f$FALL + mydf$BEND + as.factor(mydf$Line))
##
## Residuals:
##      Min       1Q   Median       3Q      Max
## -13.4027  -2.5738  -0.2008   2.2486  24.7410
##
## Coefficients:
##                             Estimate Std. Error  t value Pr(>|t|)
## (Intercept)                3.937e+01  1.545e-01  254.768  < 2e-16 ***
## mydf$TF                   -5.631e-03  7.752e-05  -72.638  < 2e-16 ***
## mydf$TF2                   3.297e-06  3.771e-08   87.435  < 2e-16 ***
```

```
## mydf$TR                    3.427e-03  1.120e-04   30.587  < 2e-16 ***
## mydf$RISE                 -3.095e-02  2.991e-03  -10.348  < 2e-16 ***
## mydf$FALL                  1.741e-01  3.209e-03   54.263  < 2e-16 ***
## mydf$BEND                  7.987e-06  2.955e-03    0.003  0.998
## (Line)Jungang             -2.128e+00  6.784e-02  -31.375  < 2e-16 ***
## (Line)Jungang-Branch      -4.887e-01  6.678e-02   -7.318 2.54e-13 ***
## (Line)Jungbunaeryuk        6.689e-01  6.402e-02   10.449  < 2e-16 ***
## (Line)KochangDamyang      -4.773e+00  8.057e-02  -59.246  < 2e-16 ***
## (Line)MuanGwangju         -1.701e+00  9.893e-02  -17.190  < 2e-16 ***
## (Line)PyungtaekJaecheon -4.585e+00  5.778e-02  -79.343  < 2e-16 ***
## (Line)SangjuYoungduk      -4.390e+00  5.767e-02  -76.115  < 2e-16 ***
## (Line)SeoulYangyang       -5.866e+00  5.100e-02 -115.026  < 2e-16 ***
## (Line)SuncheonWyanju      -1.777e+00  6.087e-02  -29.198  < 2e-16 ***
## (Line)TongyoungDaejeon    -1.199e+00  6.267e-02  -19.125  < 2e-16 ***
## ---
## Signif. codes:  0 '***' 0.001 '**' 0.01 '*' 0.05 '.' 0.1 ' ' 1
##
## Residual standard error: 3.891 on 147814 degrees of freedom
## Multiple R-squared:  0.2661, Adjusted R-squared:  0.266
## F-statistic:  3350 on 16 and 147814 DF,  p-value: < 2.2e-16
```

"MODEL2-2": FE model by brightness (day and night time)

The entity of brightness is for time-fixed modelling that identifies how both daytime and nighttime can affect travel time. As mentioned in Section 4.2.2, day time was treated as falling between 07.00 and 19.00; and night time during the remaining hours of a day and night. The result of FE modelling suggests that during the night time FFTT is larger by 1.3 (seconds per km) than that during daytime (Table 4-15). However, the overall R-squared (9.8%) of this model is little improved compared to MODEL2.

Table 4-15 Result of FE modelling (LSDV) with the 'Brightness' entity

```
#Model with brightness dummies
MODEL2_2<-lm(mydf$Inv_SPD~mydf$TF+mydf$TF2+mydf$TR+mydf$RISE+mydf$FALL+mydf$B
END+as.factor(mydf$night))
summary(MODEL2_2)
##
## Call:
## lm(formula = mydf$Inv_SPD ~ mydf$TF + mydf$TF2 + mydf$TR + mydf$RISE +
##     mydf$FALL + mydf$BEND + as.factor(mydf$night))
##
## Residuals:
##      Min       1Q   Median       3Q      Max
## -13.2084  -3.0274  -0.5624   2.6824  24.4239
##
## Coefficients:
##                            Estimate Std. Error t value Pr(>|t|)
## (Intercept)_FFTT          3.488e+01  9.754e-02 357.555  < 2e-16 ***
## mydf$TF                  -1.727e-03  8.725e-05 -19.794  < 2e-16 ***
## mydf$TF2                  1.699e-06  4.200e-08  40.448  < 2e-16 ***
## mydf$TR                   1.476e-03  9.154e-05  16.120  < 2e-16 ***
## mydf$RISE                -1.785e-02  2.390e-03  -7.466 8.29e-14 ***
## mydf$FALL                 2.126e-01  2.846e-03  74.701  < 2e-16 ***
## mydf$BEND                 9.833e-02  2.213e-03  44.436  < 2e-16 ***
```

```
## as.factor(mydf$night)1  1.269e+00  2.807e-02  45.224  < 2e-16 ***
## ---
## Signif. codes:  0 '***' 0.001 '**' 0.01 '*' 0.05 '.' 0.1 ' ' 1
##
## Residual standard error: 4.313 on 147823 degrees of freedom
## Multiple R-squared:  0.09835,    Adjusted R-squared:  0.09831
## F-statistic:  2304 on 7 and 147823 DF,  p-value: < 2.2e-16
```

"MODEL2-3": FE model by day (weekday and weekend)

As a result of FE modelling with the dummy variables of weekday and weekend, the overall R-squared of the model increased from 8.6% (MODEL2) to 13.7% (MODEL2-3), and FFTT during weekends is found to be lower by 2.2 (seconds per km) than on weekdays (Table 4-16).

Table 4-16 Result of FE modelling (LSDV) with the 'Day (weekday and weekend)' entity

```
#Model with day dummies
MODEL2_3 <-lm(mydf$Inv_SPD~mydf$TF+mydf$TF2+mydf$TR+mydf$RISE+mydf$FALL+mydf
$BEND+as.factor(mydf$Weekend))
summary(MODEL2_3)
##
## Call:
## lm(formula = mydf$Inv_SPD ~ mydf$TF + mydf$TF2 + mydf$TR + mydf$RISE +
##     mydf$FALL + mydf$BEND + as.factor(mydf$Weekend))
##
## Residuals:
##      Min       1Q   Median       3Q      Max
## -13.1775  -2.9247  -0.5007   2.5178  26.6557
##
## Coefficients:
##                             Estimate Std. Error t value Pr(>|t|)
## (Intercept)_FFTT           3.656e+01  9.124e-02 400.660   <2e-16 ***
## mydf$TF                   -2.481e-03  7.986e-05 -31.063   <2e-16 ***
## mydf$TF2                   1.952e-06  3.975e-08  49.108   <2e-16 ***
## mydf$TR                    1.252e-03  8.934e-05  14.020   <2e-16 ***
## mydf$RISE                 -2.301e-02  2.333e-03  -9.862   <2e-16 ***
## mydf$FALL                  2.202e-01  2.774e-03  79.386   <2e-16 ***
## mydf$BEND                  9.522e-02  2.164e-03  44.003   <2e-16 ***
## as.factor(mydf$Weekend)1 -2.171e+00  2.324e-02 -93.389   <2e-16 ***
## ---
## Signif. codes:  0 '***' 0.001 '**' 0.01 '*' 0.05 '.' 0.1 ' ' 1
##
## Residual standard error: 4.22 on 147823 degrees of freedom
## Multiple R-squared:  0.1368, Adjusted R-squared:  0.1368
## F-statistic:  3347 on 7 and 147823 DF,  p-value: < 2.2e-16
```

"MODEL2-4": FE model by weather (rainy days)

As mentioned in Section 4.2.2, in order to identify the effects of different weathers more clearly, the data for local rainy days were excluded. After excluding such data, only nationwide rainy days and dry days remained in the dataset. FFTT in rainy days is higher by 1.2 (seconds per km) than its equivalent on dry days (Table 4-17). However, as with MODEL2-2, the R-squared of MODEL2-4 was slightly improved.

Table 4-17 Result of FE modelling (LSDV) with the 'Weather' entity

```
#Model with Weather dummies
mydf<-mydf[mydf$rainy2=="0",]   #locally rainy days exclusion
MODEL2_4 <-lm(mydf$Inv_SPD ~ mydf$TF + mydf$TF2 + mydf$TR +
mydf$RISE + mydf$FALL + mydf$BEND + as.factor(mydf$rainy1))
summary(MODEL2_4)
##
## Call:
## lm(formula = mydf$Inv_SPD ~ mydf$TF + mydf$TF2 + mydf$TR +
mydf$RISE + mydf$FALL + mydf$BEND + as.factor(mydf$rainy1))
##
## Residuals:
##      Min       1Q   Median       3Q      Max
## -12.8878  -3.0908  -0.5738   2.6743  24.4976
##
## Coefficients:
##                               Estimate Std. Error t value Pr(>|t|)
## (Intercept)_FFTT             3.595e+01  1.262e-01  284.94   <2e-16 ***
## mydf$TF                     -2.976e-03  1.056e-04  -28.18   <2e-16 ***
## mydf$TF2                     2.138e-06  5.067e-08   42.20   <2e-16 ***
## mydf$TR                      1.324e-03  1.233e-04   10.74   <2e-16 ***
## mydf$RISE                   -3.020e-02  3.217e-03   -9.39   <2e-16 ***
## mydf$FALL                    2.357e-01  3.837e-03   61.44   <2e-16 ***
## mydf$BEND                    1.043e-01  2.983e-03   34.96   <2e-16 ***
## as.factor(mydf$raining1)1  1.205e+00  3.390e-02   35.54   <2e-16 ***
## ---
## Signif. codes:  0 '***' 0.001 '**' 0.01 '*' 0.05 '.' 0.1 ' ' 1
##
## Residual standard error: 4.385 on 84024 degrees of freedom
## Multiple R-squared:  0.1055, Adjusted R-squared:  0.1054
## F-statistic:  1416 on 7 and 84024 DF,  p-value: < 2.2e-16
```

"MODEL2-5": time-fixed effects model by date

Time-fixed effects models can capture individual-invariant effects varying across every day. The entity of date can find the unobserved fixed effects more than the entities of weather and day because the date entity splits both entities more. As can be seen from Table 4-18, the daily change was investigated. Compared to FFTT (intercept of the model) on 1st September 2018, the coefficients of the other 29 days in September vary from -1.2 (23rd) to 3.2 (11th). The R-squared of this FE model is 19.4%, which is higher by 10.8% than that of MODEL2.

Table 4-18 Result of FE modelling (LSDV) with the 'Date' entity (with geometric variables)

```
#Model with date dummies
MODEL2_5<-lm(mydf$Inv_SPD ~ mydf$TF + mydf$TF2 + mydf$TR +
mydf$RISE + mydf$FALL + mydf$BEND + as.factor(mydf$Date))
summary(MODEL2_5)
##
## Call:
```

```
## lm(formula = mydf$Inv_SPD ~ mydf$TF + mydf$TF2 + mydf$TR + mydf$RISE +
##     mydf$FALL + mydf$BEND + as.factor(mydf$Date))
##
## Residuals:
##      Min       1Q   Median       3Q      Max
## -13.7344  -2.7816  -0.4828   2.4113  26.0050
##
## Coefficients:
##                         Estimate Std. Error t value Pr(>|t|)
## (Intercept)            3.427e+01  1.056e-01 324.515  < 2e-16 ***
## mydf$TF               -2.491e-03  7.757e-05 -32.111  < 2e-16 ***
## mydf$TF2               2.373e-06  3.906e-08  60.755  < 2e-16 ***
## mydf$TR                1.378e-03  8.637e-05  15.954  < 2e-16 ***
## mydf$RISE             -1.929e-02  2.256e-03  -8.551  < 2e-16 ***
## mydf$FALL              2.158e-01  2.682e-03  80.470  < 2e-16 ***
## mydf$BEND              9.882e-02  2.092e-03  47.232  < 2e-16 ***
## as.factor(mydf$Date)2  -6.480e-01  8.221e-02  -7.882 3.24e-15 ***
## as.factor(mydf$Date)3   2.384e+00  8.366e-02  28.502  < 2e-16 ***
## as.factor(mydf$Date)4   2.683e+00  8.351e-02  32.130  < 2e-16 ***
## as.factor(mydf$Date)5   2.817e+00  8.292e-02  33.970  < 2e-16 ***
## as.factor(mydf$Date)6   2.649e+00  8.279e-02  32.001  < 2e-16 ***
## as.factor(mydf$Date)7   1.569e+00  8.178e-02  19.188  < 2e-16 ***
## as.factor(mydf$Date)8  -8.155e-02  8.011e-02  -1.018    0.309
## as.factor(mydf$Date)9  -7.852e-01  8.119e-02  -9.671  < 2e-16 ***
## as.factor(mydf$Date)10  2.060e+00  8.241e-02  25.001  < 2e-16 ***
## as.factor(mydf$Date)11  3.187e+00  8.300e-02  38.396  < 2e-16 ***
## as.factor(mydf$Date)12  2.898e+00  8.288e-02  34.965  < 2e-16 ***
## as.factor(mydf$Date)13  2.758e+00  8.258e-02  33.400  < 2e-16 ***
## as.factor(mydf$Date)14  2.073e+00  8.162e-02  25.401  < 2e-16 ***
## as.factor(mydf$Date)15  5.173e-01  8.086e-02   6.397 1.59e-10 ***
## as.factor(mydf$Date)16 -7.020e-01  8.228e-02  -8.532  < 2e-16 ***
## as.factor(mydf$Date)17  2.484e+00  8.231e-02  30.176  < 2e-16 ***
## as.factor(mydf$Date)18  2.940e+00  8.270e-02  35.550  < 2e-16 ***
## as.factor(mydf$Date)19  2.893e+00  8.265e-02  35.005  < 2e-16 ***
## as.factor(mydf$Date)20  2.824e+00  8.298e-02  34.037  < 2e-16 ***
## as.factor(mydf$Date)21  1.974e+00  8.179e-02  24.138  < 2e-16 ***
## as.factor(mydf$Date)22 -4.732e-01  7.975e-02  -5.933 2.98e-09 ***
## as.factor(mydf$Date)23 -1.242e+00  7.973e-02 -15.573  < 2e-16 ***
## as.factor(mydf$Date)24 -1.171e+00  8.267e-02 -14.171  < 2e-16 ***
## as.factor(mydf$Date)25 -8.035e-01  8.044e-02  -9.989  < 2e-16 ***
## as.factor(mydf$Date)26 -1.019e+00  8.089e-02 -12.595  < 2e-16 ***
## as.factor(mydf$Date)27  1.524e+00  8.341e-02  18.268  < 2e-16 ***
## as.factor(mydf$Date)28  2.000e+00  8.201e-02  24.387  < 2e-16 ***
## as.factor(mydf$Date)29  6.443e-01  8.161e-02   7.895 2.92e-15 ***
## as.factor(mydf$Date)30 -4.988e-01  8.370e-02  -5.960 2.53e-09 ***
## ---
## Signif. codes:  0 '***' 0.001 '**' 0.01 '*' 0.05 '.' 0.1 ' ' 1
##
## Residual standard error: 4.079 on 147795 degrees of freedom
## Multiple R-squared:  0.1937, Adjusted R-squared:  0.1935
## F-statistic:  1014 on 35 and 147795 DF,  p-value: < 2.2e-16
```

4.4.4. Comparison between fixed effects models

The above results by FE modelling by LSDV from the one-month dataset can be summarised in Table 4-19 and Table 4-20: The first table compares pooled OLS model and FE models without geometric variables because the perfect correlation happens between the link entity and the geometric variables; and the latter table compares pooled OLS model and FE models with geometric features. FE modelling in this section focused more on the change in the values of estimated coefficients with the overall coefficient of determination (adjusted R-squared) rather than the statistical significance of each coefficient. The statistical significance of estimated coefficients is examined in detail in Chapter 5 because it is imperative to develop the feasible models for traffic assignment.

First of all, as can be seen from Table 4-19, it can be concluded that there are many unobserved effects affecting travel time across links. The adjusted R^2s of two FE models (MODEL1-1 and MODEL1-3) which take into account the link entity are much higher than MODEL1 and other FE models without the link entity. Moreover, in comparison with the coefficients of MODEL1, the coefficients of the two FE models including the link entity fluctuated more than those of other FE models. This result suggests therefore that unobserved effects resulting from the entity of link would affect travel time more than those from the entity of date. It also implies that link geometry, which is one of the link attributes, needs to be reflected in travel time estimation models.

Secondly, Table 4-20 compares the pooled OLS estimation model (MODEL2) including geometric variables with FE models across other entities, which are routes (lines), brightness, day, weather and date. The analysis has some implications for both this thesis and future study. When looking at MODEL2-1 including the route entity, the adjusted R^2 and the coefficients of the model differ widely from MODEL2. This finding is in line with the observation between MODEL1 and MODEL1-1in that routes (lines) are the collective groups of links. With regards to MODEL2-2, most percentage changes of the model's coefficients with those of MODEL2 are higher than any other model with time-fixed effects. This indicates that there is a difference in traffic characteristics between day and night time[9].

[9] This finding is also useful for filtering data in developing feasible models (Chapter 5). Brightness needs to be considered in travel time estimation models.

Table 4-19 Summary of FE modelling by LSDV (without geometric variables)

Model	MODEL1	MODEL1-1	MODEL1-2	MODEL1-3
Fixed effects	-	Link	Date	Link&Date
Variables	Coef.	Coef.	Coef.	Coef.
(Intercept)	3.66E+01 ***	3.70E+01 ***	3.50E+01 ***	3.53E+01 ***
TF	-2.96E-03 ***	-6.42E-03 ***	-2.29E-03 ***	-5.28E-03 ***
		-117%	22%	-79%
TF^2	2.09E-06 ***	3.49E-06 ***	2.26E-06 ***	3.51E-06 ***
		67%	8%	68%
Degrees of Freedom	147,828	147,757	147,799	147,728
Adjusted R-squared	0.0252	0.5940	0.1339	0.6823

Note 1. '***' means that coefficients are statistically significant at 99.9% confidence level.
2. The underlined values are percentage changes of coefficients between MODEL1 and each model.

Table 4-20 Summary of FE modelling by LSDV (with geometric variables)

Model	MODEL2	MODEL2-1	MODEL2-2	MODEL2-3	MODEL2-4	MODEL2-5
Fixed effects	-	Route	Brightness	Day	Weather	Date
Variables	Coef.	Coef.	Coef.	Coef.	Coef.	Coef.
(Intercept)	3.62E+01 ***	3.94E+01 ***	3.49E+01 ***	3.66E+01 ***	3.60E+01 ***	3.43E+01 ***
TF	-3.16E-03 ***	-5.63E-03 ***	-1.73E-03 ***	-2.48E-03 ***	-2.98E-03 ***	-2.49E-03 ***
		-78%	45%	22%	6%	21%
TF^2	2.20E-06 ***	3.30E-06 ***	1.70E-06 ***	1.95E-06 ***	2.14E-06 ***	2.37E-06 ***
		50%	-23%	-11%	-3%	8%
TR	1.18E-03 ***	3.43E-03 ***	1.48E-03 ***	1.25E-03 ***	1.32E-03 ***	1.38E-03 ***
		191%	25%	6%	12%	17%
RISE	-2.57E-02 ***	-3.10E-02 ***	-1.79E-02 ***	-2.30E-02 ***	-3.02E-02 ***	-1.93E-02 ***
		-21%	30%	10%	-18%	25%
FALL	2.24E-01 ***	1.74E-01 ***	2.13E-01 ***	2.20E-01 ***	2.36E-01 ***	2.16E-01 ***
		-22%	-5%	-2%	5%	-4%
BEND	9.49E-02 ***	7.99E-06	9.83E-02 ***	9.52E-02 ***	1.04E-01 ***	9.88E-02 ***
		-100%	4%	0%	10%	4%
Degrees of Freedom	147,824	147,814	147,823	149,193	84,024	147,795
Adjusted R-squared	0.0858	0.2660	0.0983	0.1340	0.1054	0.1935

Note: The underlined values are percentage changes between MODEL2 and each model.

4.4.5. Model finding with panel data: POLS, FE and RE modelling

This section implements POLS, FE and RE modelling after recognising the one-month dataset as the panel data having the cross sections of links and time-series with 15-minute intervals. The reason behind this is that FE modelling by LSDV in Section 4.4.2 and 4.4.3 found that the entity of links is the most influential factor of all the entities. However, as already mentioned in the above section, geometric independent variables by the panel data cannot be included in FE modelling because the geometric features are time-invariant variables across links. Therefore, this section compares three models of pooled OLS, FE and RE models after deriving models with the independent variables of TF and TF2 only and by using the one-month dataset[10]. The library that is used for the model estimation in the software package of "R" is ***"plm"*** and the *'plm()'* function was applied to the dataset with the different arguments of *'pooling'*, *'within'* and *'random'*.

Panel data definition

Unlike FE modelling by LSDV, in order to implement *'plm()'* function in "R" and compare the estimated functions, the dataset needs to be defined as the panel data. As mentioned above, the one-month dataset was firstly defined as the panel data with the entity of links and 15-minute time intervals as follows;

Table 4-21 Panel data definition with the entity of links and 15-minute intervals

```
# Panel Data Definition with the entity of links and time
PanelData_Link_Time <- plm.data(mydf,index=c("Link","Time"))
```

Pooled OLS modelling

Table 4-22 shows the result of pooled OLS estimation by using *'plm()'* function, which has the same result of 'MODEL1' in Section 4.4.2.

Table 4-22 Pooled OLS estimation with the panel data

```
# Pooled OLS estimation with the panel data
Model_POLS_TF_Panel <- plm(Inv_SPD~TF+TF2, data=PanelData_Link_Time, model="p
ooling")
summary(Model_POLS_TF_Panel)
## Pooling Model
##
## Call:
```

[10] Although RE modelling can include geometric variables in the estimated models, this chapter does not suggest the results because this chapter mainly aims to find the influential factors on travel time estimation models from one-month dataset. Chapter 5 scrutinises the detailed measurement of coefficients and their statistical significances.

```
## plm(formula = Inv_SPD ~ TF + TF2, data = PanelData_Link_Time,
##     model = "pooling")
##
## Unbalanced Panel: n = 72, T = 1299-2725, N = 147831
##
## Residuals:
##      Min.   1st Qu.    Median   3rd Qu.      Max.
## -12.47743  -3.24498  -0.70206   2.68517  23.84815
##
## Coefficients:
##                Estimate  Std. Error  t-value  Pr(>|t|)
## (Intercept)  3.6632e+01  3.3037e-02 1108.789 < 2.2e-16 ***
## TF          -2.9572e-03  8.4341e-05  -35.062 < 2.2e-16 ***
## TF2          2.0875e-06  4.2100e-08   49.584 < 2.2e-16 ***
## ---
## Signif. codes:  0 '***' 0.001 '**' 0.01 '*' 0.05 '.' 0.1 ' ' 1
##
## Total Sum of Squares:    3049300
## Residual Sum of Squares: 2972300
## R-Squared:      0.025239
## Adj. R-Squared: 0.025226
## F-statistic: 1913.84 on 2 and 147828 DF, p-value: < 2.22e-16
```

FE modelling within entities

Table 4-23 shows the result of FE modelling by *'plm()'* function with the argument of *'within'*, whose coefficients of TF and TF2 are identical with the result of FE modelling by LSDV (Table 4-10).

Table 4-23 FE modelling by the method of 'within' estimation

```
# FE modelling with the panel data by 'within' estimation
Model_FE_within_Panel <- plm(Inv_SPD~TF+TF2, data=PanelData_Link_Time, model=
"within")
summary(Model_FE_within_Panel)
## Oneway (individual) effect Within Model
##
## Call:
## plm(formula = Inv_SPD ~ TF + TF2, data = PanelData_Link_Time,
##     model = "within")
##
## Unbalanced Panel: n = 72, T = 1299-2725, N = 147831
##
## Residuals:
##      Min.   1st Qu.    Median   3rd Qu.      Max.
## -12.33278  -1.74056  -0.22462   1.37627  23.46250
##
## Coefficients:
##        Estimate  Std. Error t-value  Pr(>|t|)
## TF  -6.4169e-03  5.8266e-05 -110.13 < 2.2e-16 ***
## TF2  3.4916e-06  2.8355e-08  123.14 < 2.2e-16 ***
## ---
## Signif. codes:  0 '***' 0.001 '**' 0.01 '*' 0.05 '.' 0.1 ' ' 1
```

```
##
## Total Sum of Squares:    1367200
## Residual Sum of Squares: 1237400
## R-Squared:      0.094921
## Adj. R-Squared: 0.094474
## F-statistic: 7748.1 on 2 and 147757 DF, p-value: < 2.22e-16
```

RE modelling

Based on the assumption that each entity of links is not correlated with the explanatory variables, the coefficients were derived by RE modelling (Table 4-24). The coefficient values in RE modelling, which are -6.41e-03 for TF and 3.49e-06 for TF2 respectively, are not very different from those in FE modelling, which are -6.42e-03 and 3.50e-06. In comparison to FE modelling, RE modelling can estimate the intercept with 3.78e+01.

Table 4-24 RE modelling with panel data

```
# Random Effects Model
Model_RE_Panel <- plm(Inv_SPD~TF+TF2, data=PanelData_Link_Time, model="random
")
summary(Model_RE_Panel)
## Oneway (individual) effect Random Effect Model
##    (Swamy-Arora's transformation11)
##
## Call:
## plm(formula = Inv_SPD ~ TF + TF2, data = PanelData_Link_Time,
##     model = "random")
##
## Unbalanced Panel: n = 72, T = 1299-2725, N = 147831
##
## Effects:
##                   var std.dev share
## idiosyncratic  8.375   2.894 0.444
## individual    10.475   3.236 0.556
## theta:
##    Min. 1st Qu.  Median    Mean 3rd Qu.    Max.
##  0.9752  0.9799  0.9810  0.9804  0.9814  0.9829
##
## Residuals:
##     Min.  1st Qu.   Median     Mean  3rd Qu.     Max.
## -12.1801  -1.7429  -0.2320   0.0023   1.3703  23.3986
##
## Coefficients:
##                Estimate  Std. Error  z-value  Pr(>|z|)
## (Intercept)  3.7757e+01  3.8210e-01   98.815 < 2.2e-16 ***
## TF          -6.4152e-03  5.8265e-05 -110.104 < 2.2e-16 ***
## TF2          3.4909e-06  2.8355e-08  123.115 < 2.2e-16 ***
```

[11] In order to transform the variance of errors from OLS estimation, there are many studies to predetermine the variance of cross-sectional specific effects (σ_μ^2 in Equation 3-26) and the variance of the random error (σ_ε^2) (see Baltagi (2013) in detail). However, since this study implements RE modelling for the comparison with pooled OLS and FE modelling rather than for coefficient estimation, the default method of RE modelling in 'plm()' function, which is Swamy and Arora (1972)'s transformation, was applied without a further discussion.

```
## ---
## Signif. codes:  0 '***' 0.001 '**' 0.01 '*' 0.05 '.' 0.1 ' ' 1
##
## Total Sum of Squares:    1368000
## Residual Sum of Squares: 1238100
## R-Squared:      0.094999
## Adj. R-Squared: 0.094987
## Chisq: 15517.5 on 2 DF, p-value: < 2.22e-16
```

Comparison between the modelling methods

In order to find the most appropriate modelling method among the three methods, which are closely related to the establishment of the direction for the feasible model development in Chapter 5, three tests were implemented. Firstly, F-test between pooled OLS modelling and FE modelling was used for investigating the significance of individual effects (Hamilton, 2012). Secondly, the Hausman test (also called Durbin–Wu–Hausman test) between FE and RE modelling was conducted for the model selection (Hausman, 1978). Lastly, the Breusch and Pagan Lagrangian Multiplier (LM) test was applied for investigating random effects (Baltagi, 2008).

The result of F-test rejects the null hypothesis that pooled OLS modelling is better than FE modelling (Table 4-25). In addition, the result of the Hausman test shows that FE modelling is superior to RE modelling. Lastly, it is confirmed that there are panel effects in the one-month dataset by the Breusch and Pagan LM test. Overall, it can be concluded that FE modelling is the most appropriate approach among the three modelling methods.

Table 4-25 F-test for investigating individual effects

```
# Testing for fixed effects, null: OLS better than FE modelling
pFtest(Model_FE_within_Panel, Model_POLS_TF_Panel)
##
##  F test for individual effects
##
## data:  Inv_SPD ~ TF + TF2
## F = 2917.7, df1 = 71, df2 = 147760, p-value < 2.2e-16
## alternative hypothesis: significant effects
```

Table 4-26 Hausman test for model selection between FE and RE modelling

```
# Fixed vs Random: null hypothesis is that the preferred model is random effe
cts
phtest(Model_FE_within_Panel, Model_RE_Panel)
##
##  Hausman Test
##
## data:  Inv_SPD ~ TF + TF2
## chisq = 11.432, df = 2, p-value = 0.003293
## alternative hypothesis: one model is inconsistent
```

Table 4-27 Breusch and Pagan Lagrangian Multiplier (LM) test

```
# Breusch-Pagan Lagrange Multiplier for random effects. Null is no panel effe
ct (i.e. OLS better).
plmtest(Model_POLS_TF_Panel, type=c("bp"))
##
##  Lagrange Multiplier Test - (Breusch-Pagan) for unbalanced panels
##
## data:  Inv_SPD ~ TF + TF2
## chisq = 56699000, df = 1, p-value < 2.2e-16
## alternative hypothesis: significant effects
```

4.4.6. Summary

In Section4.4, in order to find the factors which have an influence on travel time, the statistical linear estimation was implemented in the following three ways: pooled OLS estimation, FE modelling, and RE modelling.

Firstly, the comparison between MODEL1 and MODEL2 concluded that four geometric variables, namely TR, RISE, FALL and BEND, improve the coefficient of determination of the estimated model. The difference of adjusted R^2s between two models with and without the geometric variables is 6.1%. This suggests that link geometric variables need to be included in travel time estimation models as with the result of NLS estimation (Section 4.3).

Secondly, FE modelling by LSDV was an efficient way to identify the influential factors on travel time in the one-month dataset. As is summarised in Table 4-19 and Table 4-20, the influential factors affecting the dependent variable were selected by comparing the change in model goodness of fit, introducing many entities, which are links, routes (lines), brightness, day, weather and date. The link entity is the most influential factor of the classified entities when investigating the goodness of fit in one-way FE modelling with the link entity and two-way FE modelling with both entities of links and date (Table 4-19). In addition, the big difference in the coefficients between FE models including the link entity and other models, was demonstrated.

Lastly, of the three different models of pooled OLS, FE and RE modelling, FE modelling across links is the most appropriate for one-month data analysis. Since FE modelling by LSDV suggested that the entity of links is the most influential factor in this study, the one-month dataset was defined as the panel data with the link entity and 15-minute intervals. Three statistical tests for comparing three methods indicated that the FE model, to control unobserved fixed effects across links, is the best of the analysed models.

The intermediate result by the linear estimation from the one-month dataset concludes that the different link attributes affect travel time estimation models on each link. FE modelling confirmed that the link entity is one of the most influential factors in the models. In addition, other variables such as brightness, weather and day need to be considered in the models. Although link geometry cannot explain all link attributes, it is an important factor in the models and needs to be developed in this study.

4.5. Findings

Unlike previous studies about travel time estimation, this study used the dataset that was collected from Korean ITS including ILDs and DSRCs during a comparatively long period of time (one month). There would be many factors (or situations) affecting travel time while traffic data was measured over this time. Statistical models by the NLS (based on the BPR function) and OLS estimation were developed for identifying those factors and the main findings are as follows. For the comparison between models in this chapter, BPR1 is used as the reference model that customises the current BPR function by the one-month dataset.

Geometric features consideration

This chapter investigated how geometric variables change estimated models. In NLS estimation models, which are based on the BPR function. RMSE can be used in this study for comparing the accuracy of NLS estimation models because R-squared is not an appropriate criterion for NLS models (Spiess and Neumeyer, 2010). RMSEs in two models (BPR1 and BPR2 in Table 4-28), one of which is the same as the BPR function and the other of which is the function that adds the four geometric variables referred to above to the BPR function, are 4.490 on 147,828 degrees of freedom and 4.350 on 147,824 degrees of freedom respectively. In other words, RMSE for measuring accuracy of forecasting models was improved by 0.140 after considering link geometry in NLS models.

The above result can also be confirmed in the OLS estimation, the coefficients of determination (R-squared) are 2.5% and 8.6% in the two models (MODEL1 and MODEL2). Only the independent variables of TF and TF2 were included in MODEL1 and the geometric variables of TR, RISE, FALL and BEND were added in MODEL2. It is noteworthy that the increase of R-squared between the two models is 6.1% even if both the R-squared values are not that high because of many influential factors other than geometric features.

Therefore, both NLS and OLS estimation models demonstrate that geometric variables can improve the accuracy of travel time estimation models to some extent even if the negative sign of IV3 (RISE) estimated in OLS and NLS models, which produces the opposite result of scatter plots, requires more detailed analysis after testing statistical assumptions and applying a different estimation. (Chapter 5)

Significance of FE modelling

This chapter investigated how unobserved fixed effects influence travel time estimation models. FE modelling was used for identifying unobserved fixed effects in the OLS estimation. Six entities, which are links, routes, brightness, day, weather and date, were defined from a one-month dataset.

From the comparison and investigation of coefficients between pooled OLS models and FE models, it can be concluded that most entities exhibit different patterns of travel time. In other words, a one-month dataset contains various road and external situations. In particular, in FE modelling, there are more unobserved effects across cross-sectional entities (links and routes) than across time-related entities (day and date). This finding suggests that geometric features, which are closely related to link entities, must not be ignored in modelling.

However, when a cross-sectional entity is defined for FE modelling, the FE model has one limitation which is that it cannot explain the effects by time-invariant characteristics of the entity because they have perfect collinearity with the entity (Torres-Reyna, 2007). Likewise, the coefficients of geometric variables, which are time-invariant effects varying across the entity of link, cannot be estimated in FE modelling. In the process of FE modelling by the entity of link (Section 4.4.2), it was confirmed that once geometric variables are included in the model, the coefficients of some link dummy variables cannot be measured because of the perfect correlation (denoted as 'NA'). Therefore, FE modelling is not appropriate for quantifying the effects of separate geometric features in models.

Comprehensive evaluation between OLS and NLS estimation models

In order to compare NLS and OLS estimation models, RMSE in each model was scrutinised. As both estimations used the same dataset, the low RMSE can explain the statistical consistency and unbiasedness within the dataset (Washington *et al.*, 2010). Based on RMSE comparison through one-month data analysis (Table 4-28), it is concluded that MODEL1 (the OLS estimation model without geometric variables) and MODEL2 (with geometric variables), which are suggested as new approaches in this study, are not inferior to BPR1 (the customised BPR function) and BPR2 (inclusion of geometric variables) respectively. In addition, FE modelling can be said to improve model accuracy through the comparison between OLS estimated models (e.g. MODEL1 and MODEL1-1). However, as can also be seen from FE modelling results, it is difficult to develop feasible VDFs by using a one-month dataset because there are many unobserved influential factors within the period. Therefore, this study investigates modelling processes statistically in more detail by using the one-day dataset in Chapter 5.

Table 4-28 RMSE comparison between OLS and NLS estimation (one-month data analysis)

Model	MODEL1	MODEL2	BPR1	BPR2	MODEL1-1	MODEL2-5
Degrees of freedom	147,828	147,824	147,828	147,824	147,757	147,795
RMSE	4.484	4.342	4.490	4.350	2.894	4.079

Chapter 5. Development of Feasible Models

5.1. Introduction

The previous chapter sought to establish the factors that would affect travel time estimation models based on one-month data analysis. Whilst the analysis of data collected over a one-month period has the advantage of making it possible to estimate models with reference to many factors, its corresponding drawback is that it is not hard to establish the feasible models for traffic assignment when there are so many differing situations such as weather conditions and vehicle composition. In order to clarify geometric features in travel time estimation models, it is necessary to minimise the impact of other factors except for link geometry through the use of one-day data analysis. This chapter selects the most appropriate one-day dataset for modelling after considering the data distribution and other factors which influence on travel time. In addition, three statistical estimation methods are used for modelling: OLS, GLS and NLS. Each of these estimation methods identifies the statistical significance of the developed models including their coefficients of variables.

Firstly, the one-day dataset is extracted from the one-month dataset by focusing mainly on the distribution of traffic flow on each day. In addition, the dataset is cleaned and filtered in order to reduce unobserved fixed effects. As with the one-month data analysis in Section 4.2, the descriptive analysis of the dataset including scatter plots is illustrated.

Secondly, NLS estimation models, which are customised from BPR function as a reference model, are investigated. Like Section 4.3, the sensitivity analysis by different road capacity is performed in order to clarify the impact on the model estimation of road capacity.

Thirdly, the OLS estimation is performed based on the quadratic function and the interaction effects and model transformation were scrutinised. After the comparison between models with geometric variables, this study tests whether the developed models satisfy the assumptions for the OLS estimation, which are prerequisites for best linear unbiased estimators (BLUE).

Lastly, as mentioned in Section 3.3.2, the GLS estimation generalises the variance-covariance matrix of errors more than the OLS estimation does. In other words, the GLS estimation is more effective in treating the statistical violations such as heteroscedasticity and serial correlation. Various variance-covariance structures for dealing with heteroscedasticity and serial correlation including autoregressive and moving average (ARMA) models are considered in the GLS estimation process.

5.2. Data selection

5.2.1. Data filtering

The one-day dataset is used for the development of feasible models by selecting a day from one-month dataset. As discussed in Section 4.4, the unobserved fixed effects that could potentially affect travel time were excluded from model estimations in so far as was possible.

The first consideration for data filtering is the distribution of traffic flow. Well-distributed traffic flows would help the feasible model estimation. Therefore, the distribution was examined in detail because high traffic flows do not always happen every day in all motorway sections. Figure 5-1 shows the daily distribution in September 2018. Many vehicles moved across regions during the period from the 23rd to the 25th of the month because the period is a national holiday in South Korea. In particular, the data recorded on the 24th of September was used in model estimations because the variation in traffic flows on that day is the widest recorded for all the dates in the month without it having outliers[12] from the box plot. Data from the day would be useful in helping to explain the relationship between travel time and high traffic flow compared to other days. Helpfully, the weather on that particular day was sunny, which means that weather effects are automatically excluded from estimated models.

Figure 5-1 Box plot of daily traffic flows in September of 2018

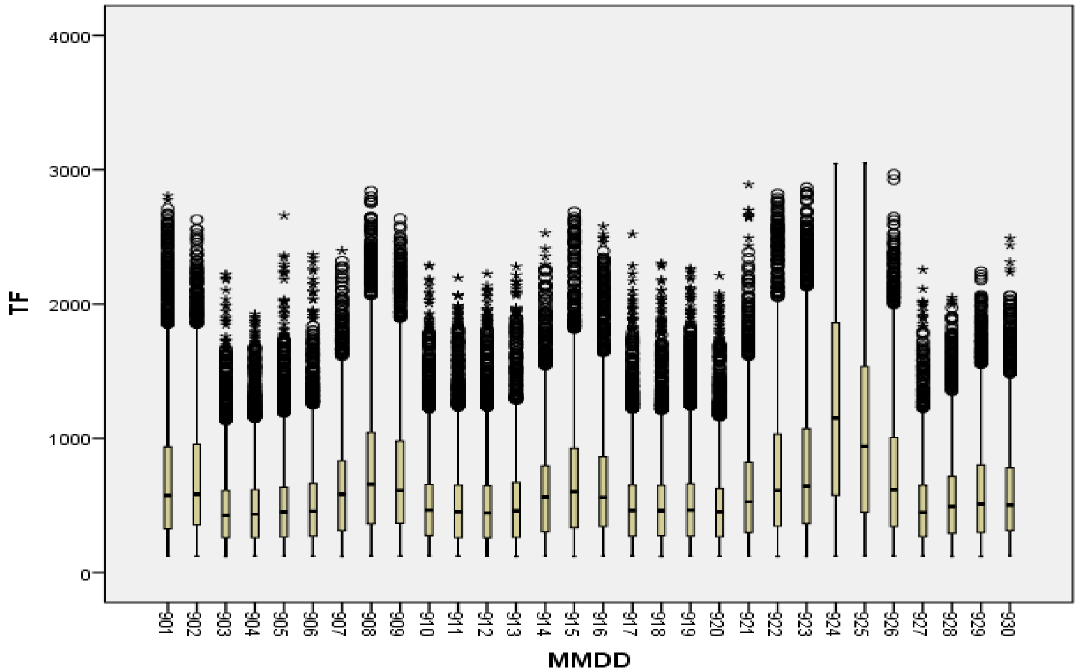

[12] Box plot recognises the data whose absolute value is over 3/2 times of upper and lower quartiles as outliers.

The second consideration for data filtering is brightness. In Section 4.4.3, models between daytime and night time were estimated differently; in particular, the brightness variable had more of an impact on the coefficients of the models compared to other time-fixed effects. Only the data between 07.00 and 19.00 was extracted from the dataset on the 24th of September. The last consideration for data filtering is the exclusion of congested traffic situations used by the congestion speed of 60kph (Section 3.4.3).

5.2.2. Discussion on one-day data selection

As mentioned in Section 5.2.1, the one-day dataset for modelling was extracted from the one-month dataset with consideration given to the distribution of traffic flows. This section investigates how different daily datasets affect models using the OLS linear estimation. The OLS estimation, which can be a starting point of linear estimation, shows the basic coefficients of model determination as well as the coefficients for each variable together with their statistical significance. In addition, this investigation will help justify the dataset selection of the 24th of September. Table 5-1 provides the key information derived from the models and according to the different dates selected. The main discussion points arising are as follows.

The first discussion point is about the traffic flow distribution and the coefficient of determination for the different daily datasets. Table 5-1 shows the mean and the maximum traffic flows on each day. Most daily data are skewed towards low traffic flow, especially on weekdays. These skewed datasets recognise the data corresponding to relatively high traffic flows as outliers in box plot observation (Figure 5-1) and as such they would lower the goodness of fit of the estimated models. For example, when examining the daily datasets below the mean traffic flow of 600vph and over the outlier ratio of 5%, the adjusted R^2s range from 12.8% on the 4th to 17.8% on the 20th of September. However, when investigating the datasets over the mean traffic flow of 900vph and below the outlier ratio of 2%, most of which were recorded during weekends or holidays, the adjusted R^2s were more improved from 30.9% on the 23rd and 43.8% on the 24th of September. In particular, the dataset on the 24th of September, which is used for the development of feasible models in this study, produces the highest R^2. This result indicates that the one-day dataset including both low and high traffic flows increases the goodness of fit of an estimated model by explaining the relationship between travel time and traffic flow without weighting.

The second discussion point is about the statistical significance of estimated coefficients. Firstly, all coefficients of the FALL variable have a statistical significance at a 95% confidence level regardless of the traffic flow distribution. This means that the FALL variable can affect the estimated models significantly in both low and high traffic flow. Secondly, most coefficients of both TR and RISE do not have statistical significance in the models estimated from the datasets with relatively low mean traffic flow. This result implies that both the variables of TR and RISE would affect travel time more in relatively high traffic flow. Lastly, the coefficients of the TF2 variable have more explanatory power in relatively high traffic flow, having the trade-off relationship with the coefficients of TF variable. Whilst the coefficients of TF and TF2 are statistically significant at a 95% confidence level in the dataset including both low and high traffic flows, but one of the coefficients is not statistically significant in the dataset with relatively low traffic flows. Therefore, it can be confirmed that the one-day dataset with well-distributed traffic flow is an important condition for travel time model estimation.

The third discussion point is about the negative coefficients of independent variables in the models estimated from many datasets on the 1st, 7th, 8th, 11th, 12th, 14th, 15th, 17th, 18th, 21st and 22nd of September. The negative coefficients of TF variable in estimated models indicate that in situations with low traffic, travel time reduces as traffic increases. This not only violates the necessary conditions of link cost functions in traffic assignment (Ortúzar and Willumsen, 2012), but also is not in line with the fundamental traffic theory (Section 2.3.1). In addition, since the models with the negative coefficients of TF2 variable are concave functions, they cannot be applied to traffic assignment as a convex function is required (Ortúzar and Willumsen, 2012). Lastly, two coefficients of TR and RISE on the 14th and 17th of September have negative signs with their statistical significance at a 95% confidence level. It is also questionable whether they can be used in estimated models from the viewpoint of physics. Therefore, it would be not desirable to use the estimated models with negative coefficients in this study.

The last discussion point is about the coefficients of the BEND variable and their statistical significance. The coefficients in the estimated models fluctuated on a daily basis. The coefficients become lower or statistically insignificant in the models using one-day datasets with high traffic flows rather than with low traffic flows. In particular, when confining the analysis to the models using the datasets from the 22nd to the 26th of September, it was found that the coefficients of the BEND variable are much less than those on other days or that they become not statistically significant. Although the model estimated from the dataset on 25th of September has the statistically significant coefficient of the BEND variable, the modelling result without the BEND variable shows just a small difference (0.12%) of adjusted R-squares between the two models (Table 5-2), which indicates that the BEND variable contributes little to the model's accuracy. Therefore, it needs to be prudent to include the BEND variable in the models.

In summary, it is very important to select the reasonable dataset in regression models. Since this study focuses on travel time estimation with geometric features in relatively high traffic flows as well as in low traffic ones, it can be inferred that it is desirable to estimate models by reflecting as wide a distribution of traffic flow as possible. Moreover, it was confirmed that different traffic flow distribution affects the overall accuracy of estimated models and their coefficients. Although the dataset collected on the 24th of September could have a limitation in that it was a certain date (national holiday), it is not easy to find the well-distributed dataset in most motorways except for the day in a year. Therefore, the selected dataset is deemed to be the best in travel time estimation modelling than any other daily dataset in the whole month.

Table 5-1 OLS estimation by different daily data selection

Date	Mean_TF	Max_TF	Outlier ratio	Adj.R2	(Intercept)	FFS (kph)	TF	TF2	TR	RISE	FALL	BEND
0901	815	2,806	3.79%	20.3%	3.47	111.54	-3.01E-05	4.80E-08	7.84E-05	1.59E-03	2.98E-03	5.94E-04
0902	787	2,503	1.91%	16.1%	3.45	114.26		2.63E-08	5.27E-05	2.14E-03	3.23E-03	1.00E-03
0903	543	2,220	4.20%	15.6%	3.53	105.79	8.59E-05				5.25E-03	2.11E-03
0904	557	1,925	5.20%	12.8%	3.53	105.12	1.01E-04				4.37E-03	1.72E-03
0905	576	2,660	5.31%	14.4%	3.57	101.10	1.08E-04				4.76E-03	
0906	592	2,368	4.64%	15.3%	3.55	103.15	1.17E-04				4.48E-03	
0907	690	2,398	2.16%	13.3%	3.56	102.32	-4.83E-05	6.78E-08			4.70E-03	1.33E-03
0908	897	2,840	1.57%	23.0%	3.47	111.88	-3.54E-05	5.45E-08	7.96E-05	1.43E-03	3.58E-03	7.02E-04
0909	830	2,636	1.58%	14.8%	3.45	114.50		1.93E-08	5.93E-05	1.96E-03	3.15E-03	6.73E-04
0910	593	2,288	5.77%	12.0%	3.56	102.11	9.10E-05				4.43E-03	
0911	588	2,195	5.57%	13.8%	3.50	108.21	1.33E-04	-2.49E-08	6.62E-05		5.12E-03	1.69E-03
0912	583	2,225	4.71%	16.8%	3.51	107.54	1.40E-04	-2.42E-08	3.44E-05		5.27E-03	2.19E-03
0913	593	2,280	3.19%	18.9%	3.54	104.70	1.02E-04				4.91E-03	1.63E-03
0914	675	2,529	2.48%	13.7%	3.64	94.80	-9.80E-05	9.37E-08	-3.69E-05		4.80E-03	8.02E-04
0915	812	2,623	2.23%	18.2%	3.52	107.06	-3.21E-05	5.22E-08	4.70E-05		3.80E-03	5.99E-04
0916	732	2,312	1.92%	10.4%	3.46	112.73	3.59E-05		3.68E-05	1.03E-03	3.10E-03	6.06E-04
0917	591	2,520	5.90%	15.0%	3.51	107.39	1.76E-04	-4.67E-08	3.88E-05	-9.04E-04	6.27E-03	1.40E-03
0918	591	2,304	6.20%	16.0%	3.49	109.85	1.78E-04	-4.02E-08	4.27E-05		4.52E-03	1.80E-03
0919	601	2,265	6.88%	13.6%	3.50	108.80	1.07E-04		3.70E-05		3.61E-03	2.38E-03
0920	575	2,076	7.26%	17.8%	3.53	105.02	4.61E-05	3.79E-08			4.58E-03	2.84E-03
0921	673	2,890	2.39%	13.5%	3.58	100.61	-4.56E-05	6.31E-08			4.27E-03	1.73E-03
0922	882	2,820	1.67%	31.0%	3.47	112.04	-4.27E-05	6.26E-08	6.71E-05	1.24E-03	2.68E-03	
0923	938	2,868	1.50%	30.9%	3.43	116.44		4.89E-08	8.38E-05	1.51E-03	2.44E-03	
0924	1,423	3,045	0%	43.8%	3.37	123.19	5.02E-05	2.30E-08	1.25E-04	2.19E-03	3.44E-03	
0925	1,196	2,947	0%	37.1%	3.39	120.77	2.81E-05	3.15E-08	1.17E-04	2.46E-03	3.65E-03	8.20E-04
0926	876	2,648	0.72%	16.2%	3.46	113.02		2.33E-08	5.65E-05	1.24E-03	3.62E-03	6.84E-04
0927	571	2,256	2.40%	13.9%	3.52	106.93	8.72E-05				5.45E-03	2.15E-03
0928	617	2,049	3.11%	11.7%	3.57	101.41		5.76E-08			5.54E-03	2.14E-03
0929	698	2,241	2.24%	9.2%	3.52	106.68	3.41E-05		2.77E-05		4.50E-03	6.63E-04
0930	649	2,489	2.43%	8.6%	3.49	109.71		2.52E-08	3.43E-05	1.35E-03	3.48E-03	9.06E-04

Note 1. Outlier ratio is calculated from the number of samples over 3/2 times of upper and lower quartiles divided by the number of whole samples in the box plot.
2. Yellow cells show weekends or holidays; and blue cells show nationwide rainy days.
3. Grey cells show negative values of estimated coefficients.
4. Empty cells mean that the estimated coefficients are not statistically significant at a 95% confidence level.

Table 5-2 Impact of BEND variable on estimated models from the dataset on 25th of Sep

Models	Adj.R2	(Intercept)	TF	TF2	TR	RISE	FALL	BEND
With BEND	37.14%	3.39	2.81E-05	3.15E-08	1.17E-04	2.46E-03	3.65E-03	8.20E-04
Without BEND	37.02%	3.42	2.63E-05	3.22E-08	9.80E-05	2.54E-03	3.52E-03	

5.2.3. Plot observation

Scatter plot

The scatter plot (Figure 5-2) was derived after data filtering. When recalling the one-month scatter plot (Figure 4-2), the biggest difference between two plots is the variation of traffic data when the traffic flow is low (e.g. < 500vph). From the comparison, it can be seen that travel time is affected by different situations especially when there is low traffic flow. The range of variation becomes narrower as traffic flow increases in both scatter plots. The factors which are particularly significant in low traffic flow include brightness, weather, day (weekday and weekend), accidents and maintenance work. Some of the observations was confirmed by FE modelling in Section 4.4.2 and 4.4.3.

Figure 5-2 Scatter plot between DV and IV1 (TF) from the one-day dataset

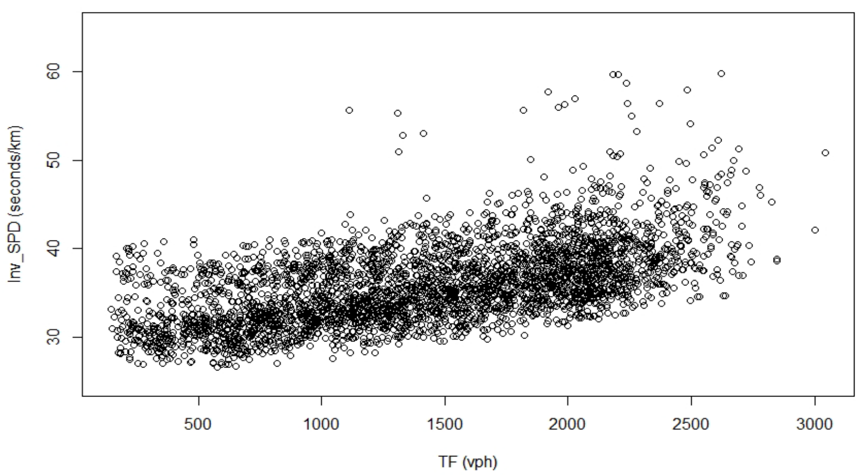

Observation of the 15th and 85th percentile values of DV depending on geometric features

As with one-month data analysis, the 15th and 85th percentile values of DV, both of which stand for the free-flow and congested (or moderate) traffic situations, were examined. Based on the observations of the linear relationships between both values and each geometric feature, the direction of overall modelling was determined. As can be seen from Figure 5-3 and Figure 5-4, the other three geometric features other than BEND have positive linear relationships with the 15th and 85th values of travel time. It can be observed that the correlations between DV and each IV from the one-day dataset are stronger than from the one-month dataset. In addition, it is noteworthy that the independent variable of BEND has the negative linear relationships with both 15th and 85th values of DV. This observation contrasts with the positive relationship shown in Figure 4-6 and Figure 4-7.

Figure 5-3 15th percentile values of DV by geometric variables from the one-day dataset

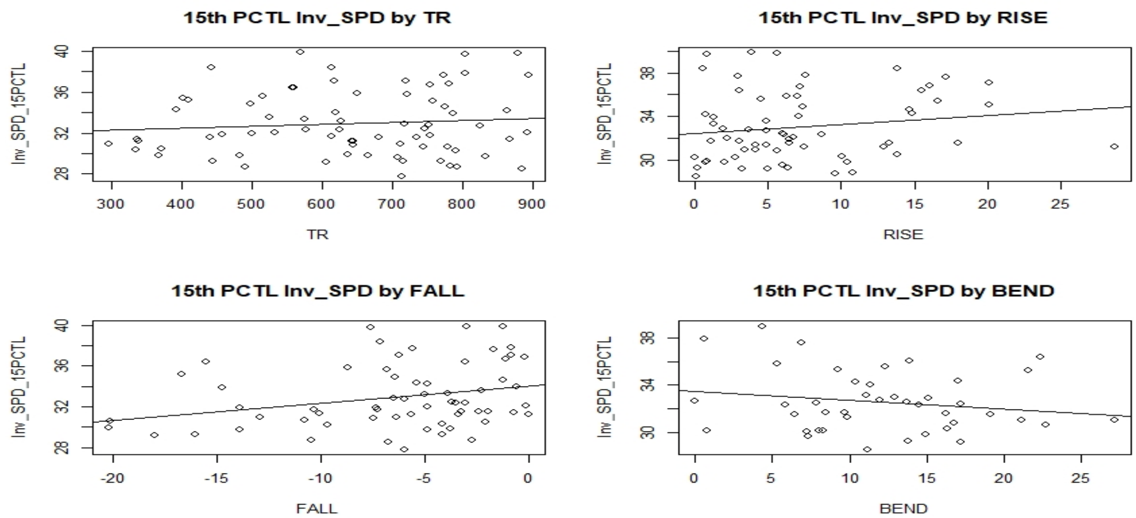

Figure 5-4 85th percentile values of DV by geometric variables from the one-day dataset

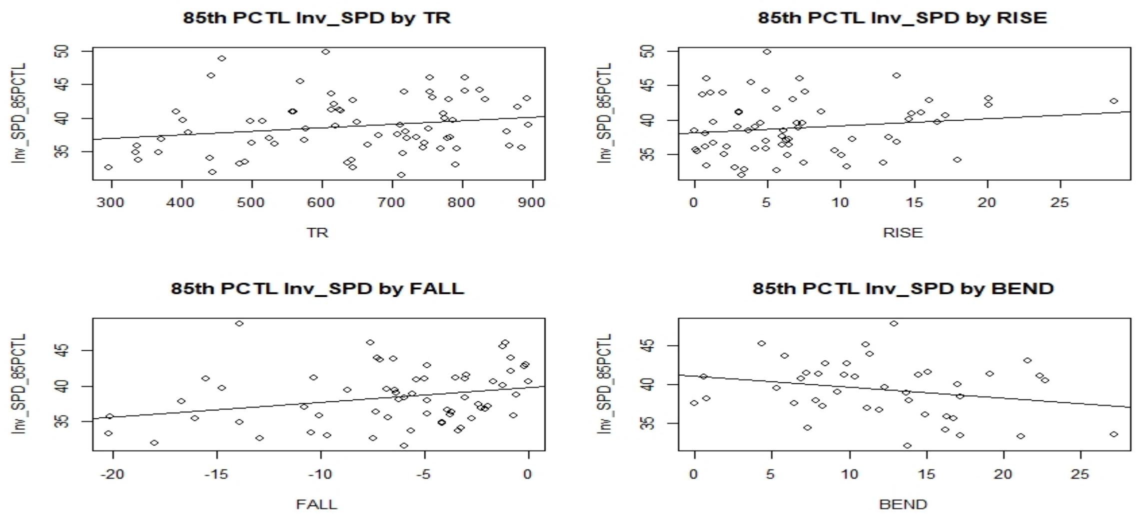

5.3. Customisation of BPR function by NLS estimation

As reference models of the OLS and GLS estimation models, NLS estimation models based on BPR function were derived by using the same dataset (Equation 5-1). The nominal road capacity (C_n) required for the NLS estimation is defined as the same value (2,404vph) as the derived value during one month based on the same conditions suggested in Section 4.3. The feasible model development by the NLS estimation can be divided into two parts. The first part finds the best NLS estimation model by investigating the change in the RMSE and MAPE of models estimated by the different combination of variables. The second part conducts the sensitivity analysis in order to determine the effect of the change in road capacity on the model. In addition to the parameter estimation by different road capacity in the sensitivity analysis, the change in RMSE and MAPE by measured road capacity from five randomly selected cases was also examined for finding how predetermined road capacity could affect total travel time prediction as mentioned in Section 3.3.3.

$$TT = FFTT\left(1 + \alpha\left(\frac{TF}{C}\right)^{\beta}\right) + \sum \boldsymbol{\gamma_k Geometry_k} + u \qquad \text{Equation 5-1}$$

The models derived by customising BPR function in this section are denoted as from FBPR1 (without geometric variables) to FBPR6 as Table 5-3 to distinguish them from those in Section 4.3. This section compares the change in statistical accuracy of the estimated models according to the included geometric variables.

Table 5-3 NLS estimation models by inclusion of geometric variables

Model Name	Independent Variables	Explanation
FBPR1	TF	Customisation of BPR function by predetermining road capacity (existing approach)
FBPR2	TF, TR, RISE, FALL, BEND	Inclusion of all collected geometric variables in addition to the customised BPR function
FBPR3	TF, TR, RISE, FALL	Inclusion of TR, RISE and FALL in addition to the customised BPR function
FBPR4	TF, TR, RISE	Inclusion of TR and RISE in addition to the customised BPR function
FBPR5	TF, TR	Inclusion of only TR in addition to the customised BPR function
FBPR6	TF, RISE, FALL	Inclusion of RISE and FALL in addition to the customised BPR function

5.3.1. Model specification

Based on the methodology mentioned in Section 3.3.3, the *'nls()'* function in "R" was used for the NLS estimation. This study estimated models based on the existing BPR function approach that considers only the relationship between travel time and traffic flow with road capacity (without geometric features). In addition, different models were estimated by including the various combinations of geometric variables. For example of FBPR2 that inclues all IVs (Table 5-4), after predetermining road capacity with 2,404vph, the coefficients for the relationship between Inv_SPD and TF as well as for the relationship between Inv_SPD and geometric variables were estimated at the same time. The starting values are the same as the one-month data analysis in Section 4.3. After six iterative calculations, the errors were converged with the tolerance of 1.351e-06. The RMSE and MAPE by this estimation are 3.36 and 7.05% respectively. Table 5-5 summarises the key information of the models by the NLS estimation. Firstly, it can be seen that free-flow travel time (FFTT) of the models considering the geometric features is smaller than FFTT from the model in which only traffic flow is taken into account. As FFTT is estimated by an intercept, it can be explained that the geometric variables take a part of FFTT when they are included in models. Secondly, since geometric variables contribute to increase travel time (Inv_SPD), it can be predicted that the coefficients of TR, RISE, and FALL[13] are estimated as positive values. Thirdly, FBPR2 and FBPR3 can be considered as better than any other model because they have fewer RMSE and MAPE. Lastly, when comparing the two models, it is concluded that FBPR3 the best model of the NLS estimation models because the coefficient of BEND is not statistically significant and it has the negative sign (this is in line with the previous OLS estimation results in Section 5.4.1and scatter plot in Section 5.2.3).

Table 5-4 Example of NLS estimation (with all geometric variables)

```
#Definition of road capacity
Data_1day$capacity <-2404

# Nonlinear estimation with geometric IVs
FBPR2 <- nls(Inv_SPD ~ FFTT*(1+a*(TF/capacity)^b) + c*TR + d*RISE + e*FALL +
f*BEND, start = list(FFTT=36, a =0.15, b =4, c=0, d=0, e=0, f=0), data=Data_1
day, trace = TRUE)

## 57730.55 :  36.00  0.15  4.00  0.00  0.00  0.00  0.00
## 56053.32 :  30.539247976  0.241691864  0.768497485  0.004421613  0.0802441
22  0.130809177 -0.010412663
## 48210.73 :  32.293055914  0.169310546  1.958072463  0.004534452  0.0787281
96  0.127479196 -0.006645969
## 39378.09 :  29.425996860  0.281585982  1.632602159  0.004545583  0.0808555
41  0.126160110 -0.007307071
## 39297.89 :  29.371359071  0.294321544  1.736666941  0.004548723  0.0807523
```

[13] Since FALL is defined as a negative value (Chapter 3.4.2), the downhill slope decreases when the value of FALL increases.

```
36  0.126083857 -0.007179447
## 39297.87 :  29.373335243  0.294445030  1.738640033  0.004548368  0.0808153
26  0.126062498 -0.007215404
## 39297.87 :  29.373549178  0.294439210  1.738760660  0.004548351  0.0808162
59  0.126062472 -0.007216331

summary(FBPR2)
##
## Formula: Inv_SPD ~ FFTT * (1 + a * (TF/capacity)^b) + c * TR + d * RISE +
##     e * FALL + f * BEND
##
## Parameters:
##        Estimate Std. Error t value Pr(>|t|)
## FFTT 29.3735492  0.4845285  60.623  < 2e-16 ***
## a     0.2944392  0.0100629  29.260  < 2e-16 ***
## b     1.7387607  0.1059991  16.404  < 2e-16 ***
## c     0.0045484  0.0004631   9.822  < 2e-16 ***
## d     0.0808163  0.0124125   6.511 8.54e-11 ***
## e     0.1260625  0.0142558   8.843  < 2e-16 ***
## f    -0.0072163  0.0110384  -0.654    0.513
## ---
## Signif. codes:  0 '***' 0.001 '**' 0.01 '*' 0.05 '.' 0.1 ' ' 1
##
## Residual standard error: 3.363 on 3475 degrees of freedom
##
## Number of iterations to convergence: 6
## Achieved convergence tolerance: 1.351e-06

# Calculation of RMSE and MAPE
RMSE.FBPR2 <- RMSE(predict(FBPR2),Data_1day$Inv_SPD)
RMSE.FBPR2
## [1] 3.359465
MAPE.FBPR2 <- MAPE(predict(FBPR2),Data_1day$Inv_SPD)
MAPE.FBPR2
## [1] 0.070535
```

where the coefficients of ‘a’ and ‘b’ represent ‘α’ and ‘β’ in Equation 5-1; and the coefficients of ‘c’, ‘d’, ‘e’ and ‘f’ represent ‘$\boldsymbol{\gamma_k}$’ (a vector) in Equation 5-1.

Table 5-5 Feasible NLS estimation models by different combinations of IVs

Coefficient \ Model	FBPR1		FBPR2		FBPR3	
	Estimate	p-value	Estimate	p-value	Estimate	p-value
FFTT (Intercept)	3.18E+01	< 2e-16 ***	2.94E+01	< 2e-16 ***	2.92E+01	< 2e-16 ***
a	2.71E-01	< 2e-16 ***	2.94E-01	< 2e-16 ***	2.97E-01	< 2e-16 ***
b	1.59E+00	< 2e-16 ***	1.74E+00	< 2e-16 ***	1.73E+00	< 2e-16 ***
c			4.55E-03	< 2e-16 ***	4.71E-03	< 2e-16 ***
d			8.08E-02	8.54e-11 ***	7.99E-02	1.05e-10 ***
e			1.26E-01	< 2e-16 ***	1.27E-01	< 2e-16 ***
f			-7.22E-03	0.513		
RMSE	3.601		3.359		3.360	
MAPE	7.748%		7.054%		7.053%	

Coefficient \ Model	FBPR4		FBPR5		FBPR6	
	Estimate	p-value	Estimate	p-value	Estimate	p-value
FFTT (Intercept)	2.72E+01	< 2e-16 ***	2.86E+01	< 2e-16 ***	3.29E+01	< 2e-16 ***
a	3.19E-01	< 2e-16 ***	3.05E-01	< 2e-16 ***	2.61E-01	< 2e-16 ***
b	1.72E+00	< 2e-16 ***	1.59E+00	< 2e-16 ***	1.72E+00	< 2e-16 ***
c	5.98E-03	< 2e-16 ***	5.02E-03	< 2e-16 ***		
d	1.49E-01	< 2e-16 ***			2.76E-02	0.0193 *
e					1.89E-01	< 2e-16 ***
f						
RMSE	3.399		3.511		3.430	
MAPE	7.195%		7.514%		7.191%	

5.3.2. Sensitivity analysis by road capacity

Table 5-6 presents the result of coefficient measurements according to the change in road capacity. Similar to the NLS estimation performed with the one-month dataset in Section 4.3, the value of 'a' coefficient (α in Equation 2-21) is proportional to road capacity, and the other coefficients, as well as FFTT, are not affected by the change in road capacity. In addition, road capacity does not change the RMSE and MAPE, which can determine the accuracy of the NLS estimation. The result that the predetermined road capacity value is only related to the estimation of 'a' coefficient correlates with the conclusion that the coefficient is flexibly determined to minimize the sum of squared errors (e.g. RMSE) by the predetermined road capacity value. Therefore, it is concluded that the uncertainty of road capacity can be transferred into the coefficient estimation of nonlinear functions such as BPR function.

Table 5-6 Coefficients of feasible NLS estimation models by different road capacity

Road Capacity \ Model	FBPR1			FBPR3					
	FFTT	a	b	FFTT	a	b	c	d	e
80% of C_n (1,923vph)	31.82	0.1901	1.5862	29.18	0.2014	1.7346	0.0047	0.0799	0.1275
90% of C_n (2,164vph)	31.82	0.2292	1.5862	29.18	0.2471	1.7346	0.0047	0.0799	0.1275
C_n (2,404vph)	31.82	0.2708	1.5862	29.18	0.2966	1.7346	0.0047	0.0799	0.1275
110% of C_n (2,644vph)	31.82	0.3149	1.5862	29.18	0.3498	1.7346	0.0047	0.0799	0.1275
120% of C_n (2,884vph)	31.82	0.3615	1.5862	29.18	0.4067	1.7346	0.0047	0.0799	0.1275
C_{Korea} (3,572vph)	31.82	0.5075	1.5862	29.18	0.5895	1.7346	0.0047	0.0799	0.1275
RMSE	3.601			3.360					
MAPE	7.748%			7.053%					

where the coefficients of 'a' and 'b' represent 'α' and 'β' in Equation 5-1; and the coefficients of 'c', 'd', 'e' and 'f' represent '$\boldsymbol{\gamma_k}$' (a vector) in Equation 5-1, which are for the geometric variables of TR, RISE and FALL.

5.3.3. Summary

Modelling by the NLS estimation can be summarised in three key points. Firstly, through the comparison with the reference model (FBPR1), which is customised based on the current BPR function, the NLS estimation showed higher statistical accuracy for models that add geometric variables to the relationship between travel time and traffic flow. Among the NLS estimation models analysed in this study, the model (FBPR3) including the geometric variables of TR, RISE, and FALL as a linear function , has the lowest RMSE and MAPE. BEND is not significant in the NLS estimation of the geometric features.

Secondly, as road capacity changes, the coefficients of models are estimated flexibly without changing the accuracy of the models. As mentioned in Section 2.4.2, road capacity cannot be defined as a single value, thus sensitivity analysis was conducted by setting road capacity ranging from 80% to 120% nominal road capacity as defined in this study. It was confirmed that the change in road capacity is proportional to the 'a' coefficients of the models even though sensitivity analysis did not help select models because road capacity did not change the accuracy of the models.

Lastly, once a model has been developed based on the predetermined road capacity, the model is not be applicable for sections with values that differ significantly from the road capacity used in the model. Although NLS estimation models can explain a given dataset well, the lack of spatial transferability is a major drawback. Therefore, it can be concluded that current VDFs including road capacity have difficulty in explaining different link attributes.

5.4. OLS estimation models

5.4.1. Model specification

The OLS estimation for the feasible travel time estimation model extended the analysis to identify the change in models' coefficients by different variable selection. When recalling Equation 3-9, the estimated models are specified according to the combination of quadratic and linear function (Equation 5-2). It is different from the one-month data estimation (Equation 4-2) in that the OLS estimation does not treat the dataset as the panel data because the GLS estimation investigates individual and time-series effects in detail. In addition, the different combination and transformation of variables in Equation 5-2 was applied to the OLS estimation. In particular, the terms of $Geometry_k$ varied according to whether the variables were included in each model.

$$TT = \beta_0 + \beta_1 TF + \beta_2 TF^2 + \sum \boldsymbol{\gamma_k Geometry_k} + u \qquad \text{Equation 5-2}$$

OLS estimation models in this section can be summarised due to included variables as Table 5-7. FMODEL represents feasible models that could replace current VDFs by analysing various statistical significances. The models have the difference from those in Chapter 4 in that they investigate the effects by geometric variables in detail.

Table 5-7 OLS estimation models by inclusion of geometric variables

Model Name	Independent Variables	Explanation
FMODEL1	TF, TF2	Quadratic model between Inv_SPD and TF. Replacement of existing BPR function without road capacity and FFTT.
FMODEL2	TF, TF2, TR, RISE, FALL, BEND	Inclusion of all geometric variables collected in this study based on quadratic model.
FMODEL3	TF, TF2, TR, RISE, FALL	Exclusion of BEND from FMODEL2.
FMODEL4	TF, TF2, TR, RISE	Exclusion of FALL from FMODEL3.
FMODEL5	TF, TF2, TR, FALL	Exclusion of RISE from FMODEL3.
FMODEL6	TF, TF2, TR	Exclusion of RISE and FALL from FMODEL3.
FMODEL7~12	TF, TF2, TR, RISE, FALL, BEND	Consideration of interaction effects between geometric variables.

5.4.2. Model findings

Model findings by different variable selection

As with the pooled OLS estimation in Section 4.3, the *'lm()'* function, provided by the software package "R", was used for this analysis (Appendix A.5.2). The result of the OLS estimation models are summarised in Table 5-8. Adjusted R^2s vary from 33.7% (without geometric variables) to 42.2% (with all variables or with the exclusion only of BEND). All intercepts and coefficients of variables in estimated models except for the IV4 of BEND are statistically significant at a 95% confidence level. As can be observed, only the BEND variable has the negative coefficient; this is not statistically significant at a 95% confidence level. In addition, standardised beta coefficients, which are denoted as 'std. Beta' in Table 5-8 are derived. The coefficients enable comparisons to be made as to how each IV affects the DV regardless of the IV's scale of units because they are calculated by dividing by the standard deviation of each variable after subtracting the mean from the variable (Freedman, 2009).

Table 5-8 Model estimations by variable selection

	FMODEL1				FMODEL2				FMODEL3			
Coeffcient	*Estimates*	*std. Error*	*std. Beta*	*P-Value*	*Estimates*	*std. Error*	*std. Beta*	*P-Value*	*Estimates*	*std. Error*	*std. Beta*	*P-Value*
(Intercept)	3.15E+01	2.86E-01		<0.001	2.91E+01	5.18E-01		<0.001	2.89E+01	4.27E-01		<0.001
TF	1.56E-03	4.44E-04	0.22	<0.001	1.02E-03	4.17E-04	0.14	0.014	1.04E-03	4.16E-04	0.15	0.013
TF2	8.95E-07	1.55E-07	0.36	<0.001	1.11E-06	1.45E-07	0.45	<0.001	1.11E-06	1.45E-07	0.45	<0.001
TR					4.55E-03	4.63E-04	0.16	<0.001	4.72E-03	3.88E-04	0.17	<0.001
RISE					8.11E-02	1.24E-02	0.11	<0.001	8.02E-02	1.23E-02	0.11	<0.001
FALL					1.26E-01	1.43E-02	0.15	<0.001	1.27E-01	1.41E-02	0.15	<0.001
BEND					-7.18E-03	1.10E-02	-0.01	0.515				
Observations	3,482				3,482				3,482			
R^2 / R^2 adjusted	0.337 / 0.337				0.423 / 0.422				0.423 / 0.422			

	FMODEL4				FMODEL5				FMODEL6			
Coeffcient	*Estimates*	*std. Error*	*std. Beta*	*P-Value*	*Estimates*	*std. Error*	*std. Beta*	*P-Value*	*Estimates*	*std. Error*	*std. Beta*	*P-Value*
(Intercept)	2.69E+01	3.68E-01		<0.001	3.03E+01	3.76E-01		<0.001	2.83E+01	3.70E-01		<0.001
TF	1.10E-03	4.21E-04	0.16	0.009	1.16E-03	4.18E-04	0.16	0.005	1.58E-03	4.33E-04	0.22	<0.001
TF2	1.09E-06	1.47E-07	0.44	<0.001	1.06E-06	1.46E-07	0.43	<0.001	9.03E-07	1.51E-07	0.37	<0.001
TR	5.98E-03	3.66E-04	0.22	<0.001	3.84E-03	3.66E-04	0.14	<0.001	5.02E-03	3.73E-04	0.18	<0.001
RISE	1.49E-01	9.77E-03	0.20	<0.001								
FALL					1.84E-01	1.11E-02	0.22	<0.001				
Observations	3,482				3,482				3,482			
R^2 / R^2 adjusted	0.410 / 0.409				0.416 / 0.415				0.370 / 0.369			

Model findings by considering interaction effects

Interaction effects can be included for better model specification. The term of $Geometry_k$ in Equation 5-2 can be extended by including the multiplication of two or more different geometric variables. Although different interactions can be combined, the interaction effects between RISE and FALL were excluded because both geometric features are incompatible (Table 5-9). After observing the change in R^2s and the p-values of coefficients in various models, it can be concluded that the effects of interaction in the models are not clear. This conclusion is supported by the finding that the signs of main variables are changed or some of the coefficients of variables no longer have statistical significance after adding interaction effects to models, these are denoted as shade cells in Table 5-9. In addition, all estimated adjusted R^2s (42.2%-42.6%) do not exhibit a big difference (0.0%-0.4%) with R^2 (42.2%) from the model (FMODEL3) without considering interaction effects. For this reason, interaction effects were no longer considered in other statistical estimations.

Table 5-9 Model estimations by interaction variables

	FMODEL7				FMODEL8				FMODEL9			
Coeffcient	*Estimates*	*std. Error*	*std. Beta*	*P-Value*	*Estimates*	*std. Error*	*std. Beta*	*P-Value*	*Estimates*	*std. Error*	*std. Beta*	*P-Value*
(Intercept)	2.96E+01	5.26E-01		<0.001	2.76E+01	5.25E-01		<0.001	2.73E+01	7.57E-01		<0.001
TF	1.04E-03	4.16E-04	0.15	0.012	1.14E-03	4.15E-04	0.16	0.006	1.08E-03	4.16E-04	0.15	0.01
TF2	1.10E-06	1.45E-07	0.45	<0.001	1.08E-06	1.45E-07	0.44	<0.001	1.12E-06	1.45E-07	0.45	<0.001
TR	3.74E-03	5.89E-04	0.14	<0.001	6.66E-03	5.80E-04	0.24	<0.001	6.96E-03	8.57E-04	0.25	<0.001
RISE	-1.34E-02	4.44E-02	-0.02	0.762	8.37E-02	1.23E-02	0.11	<0.001	8.54E-02	1.25E-02	0.12	<0.001
FALL	1.30E-01	1.42E-02	0.16	<0.001	-6.93E-02	4.58E-02	-0.08	0.13	1.22E-01	1.43E-02	0.15	<0.001
BEND									1.14E-01	3.79E-02	0.17	0.003
TR:RISE	1.45E-04	6.62E-05	0.13	0.028								
TR:FALL					3.12E-04	6.93E-05	0.23	<0.001				
TR:BEND									-1.84E-04	5.51E-05	-0.15	0.001
Observations				3,482				3,482				3,482
R^2 / R^2 adjusted				0.424 / 0.423				0.426 / 0.425				0.425 / 0.424

	FMODEL10				FMODEL11				FMODEL12			
Coeffcient	*Estimates*	*std. Error*	*std. Beta*	*P-Value*	*Estimates*	*std. Error*	*std. Beta*	*P-Value*	*Estimates*	*std. Error*	*std. Beta*	*P-Value*
(Intercept)	2.93E+01	5.33E-01		<0.001	2.99E+01	5.53E-01		<0.001	2.67E+01	8.86E-01		<0.001
TF	1.04E-03	4.17E-04	0.15	0.013	9.42E-04	4.16E-04	0.13	0.024	1.17E-03	4.16E-04	0.17	0.005
TF2	1.11E-06	1.45E-07	0.45	<0.001	1.15E-06	1.45E-07	0.47	<0.001	1.08E-06	1.45E-07	0.44	<0.001
TR	4.52E-03	4.64E-04	0.16	<0.001	4.33E-03	4.66E-04	0.16	<0.001	7.92E-03	1.17E-03	0.29	<0.001
RISE	5.56E-02	2.48E-02	0.08	0.025	7.91E-02	1.24E-02	0.11	<0.001	1.57E-01	6.06E-02	0.21	0.01
FALL	1.24E-01	1.44E-02	0.15	<0.001	2.30E-01	3.13E-02	0.27	<0.001	-1.23E-01	6.31E-02	-0.15	0.052
BEND	-2.03E-02	1.56E-02	-0.03	0.194	-4.89E-02	1.57E-02	-0.07	0.002				
RISE:BEND	1.99E-03	1.68E-03	0.04	0.235								
FALL:BEND					-7.01E-03	1.87E-03	-0.15	<0.001				
TR:RISE									-1.12E-04	9.10E-05	-0.10	0.217
TR:FALL									3.93E-04	9.54E-05	0.30	<0.001
Observations				3,482				3,482				3,482
R^2 / R^2 adjusted				0.423 / 0.422				0.425 / 0.424				0.427 / 0.426

Model findings by transformations

Based on FMODEL3, different types of models were specified by taking four transformations between DV and IVs: linear-linear; log-linear; linear-log[14]; and log-log. The estimated models are denoted as from FMODEL3-1 to FMODEL3-9. When examining R-square and the p-value of coefficients (Table 5-10), the log-linear model can be said to be the most appropriate model. In addition, the Box-Cox test, which is used for selecting linear-linear versus log-linear functional form (Maddala, 1992), supports this result (Appendix A.5.3)

Table 5-10 Model estimation by log-transformation

	FMODEL3		FMODEL3-1		FMODEL3-2		FMODEL3-3	
Coeffcient	*Estimates*	*P-Value*	*Estimates*	*P-Value*	*Estimates*	*P-Value*	*Estimates*	*P-Value*
(Intercept)	2.89E+01	<0.001	3.37E+00	<0.001	-6.67E+01	<0.001	7.75E-01	<0.001
TF	1.04E-03	0.013	5.06E-05	<0.001				
TF2	1.11E-06	<0.001	2.30E-08	<0.001				
TR	4.72E-03	<0.001	1.29E-04	<0.001				
RISE	8.02E-02	<0.001	2.17E-03	<0.001				
FALL	1.27E-01	<0.001	3.48E-03	<0.001				
log(TF + 30)					1.25E+02	<0.001	3.32E+00	<0.001
log(TF2 + 30)					-5.82E+01	<0.001	-1.54E+00	<0.001
log(TR + 30)					2.83E+00	<0.001	7.76E-02	<0.001
log(RISE + 30)					2.92E+00	<0.001	8.07E-02	<0.001
log(FALL + 30)					2.46E+00	<0.001	6.75E-02	<0.001
Observations	3,482		3,482		3,482		3,482	
R^2 / R^2 adjusted	0.423 / 0.422		0.439 / 0.438		0.406 / 0.405		0.427 / 0.426	

When considering mixed transformation according to the log-transformation of each variable (Table 5-11), most log-transformed IVs do not significantly affect the increase of R-square although log-transformed IV4 of FALL causes only 0.1% increase of R-square. Therefore, the log-linear transformation is analysed in detail hereafter.

[14] The IVs of RISE, FALL and BEND could have zero or negative values, so the integer more than the absolute value of the lowest negative value (-20.156) needs to be added to all the variables before log transformation of IVs. Although the integer needs to be specified for the generalisation of log transformed IVs, the integer of 30 in this study was temporarily added to the IVs only for the comparison of goodness of fit.

Table 5-11 Change of R-square by log-transformation of IVs

	FMODEL3-4		FMODEL3-5		FMODEL3-6		FMODEL3-7		FMODEL3-8		FMODEL3-9	
Coeffcient	*Estimates*		*Estimates*		*Estimates*		*Estimates*		*Estimates*		*Estimates*	
(Intercept)	3.19E+00	***	3.07E+00	***	3.46E+00	***	2.79E+00	***	2.98E+00	***	3.05E+00	***
TFplus30	5.06E-05	***			1.59E-04	***	5.03E-05	***	5.07E-05	***	5.04E-05	***
TF2plus30	2.30E-08	***	3.40E-08	***			2.30E-08	***	2.30E-08	***	2.30E-08	***
TRplus30	1.29E-04	***	1.29E-04	***	1.28E-04	***			1.30E-04	***	1.32E-04	***
RISEplus30	2.17E-03	***	2.19E-03	***	2.11E-03	***	2.12E-03	***			2.35E-03	***
FALLplus30	3.48E-03	***	3.46E-03	***	3.52E-03	***	3.51E-03	***	3.43E-03	***		
log(TFplus30)			2.39E-02	***								
log(TF2plus30)					-2.55E-02	***						
log(TRplus30)							7.64E-02	***				
log(RISEplus30)									8.34E-02	***		
log(FALLplus30)											6.85E-02	***
Observations	3,482		3,482		3,482		3,482		3,482		3,482	
R^2 / R^2 adjusted	0.439 / 0.438		0.438 / 0.437		0.438 / 0.438		0.437 / 0.437		0.438 / 0.437		0.440 / 0.439	

5.4.3. OLS assumption tests

Multicollinearity test

Multicollinearity happens among IVs when IVs are correlated with each other or when IVs are correlated with the variables that are not considered (Washington *et al.*, 2010). It can be problematic in that multicollinearity produces the large standard errors of the estimated coefficients of collinear IVs and thus causes the wider confidence intervals for them. Although the OLS estimated the smallest variance even when multicollinearity happens, it is uncertain that the variance is absolutely small (Greene, 2018). A variance inflation factor (VIF) as a measure of multicollinearity is widely used, which is the equation of $1/(1-\mathrm{R}_\mathrm{k}^2)$ where the subscript of k means k^{th} independent variable (x_k). In the most extreme case, in which x_k has the perfect collinear with other IVs, so that $\mathrm{R}_\mathrm{k}^2 = 1$, VIF becomes infinite (Greene, 2018). Overall, the high values of VIF would potentially cause problems in model specification, in regard to the estimation of coefficients.

The VIFs of the IVs in two models were examined: the linear-linear OLS estimation model (FMODEL3) and the log-linear OLS estimation model (FMODEL3-1). As both models have the same IVs, the results of the two VIF tests are identical. Although the VIFs of TF and TF2 are over 20 (Table 5-12) and this could be regarded as a problem (Belsley *et al.*, 1980), it is reported in many studies that the collinearity between polynomial terms can either be ignored or treated by centring the IVs in that both variables are naturally collinear because the variable of TF2 is created from the variable of TF (Yu, 2000; Kraemer and Blasey, 2004; Allison, 2012; Dalal and Zickar, 2012). Table 5-12 shows that the issue of multicollinearity can be resolved by centring the variables. With regard to the VIFs (< 1.7) of the geometric IVs, it can be said that multicollinearity does not have any significant effect on the variables.

Table 5-12 Result of the variance inflation factor (VIF)

Uncentred			Centred		
Coeffcient	*VIF*	*Tolerance (1/VIF)*	*Coeffcient*	*VIF*	*Tolerance (1/VIF)*
TF	20.860	0.048	TFc	1.008	0.992
TF2	20.883	0.048	TFc2	1.013	0.987
TR	1.185	0.844	TR	1.185	0.844
RISE	1.688	0.592	RISE	1.688	0.592
FALL	1.699	0.588	FALL	1.699	0.588

where TFc is the centred variable of TF, which is created by subtracting the mean of TF from each value of TF, and TFc2 is TFc squared.

Test for heteroscedasticity detection

As referred to Section 3.3.2, homoscedasticity is the OLS estimation assumption that the residuals should have the identical distribution, which means all residuals have one value of variance corresponding to each independent variable. The scatter residual plots were examined for detecting heteroscedasticity (Figure 5-5) and the Breusch-Pagan test was implemented in order to quantify the level of heteroscedasticity (Table 5-13 and Table 5-14). The test was used for assessing heteroscedasticity in linear regression models by examining χ^2 whether the variance of errors is dependent on the independent values (Breusch and Pagan, 1979). A large χ^2 would mean that heteroscedasticity is present in the tested model. When examining the test against fitted values for FMODEL3-1 (Table 5-13), heteroscedasticity can be doubted but uncertain because χ^2 is 3.73, indicating that a null hypothesis cannot be rejected at a 95% confidence level. It can be confirmed through the observation that the residual plot (top-left one in Figure 5-5) shows centred but non-increasing or non-decreasing points. However, when examining the test against the independent variables (Table 5-14), the χ^2s against three independent (geometric) variables of TR, RISE and FALL vary from 11.13 to 41.92. On the other hand, the χ^2s against TF and TF2 are only 0.97 and 0.00043 respectively (homoscedasticity). The residual plots (two bottom ones in Figure 5-5) show that the variations of residuals are not constant across the values of the geometric variables. Therefore, both results of the scatter plots and Breusch-Pagan test suggest that other statistical estimations for dealing with the heterogeneity need to be considered in this study.

Figure 5-5 Scatter residual plots for FMODEL3-1

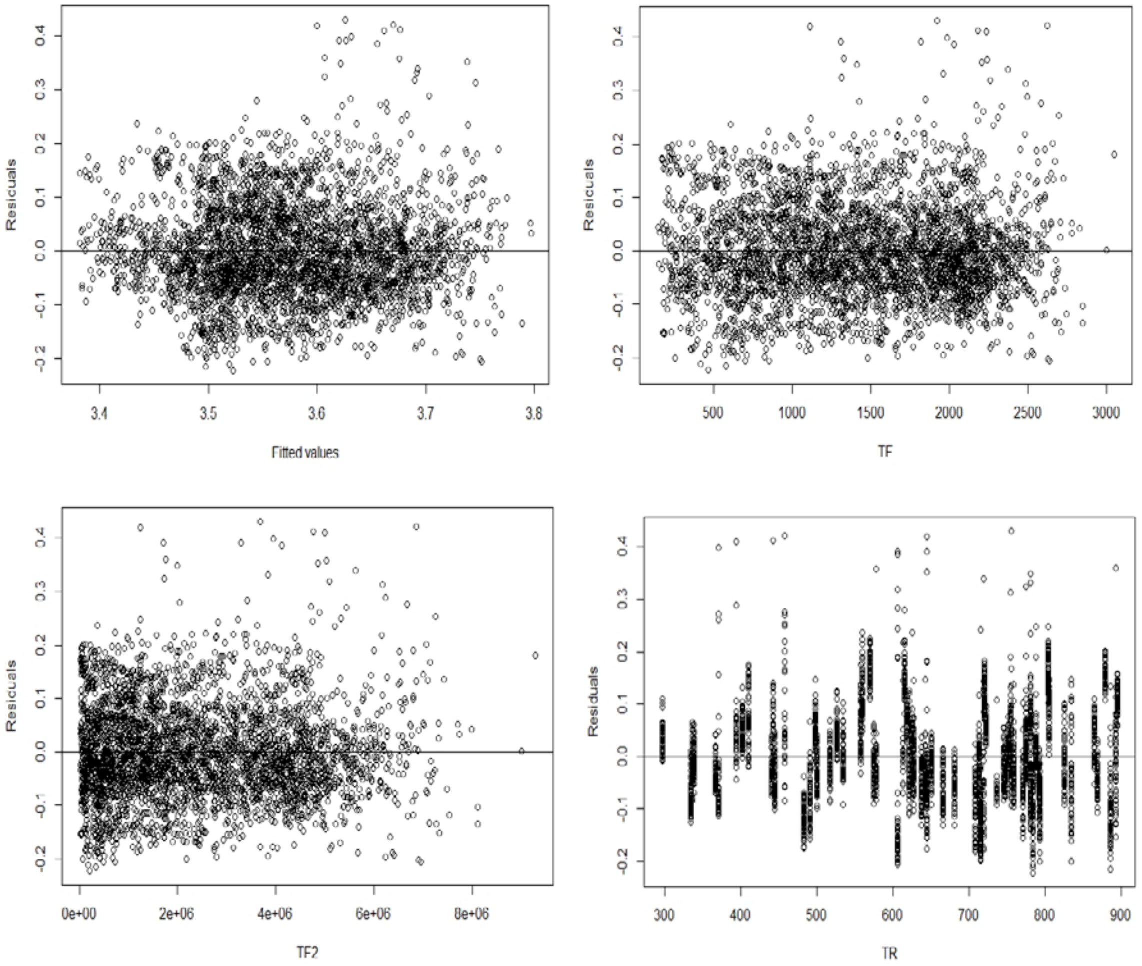

Table 5-13 Breusch-Pagan test by using fitted values for FMODEL3-1

```
ols_test_breusch_pagan(MODEL3_1)
##
##  Breusch Pagan Test for Heteroskedasticity
##  -----------------------------------------
##  Ho: the variance is constant
##  Ha: the variance is not constant
##
##                  Data
##  ----------------------------------------
##  Response : log(Inv_SPD)
##  Variables: fitted values of log(Inv_SPD)
##
##         Test Summary
##  -----------------------------
##  DF            =    1
##  Chi2          =    3.730069
##  Prob > Chi2   =    0.05344118
```

Table 5-14 Breusch-Pagan test of independent variables for MODEL3-1

```
ols_test_breusch_pagan(MODEL3_1, rhs=TRUE, multiple=TRUE)
##
##  Breusch Pagan Test for Heteroskedasticity
##  -----------------------------------------
##  Ho: the variance is constant
##  Ha: the variance is not constant
##
##              Data
##  -------------------------------
##  Response : log(Inv_SPD)
##  Variables: TF TF2 TR RISE FALL
##
##            Test Summary (Unadjusted p values)
##  ----------------------------------------------------
##   Variable             chi2        df         p
##  ----------------------------------------------------
##   TF               9.681590e-01     1          0.3251
##   TF2              4.304884e-04     1          0.9834
##   TR               4.191977e+01     1    9.509626e-11
##   RISE             1.113442e+01     1    8.474034e-04
##   FALL             2.667428e+01     1    2.408060e-07
##  ----------------------------------------------------
##   simultaneous     1.133549e+02     5    8.002381e-23
##  ----------------------------------------------------
```

Table 5-15 Breusch-Pagan test of independent variables for FMODEL3

```
ols_test_breusch_pagan(FMODEL3, rhs=TRUE, multiple=TRUE)
##
##  Breusch Pagan Test for Heteroskedasticity
##  -----------------------------------------
##  Ho: the variance is constant
##  Ha: the variance is not constant
##
##              Data
##  -------------------------------
##  Response : Inv_SPD
##  Variables: TF TF2 TR RISE FALL
##
##           Test Summary (Unadjusted p values)
##  --------------------------------------------------
##   Variable             chi2       df         p
##  --------------------------------------------------
##   TF                 46.358638     1    9.847244e-12
##   TF2                63.153982     1    1.911627e-15
##   TR                 26.893255     1    2.150079e-07
##   RISE                0.245749     1    6.200844e-01
##   FALL               44.199768     1    2.965164e-11
##  --------------------------------------------------
##   simultaneous     162.608262     5    2.751596e-33
##  --------------------------------------------------
```

Test for serial correlation detection

As with heteroscedasticity, serial correlation (which means the correlation between the errors observed in a given time series and the errors in a lagged time series) can be detected by a scatter residual plot. However, it is difficult to detect the violation from the scatter plot because of the large number of points observed from 72 cases by 15-minute intervals between 7.00 and 19.00 (Figure 5-5). Therefore, the Durbin-Watson test, which is widely used for detecting serial correlation, was implemented (Washington *et al.*, 2010). When the errors are independent of each other, the statistic from the Durbin-Watson test (hereafter "D-W statistic") is close to 2. If the errors are positively correlated, the D-W statistic is less than 2 and vice versa greater than 2. In addition, Durbin and Watson (1951) set the criteria of D-W statics that do not reject the null hypothesis only up to 200 samples. The variation becomes narrow as degrees of freedom increase or the number of independent variables decreases. Lee (2016) extended the expected values and variations of the statistic to the large samples size with the different number of IVs (Equation 5-3). According to Lee (2016), in a case where the sample size is 3,482 for the OLS estimated models, the D-W statistic should be close to 2 with the variation of around 0.0011 in order not to violate the serial correlation assumption. Table 5-16 shows the D-W statistics derived for both models of MODEL3-1 and FMODEL3. The test result indicates that the errors of the OLS estimated models are serially correlated and as such it is concluded that alternative model estimations need to be considered.

$$Var(DW) = \begin{cases} \dfrac{4}{df}, & df > 200 \\ 0.002699 + \dfrac{3.1189}{df}, & df \leq 200 \end{cases} \qquad \text{Equation 5-3}$$

Table 5-16 Durbin-Watson test for MODEL3-1 and FMODEL3

```
durbinWatsonTest(MODEL3_1)
##  lag Autocorrelation D-W Statistic p-value
##    1       0.8390613     0.3193988   <0.001
##  Alternative hypothesis: rho != 0

durbinWatsonTest(FMODEL3)
##  lag Autocorrelation D-W Statistic p-value
##    1       0.8115146     0.3741022   <0.001
##  Alternative hypothesis: rho != 0
```

5.4.4. Summary

Many OLS estimation models were constructed in order to develop feasible VDFs using different combinations of variables, interaction effects and transformations of logarithmic functions. Firstly, the IV5 of BEND in all OLS estimated models based on the one-day dataset cannot reject the null hypothesis at a 99% confidence level when applying different combinations to the estimated models. Secondly, interaction effects do not need to be considered when taking into account the change in overall R^2s, p-values of coefficients and the signs of coefficients. Lastly, the log-linear function would be the most appropriate of the four transformed function types.

On the one hand, it is prudent that the developed OLS estimated models are statistically significant because two statistical assumptions for the OLS estimation were violated. In the same context, Washington *et al.* (2010) mentioned that many transportation studies did not consider these OLS assumptions. From the strict viewpoint of OLS statistical assumption, it is not appropriate to apply the OLS estimated models to the traffic assignment process.

On the other hand, as discussed in Section 3.3.2, the violations of both heteroscedasticity and serial correlation do not affect consistency and unbiasedness but rather the efficiency of estimators (Washington *et al.*, 2010). Whilst the estimation requires that many statistical assumptions are satisfied, the OLS estimation method has traditionally been widely used because of its simplicity and clarity. Therefore, care need to be taken when excluding the OLS estimated models from this study.

To sum up, FMODEL3-1 could be the best on the statistical measures of the models by OLS linear estimation. In addition, this study introduces another statistical estimation method for resolving both statistical violations of heteroscedasticity and serial correlation in Section 5.5. Generalised least squares (GLS) estimation is adopted for developing feasible VDFs in this study as discussed in Section 3.3.2.

5.5. GLS estimation models

5.5.1. Model specification

As mentioned in Section 3.3.2, the biggest difference between the OLS and GLS estimation is the variance-covariance matrix of errors. In the OLS estimation, it is a diagonal matrix with the same value assuming that the variance of the errors is constant and the covariance is zero. By contrast, the matrix in the GLS estimation is assumed to be symmetric and non-singular. In addition, the OLS estimation assumes that the errors are normally distributed, while the GLS estimation can cover various distributions of errors including normal, gamma, Poisson and binomial distribution (as with OLS, the GLS estimation predefines the type of distribution). FMODEL3-1 with the independent variables of TF, TF2, TR, RISE and FALL in Section 5.3 is the starting point for the GLS estimation. When recalling Equation 3-35 and Equation 3-36 (Equation 5-4 and Equation 5-5), Equation 5-4 is the possible approach when the variance-covariance matrix is already known, but it is not realistic. Instead, the GLS estimation uses a maximum likelihood estimation (MLE) approach to maximise the log-likelihood (LL) by iterative calculations because it is impossible to define the matrix beforehand (Equation 5-5).

$$\widehat{\boldsymbol{\beta}_{GLS}} = \left(\boldsymbol{X^T \Omega^{-1} X}\right)^{-1} \boldsymbol{X^T \Omega^{-1} Y}$$ Equation 5-4

$$LL = -\frac{n}{2}\ln(2\pi) - \frac{1}{2}\ln(\det(\boldsymbol{\Omega})) - \frac{1}{2}(\boldsymbol{Y} - \boldsymbol{X\beta})^T \boldsymbol{\Omega^{-1}}(\boldsymbol{Y} - \boldsymbol{X\beta})$$ Equation 5-5

The GLS estimation models by different variance-covariance matrices are denoted as Table 5-17 in this section.

Table 5-17 GLS estimation models by different variance-covariance matrices

Model Name	Independent Variables	Explanation
FMODEL3-1	TF, TF2, TR, RISE, FALL	Quadratic model between Inv_SPD and IVs. Log-linear transformation based on FMODEL3. Base model for GLS estimation.
FMODEL3-1-1 ~ FMODEL3-1-11	TF, TF2, TR, RISE, FALL	Reflection by the various relationship between variances (consideration of heterogeneity effects)
FMODEL3-1-12 ~ FMODEL3-1-16	TF, TF2, TR, RISE, FALL	Reflection by the various relationship between covariances (consideration of time-series effects)
FMODEL3-1-17	TF, TF2, TR, RISE, FALL	Consideration of both heterogeneity and time-series effects.

5.5.2. Dealing with heteroscedasticity

The heteroscedasticity detection test performed in Section 5.4.3 confirmed that the homogeneity of the five assumptions for OLS linear estimation was violated. Namely, residuals do not have fixed variance of σ^2. Thus, when recalling Equation 3-37 (Equation 5-6), if heteroscedasticity exists, the variances of residuals against fitted values or explanatory variables can differ ($\sigma_1^2 \neq \sigma_2^2 \neq \ \dots \dots \neq \sigma_n^2$ in Equation 5-6).

$$\boldsymbol{E}[\boldsymbol{\varepsilon\varepsilon^T}] = \sigma^2\boldsymbol{\Omega} = \begin{pmatrix} \sigma_1^2 & 0 & . & 0 \\ 0 & \sigma_2^2 & . & 0 \\ . & . & . & . \\ 0 & 0 & . & \sigma_n^2 \end{pmatrix} \quad \text{Equation 5-6}$$

Dealing with the heteroscedasticity requires prior assumptions about the variance structure. If there are no assumptions about the variance-covariance matrix for a large number of samples in the GLS estimation process, it would either require too much computational work to transform the matrix with iterative calculations or be impossible to find estimators for maximising likelihood function (Equation 5-5). Zuur *et al.* (2009) introduced many variance structures and their functions in “R” for formulating each variance structure following Pinheiro and Bates (2000) (Table 5-18).

Table 5-18 Various variance structures for dealing with heteroscedasticity

Function in “R”	Variance function	Explanation
varFixed()	$\mathrm{Var}(\varepsilon_{ij}) = \sigma^2 \times v_{ij}$	Fixed variance
varIdent()	$\mathrm{Var}(\varepsilon_{ij}) = \sigma^2\delta^2_{s_{ij}}$	Different variances per stratum
varPower()	$\mathrm{Var}(\varepsilon_{ij}) = \sigma^2 \times \lvert v_{ij}\rvert^{2\delta_{s_{ij}}}$	Power of the variance covariate
varExp()	$\mathrm{Var}(\varepsilon_{ij}) = \sigma^2 \times \exp\left(2\delta_{s_{ij}} \times v_{ij}\right)$	Exponential of the variance covariate
varConstPower()	$\mathrm{Var}(\varepsilon_{ij}) = \sigma^2 \times \left(\delta_{1,s_{ij}} + \lvert v_{ij}\rvert^{\delta_{2,s_{ij}}}\right)^2$	Constant plus power of the variance covariate
varComb()	-	A combination of variance functions

where v_{ij} is a vector of variance covariates, δ is a vector of variance parameters and *s* is a stratification variable (Pinheiro and Bates, 2000).

GLS estimation with different variance structures

As can be seen from the Breusch-Pagan test of the residuals against each explanatory variable, the heteroscedasticity of the residuals happened against the geometric IVs except for TF and TF2 IVs.

Therefore, in order to deal with the heteroscedasticity in the modelling process, the variance structures of errors against each independent variable were applied to the GLS estimation focusing on the geometric variables. In addition, since all geometric variables can be grouped into the entity of links as investigated from FE modelling in Section 4.4.2, the stratified variance structure against each link is used for the modelling. In the modelling process, the dependent and independent variables are the same as the log-linear OLS estimation model, which is denoted as "FMODEL3-1" in Table 5-10. The functions presented in Table 5-18 are used to estimate the coefficients of the model and the statistical significance of each coefficient by the *'gls()'* function in the software package of "R". For example, the argument of *"varIdent (form = ~1|Link)"* in Table 5-19 represents the desired variance structure, which is $\mathrm{Var}(\varepsilon_{ij}) = \sigma^2\delta^2_{s_{ij}}$. This argument indicates that the variance of errors is identical within each link but the variance is different across links. The variance model plays a role of weighting in the GLS estimation process by specifying the *'weights'* argument in the *'gls()'* function. Table 5-20 summarises the results of applying different variance structures to GLS estimations by focusing on the estimated coefficients with their t-value, AIC, BIC and logLik (log-likelihood). From this comparison, it can be concluded that the stratified variance structure shows the best result.

Table 5-19 Example of GLS estimation dealing with heteroscedasticity (stratified variance)

```
varIndent_1 <- varIdent(form = ~ 1|Link)
FMODEL3_1_3 <- gls(log(Inv_SPD) ~ TF + TF2 + TR + RISE + FALL,
weights= varIndent_1, data = Data_1day, method="ML")
summary(FMODEL3_1_3)

## Generalized least squares fit by maximum likelihood
##   Model: log(Inv_SPD) ~ TF + TF2 + TR + RISE + FALL
##   Data: Data_1day
##         AIC       BIC    logLik
##   -8575.416 -8095.297 4365.708
##
## Variance function:
##  Structure: Different standard deviations per stratum
##  Formula: ~1 | Link

##Parameter estimates:
##   1. KochangDamyang (6.23-11.57k)_E   10. GwangjuDaegu (125.9-128.0K) S
##               1.0000000                                 3.9309680
## 100. Jungang (267.8-270.4) S         102. Jungang (349.3-351.4) S
##               2.2513605                                 1.3511151
## 103. Jungang-Branch (1.1-3.4) E      104. Jungang-Branch (1.1-3.4) S
##               2.5053089                                 4.8325360
## 105. Jungang-Branch (3.4-5.4) E      106. Jungang-Branch (3.4-5.4) S
##               0.8622466                                 4.2930834
## 107. Jungang-Branch (5.4-8.0) E      108. Jungang-Branch (5.4-8.0) S
##               1.7055257                                 0.9120687
## 117. TongyoungDaejeon (113.2-115.6)E 118. TongyoungDaejeon (113.2-115.6)S
##               4.4932358                                 1.1705882
## 119. TongyoungDaejeon (127.6-131.8)E  12. GwangjuDaegu (135.0-138.6K) S
##               2.3368967                                 1.8843695
```

```
## 120. TongyoungDaejeon (127.6-131.8)S 121. TongyoungDaejeon (153.1-155.9)E
##              2.4076936                                2.8298059
## 122. TongyoungDaejeon (153.1-155.9)S 123. Pyungtaek Jaecheon (48.9-52.1)E
##              1.2476784                                2.6880383
## 124. Pyungtaek Jaecheon(48.9-52.1)S  125. Pyungtaek Jaecheon(105.1-107.3)E
##              1.3979250                                2.9658649
## 126. PyungtaekJaecheon(105.1-107.3)S 127. Pyungtaek Jaecheon(112.0-115.7)E
##              1.7665557                                3.1751057
## 128. PyungtaekJaecheon(112.0-115.7)S 129. Pyungtaek Jaecheon(115.7-118.9)E
##              2.0985188                                2.7722589
## 130. PyungtaekJaecheon(115.7-118.9)S 131. Pyungtaek Jaecheon(118.9-123.9)E
##              1.2073310                                2.2780113
## 132. PyungtaekJaecheon(118.9-123.9)S  14. GwangjuDaegu (138.6-143.3K) S
##              2.0370626                                3.7151508
##   2. KochangDamyang (6.23-11.57k)_S   22. MuanGwangju (26.57-29.57) S
##              2.3986936                                2.2880818
## 25. SangjuYoungduk (105.1-110.3) E    26. SangjuYoungduk (105.1-110.3) S
##              0.7473644                                2.2261311
## 27. SangjuYoungduk(110.3-115.0) E     28. SangjuYoungduk (110.3-115.0) S
##              1.0744919                                1.0131826
## 29. SangjuYoungduk (124.7-128.1) E    30. SangjuYoungduk(124.7-128.1) S
##              1.4833480                                1.0781803
## 31. SangjuYoungduk (146.3-152.2) E    32. SangjuYoungduk (146.3-152.2) S
##              0.6528437                                1.0842468
## 35. SangjuYoungduk (172.3-176.2) E    36. SangjuYoungduk(172.3-176.2) S
##              0.7964520                                1.3246698
## 37. SangjuYoungduk (181.3-185.5) E    38. SangjuYoungduk (181.3-185.5) S
##              3.7026360                                1.7570957
## 39. SangjuYoungduk(185.5-188.7) E     40. SangjuYoungduk (185.5-188.7) S
##              4.3899208                                3.5291273
## 41. SeoulYangyang (63.8-70.1) E       43. SeoulYangyang (70.1-73.7) E
##              0.7212434                                0.8209368
## 47. Seoul Yangyang(97.7-103.9) E      48. Seoul Yangyang (97.7-103.9) S
##              1.2541598                                1.0513742
## 49. Seoul Yangyang(106.9-110.9) E      5. KochangDamyang (19.92-24.06k) E
##              1.2493440                                0.8910661
## 50. Seoul Yangyang(106.9-110.9) S     54. Seoul Yangyang(115.7-119.0) S
##              2.7432645                                1.4564409
## 55. Seoul Yangyang(143.0-149.6) E     56. Seoul Yangyang(143.0-149.6) S
##              1.9439133                                0.6557524
## 57. Suncheon Wyanju (7.8-12.5) E      59. Suncheon Wyanju (12.5-20.0) E
##              1.7209213                                1.3865743
##  6. KochangDamyang (19.92-24.06k) S   61. Suncheon Wyanju (25.1-32.6) E
##              1.9624852                                1.9552155
## 62. Suncheon Wyanju (25.1-32.6) S     65. Suncheon Wyanju (37.9-41.8) E
##              0.8243266                                2.6928160
## 66. Suncheon Wyanju (37.9-41.8) S     67. Suncheon Wyanju (41.8-46.6) E
##              0.6941331                                2.0008783
## 68. Suncheon Wyanju (41.8-46.6) S      7. GwangjuDaegu (41.2-43.7K) E
##              1.2052564                                0.9660230
##  8. GwangjuDaegu (41.2-43.7K) S       83. Jungbunaeryuk (106.4-108.1) E
##              1.8112138                                1.3713531
## 84. Jungbunaeryuk (106.4-108.1) S      9. GwangjuDaegu (125.9-128.0K) E
##              4.3872995                                1.7432063
## 93. Jungbunaeryuk (290.6-295.4) E     94. Jungbunaeryuk (290.6-295.4) S
##              0.9734423                                1.0486989
## 97. Jungang (237.4-244.9) E           99. Jungang (267.8-270.4) E
##              1.7812751                                4.0794553
```

```
## Coefficients:
##                 Value        Std.Error   t-value  p-value
## (Intercept) 3.378419e+00  0.006715026  503.1133        0
## TF          4.966598e-05  0.000006750    7.3582        0
## TF2         2.421686e-08  0.000000002   10.0692        0
## TR          8.906681e-05  0.000005954   14.9584        0
## RISE        3.156171e-03  0.000222389   14.1921        0
## FALL        4.874284e-03  0.000224615   21.7006        0

##  Correlation:
##       (Intr) TF     TF2    TR     RISE
## TF   -0.585
## TF2   0.530 -0.976
## TR   -0.677 -0.017  0.017
## RISE -0.501 -0.015  0.024  0.281
## FALL  0.572 -0.042  0.043 -0.356 -0.635

## Standardized residuals:
##        Min         Q1        Med         Q3        Max
## -2.7493173 -0.7252864  0.1205624  0.8846412  5.0995675

## Residual standard error: 0.04158249
## Degrees of freedom: 3482 total; 3476 residual
```

Table 5-20 GLS estimation considering different variance structures

Model	FMODEL3-1		FMODEL3-1-1		FMODEL3-1-2		FMODEL3-1-3	
Form			varFixed(~ TF)		varFixed(~ TR)		varIdent(form = ~ 1|Link)	
Coeffcient	*Estimates*	*t-value*	*Estimates*	*t-value*	*Estimates*	*t-value*	*Estimates*	*t-value*
(Intercept)	3.37E+00	296.04	3.39E+00	316.60	3.37E+00	311.00	3.38E+00	503.11
TF	5.06E-05	4.57	3.68E-05	3.79	4.24E-05	3.93	4.97E-05	7.36
TF2	2.29E-08	5.91	2.78E-08	7.10	2.55E-08	6.78	2.42E-08	10.07
TR	1.29E-04	12.48	1.23E-04	11.62	1.32E-04	13.64	8.91E-05	14.96
RISE	2.17E-03	6.60	1.51E-03	4.34	2.24E-03	6.83	3.16E-03	14.19
FALL	3.48E-03	9.26	3.45E-03	8.85	3.06E-03	8.25	4.87E-03	21.70
AIC	-6,909		-6,036		-6,959		-8,575	
BIC	-6,865		-5,993		-6,916		-8,095	
logLik	3,461		3,025		3,487		4,366	

Model	FMODEL3-1-4		FMODEL3-1-5		FMODEL3-1-6		FMODEL3-1-7	
Form	varIdent(form = ~ 1|RISE)		varPower(form = ~ TF)		varPower(form = ~ TR)		varExp(form = ~ TR)	
Coeffcient	*Estimates*	*t-value*	*Estimates*	*t-value*	*Estimates*	*t-value*	*Estimates*	*t-value*
(Intercept)	3.39E+00	479.52	3.37E+00	292.93	3.37E+00	307.36	3.37E+00	305.15
TF	4.14E-05	5.97	5.08E-05	4.50	4.49E-05	4.12	4.61E-05	4.22
TF2	2.75E-08	11.02	2.28E-08	5.86	2.48E-08	6.52	2.44E-08	6.40
TR	8.51E-05	13.67	1.29E-04	12.52	1.30E-04	13.30	1.28E-04	12.87
RISE	2.51E-03	10.96	2.20E-03	6.72	2.21E-03	6.75	2.19E-03	6.73
FALL	5.32E-03	21.68	3.49E-03	9.31	3.19E-03	8.56	3.25E-03	8.74
AIC	-8,413		-6,910		-6,966		-6,955	
BIC	-7,982		-6,861		-6,917		-6,906	
logLik	4,277		3,463		3,491		3,486	

Model	FMODEL3-1-8		FMODEL3-1-9		FMODEL3-1-10		FMODEL3-1-11	
Form	varExp(form = ~ RISE)		varExp(form = ~ FALL)		varConstPower(form = ~ TF)		varConstPower(form = ~ TR)	
Coeffcient	*Estimates*	*t-value*	*Estimates*	*t-value*	*Estimates*	*t-value*	*Estimates*	*t-value*
(Intercept)	3.37E+00	297.34	3.38E+00	303.07	3.37E+00	290.19	3.37E+00	307.36
TF	5.06E-05	4.56	4.66E-05	4.26	5.31E-05	4.61	4.49E-05	4.12
TF2	2.31E-08	5.96	2.39E-08	6.25	2.21E-08	5.57	2.48E-08	6.52
TR	1.31E-04	12.74	1.19E-04	11.78	1.29E-04	12.53	1.30E-04	13.30
RISE	2.23E-03	7.04	1.98E-03	5.89	2.20E-03	6.73	2.21E-03	6.75
FALL	3.43E-03	9.04	3.74E-03	10.70	3.48E-03	9.28	3.19E-03	8.56
AIC	-6,916		-6,938		-6,912		-6,964	
BIC	-6,866		-6,888		-6,856		-6,909	
logLik	3,466		3,477		3,465		3,491	

Model selection by ANOVA

As mentioned in Section 3.6.1, the smallest AIC and BIC can be the criteria used for selecting GLS estimation models if both outputs are produced from the same dataset. In addition, the ANOVA test can statistically confirm whether there is a difference between GLS estimation models (Pinheiro and Bates, 2000; Zuur *et al.*, 2009; Fox and Weisberg, 2010). The ANOVA test (Table 5-21) shows that four models, which are FMODEL3-1-3, FMODEL3-1-4, FMODEL3-1-5 and FMODEL3-1-10, have statistical differences with the adjacent model based on the likelihood ratio which is denoted as “L. Ratio”. Moreover, the statistical difference between FMODEL3-1 and FMODEL3-1-3 was confirmed. Therefore, when investigating AIC and BIC with the ANOVA test, FMODEL3-1-3 model can be regarded as the best of the analysed models with reference to heteroscedasticity. The result can be supported by the residual plot of FMODEL3-1 (Figure 5-6) which shows different variances against each link. This can also be due to the difference in sample size or the different variation of the dependent variable (Inv_SPD) (Zuur *et al.*, 2009).

Table 5-21 ANOVA after dealing with heteroscedasticity

```
anova(FModel_OLS_Base, FMODEL3_1_1, FMODEL3_1_2, FMODEL3_1_3, FMODEL3_1_4, FM
ODEL3_1_5, FMODEL3_1_6, FMODEL3_1_7, FMODEL3_1_8, FMODEL3_1_9, FMODEL3_1_10,
FMODEL3_1_11)

##                       Model df   AIC   BIC logLik   Test     L.Ratio  p-value

## FMODEL3_1                 1  7 -6908 -6865 3461
## FMODEL3_1_1               2  7 -6036 -5993 3025
## FMODEL3_1_2               3  7 -6959 -6916 3486
## FMODEL3_1_3               4 78 -8575 -8095 4365   3 vs 4   1757.9990  <.0001
## FMODEL3_1_4               5 70 -8413 -7982 4276   4 vs 5    178.4078  <.0001
## FMODEL3_1_5               6  8 -6910 -6861 3463   5 vs 6   1626.7004  <.0001
## FMODEL3_1_6               7  8 -6966 -6916 3491
## FMODEL3_1_7               8  8 -6955 -6905 3485
## FMODEL3_1_8               9  8 -6915 -6866 3465
## FMODEL3_1_9              10  8 -6937 -6888 3476
## FMODEL3_1_10             11  9 -6911 -6856 3464 10 vs 11     23.8304  <.0001
## FMODEL3_1_11             12  9 -6964 -6908 3491

anova(FMODEL3_1, FMODEL3_1_3)

##                       Model df   AIC   BIC logLik   Test     L.Ratio  p-value
## FMODEL3_1                 1  7 -6908 -6865 3461
## FMODEL3_1_3               2 78 -8575 -8095 4365   1 vs 2    1808.888  <.0001
```

Figure 5-6 Residual plot of FMODEL3-1 against the entity of links

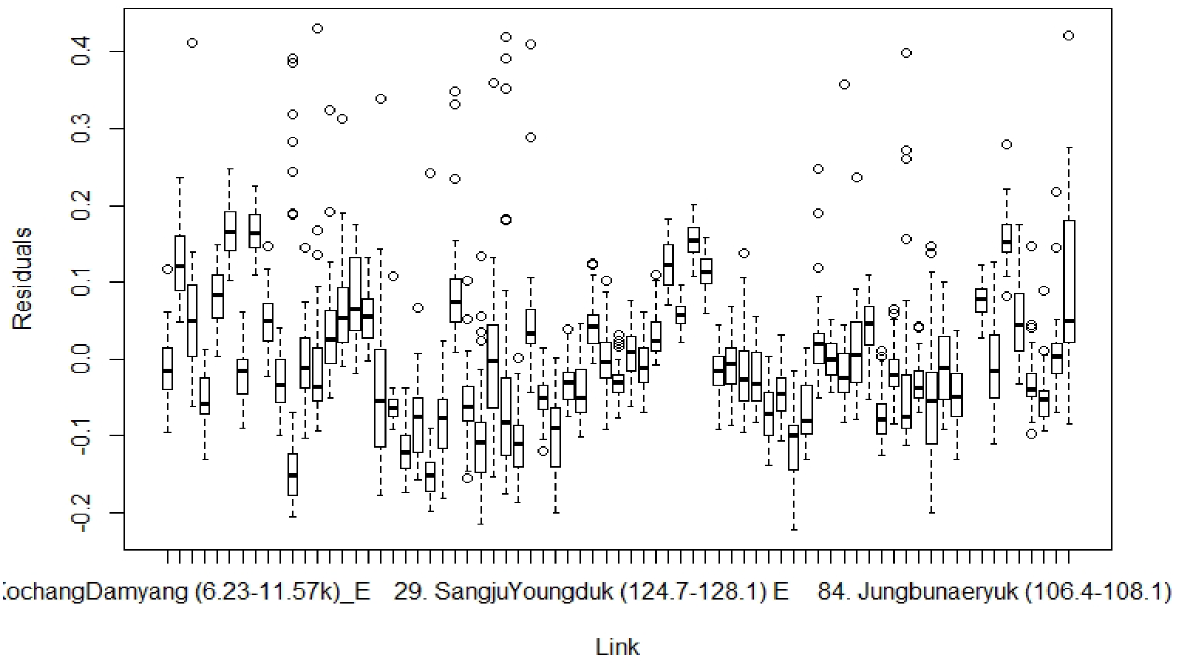

5.5.3. Dealing with serial correlation

The Durbin-Watson test performed in Section 5.4.3 shows that previous and lagged errors measured over 15-minute time intervals are not independent of each other in time-series data modelling. The test result shows that travel time measured in the current time interval can be affected by that in the previous time intervals. When recalling Equation 3-38 (Equation 5-7), if serial correlation exists in OLS linear estimation, the covariance (ρ_i) in the variance-covariance matrix of errors is not zero.

$$\sigma^2\boldsymbol{\Omega} = \sigma^2 \begin{pmatrix} 1 & \rho_1 & \rho_2 & . & \rho_{n-1} \\ \rho_1 & 1 & \rho_1 & . & \rho_{n-2} \\ \rho_2 & \rho_1 & 1 & . & \rho_{n-3} \\ . & . & . & . & . \\ \rho_{n-1} & \rho_{n-2} & \rho_{n-3} & . & 1 \end{pmatrix} \qquad \text{Equation 5-7}$$

In order to deal with serial correlation violation, ARMA models introduced in Section 3.3.2 are applied to the GLS estimation. If high-order ARMA models are included in the GLS estimation process with a large number of samples (3,482 observations in this study), it causes too much computational work to find the estimators through iterative calculations by transforming the variance-covariance matrix. Therefore, in this study, AR (1), AR (2), ARMA (1, 1), ARMA (2, 1) and ARMA (2, 2) models were considered during the GLS estimation process.

GLS estimation with different time-series correlation

In order to deal with the serial correlation, the argument of *'correlation=corARMA (form=~1|Link, p=, q=)'* in the 'R' package was used for assuming various serial correlation structures of errors in the GLS estimation. For example, *'correlation=corARMA (form=~1|Link, p=2, q=2)'* represents an AR (2, 2) model that has the second-order autoregressive and the second-order moving average correlation between residuals in each separated link. Table 5-22 shows the example of the GLS estimation with ARMA (2, 2) in the software package "R". The base model for dealing with serial correlation is FMODEL3-1; it is also the model for treating heteroscedasticity as referred to in the previous section. Table 5-23 summarises GLS estimation models with different serial correlation structures. First of all, the AIC and BIC of the GLS estimation models when combined with AR and ARMA models decreased significantly, compared to the OLS estimation model (FMODEL3-1). This indicates that the accuracy of models is much improved. Secondly, it can be seen that the coefficient values change significantly, which proves that the observed travel time is strongly correlated with previous observation. Lastly, it is noteworthy that some coefficients of independent variables cannot reject the null hypothesis that they can affect the estimated model at the confidence level of 95% after consideration of serial correlation. In particular, the coefficients of

TR, RISE and FALL become less significant as higher-order ARMA models are applied in the GLS estimation.

Table 5-22 Example of GLS estimation dealing with serial correlation (ARMA (2, 2))

```
FMODEL3_1_16 <- gls(log(Inv_SPD) ~ TF + TF2 + TR + RISE + FALL,
correlation=corARMA(form=~1|Link, p=2, q=2), data = Data_1day, method="ML")
summary(FMODEL3_1_16)

## Generalized least squares fit by maximum likelihood
##   Model: log(Inv_SPD) ~ TF + TF2 + TR + RISE + FALL
##   Data: Data_1day
##          AIC       BIC   logLik
##    -12017.37 -11949.66 6019.683

## Correlation Structure: ARMA(2,2)
##  Formula: ~1 | Link

##  Parameter estimate(s):
##       Phi1       Phi2     Theta1     Theta2
##  0.1335614  0.8145693  0.3490224 -0.4433140

## Coefficients:
##                   Value       Std.Error   t-value  p-value
## (Intercept) 3.418510e+00  0.04894284  69.84701   0.0000
## TF          4.741335e-05  0.00001246   3.80642   0.0001
## TF2         1.848031e-08  0.00000000   4.88693   0.0000
## TR          8.362728e-05  0.00005544   1.50838   0.1315
## RISE        1.628975e-03  0.00173585   0.93843   0.3481
## FALL        3.016913e-03  0.00201498   1.49724   0.1344

##  Correlation:
##      (Intr)    TF     TF2    TR     RISE
## TF   -0.185
## TF2   0.162 -0.957
## TR   -0.894  0.019 -0.015
## RISE -0.627  0.007 -0.003  0.350
## FALL  0.641 -0.022  0.020 -0.363 -0.624

## Standardized residuals:
##        Min         Q1         Med         Q3         Max
## -2.4319697 -0.6745891 -0.1646449  0.5458534  4.6720321

## Residual standard error: 0.09313556
## Degrees of freedom: 3482 total; 3476 residual
```

Table 5-23 GLS estimation considering different serial correlation structures

Model	FMODEL3-1		FMODEL3-1-12		FMODEL3-1-13	
Structrue	-		AR (1)		AR (2)	
Correlation Parameters			φ_1 =0.86468		φ_1 =0.5641235	
					φ_2 =0.3488619	
Coeffcient	*Estimates*	*t-value*	*Estimates*	*t-value*	*Estimates*	*t-value*
(Intercept)	3.37E+00	296.04	3.39E+00	105.03	3.40E+00	83.37
			1%		1%	
TF	5.06E-05	4.57	6.82E-05	4.78	6.46E-05	4.69
			35%		28%	
TF2	2.29E-08	5.91	1.09E-08	2.55	1.21E-08	2.95
			-52%		-47%	
TR	1.29E-04	12.48	1.11E-04	3.16	9.86E-05	2.17
			-14%		-24%	
RISE	2.17E-03	6.60	1.82E-03	1.65	1.74E-03	1.22
			-16%		-20%	
FALL	3.48E-03	9.26	3.39E-03	2.67	3.12E-03	1.89
			-3%		-10%	
AIC	-6,909		-11,458		-11,882	
BIC	-6,865		-11,409		-11,827	
logLik	3,461		5,737		5,950	

Model	FMODEL3-1-14		FMODEL3-1-15		FMODEL3-1-16	
Structrue	ARMA (1,1)		ARMA (2,1)		ARMA (2,2)	
Correlation Parameters	φ_1 =0.9707356	θ_1 =-0.4986121	φ_1 =1.0393624	θ_1 =-0.5560434	φ_1 =0.1335614	θ_1 =0.3490224
			φ_2 =-0.0640038		φ_2 = 0.8145693	θ_2 =-0.4433140
Coeffcient	*Estimates*	*t-value*	*Estimates*	*t-value*	*Estimates*	*t-value*
(Intercept)	3.32E+00	70.31	3.42E+00	69.09	3.42E+00	69.85
	-2%		1%		1%	
TF	9.94E-05	3.86	4.62E-05	3.74	4.74E-05	3.81
	96%		-9%		-6%	
TF2	4.84E-09	4.78	1.90E-08	5.05	1.85E-08	4.89
	-79%		-17%		-19%	
TR	1.43E-04	1.53	8.30E-05	1.48	8.36E-05	1.51
	11%		-36%		-35%	
RISE	3.13E-03	0.95	1.63E-03	0.93	1.63E-03	0.94
	45%		-25%		-25%	
FALL	1.16E-03	1.51	3.01E-03	1.48	3.02E-03	1.50
	-67%		-13%		-13%	
AIC	-12,016		-12,016		-12,017	
BIC	-11,960		-11,955		-11,950	
logLik	6,017		6,018		6,020	

Model selection by ANOVA

As with the model comparison for dealing with heteroscedasticity, the ANOVA test was performed while comparing the AIC and BIC measures of the estimated models. Table 5-24 shows that two models, which are FMODEL3-1-12 and FMODEL3-1-13, are statistical different from the adjacent models. Both models of FMODEL3-1-13 and FMODEL3-1-14 are similar through the ANOVA test in spite of the difference of AIC and BIC measures the two models. In addition, Fox and Weisberg (2010) recommended that a simpler model, which has less order of ARMA, would be best if there is no significant difference between models. Therefore, FMODEL3-1-13 in this study can be chosen after treating serial correlation. The model suggests that the previous dependent variable can affect lagged and two lagged dependent variables.

Table 5-24 ANOVA after dealing with serial correlation

```
> anova(FMODEL3_1, FMODEL3_1_12, FMODEL3_1_13, FMODEL3_1_14, FMODEL3_1_15, FM
ODEL3_1_16)

##              Model df        AIC       BIC   logLik   Test  L.Ratio p-value
## FMODEL3_1        1  7  -6908.528  -6865.44 3461.264
## FMODEL3_1_12     2  8 -11457.782 -11408.54 5736.891 1 vs 2 4551.254  <.0001
## FMODEL3_1_13     3  9 -11882.386 -11826.99 5950.193 2 vs 3  426.604  <.0001
## FMODEL3_1_14     4  9 -12015.841 -11960.44 6016.921
## FMODEL3_1_15     5 10 -12016.426 -11954.87 6018.213 4 vs 5    2.584  0.1079
## FMODEL3_1_16     6 11 -12017.367 -11949.66 6019.683 5 vs 6    2.941  0.0863

> anova(FMODEL3_1, FMODEL3_1_13)

##              Model df        AIC       BIC   logLik   Test  L.Ratio p-value
## FMODEL3_1        1  7  -6908.528  -6865.44 3461.264
## FMODEL3_1_13     2  9 -11580.240 -11524.84 5799.120 1 vs 2 4675.712  <.0001

> anova(FMODEL3_1, FModel_GLS_AR11)

##              Model df        AIC       BIC   logLik   Test  L.Ratio p-value
## FMODEL3_1        1  7  -6908.528  -6865.44 3461.264
## FMODEL3_1_14     2  9 -11649.292 -11593.89 5833.646 1 vs 2 4744.764  <.0001
```

5.5.4. Dealing with both heteroscedasticity and serial correlation

As mentioned in Section 5.5.2, if heteroscedasticity exists in the OLS estimation, the GLS estimation assumes that the variance in the variance-covariance matrix of errors is not identical (Equation 5-6). In addition, as mentioned in Section 5.5.3, if serial correlation is identified in the OLS estimation, it is assumed that the covariance in the variance-covariance matrix of errors is not zero (Equation 5-7). Therefore, the variance-covariance matrix structure for dealing with both heteroscedasticity and serial correlation can be derived after combining both matrices as follows.

$$\sigma^2\boldsymbol{\Omega} = \sigma^2 \begin{pmatrix} 1 & \rho_1 & \rho_2 & . & \rho_{n-1} \\ \rho_1 & 1 & \rho_1 & . & \rho_{n-2} \\ \rho_2 & \rho_1 & 1 & . & \rho_{n-3} \\ . & . & . & . & . \\ \rho_{n-1} & \rho_{n-2} & \rho_{n-3} & . & 1 \end{pmatrix} + \begin{pmatrix} \sigma_1^2 & 0 & 0 & . & 0 \\ 0 & \sigma_2^2 & 0 & . & 0 \\ 0 & 0 & \sigma_2^2 & . & 0 \\ . & . & . & . & . \\ 0 & 0 & 0 & . & \sigma_n^2 \end{pmatrix} \quad \text{Equation 5-8}$$

The *'gls()'* function in the software package of "R" supports the arguments of *'weights = varIdent (form = ~1 | Link)'* and *'correlation = corARMA (form = ~1|Link, p=2, q=0)'* at the same time, which are selected as the most appropriate variance-covariance structures. Table 5-25 shows a GLS estimation result dealing with both violations in the OLS estimation. The log-likelihood value was estimated at 6,741; and as such AIC and BIC were derived as -13,321 and -12,829, which are the lowest values among the estimated models in this study. With regard to coefficient estimation, the coefficients of TF and RISE are not statistically significant any more at a 95% confidence level.

Table 5-25 GLS estimation dealing with heteroscedasticity and serial correlation

```
FMODEL3_1_17  <- gls(log(Inv_SPD) ~ TF + TF2 + TR + RISE + FALL,
weights= varIndent_1, correlation=corARMA(form=~1|Link, p=2, q=0),
data = Data_1day, method="ML")
summary(FMODEL3_1_17)

##  Generalized least squares fit by maximum likelihood
##  Model: log(Inv_SPD) ~ TF + TF2 + TR + RISE + FALL
##  Data: Data_1day
##         AIC       BIC  logLik
##  -13321.82 -12829.39 6740.91

##  Correlation Structure: ARMA(2,0)
##  Formula: ~1 | Link
##  Parameter estimate(s):
##       Phi1      Phi2
##  0.5551263 0.4038067

##  Variance function:
##  Structure: Different standard deviations per stratum
##  Formula: ~1 | Link
##  Parameter estimates:
##   1. KochangDamyang (6.23-11.57k)_E    10. GwangjuDaegu (125.9-128.0K) S
##             1.0000000                             1.2115718
## 100. Jungang (267.8-270.4) S          102. Jungang (349.3-351.4) S
##             2.8437465                             1.0635928
## 103. Jungang-Branch (1.1-3.4) E       104. Jungang-Branch (1.1-3.4) S
##             0.8470087                             0.8152215
## 105. Jungang-Branch (3.4-5.4) E       106. Jungang-Branch (3.4-5.4) S
##             0.7824435                             0.8033950
## 107. Jungang-Branch (5.4-8.0) E       108. Jungang-Branch (5.4-8.0) S
##             0.7591350                             0.9174394
## 117. TongyoungDaejeon (113.2-115.6)E  118. TongyoungDaejeon (113.2-115.6)S
##             3.6854748                             1.4567642
## 119. TongyoungDaejeon (127.6-131.8)E   12. GwangjuDaegu (135.0-138.6K) S
##             2.4284418                             2.1777825
## 120. TongyoungDaejeon (127.6-131.8)S  121. TongyoungDaejeon (153.1-155.9)E
```

```
##                 2.1023616                                      0.9295036
## 122. TongyoungDaejeon (153.1-155.9)S 123. Pyungtaek Jaecheon (48.9-52.1)E
##                 0.7779605                                      2.8839645
## 124. Pyungtaek Jaecheon(48.9-52.1)S  125. Pyungtaek Jaecheon(105.1-107.3)E
##                 1.7134759                                      0.9874397
## 126. PyungtaekJaecheon(105.1-107.3)S 127. Pyungtaek Jaecheon(112.0-115.7)E
##                 1.1039314                                      2.3568067
## 128. PyungtaekJaecheon(112.0-115.7)S 129. Pyungtaek Jaecheon(115.7-118.9)E
##                 1.3629824                                      2.1809797
## 130. PyungtaekJaecheon(115.7-118.9)S 131. Pyungtaek Jaecheon(118.9-123.9)E
##                 1.1948284                                      1.8472261
## 132. PyungtaekJaecheon(118.9-123.9)S  14. GwangjuDaegu (138.6-143.3K) S
##                 2.4151600                                      3.3638369
## 2. KochangDamyang (6.23-11.57k)_S     22. MuanGwangju (26.57-29.57) S
##                 1.3761485                                      2.7859487
## 25. SangjuYoungduk (105.1-110.3) E    26. SangjuYoungduk (105.1-110.3) S
##                 0.8784543                                      1.4647244
## 27. SangjuYoungduk(110.3-115.0) E     28. SangjuYoungduk (110.3-115.0) S
##                 0.8944811                                      0.9543687
## 29. SangjuYoungduk (124.7-128.1) E    30. SangjuYoungduk(124.7-128.1) S
##                 0.8979334                                      1.3470280
## 31. SangjuYoungduk (146.3-152.2) E    32. SangjuYoungduk (146.3-152.2) S
##                 0.8309647                                      1.0431039
## 35. SangjuYoungduk (172.3-176.2) E    36. SangjuYoungduk(172.3-176.2) S
##                 1.1320569                                      0.6975661
## 37. SangjuYoungduk (181.3-185.5) E    38. SangjuYoungduk (181.3-185.5) S
##                 0.4085000                                      0.4057204
## 39. SangjuYoungduk(185.5-188.7) E     40. SangjuYoungduk (185.5-188.7) S
##                 0.5138131                                      0.4328641
## 41. SeoulYangyang (63.8-70.1) E       43. SeoulYangyang (70.1-73.7) E
##                 1.0534969                                      1.2077253
## 47. Seoul Yangyang(97.7-103.9) E      48. Seoul Yangyang (97.7-103.9) S
##                 1.4906727                                      0.8768663
## 49. Seoul Yangyang(106.9-110.9) E      5. KochangDamyang (19.92-24.06k) E
##                 1.4006033                                      0.9182540
## 50. Seoul Yangyang(106.9-110.9) S     54. Seoul Yangyang(115.7-119.0) S
##                 1.1820039                                      1.2293540
## 55. Seoul Yangyang(143.0-149.6) E     56. Seoul Yangyang(143.0-149.6) S
##                 1.8538189                                      0.8053592
## 57. Suncheon Wyanju (7.8-12.5) E      59. Suncheon Wyanju (12.5-20.0) E
##                 2.8203939                                      1.2977953
## 6. KochangDamyang (19.92-24.06k) S    61. Suncheon Wyanju (25.1-32.6) E
##                 0.8644404                                      0.7033792
## 62. Suncheon Wyanju (25.1-32.6) S     65. Suncheon Wyanju (37.9-41.8) E
##                 0.8727327                                      2.2955222
## 66. Suncheon Wyanju (37.9-41.8) S     67. Suncheon Wyanju (41.8-46.6) E
##                 0.8861990                                      1.3207914
## 68. Suncheon Wyanju (41.8-46.6) S      7. GwangjuDaegu (41.2-43.7K) E
##                 1.4003406                                      0.9385751
## 8. GwangjuDaegu (41.2-43.7K) S        83. Jungbunaeryuk (106.4-108.1) E
##                 0.7334058                                      1.2292920
## 84. Jungbunaeryuk (106.4-108.1) S      9. GwangjuDaegu (125.9-128.0K) E
##                 0.7069811                                      0.9762135
## 93. Jungbunaeryuk (290.6-295.4) E     94. Jungbunaeryuk (290.6-295.4) S
##                 1.4816811                                      0.9030070
## 97. Jungang (237.4-244.9) E           99. Jungang (267.8-270.4) E
##                 1.7636100                                      2.8878767

## Coefficients:
```

```
##                   Value      Std.Error   t-value  p-value
## (Intercept)  3.445633e+00  0.04741045  72.67666   0.0000
## TF           1.751086e-05  0.00000969   1.80693   0.0709
## TF2          2.018223e-08  0.00000000   6.46729   0.0000
## TR           1.881290e-04  0.00005117   3.67647   0.0002
## RISE        -1.543135e-03  0.00189283  -0.81525   0.4150
## FALL         5.906981e-03  0.00198397   2.97736   0.0029

##  Correlation:
##      (Intr)   TF     TF2    TR     RISE
## TF   -0.149
## TF2   0.129 -0.947
## TR   -0.913  0.038 -0.029
## RISE -0.675  0.001 -0.002  0.436
## FALL  0.688 -0.012  0.014 -0.447 -0.620

## Standardized residuals:
##        Min         Q1        Med         Q3        Max
## -2.7313871 -0.7717273 -0.2352308  0.3474124  3.7854876

## Residual standard error: 0.08913695
## Degrees of freedom: 3482 total; 3476 residual
```

5.5.5. Summary

Section 5.5 introduced the GLS estimation to deal with the violation of heteroscedasticity and autocorrelation in OLS linear estimation. OLS linear estimation assumes the zero mean and normal distribution of disturbances; non-correlation of independent variables and disturbances; homoscedasticity of disturbances; and non-autocorrelation of disturbances. However, as Washington *et al.* (2010) mentioned, many transportation studies tend to neglect these assumptions. This study assumed the structure of the variance-covariance matrix of errors in advance and then compared the statistical measures of the GLS estimated models through maximum likelihood estimation.

Table 5-26 shows four representative models by OLS and GLS linear estimation. FMODEL3-1 is the selected model after stepwise variable selection, having given consideration to interaction effects and model transformation. FMODEL3-1-3, which is based on the stratified variance structure across links, shows the best performance among the models that treat heteroscedasticity. FMODEL3-1-13 is the best model of those that consider serial correlation structures. FMODEL3-1-17 is estimated by considering both the variance-covariance structure of heteroscedasticity and serial correlation.

To investigate the coefficients and their statistical significance in Table 5-26, the GLS estimation changed the coefficients of independent variables much more than the intercept, which is FFTT in the estimated models. Whilst the stratified variance structure on each link affects the coefficients of geometric variables more than TF-related variables (TF and TF2), the AR (2) time-series structure on each link affects the coefficients of all independent variables. In other words, the heterogeneity of links mainly results in the adjustment of the impact by link geometric variables. Conversely, the effects by serial correlation not only change the values of coefficients but also their statistical significance. The consideration of serial correlation between observations would reflect the interaction between previous and lagged residuals and as such the explanatory power of each coefficient fluctuates greatly.

To summarise, it can be said that the models derived by the GLS estimation are more statistically significant than those by the OLS estimation because all of them increase log-likelihood, which is a common objective function of OLS and GLS estimations (Section 3.3.2). In particular, FMODEL3-1-17 has the highest log-likelihood measure and as such the model can be said to be the most statistically significant among the linear estimation models. If serial correlation could be considered practically in traffic assignment, FMODEL3-1-17 would be an alternative to the current VDFs. Otherwise, FMODEL3-1 and FMODEL3-1-3 which do not consider time-series relationships would be alternative feasible models. Therefore, the statistically linear estimations produced the three representative models: FMODEL3-1, FMODEL3-1-3 and FMODEL3-1-17.

Table 5-26 Selection between OLS and GLS estimated models

Model	FMODEL3-1		FMODEL3-1-3		FMODEL3-1-13		FMODEL3-1-17	
Structrue	-		varIdent(form = ~ 1|Link)		AR (2)		varIdent(form = ~ 1|Link) and AR (2)	
Correlation Parameters					φ_1 =0.5641235		φ_1 =0.5551263	
					φ_2 =0.3488619		φ_2 =0.4038067	
Coeffcient	*Estimates*	*t-value*	*Estimates*	*t-value*	*Estimates*	*t-value*	*Estimates*	*t-value*
(Intercept)	3.37E+00	296.04	3.38E+00	503.11	3.40E+00	83.37	3.45E+00	72.68
			0%		1%		2%	
TF	5.06E-05	4.57	4.97E-05	7.36	6.46E-05	4.69	1.75E-05	1.81
			-2%		28%		-65%	
TF2	2.29E-08	5.91	2.42E-08	10.07	1.21E-08	2.95	2.02E-08	6.47
			6%		-47%		-12%	
TR	1.29E-04	12.48	8.91E-05	14.96	9.86E-05	2.17	1.88E-04	3.68
			-31%		-24%		46%	
RISE	2.17E-03	6.60	3.16E-03	14.19	1.74E-03	1.22	-1.54E-03	-0.82
			46%		-20%		-171%	
FALL	3.48E-03	9.26	4.87E-03	21.70	3.12E-03	1.89	5.91E-03	2.98
			40%		-10%		70%	
AIC	-6,909		-8,575		-11,882		-13,322	
BIC	-6,865		-8,095		-11,827		-12,829	
logLik	3,461		4,366		5,950		6,741	

Note: The underlined values are percentage changes of coefficients with FMODEL3-1.

5.6. Findings

This chapter attempted to derive the representative models within three statistical estimation methods: NLS, OLS and GLS estimation. Table 5-27 summarises the key information on the selected models within each method. In particular, FBPR1 is suggested as a reference model in this study because it is in line with the current approach used in many studies for customising VDFs. FBPR3 has lower RMSE and MAPE by around 10% than FBPR1 by adding geometric variables to the current BPR functional form. Nevertheless, FBPR1 and FBPR3 do not overcome the limitation of including road capacity in their functional forms. On the other hand, linear estimated models (FMODEL3-1, FMODEL3-1-3 and FMODEL3-1-17) do not need to predetermine road capacity and show statistical measures (e.g. RMSE and MAPE) equivalent to FBPR1 and FBPR3. Moreover, the GLS estimation models (FMODEL3-1-3 and FMODEL3-1-17) have better statistical significance rather than the OLS estimation model (FMODEL3-1). The five models selected in this chapter are discussed in detail from a statistical and practical perspective in Chapter 6.

Table 5-27 Summary of feasible models within each estimation method

Model Name	FBPR1		FBPR3		FMODEL3-1		FMODEL3-1-3		FMODEL3-1-17	
Estimation	NLS estimation				OLS estimation		GLS estimation			
Base function	BPR function (current approach)		BPR function		Quadratic function | log-linear transformation					
Equation (underline: variables)	TT = FFTT*(1 + a*(1 + (TF/Capacity)^b)		TT = FFTT*(1 + a*(1 + (TF/Capacity)^b) + c*TR + d*RISE + e*FALL		TT = Exp (FFTT + a*TF + b *TF^2 + c*TR + d*RISE + e*FALL)					
Road Capacity	Predetermined		Predetermined		Not predetermined		Not predetermined		Not predetermined	
Coefficient	*Estimate*	*p-value*	*Estimate*	*p-value*	*Estimates*	*p-value*	*Estimates*	*p-value*	*Estimates*	*p-value*
FFTT	3.18E+01	< 2e-16 ***	2.92E+01	< 2e-16 ***	3.37E+00	< 2e-16 ***	3.38E+00	< 2e-16 ***	3.45E+00	< 2e-16 ***
a	2.71E-01	< 2e-16 ***	2.97E-01	< 2e-16 ***	5.06E-05	5.13e-06 ***	4.97E-05	2.31e-13 ***	1.75E-05	0.071
b	1.59E+00	< 2e-16 ***	1.73E+00	< 2e-16 ***	2.29E-08	3.76e-09 ***	2.42E-08	< 2e-16 ***	2.02E-08	1.14e-10 ***
c			4.71E-03	< 2e-16 ***	1.29E-04	< 2e-16 ***	8.91E-05	< 2e-16 ***	1.88E-04	2.40e-4 ***
d			7.99E-02	1.05e-10 ***	2.17E-03	4.78e-11 ***	3.16E-03	< 2e-16 ***	-1.54E-03	-0.415
e			1.27E-01	< 2e-16 ***	3.48E-03	< 2e-16 ***	4.87E-03	< 2e-16 ***	5.91E-03	0.003 ***
Statistical measures	RMSE: MAPE:	3.601 7.748%	RMSE: MAPE:	3.360 7.053%	AIC: BIC: RMSE: MAPE:	-6,909 -6,865 3.357 6.947%	AIC: BIC: RMSE: MAPE:	-8,575 -8,095 3.459 6.806%	AIC: BIC: RMSE: MAPE:	-13,322 -12,829 3.633 7.867%

Chapter 6. Application

6.1. Introduction

Through Chapter 4 and Chapter 5, feasible models as link cost functions have been developed by combining time-series traffic data and geometric information. This chapter will confirm the feasibility of the developed models by applying the models to the real world situation after the model selection.

Section 6.2 suggests the most appropriate model to replace the existing VDF (e.g. Korean BPR function) by comparing the feasibility of the various models developed in Chapter 6 from three different perspectives: the spatial transferability, the statistical significance, and the practical applicability. Firstly, Section 6.2.1 validates models by investigating how the models can secure the spatial transferability by 10-fold cross-validation, which shows the biases by repeating modelling and testing after dividing the dataset into training and test subsets. In addition, Section 6.2.2 deals with the statistical significance of the models by comprehensively evaluating the various statistical accuracy measures with those presented in Chapter 5. Lastly, Section 6.2.3 examines which models can be applied practically and replace existing link cost functions in terms of the data specification required for models (GLS estimation models) and the error propagation by road capacity (NLS estimation models).

Section 6.3 demonstrates quantitatively the extent to which different link cost functions affect the travel time estimation and further transport planning process between the selected model in Section 6.2 and Korean BPR functions. First of all, Section 6.3.1 identifies the extent to which differences in total travel time can be predicted by applying the models to hypothetical links which have different geometry. In addition, Section 6.3.2 emphasises the final goal of this study by presenting comparative results in traffic assignment and transport appraisal between the developed model and Korean models when planning the construction of a new hypothetical motorway.

6.2. Selection of the most appropriate link-cost function

With reference back to Table 5-27, the models discussed in this section are FBPR1, FBPR3, FMODEL3-1, FMODEL3-1-3 and FMODEL3-1-17. This section compared these models and suggested the most suitable model for traffic assignment in transport appraisal.

6.2.1. Validation of models

10-fold cross-validation is one of the statistical verifications for reducing the biases of a model as a classifier; these were mentioned in Section 3.6.2. This study used 10-fold cross-validation to confirm the spatial transferability of the estimated models. In other words, the classifier determines how well the developed models are performing when the models are applied to other sections. After dividing all the samples into 10 folds randomly, the model is calibrated on the training set of the samples in nine folds and evaluated by using the test set of the samples on one fold. Since all samples are divided into 10 folds, this process is repeated ten times without mixing samples between folds.

As 72 sections were collected in this study, the other folds have seven cases except for one fold which has nine cases. The first trial estimates models with the samples in 63 training sets (= 7 cases * 9 folds), and evaluates the developed models with the samples in nine test sets (9 cases * 1 fold). The second to tenth trials estimate models with 65 training sets (=7 cases * 8 folds + 9 cases * 1 fold), and evaluate them with seven test sets (7 cases * 1 fold). This study calculated the accuracy measures of RMSE and MAPE every trial for the evaluation of the models. In a ten iteration process, the model's spatial transferability can be determined by the average and standard deviation of the measures. Therefore, the measure of determination in a 10-fold cross-validation (denoted as 'CV_{10}' in Equation 6-1) can be calculated as follows;

$$\mathrm{CV}_{10} = \frac{1}{10}\sum_{i=1}^{10} RMSE_i \quad or \quad \frac{1}{10}\sum_{i=1}^{10} MAPE_i \qquad \text{Equation 6-1}$$

where 'i' means the *i*th trial.

The coding for 10-fold cross-validation was conducted, using the software package of "R" (Appendix A.5.4). Table 6-1 and Table 6-2 show the RMSE and MAPE for every trial in the 10-fold cross-validation. There were no big differences between the values of both measures from five groups (models). In addition, the ANOVA tests demonstrate that the difference is not statistically significant (Table 6-3). Rather, it can be seen that the other four models exhibit lower averages for

RMSEs and MAPEs than FBPR1. Therefore, it can be concluded that the other models confirm the spatial transferability as with the current VDF structure of FBPR1.

Table 6-1 RMSE derivation by 10-fold cross-validation

Trials	FBPR1 BPR function	FBPR3 BPR function with road geometry	FMODEL3-1 OLS estimation	FMODEL3-1-13 Dealing with heteroscedasticity	FMODEL3-1-17 Dealing with heteroscedasticity and serial correlation
1	2.950	3.031	2.972	3.289	3.197
2	3.018	2.715	2.714	2.822	2.964
3	4.010	3.565	3.589	3.866	3.380
4	4.320	3.729	3.696	3.459	4.025
5	3.968	3.647	3.669	3.773	3.356
6	3.187	3.278	3.262	3.396	3.860
7	3.707	3.470	3.521	3.733	3.689
8	3.647	3.856	3.865	4.082	4.080
9	2.968	3.209	3.123	3.033	4.033
10	4.070	3.801	3.808	3.682	4.206
Average	3.585	3.430	3.422	3.513	3.679
std.error	0.515	0.368	0.385	0.390	0.429

Table 6-2 MAPE derivation by 10-fold cross-validation

Trials	FBPR1	FBPR3	FMODEL3-1	FMODEL3-1-13	FMODEL3-1-17
1	6.863%	6.925%	6.685%	7.928%	6.830%
2	5.196%	4.860%	4.879%	5.319%	4.879%
3	9.167%	7.872%	7.951%	8.452%	7.404%
4	9.397%	7.436%	7.242%	5.887%	8.829%
5	9.437%	7.968%	7.895%	7.750%	7.469%
6	7.315%	7.098%	6.869%	6.747%	8.666%
7	7.738%	6.843%	6.865%	6.971%	8.112%
8	7.449%	8.158%	8.095%	8.056%	9.569%
9	6.705%	7.342%	7.066%	6.661%	9.545%
10	8.787%	8.581%	8.496%	7.764%	9.591%
Average	7.805%	7.308%	7.204%	7.154%	8.089%
std.error	1.386%	1.028%	1.023%	1.013%	1.498%

Table 6-3 ANOVA of RMSEs and MAPEs between five models

ANOVA

		Sum of Squares	df	Mean Square	F	Sig.
RMSEs_10_fold_CV	Between Groups	.439	4	.110	.276	.892
	Within Groups	17.859	45	.397		
	Total	18.298	49			
MAPEs_10_fold_CV	Between Groups	.001	4	.000	.715	.586
	Within Groups	.009	45	.000		
	Total	.010	49			

6.2.2. Investigation of statistical significance between models

In Chapter 5, the feasible models, within each estimation, were selected by comparing the statistical measures derived as a result of each estimation method. This section comprehensively investigates the accuracy measures, fitted plots, residual plots and applicability in practice to compare the accuracy of models across the estimation methods. As mentioned in Section 3.6.1, adjusted R^2, AIC and BIC can be used as statistical measures to compare linear estimation models with the same dependent variable, but it is difficult to use those measures for the comparison with non-linear estimation models. Therefore, the accuracy measures such as SSE, MAD, RMSE and MAPE, which are derived from differences between observed and fitted values, were used for model comparison. Table 6-4 compares the accuracy measures of the feasible models chosen in the previous sections. Some key points can be summarised as follows.

Firstly, all estimated models with geometric variables can explain the observed travel time values more precisely than FBPR1; this latter model shares the same model structure as the current BPR function as well as that of Korean VDFs (‘KDI (2015)’ and ‘KOTI (2009)’ in Table 6-4). Whilst the RMSE and MAPE of FBPR1 are 3.60 and 7.75% respectively, those of the other four models range from 3.36 to 3.46 and from 6.95% to 7.05% respectively. Figure 6-1 shows that the four models estimated with geometric variables can cover a wider range of observations than FBPR1 along with traffic flow (in fact, fitted values should be considered multi-dimensionally with respect to all variables).

Secondly, from examining SSE and RMSE, which impose a penalty for large errors (the effect of squares), both FMODEL3-1 and FBPR3 models show better performances than other models. In particular, FBPR3 can explain the observations better than FBPR1 by the addition of geometric variables to BPR function. Both models are similar in that they aim to minimise only the sum of square errors without considering the correlation between variables or errors.

Thirdly, FMODEL3-1-3 shows the best accuracy for MAE and MAPE, which impose comparatively the same weights to errors. In addition, Figure 6-2 shows residuals which have a relatively constant variance dependent on the fitted values in FMODEL3-1-3 compared to the other three models’ residual plots, which are clustered in the centre. Unlike the other estimations, the variance of FMODEL3-1-3 is defined differently for every link (72 variances for 72 links) without consideration of time-series structure.

Lastly, as mentioned in Section 5.5.5, the FMODEL3-1-17 model is the statistically best model in terms of maximising the log-likelihood objective function. However, when focusing on the fitted values (Figure 6-1), it can be seen that travel time does not increase much exponentially in proportion to the traffic flow. In other words, the relationship between travel time and traffic flow is close to the simple linear relationship, which is a different result from traditional traffic theory. The result can be attributed to the fact that the explanatory power of both TF and TF^2 is greatly reduced after the AR (2) correlation structure is applied to the GLS estimation.

Table 6-4 Comparison of accuracy measures between the feasible models

	FBPR1	FBPR3	FMODEL3-1	FMODEL3-1-13	FMODEL3-1-17	KDI (2015)	KOTI (2009)
SSE	39229	41651	45951	39303	45159	171998	94479
MAE	2.531	2.521	2.783	2.558	2.812	6.273	3.974
RMSE	3.357	3.459	3.633	3.360	3.601	7.028	5.209
MAPE	6.95%	6.81%	7.87%	7.05%	7.75%	18.33%	10.29%
AIC	-6909	-8575	-13322	NA	NA	NA	NA
BIC	-6865	-8095	-12829	NA	NA	NA	NA

Note. KDI (2015) and KOTI (2009) are references models, which are used in Korea

Figure 6-1 Fitted and observed values according to traffic flow on each model

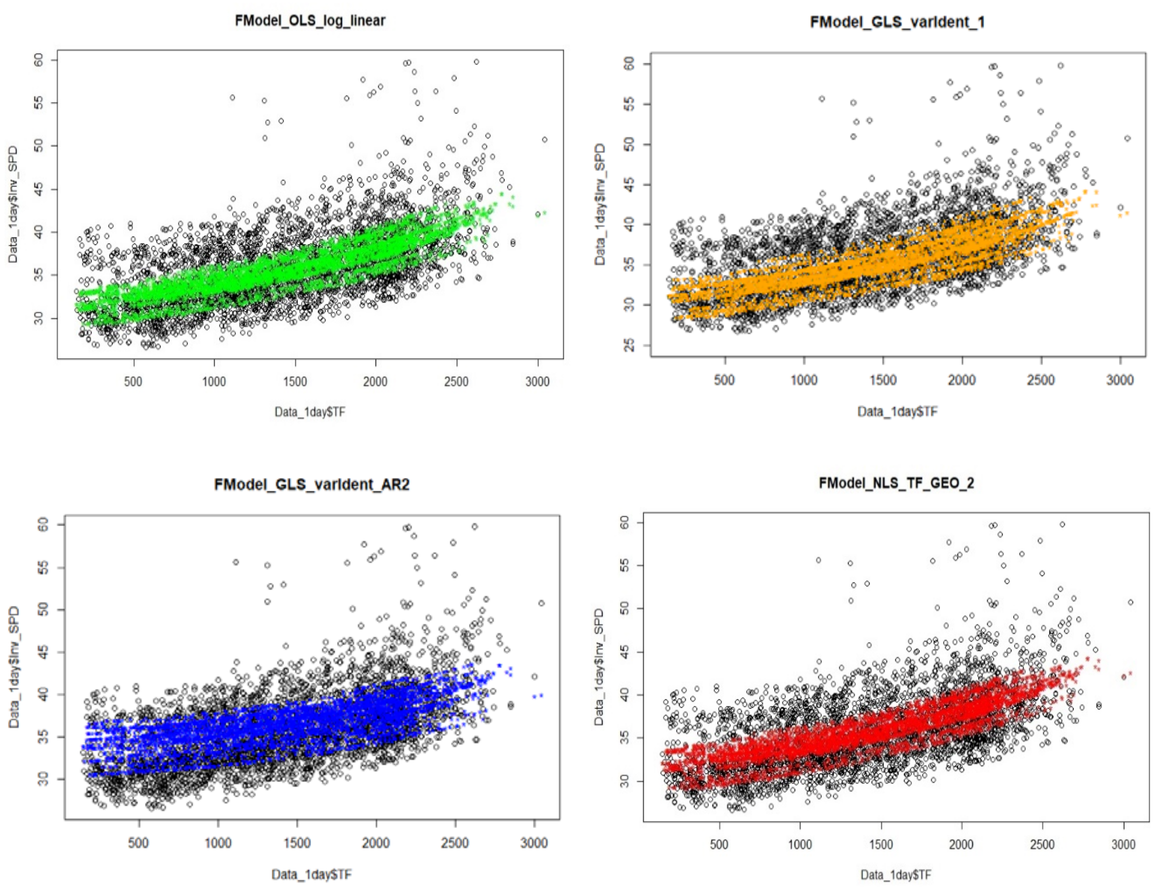

Figure 6-2 Standardised residuals vs fitted values plot on feasible models

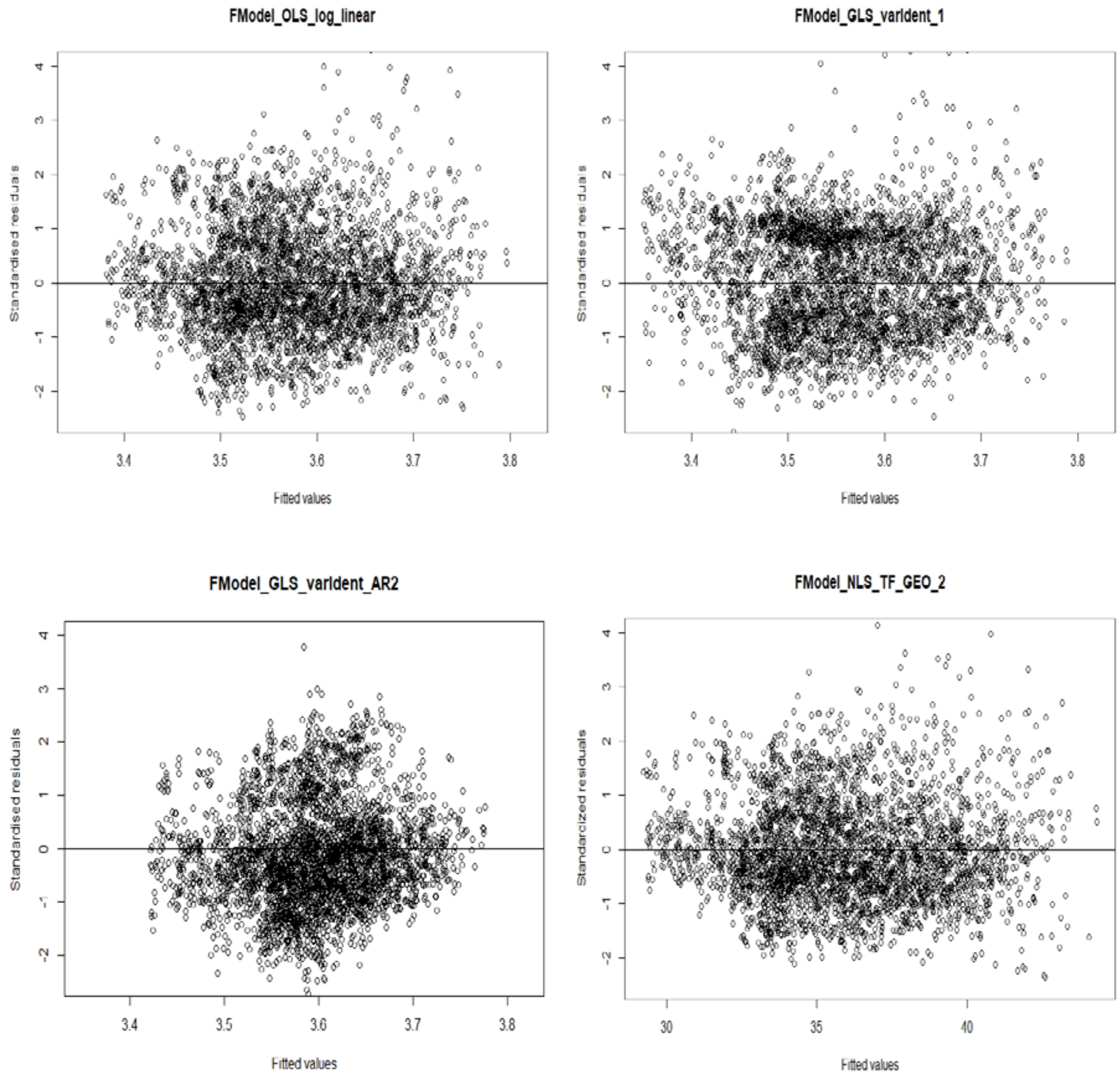

6.2.3. Practical applicability

Briefly, going back to the starting point of this study, the models developed in this study should be able to be used for traffic assignment in the traffic appraisal. Therefore, this section considers the practical applicability of the developed models. Since FMODEL3-1 developed by OLS linear estimation does not have better comparative measures including AIC, BIC and log-likelihood than other linear estimation models, the model was excluded from comparison in this section. Therefore, this section discussed the practical applicability of only those models derived by GLS and NLS estimation methods. The models by both estimations were investigated in terms of data availability and capacity uncertainty.

Applicability of GLS estimation to practice

Even though GLS estimation models are more statistically meaningful with reference to the variance-covariance structure of errors than OLS estimation models, nonetheless, even statistically accurate models need to be carefully applied in practice. As mentioned above, the two models to compare with each other in this section are FMODEL3-1-3 and FMODEL3-1-17. Whilst the first one treats the heteroscedasticity, the other treats both the heteroscedasticity and the serial correlation of errors.

Firstly, FMODEL3-1-3 was developed based on the assumption that each link has a different variance structure of the error. Washington *et al.* (2010) mentioned that spatial data can be dependent on the observed location defining the heterogeneity as samples from different populations. With reference to the 72 cases selected in this study, the assumption that the estimated model error is homoscedastic means that each case has identical variance regardless of its attributes. However, each case (link) in this study has different features affecting travel time. Therefore, it would be reasonable to assume that the 72 cases have the heteroscedastic error distribution. Figure 6-3, which is derived from Table 5-19, compares the variance ratios[15] for “1. KochangDamyang (6.23-11.57k) E” in the GLS estimation with the different error variance structure for individual links. The highest and lowest values among the estimated variances of links are 4.83 for “104. Jungang-Branch (1.1-3.4) S” and 0.65 for “31. SangjuYoungduk (146.3-152.2) E” respectively. From this result, it can be confirmed that each link has a different variance of error that could result from the unobserved heterogeneity of the links.

In addition, FMODEL3-1-17 was estimated adding the assumption that the covariance of the error is not zero and the residuals are correlated with each other. This assumption would also be reasonable in that the travel time measured in the current time interval (e.g. 15 minutes in this study) could affect the travel time in the next and subsequent time interval[16]. However, the model has limitations in two respects: the difference of data specification between modelling and traffic assignment process; and the hypothesis of time-series modelling. The first one is that FMODEL3-1-17 cannot be applied to the traffic assignment process because the O-D trip demand for traffic assignment in Korea is provided on a daily basis (Table 6-5). This highlights the fact that it is difficult to apply Korean O-D trip demand to the model estimated by considering the serial correlation from the dataset with 15-minute intervals. The other limitation is based on the assumption that a link cost function in static traffic assignment does not follow the hypothesis of time-series modelling that the current time-series trend continues in the future (Washington *et al.*,

[15] In GLS estimation, only the ratio between variances is important rather than the absolute value of variance (see Section 3.3.2).
[16] The GLS estimation model with AR (2) model means that the current value is affected by the previous two observations (travel time before 15 minutes and 30 minutes).

2010). In other words, it is inappropriate for a time-series model based on historical travel time observations to be used in current motorway planning procedures. Therefore, although time-series analysis has academic statistical significance, it is questionable whether FMODEL3-1-17 is practical in traffic assignment.

Figure 6-3 Ratio of the error variance depending on links

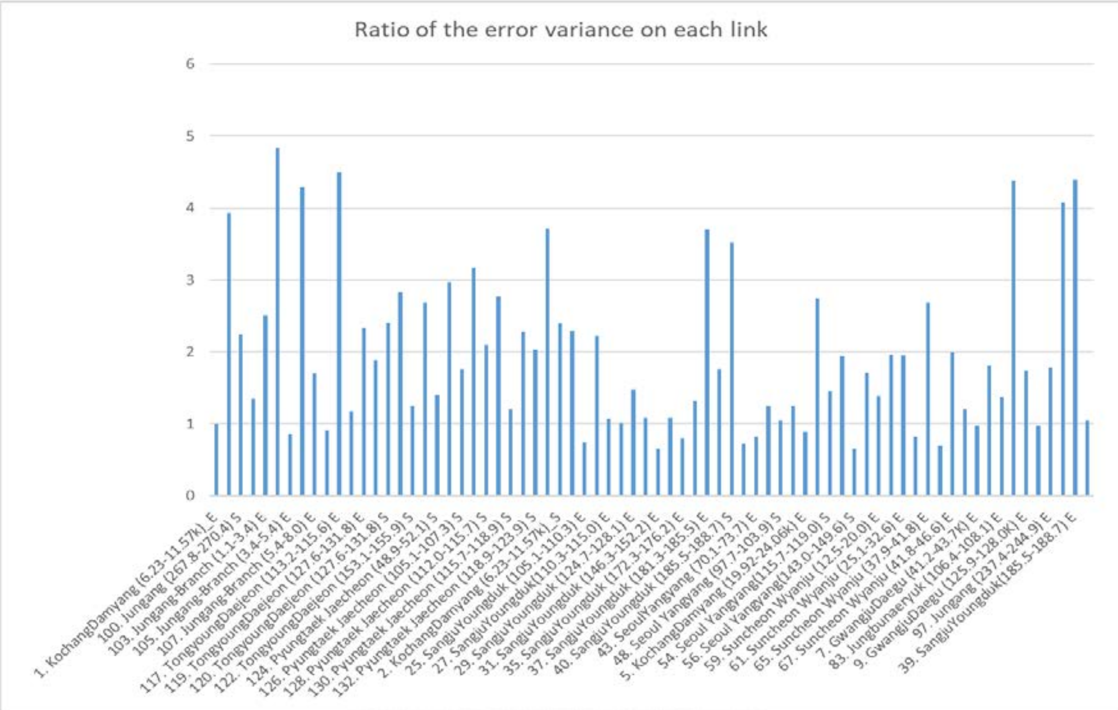

Table 6-5 O-D trip demand depending on transportation in Korea (as of 2013)

		Passenger Car	Bus	Train/ Subway	Highspeed Train	Airplane	Ship	Total
2013	Trips/day	53,413,054	18,580,517	9,820,549	140,055	60,355	36,585	82,051,115
	%	65.1	22.6	12	0.2	0.1	0	100
2015	Trips/day	55,981,759	19,440,211	10,389,324	198,817	59,158	38,168	86,107,437
	%	65	22.6	12.1	0.2	0.1	0	100
2020	Trips/day	57,039,468	19,668,285	11,417,562	194,664	60,017	38,778	88,418,774
	%	64.5	22.2	12.9	0.2	0.1	0	100
2025	Trips/day	56,935,815	19,878,385	11,511,664	197,566	66,765	39,088	88,629,283
	%	64.2	22.4	13	0.2	0.1	0	100
2030	Trips/day	56,211,307	19,646,565	11,322,806	197,033	73,766	39,256	87,490,734
	%	64.2	22.5	12.9	0.2	0.1	0	100
2035	Trips/day	54,907,198	19,132,329	10,876,490	192,867	78,837	39,374	85,227,095
	%	64.4	22.4	12.8	0.2	0.1	0	100
2040	Trips/day	53,207,396	18,469,202	10,325,562	186,749	84,257	39,453	82,312,620
	%	64.6	22.4	12.5	0.2	0.1	0	100

Note: This shows the total trip demand whose raw data consists of daily trips between small zones.
Source: MOLIT (2014)

Applicability of NLS estimation to practice (error propagation by road capacity)

Based on the investigation of the impact on the NLS models of the change in road capacity in the previous chapters, the uncertainty of road capacity, which is mentioned in the research gaps (Section 2.6), can be specified as follows:

(1) The change of a coefficient value (α in BPR function) depending on road capacity
(2) Unclear measurement method of road capacity: measurement location for link capacity and the criteria of measurement (maximum, percentile, average, breakdown traffic flow, etc.)
(3) Difficulty in the measurement of the road capacity for planned links

Of the above uncertainties, the first one could be resolved more or less by presenting various combinations of road capacity and its coefficient in NLS estimation models. However, the second and third uncertainties would still remain. This study identified how much a model with road capacity (i.e. its uncertainty) increases errors in forecasting travel time when the model is used for links which have different road capacities. As mentioned in Section 2.2 and 2.3, the calculation of total travel time in the static traffic assignment is implemented by inputting the variable of traffic flow to VDF after predetermining road capacity and free-flow travel time based on HCM. By reproducing this process, this study tried to confirm the impact of road capacity predetermination on travel time forecasting. In order to identify the impact of road capacity during the process, it was assumed that the observed traffic flow is regarded as future trip demand and that Inv_SPD is future travel time (true value) corresponding to each traffic flow.

Table 6-6 investigates how much the error occurs between the actual and the forecasted travel time in five randomly selected sections, when the model developed by using the road capacity, which is 3,572vph (C_{Korea} in Table 5-6) presented for motorways in 'Korean VDF Manual' (KDI, 2015), is applied to travel time forecasting. When a model estimated on the basis of the large road capacity is applied to the links[17] with small road capacity, the error appears to be large. In the NLS model (FBPR1 in Table 6-6) estimated without considering the geometric features, the means of RMSE and MAPE were 5.9 and 13.4%, respectively. Likewise, the model (FBPR3 in Table 6-6) estimated with the geometric variables produced errors of RMSE 4.2 and MAPE 8.5%. Therefore, this confirmed that road capacity predetermined in NLS estimation models (especially a model without link geometric variables) can cause significant errors in travel time estimation. It can thus concluded that both FBPR1 and FBPR3 are not appropriate in traffic assignment because of the uncertainty of road capacity; this is especially significant for the sections where road capacity changes drastically, i.e. where road geometry could affect traffic flow considerably.

[17] The links analysed in this study would have small road capacity in common because of the impact by tunnels and road geometry, which is similar with the initial case study (Appendix A.4)

Table 6-6 Propagation of errors by road capacity uncertainty

Selected link			FBPR1		FBPR3	
Name	C (Measured)	Obs.	RMSE	MAPE	RMSE	MAPE
56. Seoul Yangyang(143.0-149.6) S	2,221	52	4.167	9.061%	3.004	6.892%
57. Suncheon Wyanju (7.8-12.5) E	2,259	33	6.555	15.869%	4.312	9.394%
100. Jungang (267.8-270.4) S	2,533	34	4.576	8.569%	3.793	5.432%
119. TongyoungDaejeon (127.6-131.8) E	2,645	37	5.835	12.446%	4.321	7.587%
123. Pyungtaek Jaecheon (48.9-52.1) E	2,514	31	8.502	21.042%	5.732	13.341%
Average			5.927	13.397%	4.232	8.529%

Note: ‘a’ coefficients of FBPR1 and FBPR3 are 0.5075 and 0.5895 respectively assuming road capacity is 3,572vph (Table 5-6)

6.2.4. Summary

This study recommends the most appropriate model by comparing the statistical significance and practical application of five representative models selected within OLS, GLS and NLS estimation methods. Firstly, the result of 10-fold cross-validation demonstrates that all four representative models exhibit similar performances to the reference model by the NLS estimation without geometric variables, in addition to securing the spatial transferability. Secondly, the comparison of the accuracy measures of the models including AIC and BIC suggests that GLS estimation models demonstrate more statistical significance than the OLS estimation model. Lastly, the NLS estimation models and the GLS estimation model considering time-series effects are not suitable for traffic assignment because of the uncertainty of road capacity and the difference in data specification respectively. Therefore, this study concludes that FMODEL3-1-3 can be selected as the best alternative model for travel time estimation in traffic assignment when considering its statistical significance, its applicability in practice and the exclusion of road capacity comprehensively.

6.3. Application to transport planning

This section presents the quantitative difference of estimated travel time between existing Korean VDFs and FMODEL3-1-3 (hereinafter named "FModel" in this chapter) selected in this study when the models are applied to various links. In addition to travel time estimation, this section examines how the developed model changes the result of traffic assignment and the benefit estimation in transport appraisal when they are applied to a prospective motorway project plan as link-cost functions.

6.3.1. Impacts on travel time estimation

The specifications of FModel and two Korean VDFs can be seen from Table 6-7. Specifically, two Korean VDFs are suggested as the reference models, one of which is widely used for Korean traffic assignment developed by KDI (2015) and the other was developed based on the empirical data by KOTI (2009)[18]. The specifications of those models can be illustrated as equations (from Equation 6-2 to Equation 6-4).

Table 6-7 Three models for application

Models	Type	FFS	Coefficients					Road capacity
Fmodel	-	122.6kph (estimated)	4.97E-05 (TF)	2.42E-08 (TF2)	8.91E-05 (TR)	3.16E-03 (RISE)	4.87E-03 (FALL)	Not used
KDI (2015)	BPR function	90-105kph (predetermined)	0.55 (α)	2.09 (β)				3,400-4,354vph (predetermined)
KOTI (2009)	BPR function	117kph (predetermined)	0.611 (α)	2.772 (β)				4,000-4,400vph (predetermined)

Note. KDI (2015) recommends FFS as 95.2kph and road capacity as 3,572vph.

$$TT_{FModel}\ (seconds/km) = Exp(3.38 + 4.97 * 10^{-5} * TF + 2.42 * 10^{-8} * TF^2 + 8.91 * 10^{-5} * TR + 3.16 * 10^{-3} * RISE + 4.87 * 10^{-3} * FALL) \quad \text{Equation 6-2}$$

$$TT_{KDI}\ (seconds/km) = \frac{1}{95.2} * 3600 * \left(1 + 0.55 * \left(\frac{TF}{Road\ capacity}\right)^{2.09}\right) \quad \text{Equation 6-3}$$

$$TT_{KOTI}\ (seconds/km) = \frac{1}{117} * 3600 * \left(1 + 0.611 * \left(\frac{TF}{Road\ capacity}\right)^{2.772}\right) \quad \text{Equation 6-4}$$

[18] The model by KOTI (2009) is also added in this section because the model by KDI (2015) would underestimate FFS (95.2kph) for motorways too much.

Figure 6-4 shows three curves of travel time (seconds/km) estimated by those models corresponding traffic flows. The intercept and coefficients used for the curve fittings are the same as illustrated in Table 6-7. All geometric variables for FModel were assumed to be zero for comparison with the KDI (2015) and KOTI (2009) models. The FFS and road capacity values and for the KDI (2015) model are assumed to be 95.2kph and 3,572vph, which are the recommended values in KDI (2015); and both values for the KOTI (2009) model are to be 117kph and 4,400vph, which are suggested as basic values in KOTI (2009). Overall, the estimated travel time by FModel in this study falls between the model by KDI (2015) and the model by KOTI (2009) except for those in low trip demand, which are lower than those by the KOTI (2009) model. In particular, the FFTT of the KDI (2015) model, which is illustrated as the intercept of the curve, is much higher than that derived from this study and that in the KOTI (2009) model.

Figure 6-4 Curves of FModel and Korean VDFs

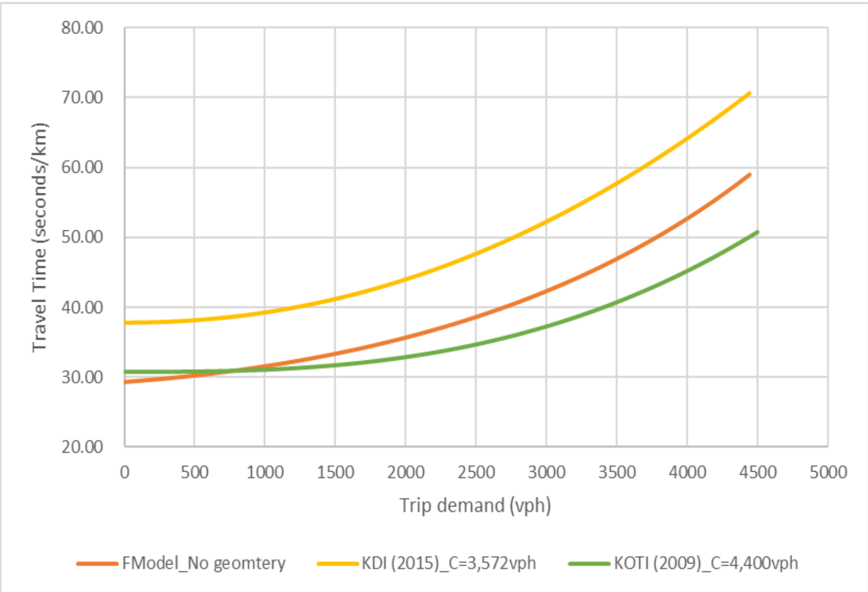

Furthermore, the models' curves shift or bend depending on link geometric features or different road capacity. When geometric features are reflected in FModel, its curve shifts up or down as shown in Figure 6-5 where the geometric features are 627.78m/km for TR, 6.51m/km for RISE and -5.70m/km for FALL[19]. In comparison, the curves of the two Korean VDFs bend upwards when applying the road capacity values of 3,400vph and 4,000vph. This study adopted both values for representing road capacity reduced by link geometry because they are suggested as the lowest limits of road capacity in both models.

[19] The geometric features for this application are the average values of 72 cases in this study (Section 3.5.2).

Figure 6-5 Curve shift by different link geometry and road capacity

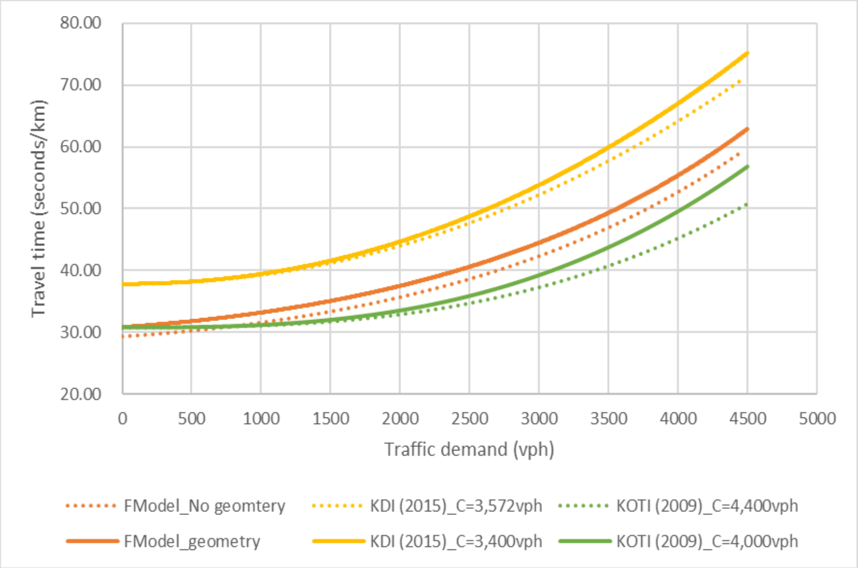

Lastly, these different specifications between models can result in lower or higher travel time estimation. In order to confirm this difference, this study applied the three models to travel time estimation on three hypothetical links having different geometry as illustrated in Table 6-8. It was assumed that the three links have varying future O-D trip demand with the different mean and standard deviation following the normal distribution. Each trip demand on each link was generated as hourly random numbers for 30 days. When each hourly trip demand is allocated to each link, the travel time of each vehicle was calculated using the three models (Appendix A.5.5). The total estimated travel time taken by all vehicles can be calculated by multiplying the estimated travel time and hourly trip demand on each link and then adding them together. Table 6-9 and Figure 6-6 show the difference in the estimated total travel time on each link as per the three different models. Compared to FModel, the KDI (2015) model predicts travel time which is higher by 18% and the KOTI (2009) model predicts a total travel time to be lower by 11%.

To summarise, the three models shows different travel time estimation results. This result is very significant in traffic assignment in that link-cost functions in transport appraisal estimate travel time not only for planned projects but also for existing transport links. When it is assumed that the link cost functions of other transport links are not changed and that there are no motorways nearby, the benefit in a planned motorway project is estimated as greater by FModel than the KDI (2015) model. However, the result could be reversed. The higher estimated travel time on existing motorways as with the KDI (2015) model could exaggerate the benefits of new transport projects (e.g. new motorways, high-speed railways, arterial roads) which compete with existing motorways. Hence, the longer travel time estimation on existing motorways could result in the unnecessary provision of new transport links because of the exaggerated benefit estimation in for example travel time savings.

Table 6-8 Three hypothetical links with different geometric features

	LINK1	LINK2	LINK3
Hourly TF (Random values)	N (1,000, 200^2)	N (1,500, 400^2)	N (2,000, 600^2)
TR	627.78	800	0
RISE	6.51	20	0
FALL	-5.70	0	0
Capacity (vph) for KDI (2015)	3,400	3,400	3,572
Capacity (vph) for KOTI (2009)	4,000	4,000	4,400

Note 1. N (M, σ^2) represents the normal distribution with the mean of M and the standard deviation of σ for 30 days.

2. Both road capacities of 3,400vph and 4,000vph for LINK1 and LINK2 were selected as the lowest values in each model for representing link geometry reducing road capacity.

Table 6-9 Sum of estimated travel times on three links for 30 days by both models

	Total Estimated Travel Time (vehicles*hours/km)		
	FModel	KDI (2015)	KOTI (2009)
LINK1	6,755	8,035	6,332
		19%	-6%
LINK2	11,820	12,912	9,873
		9%	-16%
LINK3	15,572	19,220	14,177
		23%	-9%
Sum	34,148	40,167	30,383
		18%	-11%

Note: Underlined values are percentage changes with FModel

Figure 6-6 Comparison of total travel time on three links

6.3.2. Application to traffic assignment

This study investigated two applications from the perspective of transport economics: the relationship between trip demand and link-cost function, and the impact on traffic assignment of the developed travel time estimation model. The first application reflects real life better than the second one in that trip demand is treated as elastic with regards the total cost of a route. On the other hand, the latter application assumes that the total trip demand is constant over the analysed network, which is in line with the static traffic assignment process.

In the first application, various estimated link costs in microeconomics result in different economic equilibria (Figure 6-7). In order to simplify the analysis, it was assumed that there were no alternative links or that alternative links have higher cost than the analysed motorway link. If trip demand is only dependent on journey time in the link, the equilibrium point between trip demand and journey time changes based on different link cost functions. In Figure 6-7, whilst the equilibrium point can be determined as B from the current Korean link cost function (KDI, 2015), the point moves to C based on FModel. On the other hand, trip demand derived from the KOTI (2009) model is higher than that from FModel. Therefore, it can be said that FModel determined trip demand between the KDI (2015) and the KOTI (2009) model. In particular, it allocates more trip demand on planned and existing Korean motorways links than KDI (2015) model, but less trip demand than the KOTI (2009) one. Without motorways nearby, the feasibility (e.g. benefit-cost ratio) of new motorway projects by FModel would be estimated as higher than by the KDI (2015) model. Consequently, the feasibility analysis could cause the different result.

Figure 6-7 Change in an economic equilibrium from the supply-demand relationship

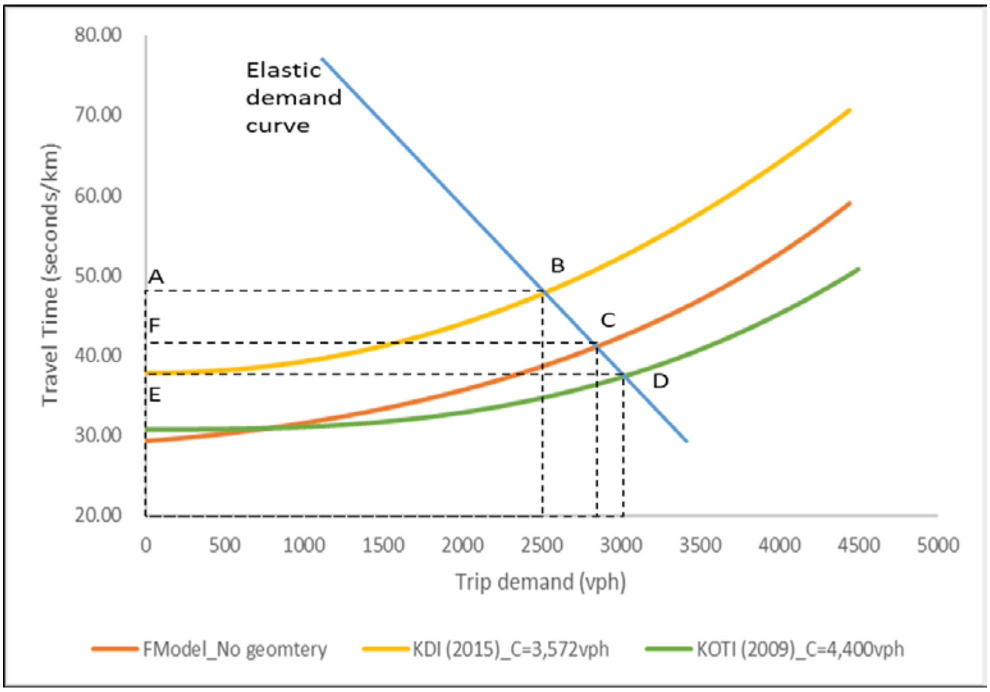

In the second application, the travel time estimation models were applied to quantitative transport appraisal to find how the result of transport appraisal changes depending on the models[20]. Figure 6-8 shows an example of a hypothetical motorway construction plan that bypasses an existing city road. As the city expands, the government is planning to construct a new motorway bypassing the city in order to resolve frequent congestion on the three routes and to prepare for growing trip demand. It is assumed that the new motorway shares only the trip demand of the city road.

Figure 6-8 Example of a local network for application to transport appraisal

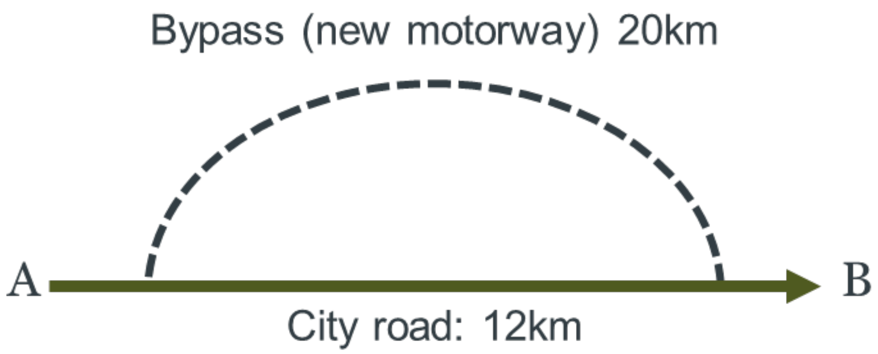

Prior to the construction of the motorway, the government implements transport appraisal as an important decision-making process. Figure 6-9 illustrates four travel time estimation model curves including the travel time estimation model for the city road (hereinafter named "Model_City"). Model_City is assumed as BPR function with FFS=80.7kph, road capacity=2,376vph, α=0.72 and β=2.14 (Equation 6-5), which is illustrated as 'BPR type 16' in Table 2-5. The link geometric features and road capacity for the three models' specifications are assumed to be the same as 'LINK1' in Table 6-8.

$$TT_{Model\_City}\ (seconds/km) = \frac{1}{80.7} * 3600 * \left(1 + 0.72 * \left(\frac{TF}{2{,}376}\right)^{2.14}\right) \quad \text{Equation 6-5}$$

This application assumes that the total trip demand over the entire network is constant. When applying O-D trip demand of 3,000vph to the above-mentioned local network, the Wardrop (1952)'s first principle can find the equilibrium points between the analysed motorway and the city road by using the three models as shown in Figure 6-9. Since the principle assumes that all vehicles have the same travel time between their origin and destinations (Section 2.2.2), the travel time by the trip demand allocated to the motorway is equal to the travel time by the trip demand allocated to the city road. In order to find the trip demand that makes travel time equal, '(3,000-TF)' needs to be applied instead of TF in Equation 6-5 because the sum of trip demand using the motorway and

[20] Although the models are not applied to the nationwide network, but the result of traffic assignment at the local network level could be applicable at a national level.

city road is 3,000vph. The curve of Model_City can be rotated as the solid line in Figure 6-9 and as such the equilibrium points can be calculated as shown in Table 6-10.

Different equilibrium points in the three models change consumer surplus (Figure 6-9), which is closely related to the benefit estimation in transport appraisal (Section 2.2.1). Whilst the total vehicle travel time is represented as ODEI before the construction of the new motorway, it changes into OCFI after sharing some of the trip demand with the constructed motorway by estimating travel time with the KDI (2015) model. In this application, the consumer surplus becomes CDEF. In comparison, when applying the other two models to the calculation, the consumer surplus increases to BDEG for FModel and ADEH for KOTI the (2009) model.

Figure 6-9 Change in consumer surplus depending on three models

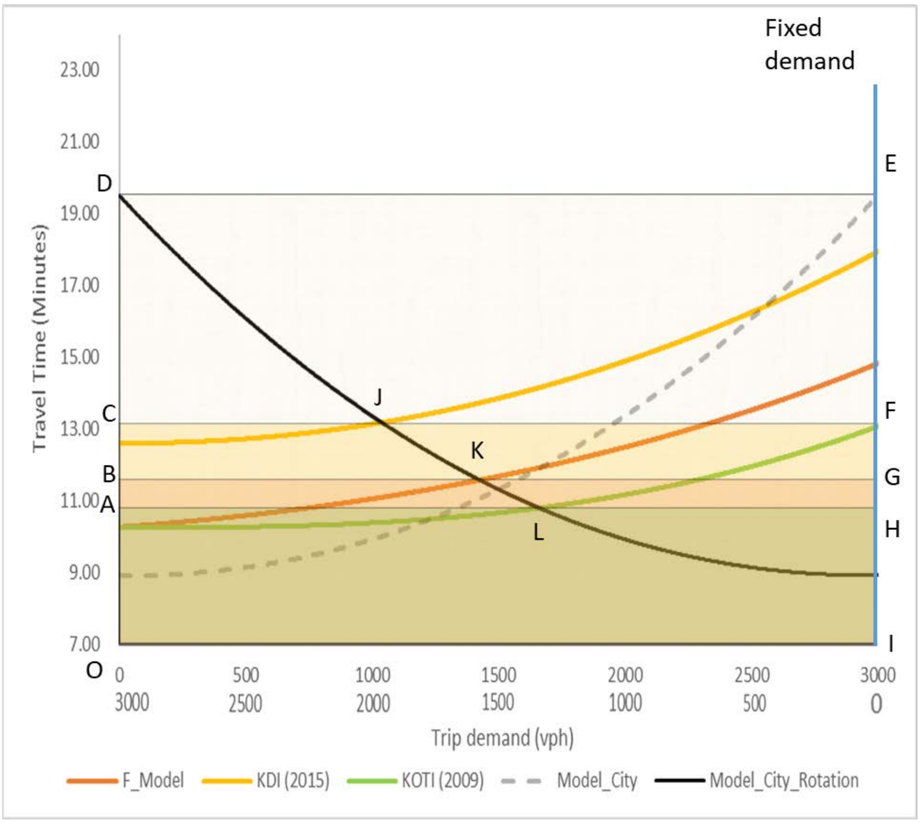

Table 6-10 Equilibrium points between motorway and city road

	Trip demand (vph)	Motorway (vph)	City road (vph)	Estimated Travel time (minutes)	Denotation
FModel	3,000	1,426	1,574	11.6	'K'
KDI (2015)	3,000	1,039	1,961	13.2	'J'
KOTI (2009)	3,000	1,661	1,339	10.8	'L'

Note: 'Denotation' represents the intersection points described in Figure 6-9

Based on this finding, the hypothetical random samples of 30 hourly trip demand following the normal distribution with the mean of 2,500vph and the standard deviation of 500vph were allocated to the local network (Figure 6-8) based on the Wardrop (1952)'s first principle. Table 6-11 summarises the result of traffic assignment and its application to the benefit estimation of vehicle travel time saving in transport appraisal (see Appendix A.5.6). As link cost functions estimate travel time as lower on the motorway as with the KOTI (2009) model, more trip demand is diverted into the planned motorway and as such the benefit of time saving in transport appraisal increases. This result implies that lower travel time estimation attracts more trip demand than comparatively higher travel time. Therefore, FModel in this study could attract trip demand to motorways more than KDI (2015)'s model, which is widely used in Korean traffic assignment, and less than the KOTI (2009) model.

In summary, a link-cost function, which is a travel time estimation model in this study, affects the result of traffic assignment to a significant degree. First of all, it plays a crucial role in determining trip demand on each link, which is a direct influential factor for the calculation of travel time savings benefit in transport appraisal. In addition, trip demand assigned over the entire network as well as its speed are the basis for the estimation of other benefits such as vehicle operating cost savings and environmental improvement such as noise, air quality and greenhouse gas emissions (Appendix A.2.2 and A.3.3)

Table 6-11 Result of traffic assignment by three models

	Do-nothing	FModel	KDI (2015)	KOTI (2009)
Sum of TD_Route3	73,984	43,117	56,269	37,629
Sum of TD_Bypass	-	30,867	17,714	36,355
Total demand	73,984	73,984	73,984	73,984
TT_Route3 (veh*hours)	1,411,798	482,363	723,783	378,493
TT_Bypass (veh*hours)	-	349,870	233,111	388,034
Total vehicle travel time (veh*hours)	1,411,798	832,232	956,894	766,526
Benefit (time savings: hours)	-	579,566	454,905	645,272
Comparison	-	-	-22%	11%

Note 1. TD is the assigned trip demand and TT is the total vehicle travel time.
2. Total trip demand of 73,984vph is randomly produced by the mean of 2,500vph and the standard deviation of 500vph with the assumption of normal distribution.
3. 'Comparison' represents the percentage change with the benefit by FModel.

6.4. Findings

This chapter has explored the application of the developed model to a real world situation. Although the developed travel time estimation models can be used in various areas[21], but this study has focused on its use for traffic assignment and further transport appraisal. Prior to its application to a real world situation, this chapter suggested the most appropriate model in terms of statistical significance and practical applicability. Furthermore, this study demonstrated the application of the selected model to transport planning including traffic assignment, which is one for the motivations of this study.

In Section 6.2, in order to decide on the most appropriate model, this study investigated the statistical criteria after the validation of models by the 10-fold cross-validation method. In particular, from among the linear estimation models, the GLS estimation models are evaluated as statistically better based on the penalized-likelihood criteria including AIC and BIC. In addition, when considering the applicability to reality, this section demonstrated that the uncertainty of road capacity causes the error propagation in travel time estimation and that the time-series data has low utilisation in traffic assignment. Therefore, this study recommended FModel, which reflects the diversity of link attributes, as the most appropriate model in practice.

In Section 6.3, this study showed quantitatively how the selected model affects transport planning compared to existing models. FModel estimates lower travel time as compared with the Korean BPR function (KDI, 2015). On the other hand, the model estimates travel time as higher than the KOTI (2009) model. When applying the three models to travel time estimation with randomly produced trip demand, whilst FModel estimated the total vehicle travel time as lower than the KDI (2015) model and higher than the KOTI (2009) model. Furthermore, it was demonstrated that the model developed in this study can affect the results of transport appraisal. When the randomly produced trip demand was assigned to the hypothetical network plan, three models predicted different equilibrium points on each link and as such they caused various levels of consumer surplus, which is closely related to benefit estimation in transport appraisal. When hypothetical trip demand pairs are allocated to a hypothetical local network, FModel estimates the total travel time savings as higher than the KDI(2015) model by 22% and lower than the KOTI(2009) by 11%. It can be concluded that the adoption of FModel would result in a significant change in Korean traffic assignment and the transport appraisal process.

---

[21] The applied areas of travel time estimation models can be other transport planning activities such as traffic demand management and periodic evaluation of link efficiency and the provision of journey time guidance.

Chapter 7. Conclusion

7.1. Main conclusions

From a microeconomic perspective based on the demand-supply principle, this study started by recognising that there are problems in the transportation investment appraisal process, which are common to many countries. Transportation investment appraisals (e.g. ex ante CBA) aiming at future predictions may involve a variety of errors (Mackie and Preston, 1998). This study focused on one of the reasons for the errors in traffic assignment, which is one of the traffic demand forecasting steps. In static traffic assignment, which is mainly used for allocating O-D trip demand to the relatively wide network over a long term period, VDFs play a role as link-cost functions in calculating the performance of links. Therefore, the detailed investigation of VDF structures became a key issue for this study.

Literature reviews showed that VDFs as travel time estimation models commonly include road capacity and free-flow speed. However, many studies on VDFs used different values for road capacity and free-flow speed for customising the parameter of VDFs. This study paid attention to whether the parameters with the two variables in VDFs can reflect the geometric features of links even though the manuals in many countries defined the values based on the geometric features of a link (USHCM, 2010; MLTM, 2013). In other words, it was examined whether geometric features are able to play a major role in travel time estimation models by replacing road capacity and free-flow speed.

As mentioned in Chapter 3, this study adopted three different statistical estimation methods, two of which are linear (OLS and GLS) and the other nonlinear (NLS), in order to analyse statistically the dataset observed from the 72 motorway sections for one month. Each estimation method considered the relationship between travel time and traffic flow with and without geometric variables, as well as identifying many factors that could affect travel time. In addition, the developed models were statistically verified to identify their feasibility and were compared with each other to assess their accuracy. In order to conclude this study, the research gaps presented in this study (Section 2.6) are recalled as follows;

(1) Uncertainty of FFTT and road capacity in VDFs
(2) Identification of influential factors on travel time (spatiotemporal data analysis)
(3) Significance of link geometric variables in VDFs
(4) Suggestion of new feasible travel time estimation models

7.1.1. Uncertainty of FFTT and road capacity in existing VDF approaches

The first conclusion is that neither road capacity nor free-flow travel time are appropriate variables in travel time estimation models. One of the focuses in the literature review is that road capacity and free-flow speed cannot be pre-determined and included in VDFs because there was no unified concept or measurement method. Many studies have applied the method to the VDF customising process without analysing the statistical impacts of both values (Kalaee, 2010; Huntsinger and Rouphail, 2011; Kim *et al.*, 2014; Kucharski and Drabicki, 2017). There has been little critical perspective on how to measure road capacity and free-flow speed in VDFs, or how much the two values would affect travel time prediction. In this study, the quantitative analysis confirmed the hypothesis that road capacity and free-flow speed are not suitable for travel time estimation modelling and demonstrated how big an impact the predetermination of road capacity and free-flow travel time have on the models and their prediction.

The initial analysis found that road capacity and free-flow travel time could not be fixed at a specific value. Road capacity was derived as different values such as the maximum; 10th largest; and breakdown traffic flow as well as free-flow speed from the different locations of six inductive loop detectors. Values of road capacity and free-flow speed were defined by measuring the discrete change in traffic flows at each detection point, but they could not represent the analysed sections very well. When road capacity and free-flow speed (travel time) with their uncertainty are included in the VDF, it was identified that the uncertainty can be propagated into travel time estimation. In the initial analysis, it was found that the change in free-flow travel time and road capacity greatly influenced the coefficient estimations in the existing BPR function. In particular, the predetermination of free-flow travel time resulted in a reduction in the accuracy of the models.

In Chapter 4 and Chapter 5, the sensitivity analysis was implemented by defining the values of road capacity ranging from 80% to 120% of nominal road capacity in the NLS estimation. In the sensitivity analysis, free-flow travel time can be derived statistically without predetermination in the NLS estimation, so it can be concluded that free-flow travel time does not need to be fixed as a specific value before modelling. With regard to the impact by road capacity, the sensitivity analysis confirmed that the change in road capacity does not affect the accuracy of the model, but it does affect the coefficients of the model. The different values of road capacity do not increase RMSE or MAPE and do not change the other coefficients including those of geometric variables. The only change is the ‘a’ coefficient (‘α’ in BPR function) that is proportional to the value of road capacity. If road capacity is used in travel time estimation models such as existing BPR functions, this correlation between ‘a’ coefficient and road capacity implies that the coefficient needs to be suggested by combining with the recommended values of road capacity in practice.

In addition, in Chapter 6, it was investigated whether the error between the true and fitted values of travel time significantly increases when an NLS estimation model is applied to sections where the actual road capacity is different from the road capacity predetermined for the BPR model estimation. A model by the NLS estimation method with the one-day dataset was derived after fixing the road capacity as 3,572vph for Korean motorways. The average of RMSE and MAPE in the NLS estimation model without geometric features are 5.9 and 13.4% respectively. In one case, RMSE and MAPE are recorded as 8.5 and 21.0%.

In summary, it can be shown that the pre-determination of road capacity can cause inappropriate coefficient estimations and/or the error propagation to the links with various geometric features. As a result, the road capacity in VDFs could cause unreasonable route selections by predicting the costs of the future links differently from what drivers will experience or receive through real-time information systems in the future. Therefore, this study can conclude that the predetermination of road capacity in travel time estimation causes the error in travel time estimation and hence potential inaccuracy in traffic assignment as shown in Section 6.3.

7.1.2. Identification of factors affecting travel time

The second conclusion in this study is that the influential factors on travel time were identified by the panel data across space (cross-sections) and time. Most previous studies on VDF modelling commonly measured road capacity and free-flow speed by incorporating the characteristics of the analysed sections first, and then they customised existing models (e.g. the BPR function) by using observed data for a few sections and for a relatively short time. By contrast, this study examined various types of factors that could influence travel time estimation models by analysing 72 sections for one month (over 147,000 samples). FE modelling using LSDV in Chapter 4 statistically identified cross-sectional and time-related fixed effects, which can be influential factors that affect travel time estimation models.

The six entities of links, routes, brightness, date, day, and weather into what all the samples are classified, had a major impact on the determination of the accuracy of models and the coefficients of independent variables. Namely, from FE modelling it can be said that the panel data from 72 sections for one month have many unobserved fixed effects. In particular, it is noteworthy that the adjusted R^2s as a coefficient of overall model determination increase from 2.5% to 59.4% and 68.2% in pooled OLS linear modelling; FE modelling within the entity of links; and the entity of both links and date respectively. By contrast, adjusted R^2s by FE modelling through setting the other entities of routes, brightness, date, day and weather range from 9.8% to 26.6%. Therefore, it can be concluded that of all the entities analysed, the entity of links has the unobserved fixed effects that most affect travel time estimation. The result of FE modelling motivated this study again because geometric features make up a large part of link characteristics.

7.1.3. Significance of link geometry for travel time estimation

The third conclusion in this study is that geometric features can play a major role in VDF as separated independent variables. Prior to travel time estimation modelling, the initial case study (Section 3.2) illustrates that the selected tunnel motorway section has smaller road capacity than that in KHCM (MLTM, 2013). Road capacity in the initial case study was defined differently as the maximum, the 10th largest traffic flow and breakdown traffic flow. The smaller values of road capacity indicate that traffic characteristics in the tunnel section are affected by link geometric features, including the tunnel environment. In other words, this indicates that tunnel sections form virtual bottlenecks without a change in the number or width of lanes and those bottlenecks would affect travel time estimation and traffic demand forecasting in these sections.

The OLS linear estimation and the NLS estimation methods in this study examined the change in the accuracy of models and the coefficients of the models when geometric features are considered in travel time estimation modelling. Since this study focuses on the travel time estimation of link intervals rather than points, all variables in the analysed models should reflect the change of traffic data and geometric features in the selected cases (links). For example, the dependent variable is the inverse of mean speed between starting and ending points in each selected case, which is equivalent to the travel time per distance. In addition, geometric feature sets of 72 sections were quantified from the road design drawings. The independent variables of geometric features in this study are TR (sum of tunnel lengths per distance), RISE (sum of rises per distance), FALL (sum of falls per distance) and BEND (sum of bendiness per unit distance). The model accuracy and the change in coefficients of independent variables were scrutinised by implementing stepwise selection methods, considering interaction effects and applying transformed functions to models in the regression analysis. A linear function for the geometric predictors in addition to a quadratic function for the predictors of TF in the OLS linear estimation was examined, and likewise, a linear function in addition to the existing BPR function in the NLS estimation was also investigated for the comparison.

Chapter 4 showed the significance of geometric features in travel time estimation models based on one month of data processing. As a result of the OLS linear estimation, it was found that the adjusted R-squared increases from 2.5% to 8.6% by the inclusion of geometric variables in the model. The result would not be negligible when considering large unobserved effects that could affect travel time significantly in FE modelling. When the same dataset is applied to the NLS estimation by iterative calculations, RMSE, which can be used for measuring the accuracy of the NLS estimation, improved from 4.490 to 4.350 after inputting geometric predictors to the model. In addition, the coefficients of all geometric variables in both estimation results are statistically significant at the confidence level of 99%.

Chapter 5 identified the impact of the geometric features based on OLS linear and NLS estimations of a one-day dataset. The one-day observations naturally eliminated some of the effects including weather, day of week and brightness from the one-month dataset. Moreover, the dataset must be ideal for the regression analysis because the values of traffic flow are well distributed on the measured day (24^{th} of September 2018). When comparing the models with and without geometric features in the OLS linear estimation, the adjusted R-squared increases from 33.7% to 42.2%. Likewise, the NLS estimation confirmed that the accuracy of a model can be improved by adding geometric features to the model by reducing RMSE from 3.601 to 3.360. In addition, whilst the coefficients of the three geometric variables of TR, RISE and FALL in both estimations are statistically significant at the confidence level of 99%, the coefficient of BEND does not have high statistical significance (p-value = 0.513).

In summary, both the results of OLS and NLS estimations demonstrate that geometric features affect the travel time estimation considerably based on modelling by one-day and one-month datasets. However, applying the BEND variable to the travel time estimation models requires more careful consideration.

7.1.4. Suggestion of new travel time estimation models

The final conclusion in this study is that new types of travel time estimation models can replace the current VDFs. This conclusion is the comprehensive result of this study which combines the previous three conclusions. Developing feasible models that could be used in practice required testing strict statistical assumptions that previous studies did not consider to any great extent. The one-day dataset was used for modelling in order to minimise impacts on travel time of factors other than geometric features. OLS, GLS and NLS estimation methods were implemented for model development, and the models developed by each method were compared by statistical measures for the optimal model selection. The detailed procedure of model development and its achievements are as follows.

Firstly, the base function for linear estimation was chosen as the quadratic function from the initial analysis that modelled the relationship between the travel time and the traffic flow of one section. The function satisfies the basic condition that link-cost functions should be convex in traffic assignment. In addition, the function was expected to have advantages in that it does not require road capacity and free-flow travel time unlike the existing VDFs as highlighted in the previous section. On the other hand, the feasible models should include geometric features in order to replace the role of road capacity and free-flow travel time.

Secondly, the OLS estimation models were developed by adding geometric variables to the base function without road capacity, but two statistical violations were observed in the models. After selecting various combinations of variables and changing the model by log transformation, the log-linear transformed model with the dependent variables of Inv_SPD and the independent variables of TF, TF2, TR, RISE, and FALL were found to have the best performance. In order for the developed model to be significant in the OLS estimation, the models must satisfy the statistical assumptions. The models were statistically tested to examine whether they met the assumptions, for example by residual plot observations. However, the models developed by the OLS estimation were found to violate homoscedasticity and non-autocorrelation assumptions.

Thirdly, the GLS estimation modelling was introduced to deal with the two violations in the OLS estimation, heteroscedasticity and serial correlation. The GLS estimation for dealing with heteroscedasticity is equivalent to the WLS estimation with different variance and covariance elements of zero in the variance-covariance matrix. In order to treat the heteroscedasticity, variance elements in the variance-covariance matrix of errors were assumed based on various structures provided in the software package of “R” and then the best variance structure was chosen through ANOVA and comparison of AIC and BIC measures. As a result of the estimation, the variance structure with constant variance on each link (different variance between links) showed the highest accuracy (lowest AIC and BIC) of the models. In addition, in order to treat the serial correlation, the correlation between covariance elements in the variance-covariance matrix was assumed in the GLS estimation based on AR and ARMA models in “R”. Time-series analysis suggested that the second-order autoregressive (AR (2)) model would be the most appropriate of different serial-correlation structures through ANOVA. The GLS estimation model derived by combining both the stratified variance structure and AR (2) model showed the most statistical significance with the lowest AIC and BIC measures maximising log-likelihood.

Fourthly, the NLS estimation developed feasible models by adding geometric variables as a linear function for generalising the BPR function. The developed models show better accuracy by smaller RMSE and MAPE than the existing BPR function without geometric variables. The coefficients of the TR, RISE, and FALL variables, except for BEND, were also statistically significant. In addition, the newly developed NLS estimation model has less error propagation than the existing BPR function (model) without geometric variables when both models are applied to the sections with different road capacity.

Finally, this study selected an alternative model by comparing accuracy measures and cross-validation results derived from five representative models by OLS, GLS, and NLS estimations. The analysed models' spatial transferability was verified through 10-fold cross-validation. The cross-validation results confirmed that the other four models have similar overall accuracy measures to the nonlinear estimation method without link geometric features, which is the current approach of the BPR function. However, as concluded in Section 7.1.1, since NLS estimation models contain the uncertainty of road capacity, the models derived by OLS and GLS estimations would be the better alternatives. AIC and BIC measures were used to compare the models derived by linear (OLS and GLS) estimation based on maximising log-likelihood estimation, and RMSE and MAPE were used for comprehensive comparison of the models derived from all three estimation methods. As a result, the GLS estimation model with both link-stratified variance structure and AR (2) time-series correlation structure was evaluated as the best model statistically. However, it is questionable whether the model is practical to use in traffic assignment, especially for static traffic assignment. It is not realistic to survey O-D trip demand every 15 minutes, which is necessary for use of the GLS estimation model with AR (2) in traffic assignment. Therefore, the model that deals with the heterogeneity of links can be an alternative model to current VDFs.

In conclusion, this study suggests the alternative travel time estimation models that have traffic flow and measurable geometric features as explanatory variables based on the statistically detailed investigation of the accuracy and the significance of coefficients in the estimated models. The alternative models can explain the relationship between travel time and road environment in a more generalised way than current VDFs.

7.2. Contributions of the thesis

This thesis developed the feasible travel time estimation models that can improve travel time prediction during traffic assignment and that can also increase the reliability of transport appraisal. From both academic and practical perspectives, this section emphasises the significance of the estimated models by suggesting their key implications are as follows.

Consideration of space-mean values

The estimated models can be used as ‘link’ cost functions in traffic assignment. In other words, the estimated models must represent the information of links. This study considered the role and principle of link cost functions while collecting the data for model estimations carefully. Many previous transportation studies collected the instantaneous traffic data observed from points. By contrast, this study used the space-mean speed from DSRC and the ratio of the link attributes (tunnel length, elevation differences and bendiness) to the total length of each link as variables. It can be expected that this consideration can serve the purpose of a link cost function more effectively than the current studies.

Replacement of FFTT and road capacity in the linear estimation models

This study started from the hypothesis that the predetermination of FFTT and road capacity would adversely affect travel time prediction on the links with different geometry. This was confirmed in this thesis. The linear estimation models that are suggested as alternatives to existing VDFs are expected to reduce the uncertainty of both values by including the various measurement methods. In light of the existing HCM that road capacity is determined by the geometric features, instead of including road capacity as an intermediate variable in the models, the linear models includes the features directly as independent variables. By minimising the unnecessary assumptions (e.g. the predetermination of road capacity) in the regression analysis, the estimated models have higher statistical significance than the existing models.

The applicability of existing VDFs

Although road capacity is inappropriate for estimating travel time, which is one of the main conclusions in this study, it is difficult to assert that existing VDFs are not useful for all links in traffic assignment. This study recommends that the existing VDFs can be used only for basic segments where the change in geometric features is not drastic. In addition, using the existing VDFs by changing the road capacities presented in manuals needs careful consideration because this study demonstrated that a different selection from the road capacity predetermined in the BPR function would cause large errors in travel time estimation. This is in line with the finding that road capacity has a proportional relationship with one of the parameters in the BPR function.

Generalised linear estimation modelling

The estimated models not only focused on the best fitting of the observed data, but also on the statistical justification. This study suggests how to deal with the violations of the statistical assumptions in OLS linear estimation. It was found that traffic data with 15-minute intervals were serially correlated and that the data from 72 different links were not homogeneous. The statistically feasible linearised models are discovered after identifying the violations and assuming different variance and covariance structures of errors. Even though the GLS linear estimation model considering serial correlation would not be practical in traffic assignment, it can imply that the serial correlation can affect traffic data analysis. Therefore, of the two models from the GLS linear estimation, the one by dealing with the heteroscedasticity can be used practically in traffic assignment, whilst the other by dealing with the serial correlation can be academically meaningful.

7.3. Limitation and future work

In spite of the contributions suggested in the previous section, this thesis has some limitations with regard to the data specification used in modelling and the assumption for modelling. This section discusses the limitations of the thesis and their probable solutions in future work.

Consideration of the variable of heavy vehicle percentage

The first limitation of this thesis is that it does not consider the important variable of heavy vehicle percentage or traffic composition due to the difficulty in data acquisition[22]. As mentioned in the thesis, current VDFs commonly include road capacity that varies depending on the heavy vehicle percentage. In other words, because of the interaction between vehicles, the heavy vehicle percentage would affect the traffic characteristics most in modest traffic flows with a small number of lanes. Therefore, the variable needs to be included in travel time estimation models in the future.

Future work is needed to reflect the value of the heavy vehicle percentage in the estimated models. The prerequisite to do so is to observe the heavy vehicle percentage every 15 minutes. As mentioned in Section 3.4, automatic vehicle identification (AVI) in ITS is difficult to use for data collection due to the sparse installation intervals even though AVI can be an easy way to classify vehicle types. Dual inductive loop detectors, which are not installed on Korean motorways, can be the alternative for classifying the vehicle types by identifying the length between axes (Cheevarunothai *et al.*, 2006). The last available option would be the field survey or the data collection from a microsimulation package[23]. After data collection, it is necessary to consider modelling through the interaction with the variable of traffic flow or piecewise modelling.

Definition of trip demand in congested situations

The second limitation of this thesis is that the estimated models would not explain the oversaturated travel time well depending on trip demand in congested situations. This thesis filtered the data of congestion in modelling by defining it as the data with a speed below 60kph. The data analysis means that the models estimated from the data in steady states and near congested states would also explain congested states that cannot be identified by the empirical data measurement because link cost functions in static traffic assignment do not represent spillback or gridlock (Section 2.2.3). For clarifying travel time estimation models in congested states, it would be necessary to define trip demand by connecting measurable traffic data with the congested traffic

[22] This study attempts to minimise the impact of the heavy vehicle percentage by selecting a national holiday for the data analysis when the traffic flow of heavy vehicles is usually low.
[23] Some transportation studies collect or validate the data from a microsimulation package, but it would not be recommended in the empirical data analysis because the microsimulation result is also based on algorithms or models.

flow. Queue length and the difference between incoming and outgoing traffic flows would be influential factors that determine trip demand on a link. However, there would be little consensus of trip demand derivation from traffic data in the field. Although Huntsinger and Rouphail (2011) predicted trip demand of a motorway link from occupancy rates and queue length at inductive loop detectors, it is based on the formula for oversaturated signalised intersections given by May (1990). In addition, the data of occupancy rates cannot be used for model estimations because of its low reliability (Section A.4.1) in Korean ITS.

Future work can be done in order to find how trip demand can be derived from the traffic flow data. Whilst the incoming traffic flow upstream of a link is similar to that of outgoing traffic flow downstream in steady states, it is known that the incoming flow exceeds the outgoing flow once the link is congested. As mentioned in Section 2.2.3, since static traffic assignment does not allow spillback effects in which traffic speed does not increase despite a decrease in traffic flow, it introduces trip demand instead of traffic flow in link cost functions. Namely, although trip demand over maximum traffic flow is a virtual concept in traffic assignment, it is definitely related to traffic flow and its cumulated rate in congested states. Therefore, it is necessary to clarify the relationship between the cumulated traffic flow in the upstream of a link and trip demand on the link. The change rate in the cumulated traffic flow would also be one of the considerations for defining trip demand. The measurement of cumulated traffic flow and its rate requires more accurate observation of queue length and its change, which cannot be done by inductive loop detectors in this study. After clarifying the definition of trip demand in travel time estimation models, it needs to be considered whether to divide the models into two regimes such as piecewise regression analysis because congested traffic characteristic could be based on the different relationships to those examined in this thesis.

Modelling for various road types with the number of lanes

The last limitation of this thesis is that the model estimation was implemented only for 2-lane motorways. This thesis confines modelling to 2-lane motorways due to the data accessibility and it assumes that the developed methodology can be applied to modelling for more diverse road types. However, it is necessary to generalise the developed methodology more. New base functions or different statistical methods might be necessary for modelling in the future. In addition, new variables that could affect travel time on a link need to be included.

Therefore, further research needs to be attempted to apply the established methodology to many types of roads. Whilst the current Korean BPR function suggests separate models that have different parameters with FFS and road capacity depending on the number of lanes even within the same type of roads, it is necessary to consider integrating the models by taking into account the number of lanes as a variable. Moreover, the additional variables for each road type would need to be included in the estimated models. For example, the intersection density and its signal interval in urban roads can be important variables.

In conclusion, this study suggests a new approach to travel time estimation through the case study of Korean motorways. Although the current VDFs are kept simple by defining road capacity and free-flow speed, the possibility of model generalisation is limited by the assumption that all link attributes are included in the two values. Therefore, this thesis can have significance and value in that it proposes extensible models to be developed in the future by encompassing road types and their attributes.

A. Appendices

A.1. Korean motorways

A.1.1. Status of motorways in South Korea

Korean government set the frame of the national arterial roads first in the 1990s, which consists of seven vertical axes and nine horizontal axes (7×9) (MOLIT, 2016b). Afterward, the frame was revised to 7×9+4R which had been combined with the arterial frame in the capital and metropolitan areas (MLTM, 2011a). All motorways (6,415km) are included in the frame and other arterial roads consist of national highways (Table A-1). It was investigated that roads accounted for 81.4% of passenger transportation by the measurement of million·passenger·kms/year and 71.1% of freight transportation by the measurement of million·tonne·kms/year in 2008 (MLTM, 2011c). In addition, it is worth noting that traffic volume of motorways was around 4 times higher than that of national highways between 2011 and 2015 based on the total vehicle kilometres (Table A-2).

Table A-1 Korean arterial road network

(Unit: km, as of 2015)

		Plan	Operation	Construction	Design	Future
	Total	7,266	4,271	743	846	1,406
	Motorway_Subtotal	6,415	4,193	694	846	682
	HIghway_Subtotal	850	78	49	0	723
Vertical Axis	Subtotal	3,606	2,367	132	463	644
	Motorway	3,277	2,348	132	463	334
	Highway	329	19			310
Horizontal Axis	Subtotal	3,066	1,715	446	226	679
	Motorway	2,587	1,686	409	226	265
	Highway	479	29	37		414
Circulation	Subtotal	594	189	165	157	83
	Motorway	551	159	153	157	83
	Highway	43	30	12		

Source: Updated from MLTM (2011a)

Table A-2 Comparison with traffic volume between Korean motorways and highways

	Road type	Length (km)	AADT (veh/day)	VKT (K·veh·km)	VKT per length (K·veh)
2015	**National Motorway**	4,149	48,505	201,247	48.5
	National Highway	12,651	11,991	151,708	12.0
2014	**National Motorway**	4,124	46,403	191,358	46.4
	National Highway	12,653	11,587	146,617	11.6
2013	**National Motorway**	4,114	15,236	186,112	45.2
	National Highway	12,648	11,471	145,080	11.5
2012	**National Motorway**	4,044	43,689	176,682	43.7
	National Highway	12,635	11,176	141,203	11.2
2011	**National Motorway**	3,912	44,276	173,186	44.3
	National Highway	12,823	11,499	147,465	11.5

Source: MOLIT (2016a)

Figure A-1 Korean motorway frame

Source: (MLTM, 2011a)

A.1.2. Design criteria for motorways in South Korea

Table A-3 Minimum width of lane by road types and design speed in Korea

Category			Minimum Width of Lane (m)		
			Rural Area	Urban Area	Small cars only
Motorway			3.50	3.50	3.25
Other roads	Design Speed (Km/h)	Over 80	3.50	3.25	3.25
		Over 70	3.25	3.25	3.00
		Over 60	3.25	3.00	3.00
		Below 60	3.00	3.00	3.00

Source: MOLIT (2015)

Table A-4 Minimum central barrier width by road types in Korea

Category	Minimum Width of Central barrier (m)		
	Rural Area	Urban Area	Small cars only
Motorway	3.0	2.0	2.0
Other roads	1.5	1.0	1.0

Source: MOLIT (2015)

Table A-5 Right clearance by road types and design speed in Korea

Category			Minimum Width of Right Clearance (m)		
			Rural Area	Urban Area	Small cars only
Motorway			3.00	2.00	2.00
Other roads	Design Speed (Km/h)	Over 80	2.00	1.50	1.00
		Over 60 Below 80	1.50	1.00	0.75
		Below 60	1.00	0.75	0.75

Source: MOLIT (2015)

Table A-6 Left clearance by road types and design speeds in Korea

Category			Minimum Width of Left Clearance (m)	
			Rural and Urban Area	Small cars only
Motorway			1.00	0.75
Other roads	Design Speed (Km/h)	Over 80	0.75	0.75
		Below 80	0.50	0.50

Source: MOLIT (2015)

Table A-7 Maximum degree of vertical slope by road types and design speed in Korea

Design Speed (Km/h)	Maximum Degree of Vertical Slope (%)							
	Motorway		Arterial		Collector		Local	
	Flat	Mountainous	Flat	Mountainous	Flat	Mountainous	Flat	Mountainous
120	3	4						
110	3	5						
100	3	5	3	6				
90	4	6	4	6				
80	4	6	4	7	6	9		
70			5	7	7	10		
60			5	8	7	10	7	13
50			5	8	7	10	7	14
40			6	9	7	11	7	15
30					7	12	8	16
20							8	16

Source: MOLIT (2015)

Table A-8 Radius of the horizontal curve by design speed and super-elevation in Korea

Design Speed (Km/h)	Minimum Radius of Horizontal curve (m)		
	Superelevation (%)		
	6 %	7 %	8 %
120	710	670	630
110	600	560	530
100	460	440	420
90	380	360	340
80	280	265	250
70	200	190	180
60	140	135	130
50	90	85	80
40	60	55	50
30	30	30	30
20	15	15	15

Source: MOLIT (2015)

A.2. Cost-Benefit Analysis (CBA) in Transportation

CBA would be firstly used in the US in the 1930s and developed as one of decision making processes for budget investment in the US in 1950s and the UK in 1960s. Afterward, it has been spread to many developed and developing countries. The early CBA did not appraise public projects in terms of regulation but afterward it began to be recognised as a regulatory way (Pearce, 1971; Price, 1999). CBA has a basic concept that a project could be determined if the total benefit by them would exceed the total cost. It is widely used in the decision process of personal affairs, corporate investment and governmental budget allocation. In governmental affairs, it would be used to justify a governmental intervention in an incomplete market (Boardman *et al.*, 2013).

CBA is mainly divided into four types, which are ex ante CBA, ex post-CBA, in medias res CBA and the comparison between ex ante CBA and one of ex post and in medias res CBA. Each type is determined depending on the point when the analysis is implemented. The first three CBAs are conducted respectively prior to, after and in the middle of projects respectively. Therefore, the most useful CBA at least in governmental affairs could be ex ante CBA because the other CBAs would be used after launching projects which are mostly irreversible (Boardman *et al.*, 2013).

CBA could be divided into several phases (Hanley and Spash, 1993; Boardman *et al.*, 2013). To summarize, they could be composed of establishing alternatives, cost and benefit identification, monetization of value including discounting, comparison through sensitivity analysis, and lastly conclusion.

A.2.1. CBA in Many Countries

Hayashi and Morisugi (2000) compared the differences of transportation projects appraisal between five international countries, which are UK, France, Japan, USA and Germany. Although it seems to be necessary to be compared based on up-to-date data of each country, it would be significant in the respect that the comparison explained its own basic appraisal direction well.

The overall planning and investment process of transportation

National governments in most countries would intervene the decision-making process of transportation planning and investment by local governments (authorities or agencies) regardless of the operational responsibility of each infrastructure. Therefore, the transportation projects appraisal such as CBA by the national government seems to have an important role in a planning and investment phase. The five countries investigated by Hayashi and Morisugi (2000) clearly used CBA to decide the priority of projects, and the results of CBA were sometimes complemented by other appraisal methods such as Multi-Criteria Analysis (MCA). Besides, although benefit factors such as travel time savings, vehicle operating cost savings, accident cost reduction and environmental factors seem to be very common, they have developed their own additional benefit factors such as regional development and defined the values of factors by reflecting their social circumstances. It would be noteworthy that they sought improvements by developing new approaches for overcoming the limitation of CBA, as well as by considering and evaluating new benefit factors. With regard to social discounting rate and project life period, they are variable from 3% to 8% and from 20 years to 60 years respectively.

The benefit factors in transportation projects appraisal

According to Hayashi and Morisugi (2000), the five countries defined the values of benefit factors differently. For example, for the value of time, the UK, the USA and Germany defined it by combining the purpose of working and non-working travels, but Japan and France did not estimate the value dependant on the purpose of work. Instead, Japan did the value of holiday higher than that of a weekday. Moreover, when calculating benefits after defining the value of time, four countries other than Germany have adjusted the uniform hourly value of time, but Germany has considered more detailed benefit of time savings based on different values at each time interval. Almost all countries using CBA would reflect the benefit of safety discreetly and there would not be distinctive characteristics in the method to measure the value of safety, which includes using insurance statistics or willingness to pay. However, the values of human life in each country are very variable, which has the range from 0.27million dollar in Japan to 2 million dollars in the USA (Hayashi and Morisugi, 2000). France, Japan and Germany considered environmental impacts in CBA whatever range they have or however values of them are high, but the UK and the USA did not even if they could be considered in another process such as NATA (Hayashi and Morisugi, 2000). Afterward, the UK and the USA included environmental factors in CBA (MLTM, 2011b; DfT, 2018). Regional development impacts would be recognised significantly in every country, but no country did include it as monetary factors in CBA because of the difficulties in measurement or a double counting problem. Instead, Germany include the monetised values related to employment and income changes.

A.2.2. CBA Benefit Estimation in the UK

Transport investment appraisal in the UK

As mentioned in Section A.2.1, many developed countries have their own process of CBA and commonly estimate the impacts by the intervention of a transportation project. In this section, it is necessary to find how to measure the costs and benefits by the intervention. In particular, focusing on the benefits of CBA is important in this study because this study aims to reappraise benefits. Of many countries' decision-making processes, the recent UK CBA was examined because it has a long history and a well-established system.

The UK government publishes Web-based Transport Analysis Guidance (WebTAG) that has been updated periodically. WebTAG includes the detailed process for transport investment appraisals such as methodology, software, modelling and policies. WebTAG introduces not only the measurement for CBA but also the expanded impacts estimation by the intervention comprehensively as the senior responsible officer, the technical project manager, the appraisal practitioner, and the modelling practitioner respectively. Figure A-2 shows the overall appraisal outputs that could be organised by many reports and worksheets.

In addition, "Transport Analysis Guidance for the Technical Project Manager" in WebTAG suggests the detailed appraisal process by dividing the process into three stages. It deals with CBA as one of the processes in the further appraisal at the second stage (Figure A-3). Lastly, many units in "Guidance for the appraisal practitioner" give advice on the overall process of CBA as well as the appraisal of many impacts such as economic, environmental, social and distributional impacts.

CBA in WebTAG

When focusing on "TAG Unit A1.1 Cost-Benefit Analysis", which is the part of "Guidance for the appraisal practitioner", the unit contains the contents about many basic factors for CBA that is originally based on "The Green Book" (HM Treasury, 2003) (Table A-9). All of the benefits and costs for 60 years or more of the appraisal period including investment period should be discounted to the value of the base year, which is currently 2010 in the UK, by using the discount rate suggested in WebTAG.

Transport appraisal results can be shown through many tables including the Analysis of Monetised Costs and Benefits (AMCB), the Public Accounts (PA) table, the Transport Economic Efficiency (TEE) table, and the Appraisal Summary Table (AST). The AMCB table would be the most crucial report for reporting CBA results of them. It summarises lists that can be estimated as monetary values and concludes the overall outputs representing Net Present Value (NPV) and Benefit to Cost Ratio (BCR).

Figure A-2 Appraisal tools and guidance for five types of business cases (UK)

		Appraisal of impacts: Study outputs	Strategic case	Economic case	Financial case	Management case	Commercial case
Guidance available in WebTAG	Stage 1: Option development	Outputs from Early Assessment and Sifting Tool (EAST)	✓	✓	✓	✓	✓
		Options Assessment Report	✓	✓	✓	✓	✓
		Appraisal Specification Report					
	Stage 2: Further Appraisal	Appraisal Summary Table	✓	✓	✓		✓
		Transport Economic Efficiency table		✓	✓		✓
		Public Accounts		✓	✓		
		Analysis of Monetised Costs and Benefits		✓			
		Greenhouse gas worksheet	✓	✓			
		Noise worksheet	✓	✓			
		Air quality worksheet	✓	✓			
		Social Distributional Impact worksheet	✓	✓			
Other guidance & tools		Social Research evidence, guidance and tools	✓				
		Carbon Tool for Local Authorities	✓	✓			
		Value for Money guidance		✓			
		Advice on Public Private Partnership (PPP) and Private Finance Initiative (PFI)					✓
		DfT's Evaluation guidance including evaluation plans and benefits realisation				✓	
		Office of Government Commerce Gateway Review guidance				✓	
		Network Rail's management & control process for enhancements (GRIP)	✓	✓	✓	✓	✓
		Highway Agency's project control framework (PCF)	✓	✓	✓	✓	✓

Source: TAG for the senior responsible officer and the technical project manager (DfT, 2018)

Figure A-3 Further appraisal process for the technical project manager (UK)

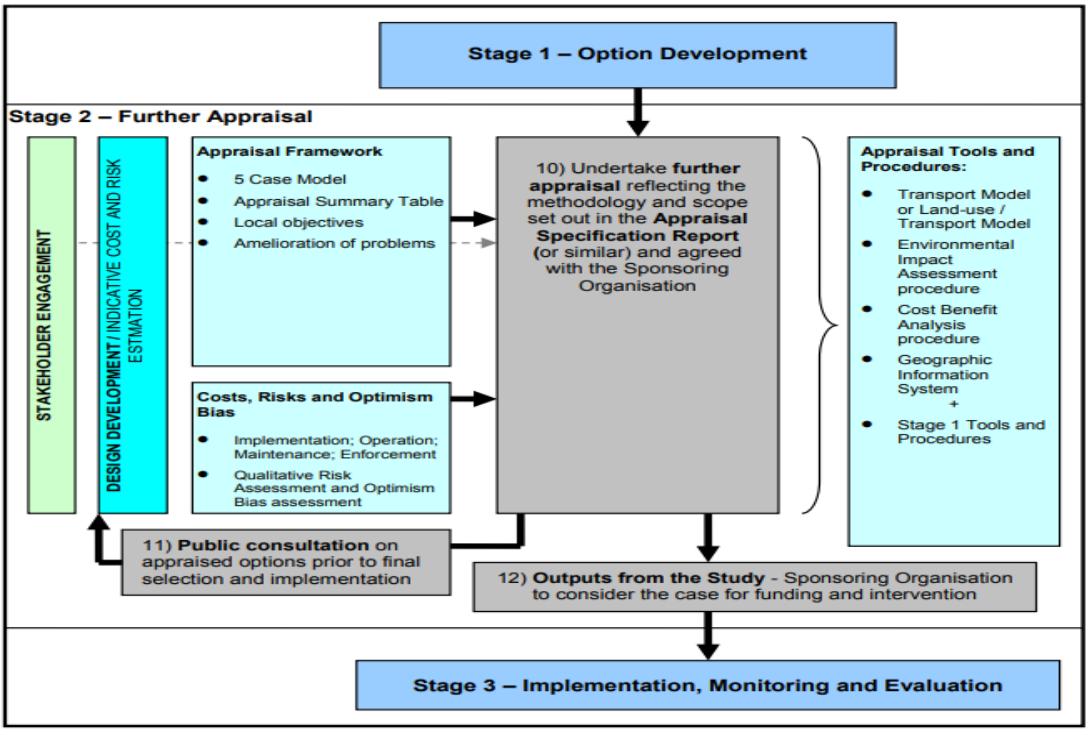

Source: TAG for the technical project manager (DfT, 2018)

Table A-9 Main contents of UK CBA in WebTAG (DfT, 2018)

Comparison	Without vs With Scheme
Appraisal Period	60 years after scheme opening
Discount rate (r_i)	3.5% (0-30 years from current year) 3.0% (31-75 years from current year)
Present Value of Benefit (PVB)	$PVB_{by} = \frac{B_{oy}}{\prod_{i=by}^{oy}(1+r_i)} + \ldots + \frac{B_{oy+59}}{\prod_{i=by}^{oy+59}(1+r_i)}$
Present Value of Cost (PVC)	$PVC_{by} = \frac{C_{by}}{\prod_{i=by}^{by}(1+r_i)} + \ldots + \frac{C_{by+oy+59}}{\prod_{i=by}^{by+oy+59}(1+r_i)}$
Outputs	Benefit-Cost Ratio (BCR) Net Present Value (NPV) NPV/capital cost
Reporting results	Public Account (PA) table Transport Economic Efficiency (TEE) table Analysis of Monetised Costs and Benefits (AMCB) table Appraisal Summary Table (AST)

Note: the subscriptions of 'by' and 'oy' are the base year (currently 2010 in WebTAG) and the opening year of a scheme respectively

Table A-10 AMCB table (UK)

Noise		*(12)*
Local Air Quality		*(13)*
Greenhouse Gases		*(14)*
Journey Quality		*(15)*
Physical Activity		*(16)*
Accidents		*(17)*
Economic Efficiency: Consumer Users (Commuting)		*(1a)*
Economic Efficiency: Consumer Users (Other)		*(1b)*
Economic Efficiency: Business Users and Providers		*(5)*
Wider Public Finances (Indirect Taxation Revenues)		*- (11) - sign changed from PA table, as PA table represents costs, not benefits*
Present Value of Benefits (see notes) (PVB)		*(PVB) = (12) + (13) + (14) + (15) + (16) + (17) + (1a) + (1b) + (5) - (11)*
Broad Transport Budget		*(10)*
Present Value of Costs (see notes) (PVC)		*(PVC) = (10)*
OVERALL IMPACTS		
Net Present Value (NPV)		NPV=PVB-PVC
Benefit to Cost Ratio (BCR)		BCR=PVB/PVC

Note : This table includes costs and benefits which are regularly or occasionally presented in monetised form in transport appraisals, together with some where monetisation is in prospect. There may also be other significant costs and benefits, some of which cannot be presented in monetised form. Where this is the case, the analysis presented above does NOT provide a good measure of value for money and should not be used as the sole basis for decisions.

Source: "Appraisal tables" in WebTAG (DfT, 2018)

In addition, it would be necessary to examine the principle of benefit quantification and valuation so that benefits in this study should be reappraised with sufficient grounds from the existent CBA result. Benefit factors for CBA, which would be listed in AMCB table (Table A-10), are noise, local air quality, greenhouse gases, journey quality, physical activity, accidents, economic efficiency and wider public finances.

Economic efficiency and wider public finances

"TAG unit A1.3 user and provider impacts" in WebTAG classifies the benefits about economic efficiency into values of travel time savings (VTTS), vehicle operating costs (VOC), reliability, impacts on transport providers and impacts on indirect tax revenue. In particular, the impacts by VTTS and VOC are described in detail because they would occupy a great part of the whole benefit. Both impacts are recorded in the TEE table and they are also recorded in the AMCB and AST table. At the same time, user charge and costs during construction and maintenance would be considered. These four impacts are divided by beneficiaries, which are non-business users (for commuting and other) and business users. In addition, impacts on private sector provider and other business would be predicted. Lastly, the change in indirect taxation revenue of the government by fuel costs, fare and charges and non-fuel operating costs would be reflected in the PA table and be recorded in the AMCB and AST table.

Another essential step for appraising these impacts is the valuation of the benefits. "TAG unit A1.3 user and provider impacts" in WebTAG suggests the valuation technique for VTTS and VOC of the economic efficiency benefits as mentioned above. Table A-11 shows the methodology of converting the impacts of VTTS and VOC to monetary values. The valuation of VTTS would be suggested by willingness to pay (WTP) and cost saving approach (CSA), which are classified into two main purposes of business and non-business. In addition, the valuation of VOC would be based on the statistical analysis dependent on the average speed about each vehicle type. The unit of VTTS is expressed in money (£) per hour and that of VOC is in money (pence) per km.

Environmental factors

"TAG UNIT A3 Environmental Impact Appraisal" in WebTAG defines the process appraising the impacts quantitatively and qualitatively, which are noise, air pollution and greenhouse gases, landscape, townscape, biodiversity, heritage and the water environment (DfT, 2018). It classifies them into two main groups, one of which is dependent by the traffic flow data and the other one is dependent by environmental changes in the area surrounded by a project. In particular, the three impacts, which are noise, air pollution and greenhouse gases, could be emphasised in CBA because they can be estimated quantitatively and the monetary valuation technique of them would be established well. Table A-12 summarises the core contents about the impacts appraisal including quantification and valuation.

Table A-11 Valuation of VTTS and VOC in UK

	Impact	Guideline or Document	Methodology of Valuation	Marginal monetary values
VTTS	Values of working time per person	ITS Leeds (2013) 'Valuation of Travel Time Savings for Business Travellers: Main Report', Prepared for the Department for Transport TAG Unit M4 – Forecasting and Uncertainty TAG Data Book Table A1.3.1	Businesses excluding professional and freight drivers: Willingness-To-Pay (WTP) based on stated preference evidence Professional and freight drivers: Cost Saving Approach (CSA)	Continuous function for car and rail employer's business only: $VTTS = \frac{U}{\left(1+e^{\frac{x_{mid}-D}{k}}\right)}$, where U, X_{mid}, k are suggested parameters and D is travel distance(independent variable) Values of other workind time by modes such as goods vehicle, taxi, underground are suggested in TAG Data Book
	Values of non-working time per person	ITS Leeds (2015) and Accent for DfT: 'Provision of market research for value of travel time savings and Reliability: Phase 2 Report'. TAG Data Book Table A1.3.1	WTP by using national average values (e.g. income)	Value of perceived cost (market price, 2010) Commuting: 9.95 £/hour Other: 4.54 £/hour
VOC	Fuel operating costs	HMT supplementary Green Book guidance National Atmospheric Emissions Inventory (NAEI)	Fuel consumption function : $L = (a + b \cdot v + c \cdot v^2 + d \cdot v^3) / v$, where v is speed and a,b,c,d are parameters The parameters for the function are the same with those in NAEI Vehicles proportion, fuel efficiency improvement and fuel prices in the future are considered	The fuel cost function (same as fuel consumption function) is suggested in TAG Data Book: $L = (a + b \cdot v + c \cdot v^2 + d \cdot v^3) / v$, where L= fuel costs (pence/km), v = average speed (km/h), and a, b, c, d are parameters by vehicle categories
	Non-fuel operating costs	EEA Division of DoT (1990-91) 'Review of Vehicle Operating Costs in COBA' DfT (2001) 'Transport Economics Note'	Costs are almost constant over the forecast period, but slight changes in each year are suggested in TAG Data Book	Non-fuel operating costs function C = a1 + b1/V where, C is cost (pence/km), V is speed (km/h), and a1, b1 are parameters by vehicle types (b1 is only for working vehicles)

Source: Adapted from "TAG unit A1.3 user and provider impacts" in WebTAG (DfT, 2018)

Table A-12 Impacts appraisal on noise, air quality and greenhouse gases in UK

Impact		Guideline or Document	Quantification or Estimation	Marginal monetary values
Noise		Noise and Vibration (DMRB 11.3.7) Calculation of Road Traffic Noise (DoT, 1988) Environmental noise: Valuing impacts on: sleep disturbance, annoyance, hypertension, productivity and quiet (Defra, 2014) TAG Data Book Table A3.1	Noise level prediction considering a distance, layout, traffic flow, etc. Number of noise exposed people prediction (average household has 2.3 persons) $L_{Aeq,16h} = L_{A10,18h} - 2dB$	Defra's noise modelling tool (dose-response functions) Risks: sleep disturbance, amenity, AMI, stroke, dementia Noise threshold for valuation: 45dB to 81dB $L_{Aeq,16h}$
Air Quality	Local Air Quality PM10 (Particulate matter less than 10μm aerodynamic diameter) NO2 (Nitrogen dioxide)	Air Quality (DMRB 11.3.1) Highways Agency's Interim Advice Note (IAN) 170/12 Group on Costs and Benefits (Air Quality) (IGCB(A)) HMT supplementary Green Book guidance TAG Data Book Table A3.2	Local air quality for PM_{10}, NO_2 Band division: 50 m, 50-100m, 100-150m, 150-200m from link centres Calculation of annual mean PM_{10}, NO_2: at 20m, 70m, 115m, 175m from each link centre Calculation of the number of properties exposed on PM_{10}, NO_2	Valuation through damage cost and marginal abatement cost (MAC) approach PM_{10}: damage cost NO_2: damage cost + MAC about emissions exceeding EU NO_2 annual limit value
	Regional Air Pollution oxides of nitrogen (NOx) and carbon dioxide (CO2)		Impact assessment at a national level by using simplified traffic model (e.g. COBA and TUBA)	
Greenhouse Gases		The Climate Change Act 2008 "Carbon budgets" every five years Air Quality (DMRB 11.3.1) TAG Data Book Tables A1.3.8, A1.3.9, A1.3.10, A1.3.11, A3.3, A3.4	Fuel consumption prediction by vehicle types and conversion to CO_2e emissions Separation of the traded sector (e.g. emission by electric vehicles) to the non-traded sector (e.g. emissions by petrol, diesel consumption)	Valuation for the non-trade sector: MAC approach per kg·CO_2e tonne published by Department for Energy and Climate Change (DECC) Valuation for the trade sector: reflection in the purchase price

Source: Adapted from "TAG UNIT A3 Environmental Impact Appraisal" in WebTAG (DfT, 2018)

A.2.3. CBA limitation or difficulties

Issues about the selection of benefit and cost factors

When considering benefits and costs in CBA, the selection of them is a very important phase that could depend on the result of CBA. According to who are the main agencies of CBA, the range of benefits and costs could be different. Local authorities want to consider the benefits only for their residents, not ones for adjacent or global area residents (Boardman *et al.*, 2013). Likewise, local authorities who are given subsidies by the central government tend to want to consider only their own costs that exclude subsidies even if a guideline or manual in the central government seems to control the misbehaviour when allocating budgets. There have been also many critical opinions that CBA only emphasised on the economic values (Price, 1999).

In addition, although the current benefit and cost factors in CBA could be said to be defined extensively, there are many opposite views that crucial factors should be included in CBA. Those that give fewer impacts on human beings do not tend to be considered. Environmental effects could be one of the representative examples. From the point of view of politicians, some factors which have a negative impact on their voters would sometimes be ignored. There could be CBAs which do not include benefit and cost factors because the demonstration about cause-and-effect relationships would be obscure and the indicators of factors could not be established easily (Boardman *et al.*, 2013).

Issues about the quantification of benefit and cost factors

Boardman *et al.* (2013) stated that the quantification of benefit and cost factors would be very difficult; especially in the CBAs of unusual, complex and opinions-divided projects. They also asserted that opponents to CBA such as environmentalists should change their perspectives because rationality could not be based on emotional or ethical reasons. If benefit and cost factors could be identified but could not be quantified, they could not but be excluded in CBA.

Although those factors passed two phases, which are identification and quantification, there would be another important monetization of value left to include benefits and costs in CBA. It is known that some agencies deny using CBA because the monetization of environmental and other social effects is not clear (Boardman *et al.*, 2013). The value of money for each benefit or cost factor in many countries is calculated based on investigation such as statistics or surveys for willingness to pay, but is sometimes debatable because life values and environmental effects could not be converted to money simply through statistics or surveys. In the case of the environmental benefit, monetary values were not established until 1995 (Price, 1999). Nevertheless, it is necessary to monetise the identified values in order to include them in current CBAs. It would originate from the principle that benefits should match with costs; that is, inputs as a monetary value.

Issues about inaccuracy of traffic demand forecasts

Flyvbjerg et al. (2005) pointed out the inaccuracy of traffic demand forecasts by illustrating 210 transportation projects in 14 countries, which include 183 road and 10 rail projects. Although the trip demand for road projects seems to be forecasted more accurately than that of rail projects, over half of the road projects had over ±20% error between the actual and forecasted demand. With regard to underestimation of traffic demand forecasts, it could cause unintended traffic congestion before the project life period assumed in CBA. However, a bigger problem could be an overestimation of traffic demand forecasts because it causes negative recognition about transportation investment and public criticism about wrong budget allocation in the general trend that welfare budget needs to increase more and more. According to Korean National Assembly (2017), it is examined that actual traffic of 23 motorway road projects newly constructed after 2000 recorded only 60% of the forecasted traffic.

A.3. CBA in Korea

A.3.1. History and significance of CBA in Korean transportation projects

CBA in National Finance Act (Republic of Korea, 2016b)

CBA is used for the preliminary feasibility assessment in National Finance Act (2016), which was introduced first in 1999. CBA in National Finance Act (2016) is now applied to all projects which are invested by national budget and whose total costs are over 50B won (45M $). The projects consist of not only ones by the national government but also ones by local governments. In the case of the projects by local governments, CBA would be implemented about only the projects that satisfy both conditions which are that total cost of the project is over 50B won and that the subsidy for it by the national government is over 30B won. According to KDI (2008a), transportation projects occupy around 70% of 372 projects from 1999 to 2008, which includes 165 road, 74 railroad and 23 port projects (Table A-13). The result of CBA in this system is directly connected to the budget allocation, it has seemed to be recognised the most important compared to other results of CBAs.

Table A-13 Preliminary feasibility assessment by project types in Korea

(Unit: case)

Year	Road	Railroad	Port	Culture & Tourism	Water Resources	Others	Total
1999	11	2	1	3	1	1	19
2000	11	7	5	2	1	4	30
2001	20	14	1	5	0	1	41
2002	9	8	2	2	5	4	30
2003	11	7	3	5	5	2	33
2004	24	13	1	2	3	12	55
2005	11	6	2	1	3	7	30
2006	27	11	3	6	1	4	52
2007	30	4	1	1	1	8	45
2008	1	2	4	3	2	15	37

Source : KDI (2008a)

Note: Others could include many projects such as welfare, R&D, IT

CBA in National Transport System Efficiency Act (Republic of Korea, 2017)

National Transport System Efficiency Act (2017) is prescribing using CBA as a mandatory requirement of transportation agencies and planners, which is called “appraisal of investment about the development of public transportation infrastructure”. Korean Ministry of Land, Infrastructure and Transport (MLTM) stipulated the act first in 1999, but it was not mandatory at that time. After 2013, it has been mandatory about the projects whose total costs are over 30B won (27M $) implemented by public agencies or public-private partnership.

CBA in Construction Technology Promotion Act (Republic of Korea, 2016a)

Construction Technology Promotion Act, which was called “Construction Technology Management Act” until 2014, seems to introduce CBA as a form of feasibility investigation in 2000. The act prescribes procedures of construction projects, so CBA seemed to be recognised as one of those procedures. The projects which are dependent on this act are those which total cost is over 50B won (45M $) same as those in CBA for preliminary feasibility studies in National Finance Act (2016). Although the CBA was stipulated to be implemented several years before major budget allocations, it did not play an important role in Korea because it could not affect budget allocations in actual cases. Therefore, CBA by the agencies of projects in the act would have lost its prestige increasingly because they intend to overestimate the benefits of projects and to enhance the feasibilities of projects.

Ex-post CBA in Construction Technology Promotion Act (Republic of Korea, 2016a)

The abovementioned CBAs are Ex-ante feasibility analyses, but there is Ex-post CBA in Korea. Construction Technology Promotion Act also prescribes Ex-post CBA, as well as Ex-ante CBA. All agencies that completed projects whose total costs are over 30B won (27M $) should implement post evaluation as a form of Ex-post CBA within 5 years after completion of each project. The post evaluation includes the comparison between Ex-ante CBA and Ex-post CBA. However, Ex-post CBA would not be concrete because it does not include evaluation of benefits which are analysed in the Ex-ante CBA other than traffic demand forecast, even if it compares total costs and examines the advocacy of residents and the satisfaction level of users such as the changes of population, employment, Gross Regional Domestic Product (GRDP) and land price.

A.3.2. The procedure of Korean CBA

The feasibility analysis in Korea is the system that examines the justification of large projects and has the purpose of enhancing the governmental finance efficiency through the careful launch of new large-scale projects by mainly using CBA. The guideline for feasibility analysis has the contents that consist of an introduction, the fundamental data analysis, cost forecast, traffic demand forecast, benefit calculation, economic analysis, financial analysis including public-private partnership, policy analysis and overall estimation (KDI, 2008b).

Fundamental data analysis

It has the important process such as reviewing the relation with a higher ranked plan and setting the alternatives. The alternatives include routes, the scale of the project and construction plan, as well as diverse scenarios determined by nearby development plans (KDI, 2008b).

Prediction of the cost of road projects

Planners should consider detailed cost or the average cost of the construction. It is mainly based on the past data of actual cases and it is predicted proportional to the width of lanes in the case of other road types. It can be predicted after reflecting the uniqueness of the project if reasonable data would be suggested (KDI, 2008b). The cost of projects could be predicted more accurately than the benefit because it is based on the past accumulated data of construction projects and it does not seem to be important because it would be finally determined by passing several stages such as bids as a principle of competition, which mostly resulted in the cost reduction.

Economic impact analysis

All benefits and costs should be discounted to the present value by using discount rate in the process of economic analysis because they happen at different periods. The total period of analysis is normally 30 years, and the Benefit-Cost (BC) ratio, Net Present Value (NPV) and Internal Rate of Return (IRR) are derived (KDI, 2008b).

Financial analysis

This stage includes public-private partnership, mainly in the case which has over 1 of BC ratio. Although the result of financial analysis does not meet the profit rate which private sectors require, the financial feasibility would be sometimes attained through the public budget support (KDI, 2008b).

Overall estimation

The overall estimation is completed after adding economic analysis to policy analysis, which is composed of the balanced development between regions, the policy consistency and drive, the risk factors of a project and other unique factors of a project. They are quantified by using the method of Analytic Hierarchy Process (AHP), where decision makers participate (KDI, 2008b).

A.3.3. The benefit factors in Korean CBA

In this section, the benefit factors, which are used in CBA for Korean Preliminary Feasibility Analysis by National Finance Act, will be examined. Korean preliminary feasibility analysis seems to be recognised as the most important method of all CBAs in Korea because it has an essential role in budget allocation. The benefit factors in Korean CBA could be classified into two groups: direct and indirect. In road project analysis, the direct benefits include vehicle operating cost savings, travel time savings, accident cost savings, increased pleasure, improvements in punctuality, improvements in reliability. The first three benefit factors are quantified and reflected in CBA, but others are hardly being considered in CBA because they could not be quantified. The indirect benefits include environmental impacts (pollution and noise) cost savings, regional development, expansion of markets, regeneration in regional industrial structures. The only first benefit factor is quantified and reflected in CBA, but others are not.

Vehicle Operating Costs (VOC)

VOC consists of fuel consumption, engine oil, tyres abrasion, maintenance and depreciation in Korean CBA. Fuel consumption, which is the largest percentage of VOC, is calculated related to vehicles' velocities. The methodology for calculating the current fuel consumption was based on the research "Establishment of road projects investment analysis method" by Korea Research Institute for Human Settlements (Krihs) in 1999. Fuel consumption changes dependant on vehicle types and speeds are examined by selecting representative vehicle types and testing to drive. The price was converted into that at the time of 2007. The distinguishing thing is that the fuel

Figure A-4 Overall vehicle operating costs (KRW/km) in Korea

(Price in 2007)

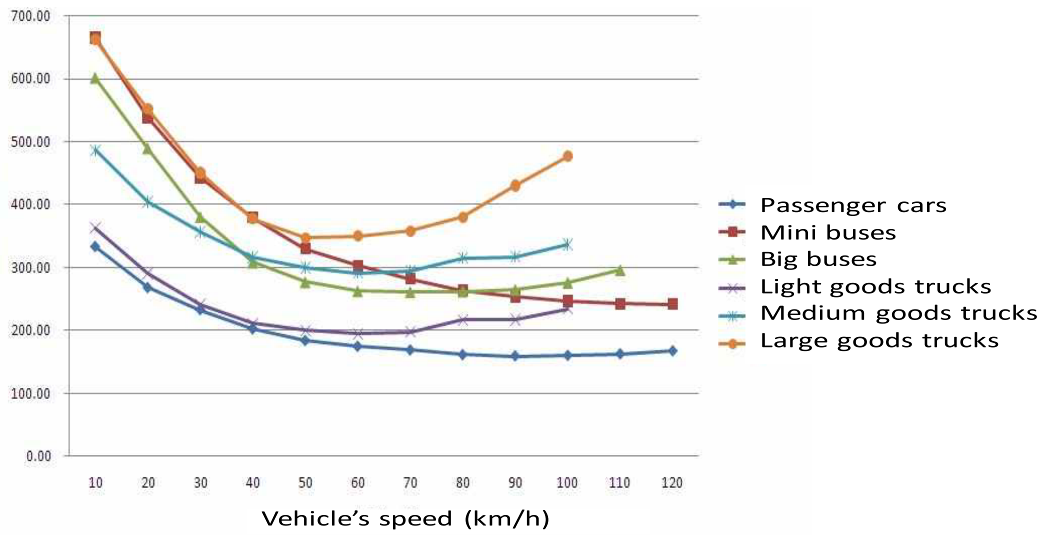

Source: KDI (2008b)

consumption of passenger cars is only based on petrol in Korea. Other costs other than fuel consumption are based on the research by Weille (1966) and Krihs (1999). Each cost is monetised per a distance (km) and suggested as tables by vehicles' speed, not equations. VOC has the lowest value at the speed of 90km/h for passenger cars, 120km/h for minibuses, 70km/h for big buses, 60km/h for light and medium goods trucks, and 50km/h for heavy goods trucks (Figure A-4).

Travel time savings

Travel time savings in Korean CBA are directly related to the purposes passing roads affected by a project. In general, most countries divide the value of time into many categories such as working and non-working purposes. When calculating the working value of time in Korean CBA, wages and other relevant expenses that are paid for each group of employees from the viewpoint of employers could be considered, so the value of time is usually higher than the level of wage in each group. In the case of the non-working value of time, the value in Korean CBA was examined by the method of Stated Preference (SP). The ratio of non-working value to working value is suggested by 32.7% for car passengers and 16.3%[24] for bus passengers (KDI, 2008b). Another element for predicting travel time savings is the ratio of working travelling volume to non-working travelling volume in the trip assignment. The ratio was suggested differently dependant on analysed regions from the fifth edition of guideline of Korean CBA (KDI, 2008b). The regions are classified into six areas and the guideline suggests seven ratios including the travelling volume through the entire area (Table A-14).

Table A-14 Average value of time per vehicle (entire area) in Korea

(Price in 2007)

	Passenger cars		Buses		Goods vehicles	
	Working	Non-working	Working	Non-working	Working	Non-working
Person	0.44	1.11	2.35	7.63	1.00	0.00
VOT (KRW/person)	18,626	6,091	10,228 (driver) 18,626 (passenger)	3,036	16,571	-
VOT (KRW/veh·hr)	8,245	6,744	35,401	23,161	16,571	2,341
Average VOT(KRW/veh)	14,990		58,561		16,571	

Source: KDI (2008b)

Traffic accidents reduction benefit

Korea has had more vehicles as the economy has grown steadily in recent decades. The traffic accidents have increased proportional to the rise of registered vehicles even if the recent statistics

[24] The percentage means the ratio of non-working value in bus passengers to working value in car passengers.

shows that the number of death persons per vehicle tends to decrease continuously. Therefore, the traffic accidents reduction benefit is included naturally in Korean CBA similarly with other countries. The guideline states that the accident costs in Korean CBA include costs for medical treatment, the loss of production by the victims of accidents, physical and mental damage, and administrative fees by the police and insurance company, as well as so-called cost for mitigating PGS (Pain, Grief and Suffering). The accident rates due to road types, which are motorway, national highway, provincial road, metropolitan road and county road above suggested, are considered by “The Statistics of Road Accidents” of the Korean Police Agency (2008) and the cost of each accident is calculated by “The Analysis and Assessment of Road Traffic Accidents” of the Korean Road Transportation Safety Corporation. For example, the cost for each death by a traffic accident is suggested as 527.4 million KRW, the cost for each injury is as 21.6 million KRW, the cost for each number of accidents is as 41.6 million KRW.

Environmental costs reduction benefit

Environmental costs by transportation projects in Korean CBA are defined as atmospheric pollution and damages by noises. Other impacts such as ecological damage are considered in the process of Environmental Impact Assessment (EIA) by environmental agencies. Atmospheric pollutants arise from vehicles’ emissions, which include CO, CO_2, HC, NO_X and PM, and noises are mainly caused by vehicles. They are dependent on elements such as a vehicle’s types, fuel types, speed, and road conditions in Korean CBA. Korean CBA guideline stipulates abovementioned five pollutant emissions per distance (km) with the speed of each vehicle’s type and the amount of cost for each pollutant as a table (Table A-15).

Table A-15. Cost of reducing atmospheric pollutants in Korea

Pollutant Type	CO	HC	NOx	PM	CO2
Cost (KRW/kg)	7,877	9,155	9,477	30,941	42.4

Source: KDI (2008b)

A.4. Initial case study

A.4.1. Case selection and Data collection

Initial case selection: 'Songsan (E) Tunnel' section in "Seoul-Chuncheon Motorway"

The motorway route selected for an initial study is Seoul-Chuncheon Motorway (Figure A-5), which was constructed in 2009 by a public-private partnership. Seoul is the capital city of Korea and Chuncheon is one of the main cities in Gangwon Province, which is the eastern area of Korea. As Gangwon Province has many attractive places for tourists, a lot of traffic passing through this route aims for the tourism and congestion would tend to happen on weekends or holidays. The total length of the motorway is 61.4km and there are nine interchanges including the starting and ending points. This road has 41 tunnels and 103 bridges because it penetrates mountainous terrain. The Average Daily Traffic (ADT) is 40,046 veh/day as of 2016, which is the traffic volume corresponding to four lanes by 12-hour observation. The enforcement speed limit of this route is 100kph. The number of lanes in this motorway is eight from the starting point to 1.9km, six from 1.9km to 14.9km, and four from 14.9km to the ending point (61.4km). The recent heavy vehicle percentage of this motorway is 18.1% measured from Road Traffic Survey (2016).

Figure A-5 Initial case location

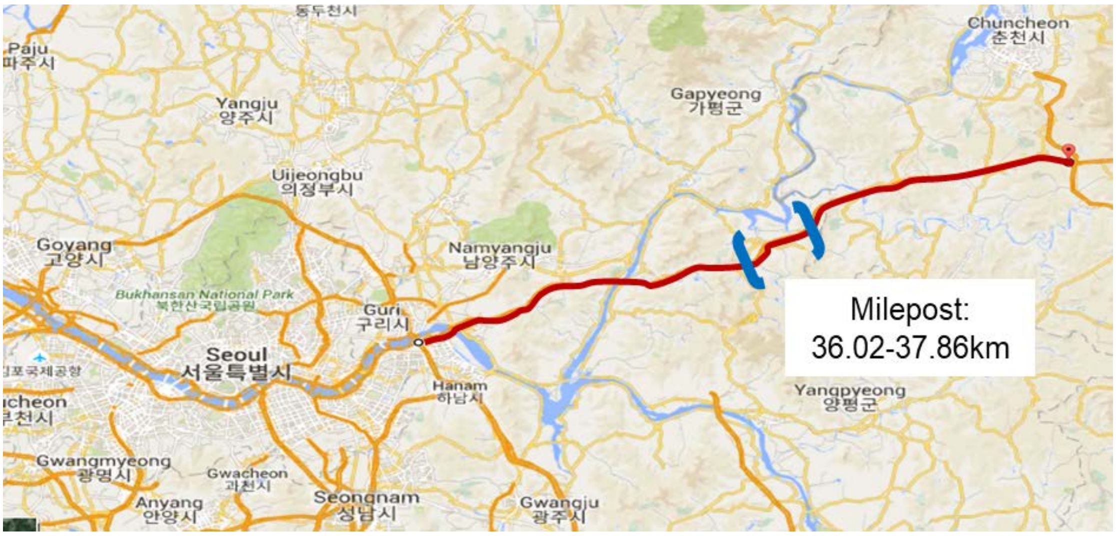

Source: Google map

Data collection from inductive loop detectors

The data for the initial case study was collected from inductive loop detectors (ILDs) in Korean ITS. The six detectors collected traffic information about all vehicles passing through 1.84km section of this case. Two of the detectors are located before the tunnel entrance respectively with 840m and 310m, and others of them are located in the tunnel with the approximate interval of

300m. According to Korean Express Corporation (KEC), the ILDs are installed in all sections of the motorway with the average distance of 1.8km between devices and the minimum distance is 2km. The distance decreases to 1km for the section of LOS D or E and to 0.5km for that of LOS F. Another notable thing is that ILDs are installed with at least 400m interval in recently constructed tunnel sections. Korean ITS produces the traffic data every 5 minute and store it to the central server for 5 years. Therefore, a recently constructed tunnel section makes the precise analysis possible because ILDs with closer intervals enable to record the spatial change in the traffic data more precisely. In addition, in the initial data analysis travel time can be calculated from the measured vehicle's speed at each detector and the distance between detectors.

Figure A-6. Design Map of the initial case

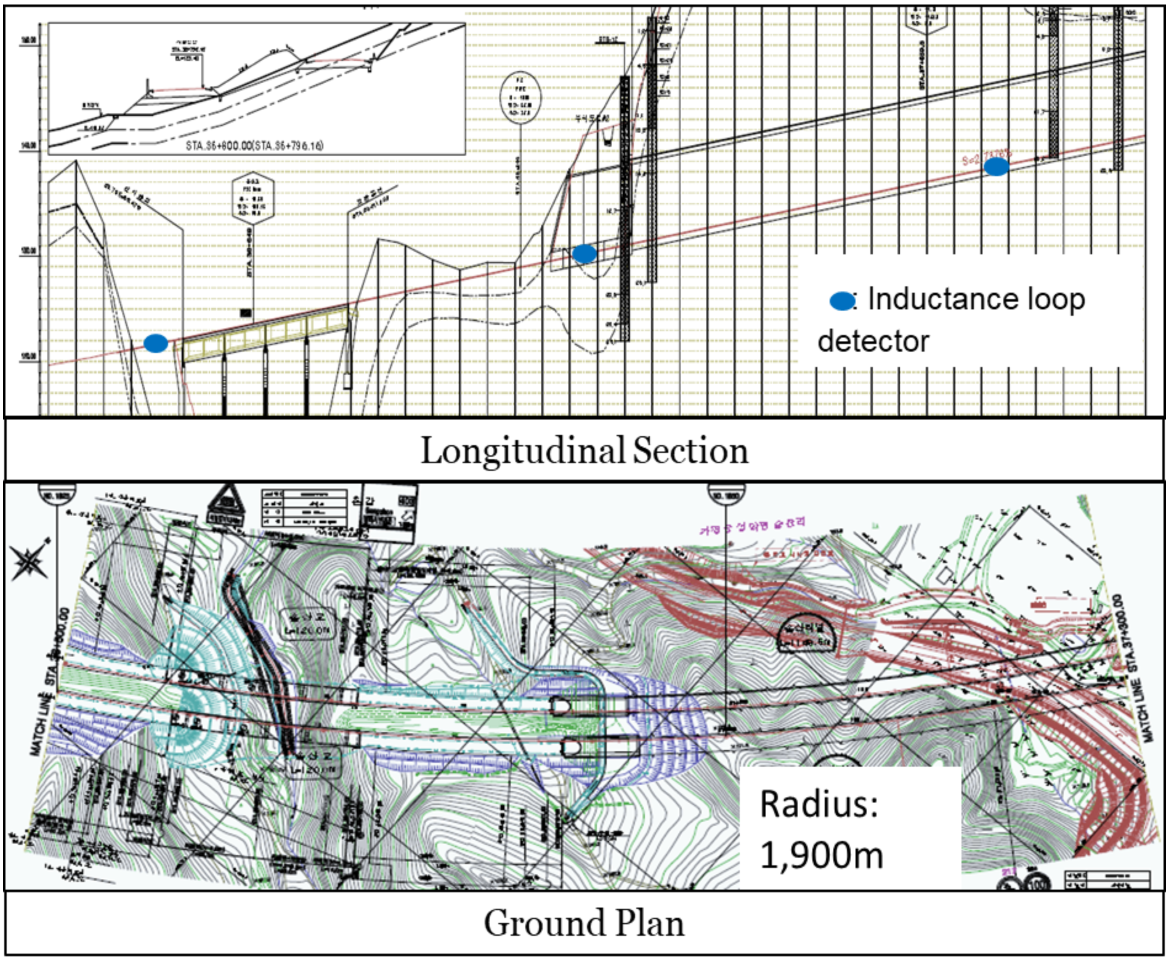

The traffic information mainly produced by an inductive loop includes time, location (ID), traffic volume, average speed and occupancy rate. As mentioned above, five-minute traffic data is stored in ITS main servers for five years without the consideration of vehicle's types even though the traffic data is measured every minute. The occupancy rate is made by recognising existing time on a loop, but the accreditation for the occupancy is not established in Korea and the accuracy would not be guaranteed. Therefore, it was not used in this study. The data with zero traffic flow for five minutes and the data with errors during measurement, which is stored as “-1” in the data set, are excluded in this analysis.

5-min average speed, which could be the most important data in the initial study, is stored through three steps (Figure A-7). Firstly, the speed measured with traffic volume per each lane is transformed into the arithmetical traffic-weighted average speed for 30 seconds. In this process, the average speed for the previous 30 seconds is weighted by 30% for calculating the current 30-second average speed. In other words, the current 30-second average speed is reflected only by 70% in calculating the 30-second average speed because the drastic change of speed could give confusion to drivers according to KEC. Secondly, 1-minute average speed is simply stored by calculating the average of two series of 30-second average speed without the consideration of traffic volume. Lastly, 5-minute speed is calculated from the arithmetical average of 1-min average speed weighted by 1-minute traffic volume.

Figure A-7 Example of speed calculation from ILD

Data per each lane for 30 secs				Data for 30 secs			Data for 1 min			Data for 5 mins		
Time	Lane	Traffic flow	Speed	Traffic flow	Speed (provisional)	Speed (used)	Time	Traffic flow	Speed	Time	Traffic flow	Speed
10:49:00						90.00						
10:49:30	1	13	90	23	85.65	86.96	10:50:00	57	79.17	10:50:00	196	74.76
	2	10	80									
10:50:00	1	16	70	34	64.71	71.38						
	2	18	60									
10:50:30	1	20	50	38	45.26	53.10	10:51:00	64	53.63			
	2	18	40									
10:51:00	1	12	60	26	54.62	54.16						
	2	14	50									
10:51:30	1	10	90	22	84.55	75.43	10:52:00	37	80.65			
	2	12	80									
10:52:00	1	8	95	15	90.33	85.86						
	2	7	85									
10:52:30	1	7	100	13	97.69	94.14	10:53:00	22	97.75			
	2	6	95									
10:53:00	1	4	110	9	104.44	101.35						
	2	5	100									
10:53:30	1	6	105	11	100.45	100.72	10:54:00	16	98.37			
	2	5	95									
10:54:00	1	2	100	5	94.00	96.02						
	2	3	90									

Travel time estimation depending traffic flow

Travel time is calculated by dividing the distance between one ILD and another detector into the 5-min average speed. If the variation of speeds in the section between detectors were measured, the travel time could be estimated more accurately. However, speed and traffic flow respectively in this study was regarded as a constant value between two detectors because this study is using the values on each detector location and does not recognise the variation between them. Even though travel time could be calculated more accurately by the car-following model (Wilson, 2008; Wilson and Ward, 2011), the model would not be applied to this study. It is because their study was based on the 1-min average speed with the average distance of 100m in M42 motorway, UK, but the data used in this study was stored every five minutes and the minimum distance between detectors is 300m. Besides, they suggested that the model is suitable for platoon flow, but this study aims to find unstable traffic pattern in unusual geometry. Therefore, this study assumes that traffic speed is constant between detectors.

In the process of calculating travel time in the selected sections of this study, the scope of the area that each detector could influence was defined as a half of distance between the previous detector and the next detector. For the example of Figure A-8, the total travel time of all vehicles passing before and after Detector 1 was calculated by dividing the influenced distance ($\mathrm{D}_1 = \mathrm{d}_0 + \mathrm{d}_1$) into the measured average speed (S_1) and multiplying the passing traffic flow (V_1) in Equation A-1. Then, all the series of total travel time on each location should be added for the selected cases (Equation A-3). It is necessary that the total travel time should be divided by the average of the series of traffic flow passing all the detectors in each selected case because VDFs are focusing on each vehicle's travel time (Equation A-4) and it could be generalised like Equation A-5.

Figure A-8 Calculation of travel time in a section

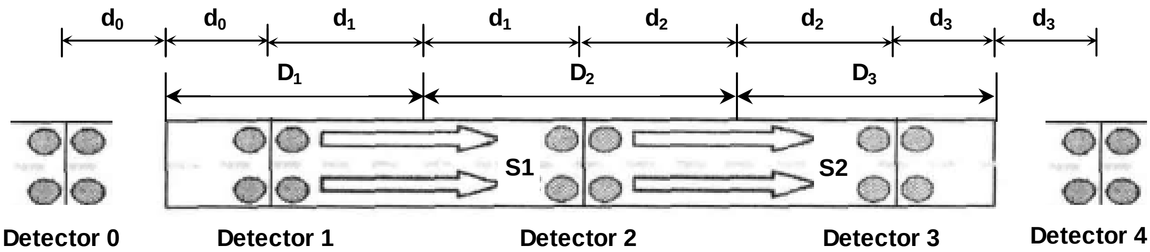

$$Total\ travelling\ time\ in\ Detector\ 1 = \frac{V_1 D_1}{S_1}$$ **Equation A-1**

$$Total\ travelling\ time\ in\ Detector\ 2 = \frac{V_2 D_2}{S_2}$$ **Equation A-2**

$$Total\ travelling\ time\ in\ Detector\ 1,2 = \frac{V_1 D_1}{S_1} + \frac{V_2 D_2}{S_2}$$ **Equation A-3**

$$Individual\ travelling\ time\ in\ d_1 + d_2 = \left(\frac{V_1 d_1}{S_1} + \frac{V_2 d_2}{S_2}\right) \Big/ \frac{V_1 + V_2}{2}$$ **Equation A-4**

where V_1 and V_2 are the traffic flow on detector 1 and 2; D_1 and D_2 are the influenced distance on detector 1 and 2; and S_1 and S_2 are the average speed on detector 1, 2.

$$Individual\ travelling\ time\ in\ the\ section\ = \sum_{i=1}^{n} \frac{V_i d_i}{S_i} \Big/ \frac{\sum_{i=1}^{n} V_i}{n}$$ **Equation A-5**

Since the collected data from Korean ITS was classified by date and location, the travel time on each location was calculated from the average speed and then the travel time passing the section was derived by adding up the series of travel time of all locations. Table A-16 shows the range of each detector's influenced distance and locational travel time was calculated through dividing the influenced distance by the measured average speed on each detector. Even though the distance between the first detector and the last detector is 1.84km, the distance with consideration of the influenced distance by detectors becomes 2.88km.

Table A-16 Influenced distance by each detector in the initial case

	Distance to previous detector (km)	Distance to the next detector (km)	Influenced distance (km)
ID No. 29	0.38	0.53	0.455
ID No. 30	0.53	0.34	0.435
ID No. 31	0.34	0.3	0.320
ID No. 32	0.3	0.3	0.300
ID No. 33	0.3	0.37	0.335
ID No. 34	0.37	1.7	1.035
SUM			2.880

A.4.2. Measurement of Traffic data in the intial case study

Plot observation for 45 days

Prior to the long period analysis, the data from 5th of October to 18th of November in 2016 (45 days) was examined initially in this study to find the change of traffic characteristics in a tunnel section because 1-year data analysis tends to show more aggregated plots in graphs. Traffic observation in autumn can be reliable and little affected by the external environment such as weather condition. The number of data rows on each location is 12,787 except for measurement errors from the total measurable time intervals of 12,960 (= 45 days * 24 hours * 12 intervals (60min/5min)). The scatter plots between the traffic volume and speed on six locations for 45 days were drawn. The plots shows the pattern of the traditional traffic theory models (Figure A-9). They also present the overall change of traffic characteristics in the tunnel section such as the free flow speed, maximum traffic volume and breakdown effect more or less.

Figure A-9 Volume-speed relationship for 45 days in the initial case

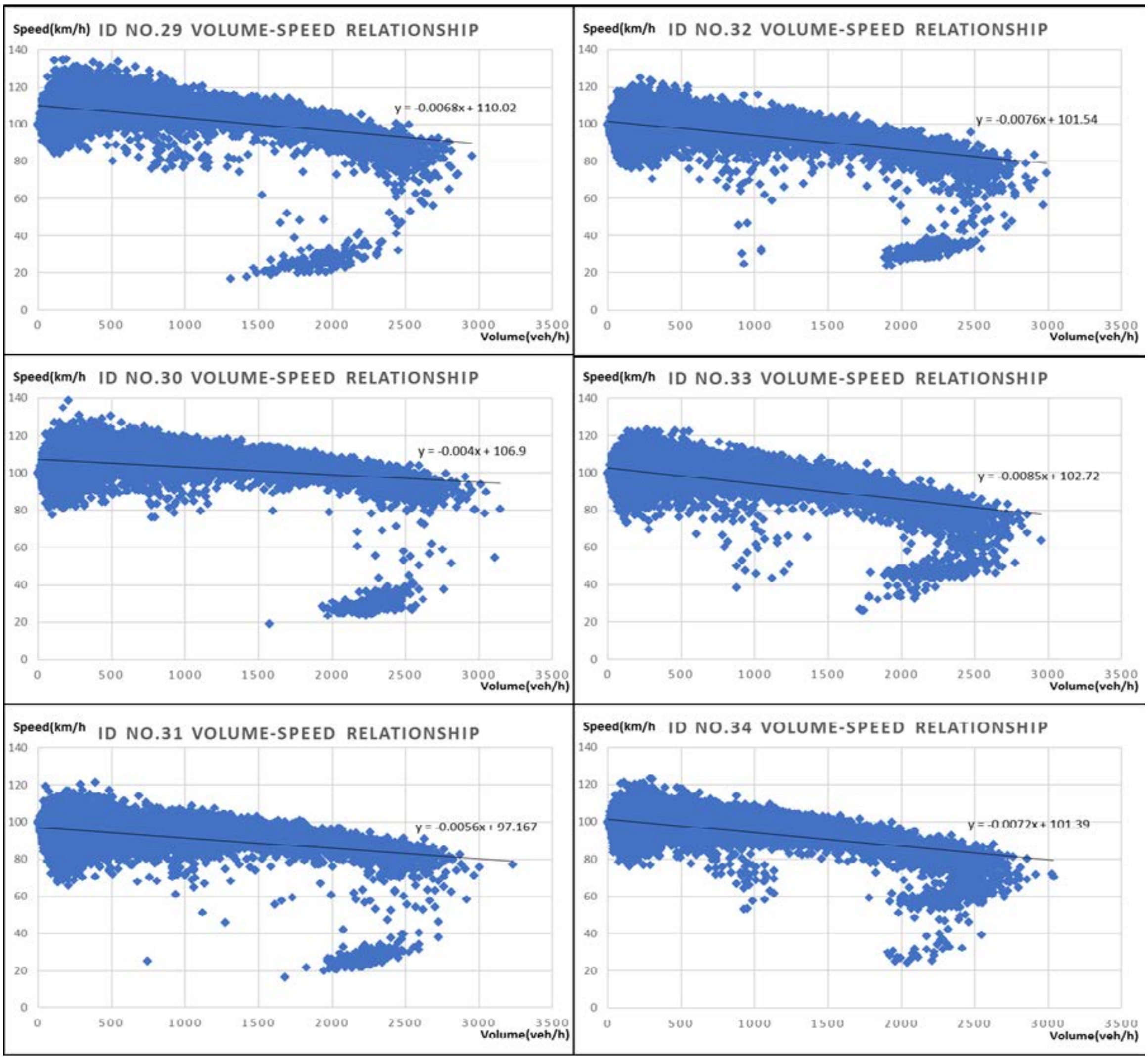

Measurement of free-flow speed

USHCM (2010) defines free-flow speed as “the mean speed of passenger cars under low to moderate flow rates that can be accommodated on a uniform roadway under prevailing roadway and traffic conditions”. In addition, it also suggests that free-flow speed for a motorway could be measured as a mean speed when the traffic volume is below 1,300 passenger cars per hour per lane (pcphpl). This means that the mean of speeds corresponding to the traffic below 2,600 passenger cars per hour (pcph) for two lanes becomes the free-flow speed. However, it could not be applied to this study because the level of traffic volume would already cause the congestion. Instead, Kalaee (2010) measured the free-flow speed as the mean of speeds corresponding to each traffic volume under 360vph. Similarly, this assumption applied to the initial case study.

FFS on each ILD for one year in this study was measured as showed in Table A-17. The free-flow speed decreases from 106.0kph at ID No. 29 to 98.6kph at ID No. 34 and the minimum free-flow speed is recorded as 95.4kph just after the tunnel entrance (ID No. 31). This result would be understandable because most vehicles tend to decelerate as they approach the tunnel entrance. The free-flow speed increases in the middle of the tunnel and stayed steadily towards the end of the tunnel. This behaviour seems to result from vehicle's movements to adapt the tunnel environment.

Table A-17. Observation of free-flow speed on ILDs in the initial case

ILD ID No.	Free-flow Speed (kph)	Distance from the tunnel
29	106.0	840m (before)
30	103.1	310m (before)
31	95.4	30m (after)
32	98.5	330m (after)
33	99.2	630m (after)
34	98.6	1,000m (after)

Measurement of road capacity

The actual road capacity for the initial case was measured from the collected dataset. MLTM (2013) and USHCM (2010) theoretically define that the road capacity is the maximum traffic volume of passenger cars per hour from 15-minute observation in a representative section. In addition to the maximum traffic volume, 10th largest traffic volume and the average of top 1% values were also extracted from the dataset because the maximum traffic flow can be accidental measurement.

In order to compare the derived values with the theoretical road capacity, it is necessary to get the information of heavy vehicle percentage. Road Traffic Survey (2016), which is annually conducted from the sample data in one autumn day, suggested Seoul-Chuncheon Motorway's heavy vehicle percentage of 18.1%. According to MLTM (2013), the theoretical road capacity of this study case, whose characteristics for calculating the road capacity are 120kph design speed, 2 lanes to each direction, 3.5m lane width, 1.0m left clearance, 2.0m right clearance, 18.1% heavy vehicle percentage and hilly terrain, is calculated as 3,310vph.

The highest maximum traffic volume based on 15-min observation for one year in the initial section would be the closest definition with the road capacity of USHCM (2000). The maximum traffic volume in the selected case is 2,948vph at ID No. 30 (Table A-17). All of the maximum, the 10th largest traffic volume and the average of top 1% values tend to drop at ID No. 31 near the entrance of the tunnel (Table A-18). Compared with the value at ID No. 30, the value of each location becomes lower by 2.6%-6.8%.

Table A-18 Measurement of road capacity on ILD locations in the initial case study

ID No.	Max. traffic flow (TF)	10th largest TF	Avg. of top 1%	Theoretical road capacity
29	2,872	2,772	2,542	
	-2.6%	-3.5%	-3.5%	
30	2,948	2,872	2,635	
31	2,836	2,768	2,541	
	-3.8%	-3.6%	-3.6%	
32	2,872	2,748	2,534	3,310
	-2.6%	-4.3%	-3.8%	
33	2,748	2,704	2,501	
	-6.8%	-5.8%	-5.1%	
34	2,820	2,748	2,536	
	-4.3%	-4.3%	-3.7%	

Note 1. Shadow area indicates locations inside the tunnel.

2. Underline values are the percentage changes with the value of No. 30

Measurement of breakdown traffic volume

A breakdown, as well as free-flow speed and road capacity, is an important consideration in the initial case study because traffic flow occurring breakdown can replace road capacity (Dong and Mahmassani, 2009; Kalaee, 2010). Brilon *et al.* (2005) defined that a breakdown happens with the significant speed drop of most vehicles that causes from smooth to congested traffic flow and they mentioned that it could differ dependent on each driving environment. In addition, they described the motorway breakdown dynamics as a transition during breakdown and recovery in congested and uncongested situations (Figure A-10).

Figure A-10 Breakdown Dynamics during breakdown and recovery (German motorway)

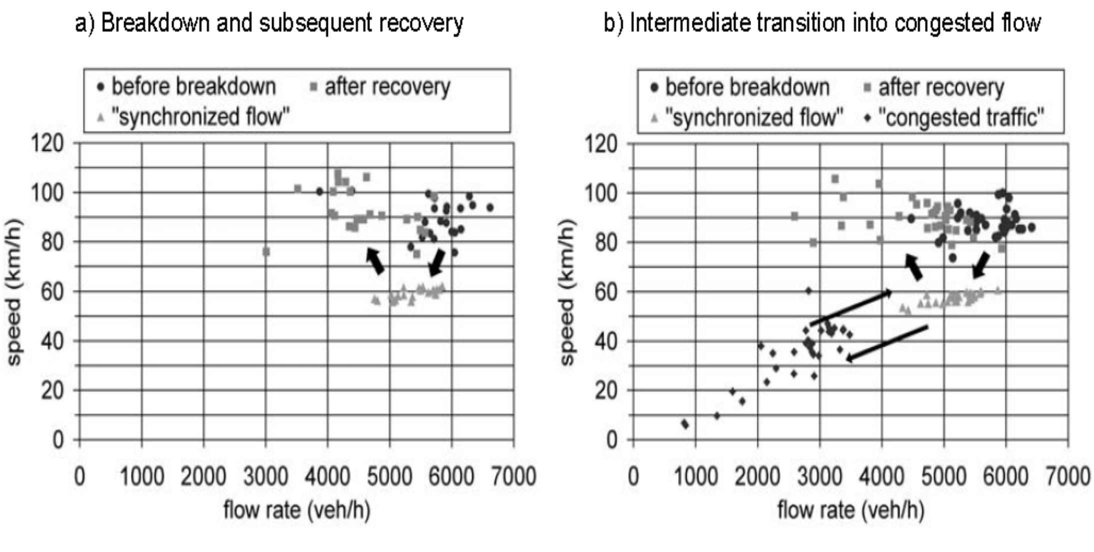

Source: Brilon *et al.* (2005)

Recalling the scatter plots for 45 days, the breakdown effect in the tunnel can be explained in Figure A-11. Every location seems to have the breakdown effect even though the frequency and the difference would be varied with each other. As can be seen from Figure A-11, the gaps of data points on each location between an uncongested and a congested situation are different; especially the gap inside the tunnel (e.g. ID No. 34) becomes smaller compared with that outside the tunnel (ID No. 30). Likewise, as the data is measured at the end of the tunnel (ID No. 34), the breakdown effect seems to be more unclear. On the other hand, the speed plots in congestion, which could be calculated in Figure A-11 as an approximate average from 20 to 40kph, are rarely dense at ID No. 34 (at the end of the tunnel) and it could be related with this breakdown effect and the virtual bottleneck point.

Figure A-11 Breakdown effect for 45 days in the initial case

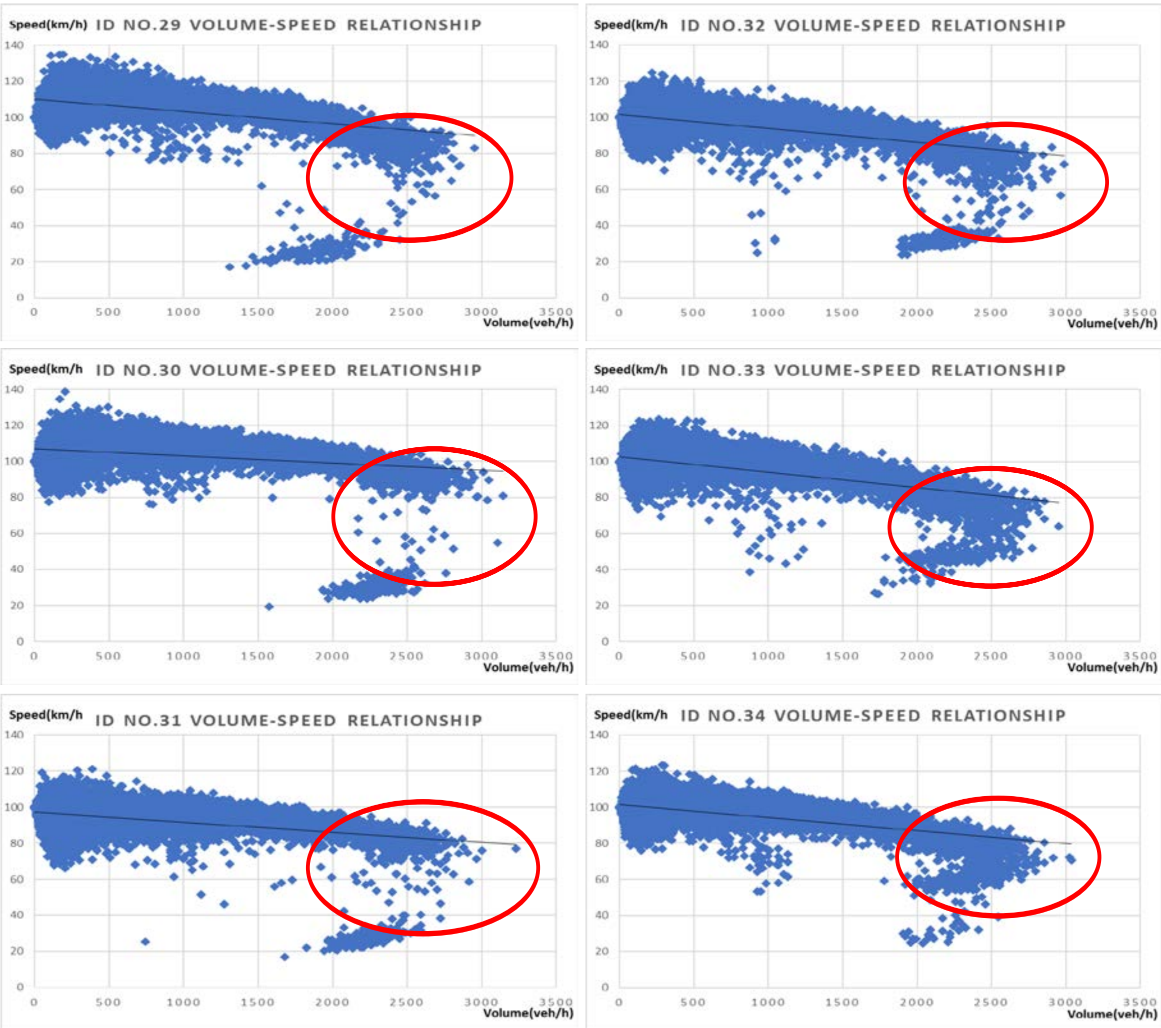

In order to confirm breakdown effects in detail, time-series data that shows fluid, congested and discharging process was extracted (Figure A-12). The breakdown happening at each detector was investigated on Saturday in 15th of October 2016. The speed drop at a breakdown point was observed after the fluent state, and the traffic volume around this point peaked at the maximum on the day. The congestion for over six hours at this location was also observed with the speed of around 20kph after a breakdown around 8.30am at ID No. 30. Although the overall congestion process at ID No. 32 and 33 would be similar with those at ID No. 30 and 31, the breakdown effects at those points were observed more unclear. In other words, the difference of speed between the fluid and congested state at ID No. 32 and 33 was smaller. Another important traffic characteristic is that as vehicles are moving away from the tunnel entrance, the overall average speed in a congested state increases. The overall speed in a congested state is higher with over 40kph at ID No. 33 than that with over 20kph at ID No. 30. These overall characteristics at breakdown points could also explain the existence of the virtual bottleneck in the tunnel like the measurement of road capacity.

Figure A-12 Congestion process from ILD No.30 to No.33 in the initial case study

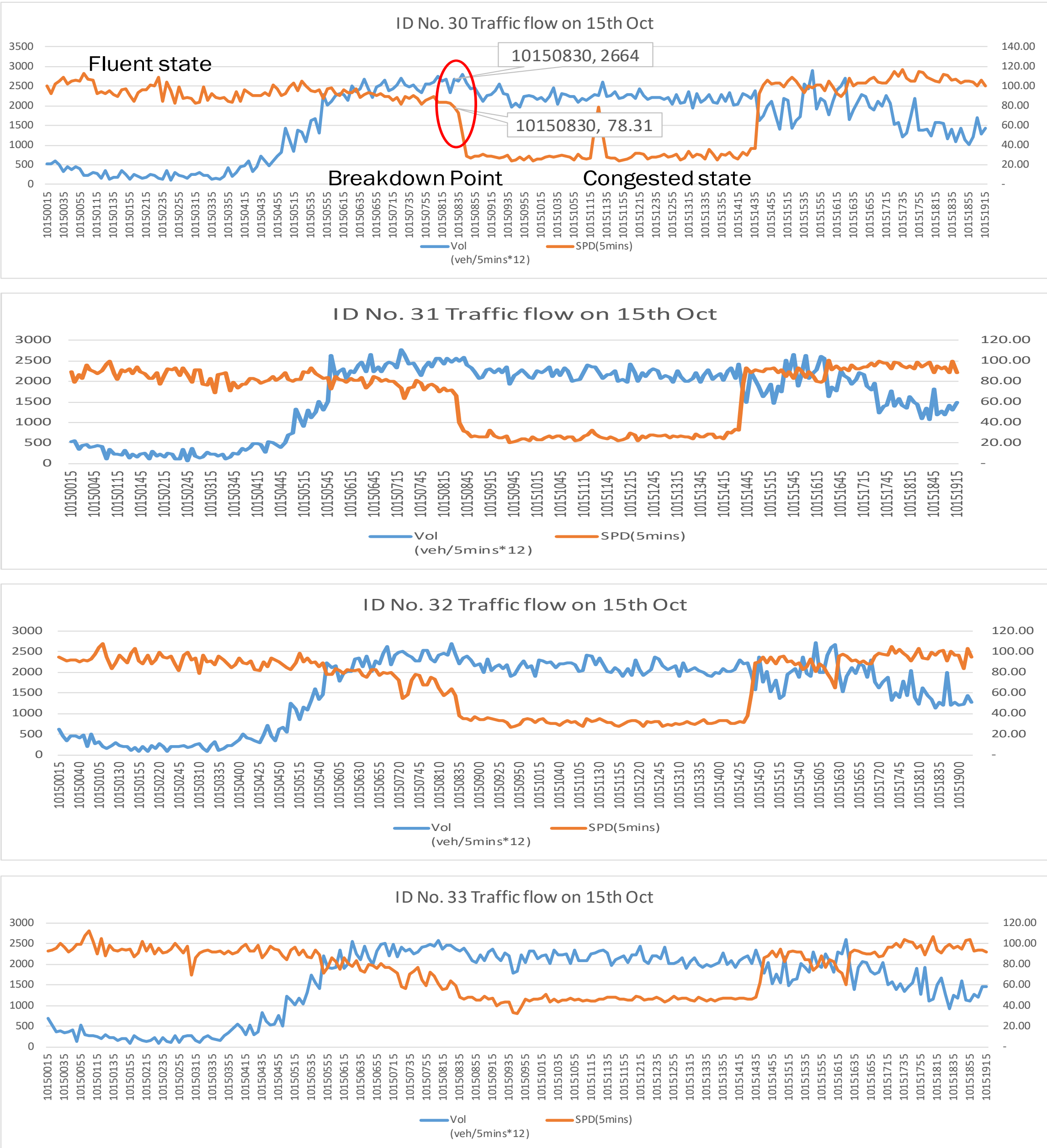

Breakdown points could be defined differently dependent on the criteria such as countries or road types, but the common traffic characteristics at the point of breakdown would be three (Brilon *et al.*, 2005; Dong and Mahmassani, 2009; Kalaee, 2010). One is a considerable speed drop, another is a lower threshold speed compared with a free-flow speed, and the other is the duration below the threshold speed. However, these three characteristics do not seem to be suggested as similar values in those studies. Brilon *et al.* (2005) suggested that the threshold speed at the breakdown point would be 70kph in German motorway conditions and other considerations were implemented by using "Product Limit Method". On the other hand, as mentioned in Section 2.4.2, Kalaee (2010) adopted the threshold speed of 55mph (88kph) and the speed drop of 10mph between consecutive time intervals in a US highway, which has free flow speed of 65mph.

In order to find the traffic volume at breakdown points in this case, 5-min average speed data for one year was examined because the breakdown point analysis should focus more on instantaneous traffic changes than on aggregated ones such as 15-min average speed change. The values from 5-min observation are necessary to be aggregated into 15-min traffic flow through the sum of three nearby values including breakdown points in order to compare with the maximum traffic flow measured above. The combinations of the low threshold speed of 70kph and 80kph; the considerable speed drop of 10kph and 16kph; and the duration time of 15 minutes were applied for this study based on the previous studies (Table A-19). To avoid finding too small traffic volume, the lowest traffic volume at a breakdown was limited to 1,500vph.

Table A-19 Various criteria for finding breakdown points

Condition	1	2	3	4
Threshold low speed	80kph	70kph	80kph	70kph
Speed drop	16kph	16kph	10kph	10kph
Duration	15minutes	15minutes	15minutes	15minutes

Table A-20 to Table A-23 show different traffic flow at breakdown points according to the given conditions (Table A-19). The key findings from the different conditions can be summarised as follows. Firstly, traffic flow at breakdown points is not always same as the maximum traffic flow. Secondly, if threshold speed or speed drop is set as a comparatively high value (e.g. 80kph > 70kph, 16kph > 10kph), traffic flow at breakdown points cannot be captured well and as such the number of breakdown points becomes smaller than other conditions. Lastly, maximum traffic flow and 10th largest traffic flow at breakdown points are the largest at ID No.30 as well as the number of breakdown points in most conditions except for condition 4 (Table A-23), which has lower conditions of threshold speed and speed drop (70kph and 10kph). This finding is in line with the measurement of maximum traffic flow. Although the conditions for finding breakdown points are stochastic like the definition of road capacity, it can be concluded that a tunnel entrance plays a role on a virtual bottleneck.

Table A-20 Finding traffic flow at breakdown points with Condition 1

ID No.	Max. traffic flow (TF, vph)	Max. TF at BPs	10th largest TF at BPs	The number of BPs
29	2,872	2,484	1,960	14
30	2,948	2,880	2,704	96
31	2,836	2,724	2,332	31
32	2,872	2,548	2,292	36
33	2,748	2,428	2,132	45
34	2,820	2,308	1,852	21

Table A-21 Finding traffic flow at breakdown points with Condition 2

ID No.	Max. traffic flow (TF, vph)	Max. TF at BPs	10th largest TF at BPs	The number of BPs
29	2,872	2,720	2,548	40
30	2,948	2,948	2,704	104
31	2,836	2,836	2,632	84
32	2,872	2,732	2,536	82
33	2,748	2,620	2,372	59
34	2,820	2,612	2,296	25

Table A-22 Finding traffic flow at breakdown points with Condition 3

ID No.	Max. traffic flow (TF, vph)	Max. TF at BPs	10th largest TF at BPs	The number of BPs
29	2,872	2,720	2,364	33
30	2,948	2,880	2,704	106
31	2,836	2,724	2,500	69
32	2,872	2,572	2,384	94
33	2,748	2,492	2,304	117
34	2,820	2,412	2,296	64

Table A-23 Finding traffic flow at breakdown points with Condition 4

ID No.	Max. traffic flow (TF, vph)	Max. TF at BPs	10th largest TF at BPs	The number of BPs
29	2,872	2,720	2,588	52
30	2,948	2,948	2,704	108
31	2,836	2,836	2,644	105
32	2,872	2,732	2,568	109
33	2,748	2,620	2,520	105
34	2,820	2,688	2,436	57

A.5. Statistical results

A.5.1. FE modelling

(1) FE Model including geometric variables with the entity of link

```
#Model including geometric features with Link dummies

MODEL_Geometry_LinkDummy<-lm(mydf$Inv_SPD ~ mydf$TF + mydf$TF2 + mydf$TR + my
df$RISE + mydf$FALL + mydf$BEND + as.factor(mydf$Link))
summary(MODEL_Geometry_LinkDummy)
```

```
Call:
lm(formula = mydf$Inv_SPD ~ mydf$TF + mydf$TF2 + mydf$TR + mydf$RISE +
    mydf$FALL + mydf$BEND + as.factor(mydf$Link))

Residuals:
     Min       1Q   Median       3Q      Max
-12.3328  -1.7406  -0.2246   1.3763  23.4625

Coefficients: (4 not defined because of singularities)
                                                        Estimate Std. Error  t value Pr(>|t|)
(Intercept)                                            2.999e+01  1.270e+00   23.621  < 2e-16 ***
mydf$TF                                               -6.417e-03  5.827e-05 -110.131  < 2e-16 ***
mydf$TF2                                               3.492e-06  2.835e-08  123.138  < 2e-16 ***
mydf$TR                                               -6.513e-03  1.438e-03   -4.529 5.93e-06 ***
mydf$RISE                                              1.241e+00  1.023e-01   12.132  < 2e-16 ***
mydf$FALL                                             -1.072e+00  7.141e-02  -15.011  < 2e-16 ***
mydf$BEND                                             -3.094e-01  1.547e-02  -20.000  < 2e-16 ***
as.factor(mydf$Link)10. GwangjuDaegu (125.9-128.0K) S  3.350e+00  3.137e-01   10.680  < 2e-16 ***
as.factor(mydf$Link)100. Jungang (267.8-270.4) S       5.798e-01  7.916e-01    0.732  0.46393
as.factor(mydf$Link)102. Jungang (349.3-351.4) S      -6.967e+00  6.538e-01  -10.657  < 2e-16 ***
as.factor(mydf$Link)103. Jungang-Branch (1.1-3.4) E    8.699e+00  1.624e-01   53.564  < 2e-16 ***
as.factor(mydf$Link)104. Jungang-Branch (1.1-3.4) S    1.175e+01  4.216e-01   27.862  < 2e-16 ***
as.factor(mydf$Link)105. Jungang-Branch (3.4-5.4) E    8.763e+00  5.909e-01   14.830  < 2e-16 ***
as.factor(mydf$Link)106. Jungang-Branch (3.4-5.4) S    1.478e+01  5.500e-01   26.880  < 2e-16 ***
as.factor(mydf$Link)107. Jungang-Branch (5.4-8.0) E    9.161e-01  3.514e-01    2.607  0.00913 **
as.factor(mydf$Link)108. Jungang-Branch (5.4-8.0) S   -1.840e+00  2.998e-01   -6.138 8.39e-10 ***
as.factor(mydf$Link)117. TongyoungDaejeon (113.2-115.6) E  9.335e+00  6.066e-01  15.390  < 2e-16 ***
as.factor(mydf$Link)118. TongyoungDaejeon (113.2-115.6) S  1.455e+01  7.437e-01  19.560  < 2e-16 ***
as.factor(mydf$Link)119. TongyoungDaejeon (127.6-131.8) E  9.260e+00  4.658e-01  19.879  < 2e-16 ***
as.factor(mydf$Link)12. GwangjuDaegu (135.0-138.6K) S -4.201e+00  9.171e-01   -4.581 4.62e-06 ***
as.factor(mydf$Link)120. TongyoungDaejeon (127.6-131.8) S  1.203e+01  2.343e-01  51.345  < 2e-16 ***
as.factor(mydf$Link)121. TongyoungDaejeon (153.1-155.9) E -3.049e+00  2.579e-01 -11.820  < 2e-16 ***
as.factor(mydf$Link)122. TongyoungDaejeon (153.1-155.9) S -6.184e+00  1.115e+00  -5.544 2.96e-08 ***
as.factor(mydf$Link)123. Pyungtaek Jaecheon (48.9-52.1) E  4.195e+00  3.560e-01  11.782  < 2e-16 ***
as.factor(mydf$Link)124. Pyungtaek Jaecheon (48.9-52.1) S  9.573e+00  2.203e-01  43.448  < 2e-16 ***
as.factor(mydf$Link)125. Pyungtaek Jaecheon (105.1-107.3) E  2.835e-01  4.988e-01  0.568  0.56985
as.factor(mydf$Link)126. Pyungtaek Jaecheon (105.1-107.3) S  2.645e-01  3.214e-01  0.823  0.41053
as.factor(mydf$Link)127. Pyungtaek Jaecheon (112.0-115.7) E  4.746e+00  6.133e-01  7.738 1.01e-14 ***
as.factor(mydf$Link)128. Pyungtaek Jaecheon (112.0-115.7) S  6.466e+00  4.236e-01  15.267  < 2e-16 ***
as.factor(mydf$Link)129. Pyungtaek Jaecheon (115.7-118.9) E  6.150e-01  7.043e-01  0.873  0.38259
as.factor(mydf$Link)130. Pyungtaek Jaecheon (115.7-118.9) S -5.014e+00  4.584e-01 -10.938  < 2e-16 ***
as.factor(mydf$Link)131. Pyungtaek Jaecheon (118.9-123.9) E  4.067e+00  6.462e-01  6.295 3.09e-10 ***
as.factor(mydf$Link)132. Pyungtaek Jaecheon (118.9-123.9) S  9.317e+00  3.364e-01  27.694  < 2e-16 ***
as.factor(mydf$Link)14. GwangjuDaegu (138.6-143.3K) S -2.154e+01  2.041e+00  -10.556  < 2e-16 ***
as.factor(mydf$Link)2. KochangDamyang (6.23-11.57k)_S -3.431e+00  1.481e-01  -23.173  < 2e-16 ***
as.factor(mydf$Link)22. MuanGwangju (26.57-29.57) S   -1.025e+01  1.143e+00   -8.963  < 2e-16 ***
as.factor(mydf$Link)25. SangjuYoungduk (105.1-110.3) E -3.165e+00  2.732e-01  -11.582  < 2e-16 ***
as.factor(mydf$Link)26. SangjuYoungduk (105.1-110.3) S -3.795e+00  2.171e-01  -17.484  < 2e-16 ***
as.factor(mydf$Link)27. SangjuYoungduk(110.3-115.0) E -1.192e+01  1.215e+00   -9.814  < 2e-16 ***
as.factor(mydf$Link)28. SangjuYoungduk (110.3-115.0) S -1.354e+01  5.871e-01  -23.061  < 2e-16 ***
as.factor(mydf$Link)29. SangjuYoungduk (124.7-128.1) E  4.961e+00  4.446e-01   11.158  < 2e-16 ***
as.factor(mydf$Link)30. SangjuYoungduk(124.7-128.1) S  5.387e+00  4.488e-01   12.004  < 2e-16 ***
as.factor(mydf$Link)31. SangjuYoungduk (146.3-152.2) E  1.405e+00  1.444e-01    9.727  < 2e-16 ***
as.factor(mydf$Link)32. SangjuYoungduk (146.3-152.2) S  3.366e+00  2.283e-01   14.741  < 2e-16 ***
as.factor(mydf$Link)35. SangjuYoungduk (172.3-176.2) E -3.870e+00  7.350e-01   -5.265 1.40e-07 ***
as.factor(mydf$Link)36. SangjuYoungduk(172.3-176.2) S -3.463e+00  2.856e-01  -12.127  < 2e-16 ***
```

```
as.factor(mydf$Link)37. SangjuYoungduk (181.3-185.5) E      1.139e+01  6.418e-01   17.754  < 2e-16 ***
as.factor(mydf$Link)38. SangjuYoungduk (181.3-185.5) S      9.218e+00  4.297e-01   21.453  < 2e-16 ***
as.factor(mydf$Link)39. SangjuYoungduk(185.5-188.7) E       7.527e+00  2.150e-01   35.008  < 2e-16 ***
as.factor(mydf$Link)40. SangjuYoungduk (185.5-188.7) S      6.327e+00  3.578e-01   17.684  < 2e-16 ***
as.factor(mydf$Link)41. SeoulYangyang (63.8-70.1) E        -7.463e+00  4.015e-01  -18.587  < 2e-16 ***
as.factor(mydf$Link)43. SeoulYangyang (70.1-73.7) E         9.474e-02  2.138e-01    0.443  0.65766
as.factor(mydf$Link)47. Seoul Yangyang(97.7-103.9) E       -9.469e+00  1.017e+00   -9.307  < 2e-16 ***
as.factor(mydf$Link)48. Seoul Yangyang (97.7-103.9) S      -7.438e+00  6.334e-01  -11.745  < 2e-16 ***
as.factor(mydf$Link)49. Seoul Yangyang(106.9-110.9) E      -1.924e+00  4.185e-01   -4.597 4.28e-06 ***
as.factor(mydf$Link)5. KochangDamyang (19.92-24.06k) E      6.873e+00  3.754e-01   18.309  < 2e-16 ***
as.factor(mydf$Link)50. Seoul Yangyang(106.9-110.9) S      -2.192e+00  2.056e-01  -10.661  < 2e-16 ***
as.factor(mydf$Link)54. Seoul Yangyang(115.7-119.0) S       7.580e+00  7.064e-01   10.730  < 2e-16 ***
as.factor(mydf$Link)55. Seoul Yangyang(143.0-149.6) E      -8.166e-01  4.770e-01   -1.712  0.08693 .
as.factor(mydf$Link)56. Seoul Yangyang(143.0-149.6) S      -1.245e+00  5.021e-01   -2.480  0.01314 *
as.factor(mydf$Link)57. Suncheon Wyanju (7.8-12.5) E        8.465e+00  3.079e-01   27.495  < 2e-16 ***
as.factor(mydf$Link)59. Suncheon Wyanju (12.5-20.0) E       3.329e+00  2.249e-01   14.799  < 2e-16 ***
as.factor(mydf$Link)6. KochangDamyang (19.92-24.06k) S      8.386e+00  5.512e-01   15.213  < 2e-16 ***
as.factor(mydf$Link)61. Suncheon Wyanju (25.1-32.6) E      -7.943e-01  6.818e-01   -1.165  0.24406
as.factor(mydf$Link)62. Suncheon Wyanju (25.1-32.6) S      -9.180e-01  3.663e-01   -2.506  0.01221 *
as.factor(mydf$Link)65. Suncheon Wyanju (37.9-41.8) E      -2.434e+00  8.787e-01   -2.770  0.00561 **
as.factor(mydf$Link)66. Suncheon Wyanju (37.9-41.8) S      -2.656e+00  2.495e-01  -10.646  < 2e-16 ***
as.factor(mydf$Link)67. Suncheon Wyanju (41.8-46.6) E       9.739e+00  6.794e-01   14.336  < 2e-16 ***
as.factor(mydf$Link)68. Suncheon Wyanju (41.8-46.6) S       1.081e+01  4.760e-01   22.715  < 2e-16 ***
as.factor(mydf$Link)7. GwangjuDaegu (41.2-43.7K) E         -7.098e+00  5.483e-01  -12.944  < 2e-16 ***
as.factor(mydf$Link)8. GwangjuDaegu (41.2-43.7K) S         -2.110e+00  1.060e+00   -1.991  0.04648 *
as.factor(mydf$Link)83. Jungbunaeryuk (106.4-108.1) E       1.568e+01  4.100e-01   38.238  < 2e-16 ***
as.factor(mydf$Link)84. Jungbunaeryuk (106.4-108.1) S       1.942e+01  5.824e-01   33.352  < 2e-16 ***
as.factor(mydf$Link)9. GwangjuDaegu (125.9-128.0K) E        9.077e-01  7.662e-01    1.185  0.23615
as.factor(mydf$Link)93. Jungbunaeryuk (290.6-295.4) E              NA         NA       NA       NA
as.factor(mydf$Link)94. Jungbunaeryuk (290.6-295.4) S              NA         NA       NA       NA
as.factor(mydf$Link)97. Jungang (237.4-244.9) E                    NA         NA       NA       NA
as.factor(mydf$Link)99. Jungang (267.8-270.4) E                    NA         NA       NA       NA
---
Signif. codes:  0 '***' 0.001 '**' 0.01 '*' 0.05 '.' 0.1 ' ' 1

Residual standard error: 2.894 on 147757 degrees of freedom
Multiple R-squared:  0.5942,    Adjusted R-squared:  0.594
F-statistic:  2964 on 73 and 147757 DF,  p-value: < 2.2e-16
```

(2) FE Model with the entities of link and date

```
#Model with date and link dummies
MODEL1_3<-lm(mydf$Inv_SPD ~ mydf$TF + mydf$TF2 +
as.factor(mydf$Date) + as.factor(mydf$Link))
summary(MODEL1_3)

##
## Call:
## lm(formula = mydf$Inv_SPD ~ mydf$TF + mydf$TF2 +
as.factor(mydf$Date) + as.factor(mydf$Link))
##
## Residuals:

##      Min       1Q   Median       3Q      Max
## -11.4554  -1.6166  -0.2194   1.2662  24.0820

##
## Coefficients:
```

```
                                                          Estimate Std. Error  t value Pr(>|t|)
(Intercept)                                              3.525e+01  6.993e-02  504.062  < 2e-16 ***
mydf$TF                                                 -5.284e-03  5.217e-05 -101.277  < 2e-16 ***
mydf$TF2                                                 3.507e-06  2.551e-08  137.469  < 2e-16 ***
as.factor(mydf$Date)2                                   -5.959e-01  5.161e-02  -11.546  < 2e-16 ***
as.factor(mydf$Date)3                                    2.189e+00  5.258e-02   41.636  < 2e-16 ***
as.factor(mydf$Date)4                                    2.395e+00  5.248e-02   45.627  < 2e-16 ***
as.factor(mydf$Date)5                                    2.554e+00  5.210e-02   49.012  < 2e-16 ***
as.factor(mydf$Date)6                                    2.389e+00  5.202e-02   45.918  < 2e-16 ***
as.factor(mydf$Date)7                                    1.476e+00  5.134e-02   28.750  < 2e-16 ***
as.factor(mydf$Date)8                                   -5.054e-02  5.029e-02   -1.005 0.314898
as.factor(mydf$Date)9                                   -6.944e-01  5.097e-02  -13.624  < 2e-16 ***
as.factor(mydf$Date)10                                   1.863e+00  5.178e-02   35.975  < 2e-16 ***
as.factor(mydf$Date)11                                   2.935e+00  5.216e-02   56.277  < 2e-16 ***
as.factor(mydf$Date)12                                   2.639e+00  5.208e-02   50.675  < 2e-16 ***
as.factor(mydf$Date)13                                   2.533e+00  5.188e-02   48.813  < 2e-16 ***
as.factor(mydf$Date)14                                   1.996e+00  5.124e-02   38.952  < 2e-16 ***
as.factor(mydf$Date)15                                   4.901e-01  5.076e-02    9.655  < 2e-16 ***
as.factor(mydf$Date)16                                  -6.935e-01  5.167e-02  -13.422  < 2e-16 ***
as.factor(mydf$Date)17                                   2.286e+00  5.171e-02   44.212  < 2e-16 ***
as.factor(mydf$Date)18                                   2.699e+00  5.196e-02   51.943  < 2e-16 ***
as.factor(mydf$Date)19                                   2.656e+00  5.192e-02   51.142  < 2e-16 ***
as.factor(mydf$Date)20                                   2.541e+00  5.215e-02   48.724  < 2e-16 ***
as.factor(mydf$Date)21                                   1.812e+00  5.135e-02   35.280  < 2e-16 ***
as.factor(mydf$Date)22                                  -4.966e-01  5.007e-02   -9.918  < 2e-16 ***
as.factor(mydf$Date)23                                  -1.226e+00  5.006e-02  -24.500  < 2e-16 ***
as.factor(mydf$Date)24                                  -1.028e+00  5.210e-02  -19.733  < 2e-16 ***
as.factor(mydf$Date)25                                  -6.397e-01  5.058e-02  -12.647  < 2e-16 ***
as.factor(mydf$Date)26                                  -9.882e-01  5.079e-02  -19.456  < 2e-16 ***
as.factor(mydf$Date)27                                   1.316e+00  5.242e-02   25.101  < 2e-16 ***
as.factor(mydf$Date)28                                   1.843e+00  5.150e-02   35.789  < 2e-16 ***
as.factor(mydf$Date)29                                   5.664e-01  5.124e-02   11.052  < 2e-16 ***
as.factor(mydf$Date)30                                  -5.353e-01  5.256e-02  -10.185  < 2e-16 ***
as.factor(mydf$Link)10. GwangjuDaegu (125.9-128.0K) S    6.190e+00  7.909e-02   78.271  < 2e-16 ***
as.factor(mydf$Link)100. Jungang (267.8-270.4) S         3.719e+00  7.773e-02   47.847  < 2e-16 ***
as.factor(mydf$Link)102. Jungang (349.3-351.4) S        -1.306e+00  8.021e-02  -16.278  < 2e-16 ***
as.factor(mydf$Link)103. Jungang-Branch (1.1-3.4) E      5.020e+00  7.702e-02   65.183  < 2e-16 ***
as.factor(mydf$Link)104. Jungang-Branch (1.1-3.4) S      6.975e+00  7.672e-02   90.921  < 2e-16 ***
as.factor(mydf$Link)105. Jungang-Branch (3.4-5.4) E     -1.756e-01  7.728e-02   -2.272 0.023065 *
as.factor(mydf$Link)106. Jungang-Branch (3.4-5.4) S      6.370e+00  7.681e-02   82.933  < 2e-16 ***
as.factor(mydf$Link)107. Jungang-Branch (5.4-8.0) E      2.069e+00  7.731e-02   26.759  < 2e-16 ***
as.factor(mydf$Link)108. Jungang-Branch (5.4-8.0) S     -8.206e-01  7.702e-02  -10.655  < 2e-16 ***
as.factor(mydf$Link)117. TongyoungDaejeon (113.2-115.6) E -1.565e+00  7.741e-02  -20.211  < 2e-16 ***
as.factor(mydf$Link)118. TongyoungDaejeon (113.2-115.6) S  2.716e+00  7.549e-02   35.984  < 2e-16 ***
as.factor(mydf$Link)119. TongyoungDaejeon (127.6-131.8) E  2.746e+00  7.771e-02   35.335  < 2e-16 ***
as.factor(mydf$Link)12. GwangjuDaegu (135.0-138.6K) S    4.632e+00  7.902e-02   58.622  < 2e-16 ***
as.factor(mydf$Link)120. TongyoungDaejeon (127.6-131.8) S  6.608e+00  7.557e-02   87.431  < 2e-16 ***
as.factor(mydf$Link)121. TongyoungDaejeon (153.1-155.9) E  2.289e+00  7.966e-02   28.739  < 2e-16 ***
as.factor(mydf$Link)122. TongyoungDaejeon (153.1-155.9) S  2.108e+00  7.786e-02   27.080  < 2e-16 ***
as.factor(mydf$Link)123. Pyungtaek Jaecheon (48.9-52.1) E -1.538e+00  7.715e-02  -19.934  < 2e-16 ***
as.factor(mydf$Link)124. Pyungtaek Jaecheon (48.9-52.1) S  4.443e+00  7.782e-02   57.091  < 2e-16 ***
as.factor(mydf$Link)125. Pyungtaek Jaecheon (105.1-107.3) E -2.143e+00  7.879e-02  -27.197  < 2e-16 ***
as.factor(mydf$Link)126. Pyungtaek Jaecheon (105.1-107.3) S -4.087e+00  7.953e-02  -51.397  < 2e-16 ***
```

```
as.factor(mydf$Link)127. Pyungtaek Jaecheon (112.0-115.7) E -3.847e+00  7.876e-02  -48.839  < 2e-16 ***
as.factor(mydf$Link)128. Pyungtaek Jaecheon (112.0-115.7) S -1.163e+00  7.828e-02  -14.858  < 2e-16 ***
as.factor(mydf$Link)129. Pyungtaek Jaecheon (115.7-118.9) E  6.258e+00  7.873e-02   79.477  < 2e-16 ***
as.factor(mydf$Link)130. Pyungtaek Jaecheon (115.7-118.9) S -2.055e+00  7.833e-02  -26.229  < 2e-16 ***
as.factor(mydf$Link)131. Pyungtaek Jaecheon (118.9-123.9) E -3.458e+00  7.889e-02  -43.835  < 2e-16 ***
as.factor(mydf$Link)132. Pyungtaek Jaecheon (118.9-123.9) S  2.800e+00  7.784e-02   35.964  < 2e-16 ***
as.factor(mydf$Link)14. GwangjuDaegu (138.6-143.3K) S       -1.995e-01  7.878e-02   -2.533 0.011319 *
as.factor(mydf$Link)2. KochangDamyang (6.23-11.57k)_S       -3.028e+00  7.827e-02  -38.678  < 2e-16 ***
as.factor(mydf$Link)22. MuanGwangju (26.57-29.57) S          7.843e-01  7.748e-02   10.122  < 2e-16 ***
as.factor(mydf$Link)25. SangjuYoungduk (105.1-110.3) E      -3.397e+00  8.737e-02  -38.885  < 2e-16 ***
as.factor(mydf$Link)26. SangjuYoungduk (105.1-110.3) S      -2.953e+00  8.794e-02  -33.585  < 2e-16 ***
as.factor(mydf$Link)27. SangjuYoungduk(110.3-115.0) E       -5.415e-01  8.745e-02   -6.192 5.95e-10 ***
as.factor(mydf$Link)28. SangjuYoungduk (110.3-115.0) S      -3.988e+00  8.771e-02  -45.470  < 2e-16 ***
as.factor(mydf$Link)29. SangjuYoungduk (124.7-128.1) E      -2.433e-01  8.530e-02   -2.852 0.004350 **
as.factor(mydf$Link)30. SangjuYoungduk(124.7-128.1) S       -4.038e-01  8.846e-02   -4.565 4.99e-06 ***
as.factor(mydf$Link)31. SangjuYoungduk (146.3-152.2) E      -1.204e+00  8.232e-02  -14.631  < 2e-16 ***
as.factor(mydf$Link)32. SangjuYoungduk (146.3-152.2) S       2.265e-01  8.439e-02    2.683 0.007290 **
as.factor(mydf$Link)35. SangjuYoungduk (172.3-176.2) E      -1.218e+00  8.982e-02  -13.562  < 2e-16 ***
as.factor(mydf$Link)36. SangjuYoungduk(172.3-176.2) S       -2.136e+00  9.072e-02  -23.545  < 2e-16 ***
as.factor(mydf$Link)37. SangjuYoungduk (181.3-185.5) E       2.685e+00  9.018e-02   29.776  < 2e-16 ***
as.factor(mydf$Link)38. SangjuYoungduk (181.3-185.5) S       1.554e+00  9.083e-02   17.114  < 2e-16 ***
as.factor(mydf$Link)39. SangjuYoungduk(185.5-188.7) E        5.313e+00  9.000e-02   59.030  < 2e-16 ***
as.factor(mydf$Link)40. SangjuYoungduk (185.5-188.7) S       3.589e+00  9.089e-02   39.485  < 2e-16 ***
as.factor(mydf$Link)41. SeoulYangyang (63.8-70.1) E         -2.510e+00  7.757e-02  -32.357  < 2e-16 ***
as.factor(mydf$Link)43. SeoulYangyang (70.1-73.7) E         -1.333e+00  7.719e-02  -17.271  < 2e-16 ***
as.factor(mydf$Link)47. Seoul Yangyang(97.7-103.9) E        -1.132e+00  7.813e-02  -14.493  < 2e-16 ***
as.factor(mydf$Link)48. Seoul Yangyang (97.7-103.9) S       -2.490e+00  8.056e-02  -30.915  < 2e-16 ***
as.factor(mydf$Link)49. Seoul Yangyang(106.9-110.9) E       -5.041e+00  7.824e-02  -64.428  < 2e-16 ***
as.factor(mydf$Link)5. KochangDamyang (19.92-24.06k) E       1.194e+00  8.289e-02   14.403  < 2e-16 ***
as.factor(mydf$Link)50. Seoul Yangyang(106.9-110.9) S       -3.602e+00  8.063e-02  -44.679  < 2e-16 ***
as.factor(mydf$Link)54. Seoul Yangyang(115.7-119.0) S       -3.470e+00  8.051e-02  -43.102  < 2e-16 ***
as.factor(mydf$Link)55. Seoul Yangyang(143.0-149.6) E       -8.939e-01  7.883e-02  -11.339  < 2e-16 ***
as.factor(mydf$Link)56. Seoul Yangyang(143.0-149.6) S        9.510e-01  8.059e-02   11.800  < 2e-16 ***
as.factor(mydf$Link)57. Suncheon Wyanju (7.8-12.5) E         3.083e+00  7.768e-02   39.691  < 2e-16 ***
as.factor(mydf$Link)59. Suncheon Wyanju (12.5-20.0) E        2.203e+00  7.777e-02   28.330  < 2e-16 ***
as.factor(mydf$Link)6. KochangDamyang (19.92-24.06k) S       2.073e+00  8.230e-02   25.187  < 2e-16 ***
as.factor(mydf$Link)61. Suncheon Wyanju (25.1-32.6) E        1.702e+00  7.802e-02   21.821  < 2e-16 ***
as.factor(mydf$Link)62. Suncheon Wyanju (25.1-32.6) S        6.635e-01  7.770e-02    8.539  < 2e-16 ***
as.factor(mydf$Link)65. Suncheon Wyanju (37.9-41.8) E        2.425e+00  7.779e-02   31.178  < 2e-16 ***
as.factor(mydf$Link)66. Suncheon Wyanju (37.9-41.8) S        3.003e-01  7.744e-02    3.877 0.000106 ***
as.factor(mydf$Link)67. Suncheon Wyanju (41.8-46.6) E        6.343e-01  7.738e-02    8.197 2.49e-16 ***
as.factor(mydf$Link)68. Suncheon Wyanju (41.8-46.6) S        2.671e+00  7.717e-02   34.608  < 2e-16 ***
as.factor(mydf$Link)7. GwangjuDaegu (41.2-43.7K) E          -2.494e+00  8.108e-02  -30.767  < 2e-16 ***
as.factor(mydf$Link)8. GwangjuDaegu (41.2-43.7K) S           5.837e+00  8.118e-02   71.900  < 2e-16 ***
as.factor(mydf$Link)83. Jungbunaeryuk (106.4-108.1) E        7.240e+00  7.459e-02   97.061  < 2e-16 ***
as.factor(mydf$Link)84. Jungbunaeryuk (106.4-108.1) S        9.922e+00  7.462e-02  132.969  < 2e-16 ***
as.factor(mydf$Link)9. GwangjuDaegu (125.9-128.0K) E         5.834e+00  7.967e-02   73.225  < 2e-16 ***
as.factor(mydf$Link)93. Jungbunaeryuk (290.6-295.4) E       -2.138e+00  8.601e-02  -24.861  < 2e-16 ***
as.factor(mydf$Link)94. Jungbunaeryuk (290.6-295.4) S       -2.486e+00  8.532e-02  -29.135  < 2e-16 ***
as.factor(mydf$Link)97. Jungang (237.4-244.9) E              7.338e-01  7.986e-02    9.188  < 2e-16 ***
as.factor(mydf$Link)99. Jungang (267.8-270.4) E              6.960e-01  7.903e-02    8.806  < 2e-16 ***
---
Signif. codes:  0 ‘***’ 0.001 ‘**’ 0.01 ‘*’ 0.05 ‘.’ 0.1 ‘ ’ 1

Residual standard error: 2.56 on 147728 degrees of freedom
Multiple R-squared:  0.6825,    Adjusted R-squared:  0.6823
F-statistic:  3113 on 102 and 147728 DF,  p-value: < 2.2e-16
```

A.5.2. OLS estimation on one-day dataset

(1) OLS estimation between DV and TF

```
# OLS model without geometric variables
FMODEL1 <- lm(Inv_SPD ~ TF + TF2, data = Data_1day)
summary(FMODEL1)
##

## Call:
## lm(formula = Inv_SPD ~ TF + TF2, data = Data_1day)
##
## Residuals:
##     Min      1Q  Median      3Q     Max
## -7.2108 -2.4999 -0.6767  2.1666 21.2738
##
## Coefficients:
##                Estimate Std. Error t value Pr(>|t|)
## (Intercept) 3.154e+01  2.859e-01 110.289  < 2e-16 ***
## TF          1.563e-03  4.443e-04   3.517 0.000441 ***
## TF2         8.946e-07  1.550e-07   5.773 8.47e-09 ***
## ---
## Signif. codes:  0 '***' 0.001 '**' 0.01 '*' 0.05 '.' 0.1 ' ' 1
##
## Residual standard error: 3.602 on 3479 degrees of freedom
## Multiple R-squared:  0.3371, Adjusted R-squared:  0.3367
## F-statistic: 884.7 on 2 and 3479 DF,  p-value: < 2.2e-16
```

(2) OLS estimation with TF and geometric independent variables

```
# OLS model with all geometric variables
FMODEL2 <-lm(Inv_SPD ~ TFc + TFc2 + TR + RISE + FALL + BEND, data = Data_1da
y)
summary(FMODEL2)
##
## Call:
## lm(formula = Inv_SPD ~ TFc + TFc2 + TR + RISE + FALL + BEND,
##     data = Data_1day)
##
## Residuals:
##     Min      1Q  Median      3Q     Max
## -7.9302 -2.2311 -0.5076  1.8017 20.0884
##
## Coefficients:
##                 Estimate Std. Error t value Pr(>|t|)
## (Intercept)  2.914e+01  5.178e-01  56.269  < 2e-16 ***
## TF           1.020e-03  4.167e-04   2.448   0.0144 ***
## TF2          1.114e-06  1.453e-07   7.663 2.33e-14 ***
## TR           4.555e-03  4.631e-04   9.836  < 2e-16 ***
## RISE         8.112e-02  1.241e-02   6.539 7.10e-11 ***
## FALL         1.256e-01  1.425e-02   8.813  < 2e-16 ***
## BEND        -7.181e-03  1.104e-02  -0.651    0.515
## ---
## Signif. codes:  0 '***' 0.001 '**' 0.01 '*' 0.05 '.' 0.1 ' ' 1
##
## Residual standard error: 3.362 on 3475 degrees of freedom
## Multiple R-squared:  0.4231, Adjusted R-squared:  0.4222
## F-statistic: 424.8 on 6 and 3475 DF,  p-value: < 2.2e-16
```

A.5.3. Box-Cox test for selecting log-linear versus linear-linear form

```
# Box-Cox test for log transformation
b <- boxcox(Inv_SPD ~ TF + TF2 + TR + RISE+ FALL  , data = Data_1day)
qqPlot(rstandard(FMODEL3))
qqPlot(rstandard(FMODEL3-1))
```

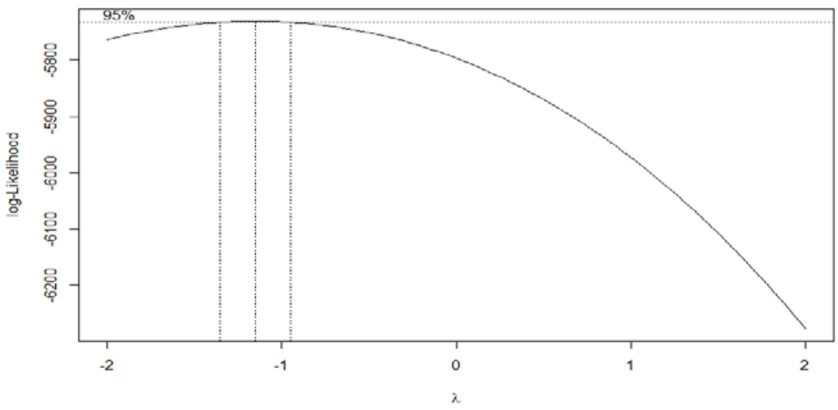

(1) q-q plot observation of the linear-linear model

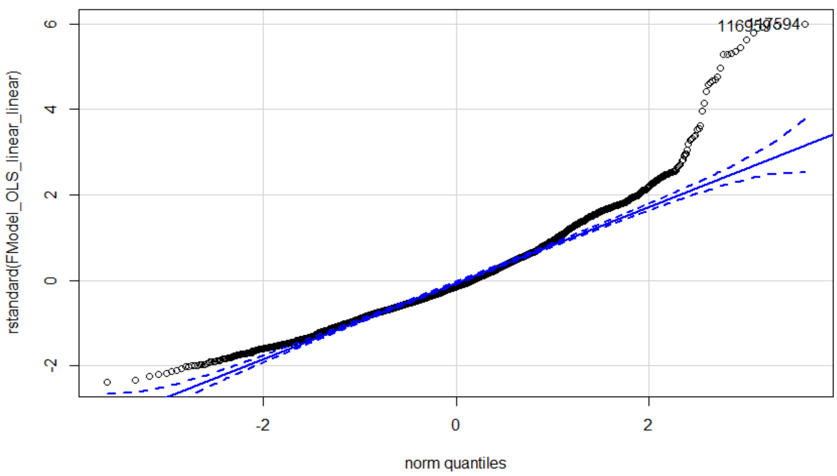

(2) q-q plot observation of the log-linear model

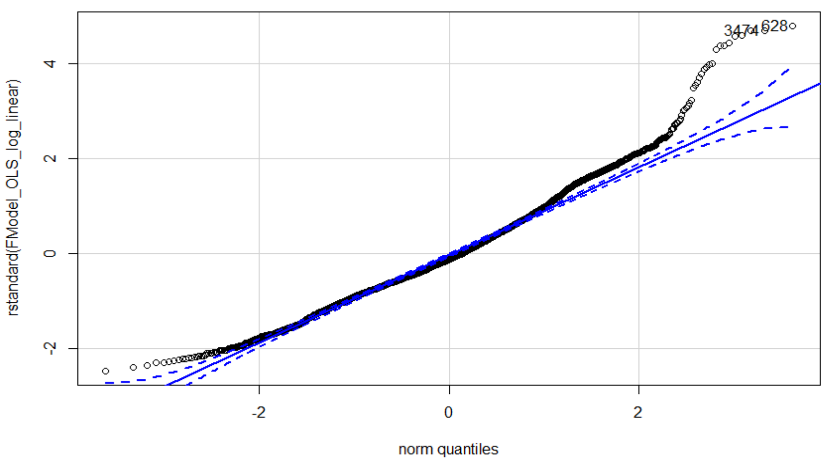

A.5.4. Coding for 10-fold cross validation

```
#Definition of road capacity
Data_1day$capacity <-2404

# 10 fold cross-validation
'%ni%' <- Negate('%in%')

fold_num <- 10
Tunnel <- levels(Data_1day$name)
Tunnel_len <- length(Tunnel)
fold_len <- floor(Tunnel_len/fold_num)
Tunnel_remain <- Tunnel

Data_1day$fold <- 0

for(i in 1:(fold_num-1)){
		sam <- sample(Tunnel_remain, fold_len)
		Data_1day[Data_1day$name %in% sam,]$fold <- i
		Tunnel_remain <- Tunnel_remain[Tunnel_remain %ni% sam]
}

Data_1day[Data_1day$name %in% Tunnel_remain,]$fold <- 10
Tunnel_remain

RMSE_k_fold_mat <- matrix(0,ncol=5,nrow=fold_num)
MAPE_k_fold_mat <- matrix(0,ncol=5,nrow=fold_num)

for(i in 1:fold_num){
		Trainset <- Data_1day[Data_1day$fold %ni% i,]
		Testset <- Data_1day[Data_1day$fold %in% i,]
		Test.true <- Testset$Inv_SPD

		### OLS Estimation ###
		FMODEL3-1 <- lm(log(Inv_SPD) ~ TF + TF2 + TR + RISE + FALL, data = Trainset)

		### GLS Estimation by dealing with heteroscedasticity###
		FMODEL3-1-3 <- gls(log(Inv_SPD) ~ TF + TF2 + TR + RISE + FALL, weights= varIdent(form = ~ 1|Link), data = Trainset, method="ML")


		### GLS Estimation by dealing with both heteroscedasticity and serial correlation###
		FMODEL3-1-17 <- gls(log(Inv_SPD) ~ TF + TF2 + TR + RISE + FALL, weights= varIdent(form = ~ 1|Link), correlation=corARMA(form = ~1|Link, p=2,q=0), data = Trainset, method="ML")

		### NLS Estimation with geometry ###
		FBPR3 <- nls(Inv_SPD ~ FFTT*(1+a*(TF/capacity)^b) + c*TR + d*RISE + e*FALL, start = list(FFTT=36, a =0.15, b =4, c=0, d=0, e=0), data= Trainset, trace = TRUE)

		### NLS Estimation without geometry ###
		FBPR1 <- nls(Inv_SPD ~ FFTT*(1+a*(TF/capacity)^b), start = list(FFTT=36, a =0.15, b =4), data= Trainset, trace = TRUE)
```

```
             OLS.pred  <- exp(predict(FMODEL3-1,Testset))
             GLS1.pred <- exp(predict(FMODEL3-1-3,Testset))
             GLS2.pred <- exp(predict(FMODEL3-1-17,Testset))
             NLS1.pred <- predict(FBPR3,Testset)
             NLS2.pred <- predict(FBPR1,Testset)

             RMSE_k_fold_mat[i,1] <- RMSE(OLS.pred,Test.true)
             RMSE_k_fold_mat[i,2] <- RMSE(GLS1.pred,Test.true)
             RMSE_k_fold_mat[i,3] <- RMSE(GLS2.pred,Test.true)
             RMSE_k_fold_mat[i,4] <- RMSE(NLS1.pred,Test.true)
             RMSE_k_fold_mat[i,5] <- RMSE(NLS2.pred,Test.true)

             MAPE_k_fold_mat[i,1] <- MAPE(OLS.pred,Test.true)
             MAPE_k_fold_mat[i,2] <- MAPE(GLS1.pred,Test.true)
             MAPE_k_fold_mat[i,3] <- MAPE(GLS2.pred,Test.true)
             MAPE_k_fold_mat[i,4] <- MAPE(NLS1.pred,Test.true)
             MAPE_k_fold_mat[i,5] <- MAPE(NLS2.pred,Test.true)
}

colnames(RMSE_k_fold_mat) <- c("FMODEL3-1","FMODEL3-1-3"," FMODEL3-1-13","
FBPR3","FBPR1")
colnames(MAPE_k_fold_mat) <- c("FMODEL3-1","FMODEL3-1-3"," FMODEL3-1-13","
FBPR3","FBPR1")

RMSE_k_fold_mat ; MAPE_k_fold_mat

Average_RMSE <- apply(RMSE_k_fold_mat,2,mean)
Average_MAPE <- apply(MAPE_k_fold_mat,2,mean)
sd_RMSE <- apply(RMSE_k_fold_mat,2,sd)
sd_MAPE <- apply(MAPE_k_fold_mat,2,sd)

Average_RMSE
sd_RMSE

Average_MAPE
sd_MAPE

write.csv(RMSE_k_fold_mat, file = "RMSE_mat_final2.csv")
write.csv(MAPE_k_fold_mat, file = "MAPE_mat_final2.csv")
```

A.5.5. Estimated travel time on three links by three models (part of result)

Demand _LINK1	Demand _LINK2	Demand _LINK3	TT_FModel _LINK1	TT_KDI_ LINK1	TT_KOTI _LINK1	TT_FModel _LINK2	TT_KDI_ LINK2	TT_KOTI _LINK2	TT_FModel _LINK3	TT_KDI_ LINK3	TT_KOTI _LINK3
1,343	1,855	2,223	34.41	40.80	31.68	36.73	43.68	33.00	38.79	46.38	34.46
1,203	995	2,322	33.88	40.19	31.44	33.17	39.41	31.17	39.41	47.19	34.93
825	1,772	2,226	32.64	38.89	31.01	36.31	43.14	32.74	38.81	46.39	34.47
926	1,609	2,089	32.95	39.19	31.09	35.54	42.17	32.28	38.00	45.33	33.87
1,116	899	1,989	33.57	39.84	31.32	32.86	39.11	31.07	37.44	44.60	33.48
557	2,030	2,138	31.92	38.29	30.85	37.67	44.90	33.64	38.28	45.70	34.08
1,014	1,373	1,463	33.23	39.47	31.19	34.53	40.94	31.74	34.90	41.38	31.93
650	2,200	1,521	32.16	38.47	30.89	38.65	46.19	34.35	35.15	41.69	32.06
1,278	1,917	1,610	34.16	40.51	31.56	37.05	44.09	33.22	35.55	42.17	32.28
825	1,643	1,414	32.64	38.89	31.01	35.70	42.36	32.36	34.70	41.14	31.82
1,221	813	2,264	33.95	40.26	31.47	32.60	38.86	31.00	39.04	46.71	34.65
1,014	1,220	2,907	33.23	39.47	31.19	33.95	40.26	31.47	43.69	52.81	38.53
996	1,438	2,367	33.17	39.41	31.17	34.80	41.26	31.87	39.70	47.57	35.16
818	1,823	2,015	32.62	38.88	31.00	36.56	43.47	32.90	37.58	44.79	33.58
964	1,719	1,827	33.06	39.31	31.13	36.06	42.82	32.58	36.58	43.49	32.91
1,037	1,480	1,909	33.30	39.55	31.21	34.97	41.47	31.96	37.01	44.04	33.19
797	1,005	2,241	32.56	38.82	30.98	33.20	39.44	31.18	38.90	46.52	34.54
1,394	2,164	1,746	34.62	41.04	31.78	38.44	45.90	34.19	36.18	42.98	32.66
1,470	1,524	2,235	34.93	41.42	31.94	35.16	41.70	32.07	38.87	46.47	34.52
607	1,039	2,709	32.05	38.38	30.87	33.31	39.56	31.22	42.12	50.76	37.15
1,057	2,097	1,753	33.37	39.63	31.24	38.04	45.39	33.91	36.22	43.03	32.68
937	736	1,410	32.98	39.22	31.11	32.39	38.66	30.94	34.68	41.12	31.81
1,025	1,864	2,122	33.26	39.51	31.20	36.78	43.74	33.03	38.19	45.58	34.01
1,298	1,710	1,362	34.24	40.59	31.60	36.01	42.76	32.55	34.49	40.89	31.72
1,061	1,727	2,631	33.38	39.64	31.24	36.09	42.87	32.60	41.53	49.99	36.66
771	2,039	1,743	32.49	38.75	30.97	37.71	44.96	33.67	36.17	42.96	32.65
937	2,354	2,320	32.98	39.22	31.11	39.61	47.46	35.09	39.39	47.17	34.92
1,224	930	2,463	33.96	40.28	31.48	32.96	39.20	31.10	40.34	48.41	35.67
1,252	1,439	1,275	34.06	40.39	31.52	34.80	41.26	31.87	34.15	40.49	31.56
1,085	1,833	2,567	33.46	39.73	31.27	36.62	43.53	32.93	41.06	49.37	36.27
1,028	1,328	2,462	33.27	39.52	31.20	34.35	40.73	31.65	40.33	48.41	35.66
862	1,468	2,003	32.75	39.00	31.04	34.92	41.41	31.94	37.52	44.70	33.53
953	1,735	1,530	33.03	39.27	31.12	36.13	42.91	32.63	35.19	41.73	32.08
1,455	1,777	3,146	34.87	41.34	31.91	36.34	43.18	32.75	45.79	55.50	40.43
924	1,463	2,514	32.94	39.18	31.09	34.90	41.39	31.93	40.69	48.88	35.96
1,238	1,312	1,180	34.01	40.33	31.50	34.29	40.66	31.62	33.80	40.09	31.41
979	908	2,205	33.11	39.36	31.15	32.89	39.13	31.08	38.68	46.23	34.37
1,111	2,086	1,768	33.56	39.82	31.31	37.98	45.30	33.86	36.29	43.12	32.73
1,042	1,606	2,345	33.32	39.57	31.22	35.53	42.15	32.27	39.56	47.38	35.05
1,147	1,419	2,253	33.68	39.96	31.36	34.72	41.16	31.83	38.98	46.62	34.60
1,178	1,625	1,354	33.79	40.08	31.40	35.61	42.26	32.32	34.46	40.85	31.70
1,016	1,425	537	33.23	39.48	31.19	34.74	41.19	31.84	31.87	38.25	30.84
1,258	1,507	2,449	34.09	40.42	31.53	35.09	41.61	32.03	40.24	48.29	35.59
868	1,654	1,365	32.77	39.02	31.04	35.75	42.43	32.39	34.50	40.90	31.72
1,029	1,961	2,012	33.28	39.53	31.21	37.28	44.40	33.37	37.57	44.77	33.57
1,381	1,779	2,678	34.57	40.98	31.76	36.35	43.19	32.76	41.88	50.44	36.95
1,227	2,406	1,903	33.97	40.28	31.48	39.96	47.91	35.36	36.98	44.00	33.17

A.5.6. Application to traffic assignment by three models

	DoNotthing		KDI (2015)				FModel			
O-D	TF_City	TT_City (veh*hours)	TF_City	TF_Bypass	TT_City (veh*hours)	TT_Bypass (veh*hours)	TF_City	TF_Bypass	TT_City (veh*hours)	TT_Bypass (veh*hours)
3,411	3,411	99,217	2,053	1,357	27,972	18,492	1,688	1,723	20,277	20,696
2,948	2,948	64,761	1,952	996	25,640	13,089	1,557	1,390	17,947	16,023
2,007	2,007	26,265	1,835	171	23,158	2,161	1,318	689	14,159	7,396
2,860	2,860	59,625	1,935	925	25,274	12,085	1,534	1,327	17,542	15,176
3,050	3,050	71,285	1,972	1,078	26,099	14,269	1,586	1,465	18,434	17,028
2,293	2,293	34,641	1,854	439	23,552	5,575	1,387	907	15,185	9,928
2,072	2,072	27,990	1,838	234	23,217	2,959	1,333	739	14,385	7,972
1,246	1,246	12,439	1,246	-	13,132	-	1,160	86	11,956	890
2,725	2,725	52,417	1,911	813	24,758	10,535	1,497	1,227	16,937	13,885
1,983	1,983	25,677	1,834	149	23,142	1,875	1,313	670	14,079	7,192
2,149	2,149	30,129	1,843	306	23,310	3,872	1,352	797	14,654	8,643
3,415	3,415	99,606	2,054	1,361	27,997	18,544	1,689	1,726	20,300	20,742
2,281	2,281	34,246	1,853	428	23,529	5,436	1,384	898	15,141	9,822
1,951	1,951	24,889	1,834	117	23,123	1,478	1,305	646	13,971	6,911
3,356	3,356	94,451	2,040	1,316	27,664	17,844	1,672	1,684	19,985	20,127
2,906	2,906	62,274	1,944	963	25,463	12,612	1,546	1,360	17,753	15,620
1,857	1,857	22,728	1,832	25	23,096	309	1,284	573	13,665	6,096
2,047	2,047	27,320	1,837	210	23,193	2,656	1,328	720	14,298	7,752
1,945	1,945	24,751	1,833	112	23,120	1,408	1,304	641	13,952	6,861
1,848	1,848	22,547	1,832	16	23,095	206	1,282	566	13,639	6,025
2,384	2,384	37,793	1,864	520	23,747	6,625	1,409	974	15,531	10,740
2,962	2,962	65,626	1,954	1,008	25,701	13,251	1,561	1,401	18,013	16,161
3,045	3,045	70,934	1,971	1,074	26,075	14,208	1,584	1,461	18,409	16,976
2,186	2,186	31,230	1,845	341	23,364	4,313	1,360	825	14,788	8,972
1,719	1,719	19,897	1,719	-	20,866	-	1,254	465	13,238	4,914
2,162	2,162	30,507	1,844	318	23,328	4,025	1,355	807	14,700	8,757
3,277	3,277	87,892	2,022	1,255	27,232	16,910	1,650	1,628	19,570	19,311
2,169	2,169	30,713	1,844	325	23,338	4,108	1,356	812	14,725	8,819
2,934	2,934	63,925	1,949	985	25,581	12,931	1,554	1,380	17,882	15,889
2,795	2,795	56,026	1,923	871	25,017	11,334	1,516	1,279	17,246	14,548
Sum of Total TT	73,984	1,411,798	56,269	17,714	723,783	233,111	43,117	30,867	482,363	349,870
Benefit (Time savings)		-				454,905				579,566
Percentage change of benefit										22%

	DoNotthing		KOTI (2009)				FMode			
O-D	TF_City	TT_City (veh*hours)	TF_City	TF_Bypass	TT_City (veh*hours)	TT_Bypass (veh*hours)	TF_City	TF_Bypass	TT_City (veh*hours)	TT_Bypass (veh*hours)
3,411	3,411	99,217	1,443	1,967	16,070	21,903	1,688	1,723	20,277	20,696
2,948	2,948	64,761	1,327	1,621	13,513	17,455	1,557	1,390	17,947	16,023
2,007	2,007	26,265	1,172	835	11,504	8,627	1,318	689	14,159	7,396
2,860	2,860	59,625	1,308	1,553	13,247	16,632	1,534	1,327	17,542	15,176
3,050	3,050	71,285	1,351	1,699	13,844	18,424	1,586	1,465	18,434	17,028
2,293	2,293	34,641	1,206	1,088	11,920	11,340	1,387	907	15,185	9,928
2,072	2,072	27,990	1,179	894	11,584	9,255	1,333	739	14,385	7,972
1,246	1,246	12,439	1,140	106	11,117	1,089	1,160	86	11,956	890
2,725	2,725	52,417	1,279	1,445	12,868	15,363	1,497	1,227	16,937	13,885
1,983	1,983	25,677	1,170	813	11,477	8,402	1,313	670	14,079	7,192
2,149	2,149	30,129	1,187	962	11,689	9,979	1,352	797	14,654	8,643
3,415	3,415	99,606	1,445	1,971	15,207	21,946	1,689	1,726	20,300	20,742
2,281	2,281	34,246	1,204	1,077	11,899	11,228	1,384	898	15,141	9,822
1,951	1,951	24,889	1,167	784	11,442	8,093	1,305	646	13,971	6,911
3,356	3,356	94,451	1,429	1,928	14,967	21,368	1,672	1,684	19,985	20,127
2,906	2,906	62,274	1,318	1,589	13,385	17,064	1,546	1,360	17,753	15,620
1,857	1,857	22,728	1,160	697	11,352	7,185	1,284	573	13,665	6,096
2,047	2,047	27,320	1,176	871	11,552	9,016	1,328	720	14,298	7,752
1,945	1,945	24,751	1,167	779	11,436	8,037	1,304	641	13,952	6,861
1,848	1,848	22,547	1,159	689	11,345	7,104	1,282	566	13,639	6,025
2,384	2,384	37,793	1,219	1,165	12,086	12,185	1,409	974	15,531	10,740
2,962	2,962	65,626	1,330	1,632	13,557	17,588	1,561	1,401	18,013	16,161
3,045	3,045	70,934	1,350	1,695	13,826	18,373	1,584	1,461	18,409	16,976
2,186	2,186	31,230	1,192	994	11,744	10,330	1,360	825	14,788	8,972
1,719	1,719	19,897	1,151	568	11,250	5,842	1,254	465	13,238	4,914
2,162	2,162	30,507	1,189	973	11,708	10,101	1,355	807	14,700	8,757
3,277	3,277	87,892	1,408	1,870	14,657	20,598	1,650	1,628	19,570	19,311
2,169	2,169	30,713	1,189	979	11,718	10,167	1,356	812	14,725	8,819
2,934	2,934	63,925	1,324	1,610	13,470	17,325	1,554	1,380	17,882	15,889
2,795	2,795	56,026	1,294	1,501	13,059	16,017	1,516	1,279	17,246	14,548
Sum of Total TT	73,984	1,411,798	37,629	36,355	378,493	388,034	43,117	30,867	482,363	349,870
Benefit (Time savings)		-				645,272				579,566
Percentage change of benefit										-11%

References

Abbas, S.K.S., Adnan, M.A. and Endut, I.R. (2011) Exploration of 85th percentile operating speed model on horizontal curve: a case study for two-lane rural highways. *Procedia-Social and behavioral sciences,* 16, 352-363.

Agarwal, M., Maze, T.H. and Souleyrette, R. (2005) Impacts of weather on urban freeway traffic flow characteristics and facility capacity *Proceedings of the 2005 mid-continent transportation research symposium*. 18-19.

Ahmed, M.M. and Abdel-Aty, M.A. (2011) The viability of using automatic vehicle identification data for real-time crash prediction. *IEEE Transactions on Intelligent Transportation Systems,* 13 (2), 459-468.

Akaike, H. (1974) A new look at the statistical model identification *Selected Papers of Hirotugu Akaike*. New York, NY: Springer, 215-222.

Akçelik, R. (1991) Travel time functions for transport planning purposes: Davidson's function, its time dependent form and alternative travel time function. *Australian Road Research,* 21 (3).

Allison, P. (2012) When can you safely ignore multicollinearity. *Statistical Horizons,* 5 (1).

Amemiya, T. (1985) *Advanced econometrics*. Massachusetts, USA: Harvard university press.

Baltagi, B. (2008) *Econometric analysis of panel data*. Chichester: John Wiley & Sons.

Baltagi, B. (2013) *Econometric analysis of panel data*, 5th edition ed. Chichester: John Wiley & Sons.

Bando, M., Hasebe, K., Nakayama, A., Shibata, A. and Sugiyama, Y. (1995) Dynamical model of traffic congestion and numerical simulation. *Physical Review E,* 51 (2), 1035.

Beckmann, M., McGuire, C.B. and Winsten, C.B. (1956) *Studies in the Economics of Transportation*. New Haven: Yale University Press.

Bell, M., Bonsall, P., Leake, G., May, A., Nash, C. and O'Flaherty, C. (1997) *Transport planning and traffic engineering*. Oxford, UK: Elsevier.

Bella, F., Calvi, A. and D'Amico, F. (2014) Analysis of driver speeds under night driving conditions using a driving simulator. *Journal of Safety Research,* 49, 45-42.

Belsley, D.A., Kuh, E. and Welsch, R.E. (1980) *Regression diagnostics: identifying influential data and sources of collinearity*. New Jersey: John Wiley & Sons.

Boardman, A., Greenberg, D. and Vining, A. (2013) *Cost-Benefit Analysis: Pearson New International Edition*. Harlow, Essex: Pearson Education Limited.

Branston, D. (1976) Link capacity functions: A review. *Transportation Research,* 10 (4), 223-236.

Breusch, T.S. (1978) Testing for autocorrelation in dynamic linear models. *Australian Economic Papers,* 17 (31), 334-355.

Breusch, T.S. and Pagan, A.R. (1979) A simple test for heteroscedasticity and random coefficient variation. *Econometrica: Journal of the Econometric Society*, 1287-1294.

Brilon, W. (2000) Traffic flow analysis beyond traditional methods *Proceedings of the 4th International Symposium on Highway Capacity*, Washington DC, USA. Transportation Research Board 26-41.

Brilon, W. and Bressler, A. (2004) Traffic flow on freeway upgrades. *Transportation Research Record: Journal of the Transportation Research Board*, 1883 (1), 112-121.

Brilon, W., Geistefeldt, J. and Regler, M. (2005) Reliability of freeway traffic flow: a stochastic concept of capacity *Proceedings of the 16th International symposium on transportation and traffic theory*. College Park Maryland.

Brilon, W., Geistefeldt, J. and Zurlinden, H. (2007) Implementing the concept of reliability for highway capacity analysis. *Transportation Research Record: Journal of the Transportation Research Board*, (2027), 1-8.

Brilon, W. and Lemke, K. (1997) *Fehmarn-Belt-Querung — Szenarische Leistungsfaehigkeitsbetrachtung für einen Tunnel, (Fixed Link across Fehmarn Belt — Capacity Considerations for Different Scenarios), Research Report for the German Federal DOT*. Ruhr-University Bochum.

Brilon, W. and Lemke, K. (1999) *Strassenquerschnitte in Tunneln (Cross Sections in Road Tunnels), Research Report 02.163 for the German Federal DOT*. Ruhr-University Bochum,.

Brilon, W. and Lemke, K. (2000) Cross Sections in Road Tunnels *2nd International Symposium on Highway Geometric Design*, Mainz, Germany. FGSV Publishers.

Bureau of Public Roads (1964) *Traffic Assignment Manual*. Washington, DC: US Department of Commerce.

Burnham, K.P. and Anderson, D.R. (2004) Multimodel inference: understanding AIC and BIC in model selection. *Sociological methods & research*, 33 (2), 261-304.

Campbell, E.W., Keefer, L.E. and Adams, R.W. (1959) A method for predicting speeds through signalized street sections. *Highway Research Board bulletin*, 230, 112-125.

Cartenì, A. and Punzo, V. (2007) Travel time cost functions for urban roads: A case study in Italy. *WIT Transactions on the Built Environment*, 96, 233-243.

Castro, M., Sánchez, J.F., Sánchez, J.A. and Iglesias, L. (2011) Operating speed and speed differential for highway design consistency. *Journal of transportation engineering*, 137 (11), 837-840.

Cheevarunothai, P., Wang, Y. and Nihan, N.L. (2006) Identification and correction of dual-loop sensitivity problems. *Transportation Research Record*, 1945 (1), 73-81.

Chen, H.-K. and Hsueh, C.-F. (1998) A model and an algorithm for the dynamic user-optimal route choice problem. *Transportation Research Part B: Methodological*, 32 (3), 219-234.

Chiu, Y.-C., Bottom, J., Mahut, M., Paz, A., Balakrishna, R., Waller, T. and Hicks, J. (2011) Dynamic traffic assignment: A primer. *Transportation Research Board*, (E-C153).

Chu, C.-Y. and Durango-Cohen, P.L. (2008) Estimation of dynamic performance models for transportation infrastructure using panel data. *Transportation Research Part B: Methodological,* 42 (1), 57-81.

Cools, M., Moons, E. and Wets, G. (2007) Investigating effect of holidays on daily traffic counts: time series approach. *Transportation Research Record*, 2019 (1), 22-31.

Correa, J.R. and Stier-Moses, N.E. (2010) Wardrop equilibria. *Wiley Encyclopedia of Operations Research and Management Science*.

Dalal, D.K. and Zickar, M.J. (2012) Some common myths about centering predictor variables in moderated multiple regression and polynomial regression. *Organizational Research Methods,* 15 (3), 339-362.

Davidson, K.B. (1978) The theoretical basis of a flow–travel time relationship for use in transportation planning. *Australian Road Research,* 8 (1), 32-35.

Dee, T.S. (1999) State alcohol policies, teen drinking and traffic fatalities. *Journal of public Economics,* 72 (2), 289-315.

DfT (2018) *Transport analysis guidance: WebTAG*. UK government. Available from: https://www.gov.uk/guidance/transport-analysis-guidance-webtag [Accessed 12 June 2018].

Diggle, P., Diggle, P.J., Heagerty, P., Heagerty, P.J., Liang, K.-Y. and Zeger, S. (2002) *Analysis of longitudinal data*, 2nd ed.: Oxford University Press.

Dong, J. and Mahmassani, H. (2009) Flow breakdown and travel time reliability. *Transportation Research Record: Journal of the Transportation Research Board,* 2124 (1), 203-212.

Dowling, R., Kittelson, W. and Skabardonis, A. (1997) *NCHRP Report 387: Planning techniques to estimate speeds and service volumes for planning applications*. Washington D.C., USA: National Academy Press.

Dowling, R.G. and Skabardonis, A. (2008) Urban arterial speed–flow equations for travel demand models *Innovations in Travel Demand Modeling Conference*, Texas, United States, 21-23 May 2006.

Durbin, J. and Watson, G.S. (1951) Testing for serial correlation in least squares regression. II. *Biometrika,* 38 (1/2), 159-177.

Elefteriadou, L., Roess, R.P. and McShane, W.R. (1995) Probabilistic nature of breakdown at freeway merge junctions. *Transportation Research Record,* 1484, 80-89.

Eskeland, G.S. and Feyzioğlu, T.N. (1997) Is demand for polluting goods manageable? An econometric study of car ownership and use in Mexico. *Journal of Development Economics,* 53 (2), 423-445.

Fagnant, D.J. and Kockelman, K.M. (2012) Outcome of Transportation Projects Under Uncertainty: Examination of Benefit–Cost Ratios and other Impacts. *Transportation research record,* 2303 (1), 89-98.

FHWA (1998) *Travel time data collection handbook*. United States. Federal Highway Administration.

Findley, D.J., Schroeder, B., Cunningham, C. and Brown, T. (2015) *Highway Engineering: Planning, Design, and Operations*. Oxford, UK: Butterworth-Heinemann.

Fitzmaurice, G.M., Laird, N.M. and Ware, J.H. (2004) *Applied longitudinal analysis*, 2nd ed. New Jersey: Wiley.

Flyvbjerg, B., Skamris Holm, M.K. and Buhl, S.L. (2005) How (in)accurate are demand forecasts in public works projects?: the case of transportation. *Journal of the American Planning Association,* 71 (2), 131-146.

Fox, J. and Weisberg, S. (2010) *An R Companion to Applied Regression*, 2nd ed. California, USA: SAGE.

Frank, M. and Wolfe, P. (1956) An algorithm for quadratic programming. *Naval Research Logistics Quarterly,* 3 (1-2), 95-110.

Freedman, D.A. (2009) *Statistical models: theory and practice*, 2nd ed. New York, USA: Cambridge University Press.

Friesz, T.L., Bernstein, D., Smith, T.E., Tobin, R.L. and Wie, B.-W. (1993) A variational inequality formulation of the dynamic network user equilibrium problem. *Operations Research,* 41 (1), 179-191.

Gao, H.O. and Niemeier, D.A. (2007) The impact of rush hour traffic and mix on the ozone weekend effect in southern California. *Transportation Research Part D: Transport and Environment,* 12 (2), 83-98.

Godfrey, L.G. (1978) Testing against general autoregressive and moving average error models when the regressors include lagged dependent variables. *Econometrica: Journal of the Econometric Society,* 1293-1301.

Goldfeld, S.M. and Quandt, R.E. (1965) Some tests for homoscedasticity. *Journal of the American Statistical Association,* 60 (310), 539-547.

Green, S.B. (1991) How many subjects does it take to do a regression analysis. *Multivariate Behavioral Research,* 26 (3), 499-510.

Greenberg, H. (1959) An analysis of traffic flow. *Operations Research,* 7 (1), 79-85.

Greene, W.H. (2018) *Econometric Analysis*, 8th ed. New York, USA: Pearson

Greenshields, B., Channing, W. and Miller, H. (1935) A study of traffic capacity *Highway research board proceedings*. National Research Council (USA), Highway Research Board.

Hamilton, L.C. (2012) *Statistics with Stata: Updated for Version 12*. Boston, USA: Cengage Learning.

Hanley, N. and Spash, C.L. (1993) *Cost-benefit analysis and the environment*. Cheltenham, UK: Edward Elgar.

Hansen, S., Byrd, A., Delcambre, A., Rodriguez, A., Matthews, S. and Bertini, R.L. (2005) Using archived ITS data to improve regional performance measurement and travel demand forecasting *2005 CITE Quad/WCTA Regional Conference,* Vancouver, BC, Canada., 7-9 April 2005.

Harrell, F.E. (2001) *Regression modeling strategies*. New York: Springer.

Hausman, J.A. (1978) Specification tests in econometrics. *Econometrica: Journal of the Econometric Society*, 1251-1271.

Hayashi, Y. and Morisugi, H. (2000) International comparison of background concept and methodology of transportation project appraisal. *Transport Policy,* 7 (1), 73-88.

He, N. and Zhao, S.-c. (2014) Urban Road Traffic Impedance Function—Dalian City Case Study. *Journal of Highway and Transportation Research and Development (English Edition),* 8 (3), 90-95.

Heydecker, B.G. and Addison, J. (2005) Analysis of dynamic traffic equilibrium with departure time choice. *Transportation Science,* 39 (1), 39-57.

HM Treasury (2003) *The Green Book*. UK government. Available from: https://www.gov.uk/government/publications/the-green-book-appraisal-and-evaluation-in-central-governent [Accessed 13 June 2018].

Hong-Di, H., Wei-Zhen, L., Yu, X. and Li-Yun, D. (2009) Dynamic characteristics and simulation of traffic flow with slope. *Chinese Physics B,* 18 (7), 2703.

Hoogendoorn, S.P. and Bovy, P.H. (2001) State-of-the-art of vehicular traffic flow modelling. *Proceedings of the Institution of Mechanical Engineers, Part I: Journal of Systems and Control Engineering,* 215 (4), 283-303.

Hsiao, C. (2014) *Analysis of Panel Data* Cambridge, UK: Cambridge University Press.

Huntsinger, L.F. and Rouphail, N.M. (2011) Bottleneck and queuing analysis: calibrating volume–delay functions of travel demand models. *Transportation Research Record,* 2255 (1), 117-124.

Irawan, M.Z., Sumi, T. and Munawar, A. (2010) Implementation of the 1997 Indonesian highway capacity manual (MKJI) volume delay function. *Journal of the Eastern Asia Society for Transportation Studies,* 8, 350-360.

ITS KOREA (2016) *ITS International Business Assistance Center*. Available from: https://intl.its.go.kr/en/02_05_04 [Accessed 17/06].

Iwasaki, M. (1991) Empirical analysis of congested traffic flow characteristics and free speed affected by geometric factors on an intercity expressway. *Transportation Research Record,* 1320, 242-250.

Jones, I.S. (1977) *Urban Transport Appraisal*. London and Basingstoke, UK: The Macmillan Press Ltd.

Kalaee, M.S. (2010) *Investigating freeway speed-flow relationships for traffic assignment applications*. Portland State University.

KDI (2008a) *General Guidelines for Preliminary Feasibility Studies*. Korea: Korean Development Institute.

KDI (2008b) *Standard Guidelines for Preliminary Feasibility Studies of Road and Railroad projects* Korea: Korean Development Institute.

KDI (2015) *VDF user's manual*. Korea: Korean Development Institute.

KEC (2016) *Practical design manual for Korean expressways*. Korea: Korean Expressway Corporation.

Kerner, B.S. (2009) *Introduction to modern traffic flow theory and control: the long road to three-phase traffic theory*. Berlin: Springer.

Kerner, B.S. (2016) Failure of classical traffic flow theories: Stochastic highway capacity and automatic driving. *Physica A: Statistical Mechanics and its Applications,* 450, 700-747.

KICT, KOTI and KST (1999) *Improvement Research for Korean Highway Capacity Manual*. Korea: Ministry of construction and transport,.

Kiefer, J. (1953) Sequential minimax search for a maximum. *Proceedings of the American mathematical society,* 4 (3), 502-506.

Kim, S., Choi, J., Lee, D. and Jang, T. (2014) Model of volume-delay formula to assess travel time savings of underground tunnel roads. *KSCE Journal of Civil Engineering,* 18 (6), 1839-1846.

Kim, S. and Seo, Y. (1999) Analysis of road capacity in basic segments of 8-lane freeway *Journal of Korean Society of Transportation*, 87-96.

Kim, Y. (2013) *Development of the Highway Capacity Estimation Method and Capacity Correction Factor for Rainfall*, Ajou Unversity.

Kim, Y.S., Cho, W.B. and Kim, J.K. (2011) Terrain classification for road design. *Korean Road Academic Association Journal* 13 (4), 221-229.

Kohavi, R. (1995) A study of cross-validation and bootstrap for accuracy estimation and model selection *International Joint Conference on Artificial Intelligence*, Stockholm, Sweden, 31 July - 6 August 1999. 1137-1145.

Komada, K., Masukura, S. and Nagatani, T. (2009) Effect of gravitational force upon traffic flow with gradients. *Physica A: Statistical Mechanics and its Applications,* 388 (14), 2880-2894.

Korean National Assembly (2017) *The final report of the audit by Korean National Assembly in 2016*. Korea: Korean national assembly.

Koshi, M. (1985) Traffic flow phenomena in expressway tunnels. *IATSS research,* 9 (1), 50-56.

Koshi, M., Kuwahara, M. and Akahane, H. (1992) Capacity of sags and tunnels on Japanese motorways. *ITE Journal,* 62 (5), 17-22.

KOTI (2009) *Survey and Research for Road Link Cost Function* Korea: Ministry of Land, Transport and Maritime affairs.

Kraemer, H.C. and Blasey, C.M. (2004) Centring in regression analyses: a strategy to prevent errors in statistical inference. *International journal of methods in psychiatric research,* 13 (3), 141-151.

Kucharski, R. and Drabicki, A. (2017) Estimating macroscopic volume delay functions with the traffic density derived from measured speeds and flows. *Journal of Advanced Transportation,* 2017.

Kurt, S. (2018) *Panel Data: Fixed and Random Effects: short guides to microeconometrics*. Unversität Basel, Switzerland. Available from: http://www. schmidheiny. name/teaching/panel2up. pdf [Accessed 05 July 2019].

Kurth, D.L., Van den Hout, A. and Ives, B. (1996) Implementation of highway capacity manual–based volume-delay functions in regional traffic assignment process. *Transportation Research Record*, 1556 (1), 27-36.

Lee, M.-Y. (2016) On the Durbin-Watson statistic based on a Z-test in large samples. *International Journal of Computational Economics and Econometrics*, 6 (1), 114-121.

Lemke, K. (2000) *Verkehrsablauf in Tunneln und dessen Auswirkungen auf die Wahl des Tunnelquerschnitts (Traffic Flow in Road Tunnels and its Consequences on the Selection of the Cross Section)*. Institute for Traffic Engineering and Transportation: Ruhr-University Bochum,.

Leong, L.V. (2017) Delay functions in trip assignment for transport planning process *AIP Conference Proceedings*. AIP Publishing LLC, 060006.

Leong, L.V. and Tan, K.Y. (2015) Volume-Delay Function in Trip Assignment *Applied Mechanics and Materials*. Trans Tech Publ, 351-356.

Leurent, F.M. (1998) Multicriteria assignment modeling: Making explicit the determinants of mode or path IN: Marcotte, P. and Nguyen, S. (eds.) *Equilibrium and Advanced Transportation Modelling*. Boston: Springer, 153-174.

Loizides, J. and Tsionas, E.G. (2002) Productivity growth in European railways: a new approach. *Transportation Research Part A: Policy and Practice*, 36 (7), 633-644.

Lorenz, M. and Elefteriadou, L. (2001) Defining freeway capacity as function of breakdown probability. *Transportation Research Record: Journal of the Transportation Research Board*, (1776), 43-51.

Mackie, P. and Preston, J. (1998) Twenty-one sources of error and bias in transport project appraisal. *Transport Policy*, 5 (1), 1-7.

Maddala, G.S. (1992) *Introduction to Econometrics*, 2nd ed. New York, USA: The Macmillan Press Ltd.

Manzo, S., Nielsen, O.A. and Prato, C.G. (2013) Investigating uncertainty in BPR formula parameters: a case study *Strategic Research in Transport and Infrastructure*.

Manzo, S., Nielsen, O.A. and Prato, C.G. (2014) Effects of Uncertainty in Speed–Flow Curve Parameters on a Large-Scale Model: Case Study of the Danish National Model. *Transportation Research Record*, 2429 (1), 30-37.

May, A.D. (1990) *Traffic flow fundamentals*.

Merchant, D.K. and Nemhauser, G.L. (1978) Optimality conditions for a dynamic traffic assignment model. *Transportation Science*, 12 (3), 200-207.

Minderhoud, M.M., Botma, H. and Bovy, P.H. (1997) Assessment of roadway capacity estimation methods. *Transportation Research Record*, 1572 (1), 59-67.

Mitsakis, E., Salanova, J.M. and Giannopoulos, G. (2011) Combined dynamic traffic assignment and urban traffic control models. *Procedia-Social and Behavioral Sciences*, 20, 427-436.

MLTM (2011a) *2nd Road Master Plan_revised (2011-2020)*. Korea: Ministry of Land, Transport and Maritime affairs.

MLTM (2011b) *Improvement Study of Transportation infrastructure investment appraisal guideline (road sector)* Korea: Ministry of Land, Transport and Maritime affairs.

MLTM (2011c) *National Transport Network Masterplan (2001-2020) 2nd revised*. Korea: Ministry of Land, Transport and Maritime affairs.

MLTM (2013) *Korean Highway Capacity Manual* Korea: Ministry of Land, Transport and Maritime affairs.

MOLIT (2014) *The Study for the Renewal of Nationwide Passenger O/D*. Korea: Ministry of Land, Infrastructure and Transport.

MOLIT (2015) *Road Standard Regulation about Structures and Facilities*. Korea: Ministry of Land, Infrastructure and Transport.

MOLIT (2016a) *2015 Road Traffic Statistics Annual Report*. Korea: Ministry of Land, Infrastructure and Transport.

MOLIT (2016b) *Road Policy Handbook*. Korea: Ministry of Land, Infrastructure and Transport.

MOLIT (2018) *Road Traffic Survey*. Korea: Ministry of Land, Infrastructure and Transport.

Montgomery, D.C., Peck, E.A. and Vining, G.G. (2012) *Introduction to linear regression analysis*. New Jersey: John Wiley & Sons.

Nagurney, A. (1998) *Network Economics: A Variational Inequality Approach*. Boston: Kluwer Academic Publisher.

Nellthorp, J. and Mackie, P.J. (2000) The UK Roads Review—a hedonic model of decision making. *Transport Policy,* 7 (2), 127-138.

Nielsen, O.A. and Jørgensen, R.M. (2008) Estimation of speed–flow and flow–density relations on the motorway network in the greater Copenhagen region. *IET Intelligent Transport Systems,* 2 (2), 120-131.

Nobel, D. and Yagi, S. (2017) Network Assignment Calibration of BPR Function: A Case Study of Metro Manila, the Philippines. *Journal of the Eastern Asia Society for Transportation Studies,* 12, 598-615.

Ortúzar, J.d.D. and Willumsen, L.G. (2012) *Modelling Transport*, 4th ed. Chiechester, West Sussex: Wiley.

Park, R.E. (1966) Estimation with heteroscedastic error terms. *Econometrica (pre-1986),* 34 (4), 888.

Patriksson, M. (2015) *The traffic assignment problem: models and methods*. New York: Dover Publications.

Pearce, D.W. (1971) *Cost-benefit analysis*. London, UK: The Macmillan Press Ltd.

Peeta, S. and Ziliaskopoulos, A.K. (2001) Foundations of dynamic traffic assignment: The past, the present and the future. *Networks and spatial economics,* 1 (3-4), 233-265.

Persaud, B., Yagar, S. and Brownlee, R. (1998) Exploration of the breakdown phenomenon in freeway traffic. *Transportation Research Record: Journal of the Transportation Research Board,* (1634), 64-69.

Petrik, O., Moura, F. and Silva, J.d.A.e. (2014) The Influence of the volume–delay function on uncertainty assessment for a four-step model IN: Sousa, J.F.D. and Rossi, R. (eds.) *Computer-based Modelling and Optimization in Transportation*. Switzerland: Springer, 293-306.

Pinheiro, J.C. and Bates, D.M. (2000) *Mixed-effects models in S and S-Plus*. New York: Springer.

Pipes, L.A. (1953) An operational analysis of traffic dynamics. *Journal of applied physics,* 24 (3), 274-281.

Preston, J. (2017) *Lecture 5: Transport Appraisal and Evaluation – Theory in Transport Economics,* lecture notes distributed in the module CENV6016, Transport Economics. at the University of Southampton, Southampton, UK, January 2017.

Price, A. (1999) The new approach to the appraisal of road projects in England. *Journal of Transport Economics and Policy,* 33 (2), 221-226.

Rakha, H. and Crowther, B. (2002) Comparison of Greenshields, Pipes, and Van Aerde car-following and traffic stream models. *Transportation Research Record,* 1802 (1), 248-262.

Rakha, H., Farzaneh, M., Arafeh, M., Hranac, R., Sterzin, E. and Krechmer, D. (2007) *Empirical studies on traffic flow in inclement weather*. Richmond, USA: Virginia Department for Transportation.

Rakha, H. and Tawfik, A. (2009) Traffic networks: dynamic traffic routing, assignment, and assessment *Encyclopedia of Complexity and Systems Science*. New York, USA: Springer, 9429-9470.

Ren, Q., Li, M. and Han, S. (2019) Tectonic discrimination of olivine in basalt using data mining techniques based on major elements: a comparative study from multiple perspectives. *Big Earth Data,* 3 (1), 8-25.

Republic of Korea (2016a) *Construction Technology Promotion Act*. Korea: Ministry of Land, Infrastructure and Transport.

Republic of Korea (2016b) *National Finance Act*. Korea: Ministry of Economy and Finance.

Republic of Korea (2017) *National Transport System Efficiency Act*. Korea: Ministry of Land, Infrastructure and Transport.

Roess, R.P. and Prassas, E.S. (2014) *The highway capacity manual: A conceptual and research history*. Springer.

Saltelli, A., Ratto, M., Andres, T., Campolongo, F., Cariboni, J., Gatelli, D., Saisana, M. and Tarantola, S. (2008) *Global sensitivity analysis: the primer*. John Wiley & Sons.

Saw, K., Katti, B. and Joshi, G. (2015) Literature review of traffic assignment: static and dynamic. *International Journal of Transportation Engineering,* 2 (4), 339-347.

Schmidt, F.L. (1971) The relative efficiency of regression and simple unit predictor weights in applied differential psychology. *Educational and Psychological Measurement,* 31 (3), 699-714.

Sheffi, Y. (1985) *Urban transportation networks: Equilibrium analysis with mathematical programming methods*. Englewood Cliffs, NJ, USA Prentice-Hall, Inc.

Singh, R. (1995) Beyond the BPR curve: Updating speed-flow and speed-capacity relationships in traffic assignment *Fifth National Conference on Transportation Planning Methods Applications-Volume II: A Compendium of Papers*, Seattle, Washington, April 1995. Transportation Research Boad.

Singh, R. and Dowling, R. (2002) Improved speed-flow relationships: application to transportation planning models *Seventh TRB Conference on the Application of Transportation Planning Methods*, Boston, Massachusetts, 7-11 March 1999. Transportation Research Board, 340-349.

Skabardonis, A. and Dowling, R. (1997) Improved speed-flow relationships for planning applications. *Transportation Research Record*, 1572 (1), 18-23.

Smock, R. (1962) An iterative assignment approach to capacity restraint on arterial networks *41st Annual Meeting of the Highway Research Board*, Washington DC, USA, 8-12 January 1962. Highway Research Board, 60-66.

Spiess, A.-N. and Neumeyer, N. (2010) An evaluation of R2 as an inadequate measure for nonlinear models in pharmacological and biochemical research: a Monte Carlo approach. *BMC pharmacology*, 10 (1), 6.

Spiess, H. (1990) Technical note—Conical volume-delay functions. *Transportation Science*, 24 (2), 153-158.

Steenbrink, P.A. (1974) *Optimization of transport networks*. New Jersey: John Wiley & Sons.

Sugden, R. (1999) *Developing a consistent cost-benefit framework for multi-modal transport appraisal*. Economics Research Centre University of East Anglia, report to Department of Transport.

Swamy, P. and Arora, S.S. (1972) The exact finite sample properties of the estimators of coefficients in the error components regression models. *Econometrica: Journal of the Econometric Society*, 261-275.

Torres-Reyna, O. (2007) *Panel data analysis fixed and random effects using Stata (v. 4.2)*. Data & Statistical Services, Princeton University.

UK Highways Agency (2002) *UK Design Manual for Roads & Bridges (DMRB)*.

Underwood, R.T. (1961) Speed, volume, and density relationships: quality and theory of traffic flow. *Yale Bureau of Highway Traffic*, 141–188.

USHCM (2000) *HCM 2000: highway capacity manual*. Washington, DC: Transportation Research Board, National Research Council.

USHCM (2010) *HCM 2010, highway capacity manual*. Washington, DC: Transportation Research Board, National Research Council.

Van Aerde, M. (1995) Single regime speed-flow-density relationship for congested and uncongested highways *74th Annual Meeting of the Transportation Research Board*, Washington DC, USA.

Wardrop, J.G. (1952) Some theoretical aspects of rad traffic research. *Proceedings of the Institution of Civil Engineers*, 1 (3), 325-362.

Washington, S.P., Karlaftis, M.G. and Mannering, F. (2010) *Statistical and econometric methods for transportation data analysis*. FL, USA: Chapman & Hall/CRC.

Weijermars, W. and van Berkum, E.C. (2004) Daily flow profiles of urban traffic. *WIT Transactions on The Built Environment*, 75, 173-182.

Weille, J.D. (1966) *Quantification of road user savings*. The World Bank.

White, H. (1980) A Heteroskedasticity-Consistent Covariance Matrix Estimator and a Direct Test for Heteroskedasticity. *Econometrica,* 48 (4), 817-838.

Wie, B.-W., Tobin, R.L., Friesz, T.L. and Bernstein, D. (1995) A discrete time, nested cost operator approach to the dynamic network user equilibrium problem. *Transportation Science,* 29 (1), 79-92.

Wilson, R.E. (2008) From inductance loops to vehicle trajectories *75 Years of the Fundamental Diagram for Traffic Flow Theory: Greenshields Symposium,* Massachusetts, 8–10 July, 2008. Transportation Research Board, 134-143.

Wilson, R.E. and Ward, J.A. (2011) Car-following models: fifty years of linear stability analysis–a mathematical perspective. *Transportation Planning and Technology,* 34 (1), 3-18.

Wooldridge, J.M. (2010) *Econometric analysis of cross section and panel data*. Massachusetts, USA: MIT press.

Wu, C.-X., Zhang, P., Wong, S. and Choi, K. (2014) Steady-state traffic flow on a ring road with up-and down-slopes. *Physica A: Statistical Mechanics and its Applications,* 403, 85-93.

Wu, N. (2017) New features in the 2015 German highway capacity manual (HBS2015) *World Conference on Transport Research - WCTR 2016,* Shanghai, 10-15 July 2016.

Yousif, S. (2009) Partial elliptical two-regime speed-flow traffic model based on the highway capacity manual *9th International Postgraduate Research Conference in the Built and Human Environment*, Salford, Greater Manchester, 28 January 2010.

Yu, C.H. (2000) An overview of remedial tools for collinearity in SAS *Proceedings of 2000 Western Users of SAS Software Conference*. WUSS, 196-201.

Yun, L. and Shengrui, Z. (2012) Analysis on actual capacity of long tunnel by using Greenshields model *2012 International Conference on Connected Vehicles and Expo*. 252-255.

Zhang, P., Wu, C.-X. and Wong, S. (2012) A semi-discrete model and its approach to a solution for a wide moving jam in traffic flow. *Physica A: Statistical Mechanics and its Applications,* 391 (3), 456-463.

Zhou, J., Shi, Z.-K. and Cao, J.-L. (2014) An extended traffic flow model on a gradient highway with the consideration of the relative velocity. *Nonlinear Dynamics,* 78 (3), 1765-1779.

Zuur, A., Ieno, E.N., Walker, N., Saveliev, A.A. and Smith, G.M. (2009) *Mixed effects models and extensions in ecology with R*. New York, USA: Springer.

A part of the initial study in this thesis was presented at a conference as follows:

Yoon, S., Preston, J. and Kaparias, I. (2018) Comparative traffic data analysis for a motorway with a tunnel segment *UTSG (The Universities' Transport Study Group) Conference*, University College of London, 3-5 January 2018.